Author:
Hidalgo Sotelo, Sergio I

Title:
Using Drosophila to model schizophrenia symptoms

Using *Drosophila* to model schizophrenia symptoms

Sergio Ignacio Hidalgo Sotelo

School of Physiology, Pharmacology and Neuroscience
UNIVERSITY OF BRISTOL

A dissertation submitted to the University of Bristol in accordance with the requirements of the degree of Doctor of Philosophy in the Faculty of Life Sciences.

February 2020

Word Count: 36,459

ABSTRACT

Schizophrenia is characterized by the presence of several symptoms including social withdrawal, cognitive impairments and psychosis. Additionally, other less known traits are observed such as olfactory deficiencies, locomotor dysfunction and circadian and sleep disruption. It is unclear what are the factors involved in the progression and onset of these symptoms. Schizophrenia shows high heritability and several genes, among those that have been associated with this disorder, are related to calcium (Ca^{2+}) signalling pathways. Genetically modified animal models of schizophrenia have started to be used to uncover the molecular and physiological mechanisms underlying the disease. However much remains to be elucidated. In this thesis the fruit fly, *Drosophila* was used to model some aspects of the classical and non-classical symptoms of schizophrenia, including olfaction, social interactions, locomotion, sleep and circadian locomotor rhythms. Characterisation of the previously proposed *Drosophila* schizophrenia model based on the *Dystrobrevin binding protein-1* (*DTNBP1*), Dysbindin (*Dysb)* mutant, was used as a proof of principle. The results were compared to characterisation of two new genes associated with schizophrenia: the *Rab-3 interacting molecule-1* (*RIMS1*) and the calcium channel subunit α1B (*CACNA1B*) called *Rim* and *cacophony (cac)* respectively in flies.

Manipulating the expression of these genes had different contributions to behaviours that were reminiscent of some schizophrenia behavioural symptoms. Olfactory performance was assessed using single-fly video tracking exposed to an aversive odorant and social interactions were assessed by using a social space paradigm to measure the clustering of the flies. Both, olfaction and social behaviours were reduced in the *Dysb* and *Rim* mutants. Moreover, the effect of *Rim* on social behaviour was explained by a dysfunction in the olfactory system, accompanied by reduced terminal area and impaired Ca^{2+} handling of the projections sent by the antennal lobe projection neurons (AL PNs) reaching the lateral horn (LH). *Rim* and *cac* manipulations differentially contributed to learning and memory which was assessed by an aversive olfactory conditioning assay. *Rim* knock-down in the mushroom body spared memory, while *cac* knock-down impaired short- and intermediate-time memory. The memory defect of *cac* mutants was explained by impaired Ca^{2+} handling namely reduced Ca^{2+} influx upon a depolarizing stimulus. Using the *Drosophila* Activity Monitoring (DAM) *Rim* and *cac* mutants were shown to display circadian rhythm and sleep deficits. The changes observed in the *Rim* mutant were accompanied by impaired day/night remodelling of the small-LNvs (s-LNvs) dorsal terminals and impaired day/night PDF neuropeptide release.

The results of this thesis add more information to the role of synaptic proteins related to Ca^{2+} signalling in schizophrenia-like pathology. Moreover, this work demonstrates the suitability of *Drosophila* genetic models to help understand the molecular and physiological basis of schizophrenia.

ACKNOWLEDGMENTS AND DEDICATION

Firstly, I would like to thank my supervisors, Drs Jorge Campusano and James Hodge, for all their guidance and patience while doing and writing my thesis. Also, for always encouraging me to try to satisfy my curiosity and for giving me the freedom to explore different scientific questions.

From the Hodge Lab, thank you to Dr Edgar Buhl for all his help and support during my stay in Bristol. Special thanks to Kiah Tasman for helping me go through the whole process and especially during the toughest moments. Thanks to all the past and current members of the Hodge Lab.

Thanks to the rest of the Campusano lab and special thanks to Rafaella and Daniela, the most amazing lab mates and friends that could ever exist. Also, to my friends Natalia, Matías, Vicente and Bastián, for all their many years of support and friendship.

Finally, I would like to thank and dedicate this work to my family: my parents, my sister and my amazing son, Gonzalo. Without you, nothing of this would have been possible.

AUTHOR'S DECLARATION

I declare that the work in this dissertation was carried out in accordance with the requirements of the University's Regulations and Code of Practice for Research Degree Programmes and that it has not been submitted for any other academic award. Except where indicated by specific reference in the text, the work is the candidate's own work. Work done in collaboration with, or with the assistance of, others, is indicated as such. Any views expressed in the dissertation are those of the author.

SIGNED: ..... DATE:.....

Table of contents

Contents

LIST OF FIGURES

LIST OF TABLES

LIST OF ABBREVIATIONS

4-MTA: 4-methylthioamphetamine
5-HT: 5-hydroxytryptamine/serotonin
AL PNs: Antennal lobe projection neurons
AL: Antennal lobe
AMPA: α-amino-3-hydroxy-5-methyl-4-isoxazolepropionic acid
AUC: Area under the curve
AZ: Active zone
Bz: Benzaldehyde
cac: cacophony
CACNA1B: Calcium Channel Subunit α1B
CACNA1C: Calcium channel subunit α1C
Calcium: Ca^{2+}
CNV: Copy number variation
CS: Canton-S
CS^{w-}: Canton-S white minus
CT: Circadian time
cVA: 11-cis-vaccenyl acetate
DAM: Drosophila Activity Monitoring
DD: Constant darkness
DISC1: Disrupted-in-schizophrenia 1
dSERT: Drosophila serotonin transporter
dsRNA: Double stranded RNA
DTNBP1: Dystrobrevin-binding protein 1
EEG: Electroencephalogram
EH: Eclosion Hormone
GCaMP: Genetically encoded calcium sensor
GWAS: Genome-wide association studies
h: Hours:
HPLC: High-performance liquid chromatography
Hz: Hertz
iACT: Inner antenno-cerebral tract
ITM: Intermediate-term memory
KCl: Potassium chloride
KCs: Kenyon cells
l-LNvs: Large ventral lateral neurons
LD: 12 h light: 12 h dark cycles
LED: Light-emitting diode
LH: Lateral horn
LNs: Local neurons
LNvs: Ventral lateral neurons
LSD: Lysergic acid diethylamide
LTP: Long-term potentiation
mACT: Median antenno-cerebral tract

MAM: Methylazoxymethanol
MBs: Mushroom bodies
MCH: 4-methylcyclohexanol
MIA: Maternal immune activation
Min: Minutes
ML: Methyl laurate
MRI: Magnetic resonance imaging
mRNA: messenger-RNA
NMDA: N-methyl-D-aspartate
NMJ: Neuromuscular junction
NREM: Non-rapid eye movement
NRG1: Neuregulin-1
NSS: Neurological signs
OCT: 3-octanol
OI: Olfactory index
ORN: Olfactory receptor neurons
PBS: Phosphate-buffered saline
PCP: Phencyclidine
PDF: Pigment dispersing factor
PET: Positron emission tomography
PFC: Prefrontal cortex
PHP: Presynaptic homeostatic potentiation
PI: Performance index
PLTX: Plectreurys toxin
PPI: Pre-pulse inhibition
REM: Rapid eye movement
RIM1: Rab-3 interactor molecule 1
RNAi: RNA-interference
RS: Rhythmicity statistic
RT-PCR: Reverse Transcription Polymerase Chain Reactions
s-LNvs: Small ventral lateral neurons
s: seconds
SEM: Standard error of the Mean
shRNA: short-hairpin RNA
siRNAi: small-interference RNA
SSI: Social space index
STM: Short-term memory
TAE: Tris-acetate-EDTA
UAS: Upstream Activating Sequences
VGCCs: Voltage-gated Calcium channels
ZT: Zeitgeber

GENE AND PROTEIN NOMENCLATURE

By convention, human genes are written uppercase and italicised (e.g. *RIM1*) and proteins are written in uppercase but not italicised (e.g. RIM1). In *Drosophila*, genes are written in lowercase and italicised while protein symbols are in regular type, (e.g. *Rim*/Rim). In *Drosophila* the first letter of the gene symbol is upper case when the mutation for which the gene is named is dominant. The convention used at FlyBase (www.flybase.org) is followed.

Chapter 1: Introduction

Several animal models have been used to start to understand the molecular and neural circuit mechanisms that underlie schizophrenia (Jones et al., 2011). However, much remains to be elucidated and there is an urge for new model systems and approaches to address the complexity of this disorder. In this thesis, I have used the highly genetically tractable model, the fruit fly, *Drosophila melanogaster*, to model some of the most recent genetic changes associated with schizophrenia-related symptoms. This introduction section gives an overview of schizophrenia, its symptoms and a brief discussion about the environmental and genetic factors underlying the aetiology of this disorder. Additionally, I summarise the animal models currently used and introduce *Drosophila* as an experimental system and how it can be used to explore schizophrenia endophenotypes. Finally, the aims and motivations of this work are described at the end of this chapter.

1.1 Schizophrenia: historical review, morbidity and traits

Schizophrenia is a neuropsychiatric disorder characterized by the presence of several symptoms including hallucination, delusion, disorganized thinking, abnormal motor skills and a diverse array of additional symptoms making it a heterogenous disorder that has been difficult to diagnose (Berrios, 1985; Cornblatt et al., 1985; Dollfus and Lyne, 2017). This disorder was first documented in 1919 by Kraepelin as *dementia praecox*, because it is a condition whose first episodes of symptoms are presented principally during late adolescence (Jablensky, 2010; Selemon and Zecevic, 2015). However, the term schizophrenia was later established, and it is still used to this day. It is estimated that schizophrenia affects around 1% of the global population and its prevalence is higher in males than females (Evensen et al., 2016; Schizophrenia Working Group of the Psychiatric Genomics Consortium, 2014).

The direct costs associated with this disorder are related to medical attention (e.g. hospitalization, drug treatment, lab testing, care, etc), however, due to the nature of this disorder, there are indirect and intangible costs (e.g. loss of work, criminality,

addiction, effects on friends and family) (Andrew et al., 2012; Evensen et al., 2016). The indirect costs are associated with the loss of productivity and social repercussions, while the intangible effects are related to other non-financial cost, side-effect of drug treatment and comorbidity with other pathologies like stress and anxiety, which are commonly observed in schizophrenia patients (Tajima-Pozo et al., 2015).

1.2 Schizophrenia classical symptoms

Schizophrenia is diagnosed by a number of symptoms that vary in their occurrence and intensity across subjects, still, there are core features that are present in most cases (Tuathaigh et al., 2013). Many classifications have been proposed for these traits, however, the model proposed by Crow in 1980 is the most refereed (Crow, 1980). Crow proposed a model in which patients with schizophrenia have positive symptoms and negative symptoms (Crow, 1985, 1980). By this definition, positive symptoms are behaviours that are exacerbated and not observed in healthy people, while negative symptoms are those functions that are absent or undermined in patients.

1.2.1 Positive symptoms

Positive symptoms of schizophrenia include delusions and hallucinations. Delusions are false perceptions of the reality, fixed ideas that do not change when conflicting evidence is presented. Although there are many types of delusions, the most common is persecutory delusion. In this case, the person has the belief that they are being focused on by others, leading to an overreaction to mundane, daily life situations. Hallucinations, on the other hand, are bizarre beliefs, sensory representations of the reality without an external stimulus being present. Although hallucinations can be related to any sensory system, the most common are the auditory (e.g. voices inside one's head) and visual (Lally and MacCabe, 2015; Pogue-Geile and Harrow, 1984).

Although it was believed that these symptoms arise from different mechanisms, new evidence suggest the opposite. A recent novel theory proposes, both, delusions and hallucinations could be the product of sensorial overreaction (Fletcher and Frith, 2009). Models using Bayesian frameworks from cognitive neuroscience, have proposed that there is a failure in the error-driven updating system in schizophrenia. According to this, schizophrenia patients would have a

strongly fixed model of reality. Conflicting new information that is not in line with this belief, instead of updating the model, could trigger a response signalling the information is abnormal.

1.2.2 Negative symptoms

The negative symptoms of schizophrenia are diverse, and include social withdrawal, avolition and anhedonia, among others. Social withdrawal is a common feature and can be presented at different levels as a lack of interest in social activities or defective interactions in social groups (Dollfus and Lyne, 2017; Riehle and Lincoln, 2017).

Commonly, deficiencies in social interactions are accompanied by blunted affect, lack of empathy and in some cases, impaired speech communication, also known as alogia. Interestingly, these symptoms have a strong correlate in term of neuronal activity. It has been suggested that reduced empathy and impaired effectiveness arise from impaired facial and body recognition (Marosi et al., 2019; Riehle and Lincoln, 2017). This is schizophrenic individuals have troubles evaluating the emotional component of faces and body postures. Nonetheless, recent studies have unveiled that this might arise from impaired sensory processing as schizophrenic patients have reduced activity in brain areas participating in early visual recognition (Campanella et al., 2006; Darke et al., 2013; Holt et al., 2015).

Avolition, on its part, is defined by a decrement in self-initiated activities and deficits in goal-directed action performance. A special case is anhedonia, which is defined as the impaired ability to find pleasure in activities or stimuli that have a rewarding positive component. Although not enclosed in this category, similar emotional and affective disorders have been linked to these symptoms such as depression and anxiety (Németh et al., 2017; Spina et al., 1994).

1.2.3 Cognitive and memory impairments

Early descriptions indicate that some cognitive functions are impaired in patients with schizophrenia. Cognitive deficits in schizophrenia span a range of cognitive functions including language, executive function, verbal memory, spatial memory, among others (Hoff et al., 1999; Takano, 2018). Decreased cognitive performance has been observed in approximately 98% first-episode schizophrenia patients and follow up reports indicate that these impairments can be observed up to the five years later, even on medication (Hoff et al., 1999).

The nature of this cognitive disfunction has started to be studied, involving structure and functional changes of several brain areas. Studies using magnetic resonance imaging (MRI) suggested that schizophrenia patients show less hippocampal volume and decreased cortical thickness (Cannon et al., 2014; Kuperberg et al., 2010; Steen et al., 2004). Although this cortical thinning is present in almost every area (grey matter loss, i.e. where most of the cell bodies sit in the brain), the most significant changes were found in the prefrontal cortex (PFC) and the temporal lobe, where hippocampus is located (Cannon et al., 2014). While the PFC is related to executive functions, the temporal lobe, where the hippocampus is located, is related to memory formation and storage (Selemon and Zecevic, 2015).

1.3 Non-classical symptoms of schizophrenia

1.3.1 Olfactory dysfunction

Olfactory dysfunctions are well-described in schizophrenia patients. They are observed at a functional and structural level and are receiving increasing attention as a prodromal symptom/marker of frontal and temporal-limbic disorders related with this disorder (Kiparizoska and Ikuta, 2017; Moberg and Turetsky, 2003; Nguyen et al., 2010). The major functional changes observed are related to acuity (i.e. detection threshold), identification and discrimination of odorants. Studies using positron emission tomography (PET) scans, have unveiled impairments in experiencing of pleasant odours in schizophrenia patients (Crespo-Facorro et al., 2001; Kiparizoska and Ikuta, 2017). Concordantly, appraisal of odour pleasantness is compromised in schizophrenia patients and interestingly, more accentuated in males (Robabeh et al., 2015). Also, smell identification is reduced in schizophrenia, similar to patients with temporal lobe epilepsy, a disorder related with neurotransmission dysregulation (Kohler et al., 2001). As in other neuropsychiatric and neurodegenerative disorders, olfactory acuity is also blunted in schizophrenia patients (Cavaco et al., 2015; Ham et al., 2016; Lelan et al., 2011; Nguyen et al., 2010) including changes in threshold for odour detection (Ugur et al., 2005).

It is important to notice that most of the studies indicate that these functional changes are not explained by external factors such as medications or smoking status, thus supporting the idea of an internal primary olfactory dysfunction (Moberg and Turetsky, 2003). Moreover, it has been suggested that genetic

components associated with schizophrenia can explain part of this dysfunction, placing olfactory deficiencies as a promising endophenotype of this disorder (Robabeh et al., 2015; Ugur et al., 2005).

In some cases, these abnormalities can be accompanied by structural changes in olfactory processing centres. It was shown that patients with schizophrenia have reduced size of cortical brain region such as the ventromedial temporal lobe that receive direct inputs from olfactory afferents (Turetsky et al., 2003). Moreover, changes in the olfactory bulb were also found, with a 23% reduction in the volume of this structure (Turetsky et al., 2000).

Most of the current knowledge on olfactory dysfunction in schizophrenia arrives from clinical descriptions, however, there is a lack of information regarding the cellular and molecular basis of these observations (Rupp, 2010). In summary, olfactory dysfunction arises as a promising new in road into schizophrenia research elucidating pathophysiology of this disorder.

1.3.2 Circadian rhythm and sleep disruption

Circadian rhythms are daily behavioural and physiology rhythms that occur and reappear approximately every 24 hours (h). In humans, sleep-wake cycles are an important output of the circadian clock and both, sleep and circadian disruptions are observed in up to 80% of schizophrenia cases (Monti et al., 2017). Recent studies have indicated that these disturbances seem to be highly variable among subjects, ranging from insomnia to increased day and night time sleep (Wulff et al., 2012). Changes in the motor patterns of daily activity are also observed with non-24 h periods as well as sleep phase advances and delays (Cosgrave et al., 2018). Sleep latency (i.e. the time to enter in sleep) and the number of awakening (i.e. times when the sleep state is disrupted) episodes are also increased in schizophrenia, highly affecting sleep quality and resting levels in these individuals (Ferrarelli et al., 2007; Monti et al., 2017).

Importantly, these disturbances may contribute to the severity of positive and negative symptoms, proposing a causal link between sleep disturbance and psychosis (Chan et al., 2017; Cohrs, 2008). Many of these disturbances can be observed in a prodromal stage of the disorder, furthermore, recent studies using healthy participants have proposed sleep deprivation as a model to obtain psychosis-like phenotypes in humans (Meyhofer et al., 2017).

Sleep architecture is composed of four main stages; a rapid eye movement (REM) phase and three stages in a phase called non-rapid eye movement (NREM), N1, N2 and N3, progressing from light sleep phases to more stable deep sleep stages. These phases are characterized and defined by the difference in the frequency of the electrical oscillations that can be seen in electroencephalogram (EEG) recordings. During REM phase, electrical waves from 15–60 Hertz (Hz), called beta waves, can be observed, like those observed in the awake state. In N1, is characterized by 4–8 Hz waves (theta waves), that can also be observed in N2. Finally, during stage N3 is possible to observe slow wave at 0.5–2 Hz, known as delta waves (Purves et al., 2004). Both REM and NREM sleep have been found to be altered in schizophrenia (Keshavan et al., 1998; Poulin et al., 2003), with changes in the latency and duration of these phases, pointing to a problem of entering into deep sleep (Chan et al., 2017).

Although the neural basis of these phenotypes are not clear, several reports suggest that it may arise from an imbalance in the thalamus-PFC circuitry (Ferrarelli and Tononi, 2017). A key signature of this imbalance is a reduction in the frequency of sleep spindles which are bursts of theta activity found in the N2-NREM sleep phase. Interestingly, this has been shown to be independent of drug treatments status and is highly linked to genetics, therefore gaining interest of features of sleep pathology as another endophenotype for schizophrenia or the effectiveness of treatment (Cosgrave et al., 2018; Ferrarelli et al., 2007). The use of second-generation antipsychotic drugs to treat chronic sleep disorders in schizophrenia have proved to be mildly effective, however, only working in a subset of patients for some symptoms and also being accompanied by heterogenous adverse effects (Monti et al., 2017).

1.3.3 Locomotor impairments

Motor dysfunctions were first documented in schizophrenia as a major feature of this disorder, however these were later eclipsed by the later introduction of delusions and hallucinations as main clinical features, making locomotor impairments phenotypes as only secondary phenomena for the disorder (Hirjak et al., 2018; Manschreck et al., 1981; Walther and Strik, 2012; Wolff and O'Driscoll, 1999).

Schizophrenic individuals display poor movement synchronization which can be accompanied by involuntary movements, known as dyskinesia, which commonly manifest in clumsiness and stereotypic movements (Walther and Strik, 2012). The dyskinesia observed in patients is found in up to 12-13% of patients with first-episode schizophrenia with the prevalence increasing with age (Cortese et al., 2005; Ismail et al., 2001; Peralta et al., 2010). Parkinsonism is also observed in schizophrenia, in up to 27% of cases, were the more prevalent signs are muscle rigidity and bradykinesia which is defined by the characteristic slowness of movements (Honer et al., 2005).

Additionally, up to 90% of first-episode schizophrenia patients display several features associated with neurological signs (NSS) (Browne et al., 2000). These are defined and characterized by poor coordination, impaired sequential motor skills and reduced sensory integration (Dazzan and Murray, 2002). Interestingly, NSS are insensitive to drug treatments and they are prevalent in up to 98% of the chronically medicated cases (Ismail et al., 2001).

Recent studies have shown that these motor defects are highly correlated with the negative symptoms. Therefore, these traits are regaining attention as clinical markers of this disorder (Walther and Strik, 2012). Nonetheless, chronic medication as in Parkinson's disease, has also been shown to contribute to the display of these motor symptoms (Hirjak et al., 2018; Manschreck et al., 1981). Hence, there is a need for animal models that help untangle the confounding effects of drugs from the basal locomotor phenotypes observed in schizophrenia.

1.4 Neuronal networks and treatments

Several hypotheses have been proposed on the neuronal mechanism underlying schizophrenia. One of these ideas is the integrative dopamine hypothesis, supported by the extensive use of anti-psychotic drugs, like haloperidol and chlorpromazine, targeting this system throughout the years. Specifically, antagonists of the dopaminergic receptor D_2, a G-coupled inhibitory receptor localised to presynaptic terminals of dopaminergic neurons. This hypothesis puts the dopaminergic system as the centre piece of a loop that also involves the glutamatergic and GABAergic systems (Goto and Grace, 2007). In this model, the loss of GABAergic parvalbumin cortical neurons directly affects pyramidal neuron activity, making them hyperactive/dysrhythmic. This would finally lead to a

hyperactivation of dopaminergic neurons in the ventral tegmental area (VTA). The later event being thought to be responsible for some of the positive symptoms (Grace, 2017, 2016). It has been shown that the dopaminergic neurons in VTA show basal increased spontaneous firing in schizophrenia, but the molecular mechanism(s) underlying this process is(are) still unknown (Owen et al. 2004). Nevertheless, one of the main caveats of this hypothesis is that it fails to explain the negative symptoms of the disorder.

Early observations on the mechanisms of action of the hallucinogenic drug lysergic acid diethylamide (LSD), suggested that the 5-hydroxytryptamine (5-HT; serotonin) might be involved in schizophrenia (Blelch et al., 1988; Eggers, 2013). LSD binds to most of the serotonergic receptors, except 5-HT_3 and 5-HT_4 receptors, causing psychedelic hallucinations that mimic those observed in schizophrenia (Meltzer, 2017; Stahl, 2018). Moreover, the serotonergic system has a well-known role in the regulation of mood and affect in humans. Therefore, several studies have supported a serotonergic involvement in the modulation of negative symptoms of schizophrenia (Spina et al., 1994). Drug treatments targeting 5-HT receptors, prevent the loss of grey matter observed in schizophrenia and improve cognitive and negative symptoms of schizophrenia patients, further agreeing with this notion (Meltzer, 2017; Štrac et al., 2016). However, the circuits involved in this regulation are not known. But it has been proposed that overactivation or expression of the excitatory G-coupled serotonin receptor, 5-HT_2, in cortical glutamatergic neurons could drive the symptoms explained by the dopaminergic deficits (Stahl, 2018). Therefore, serotonin could be upstream within the same pathway as dopamine in schizophrenia pathology.

Schizophrenia remains poorly treated. The first generation of anti-psychotic drugs, named typical anti-psychotics, were able to treat the positive symptoms of some patients efficiently, however, due to their mechanism of action, namely D2 antagonists, a number of side effects have been observed (Lally and MacCabe, 2015; Meltzer, 2017). These so-called off-target effects have been named extra-pyramidal effects and are most commonly associated with locomotor problems such as dyskinesia and Parkinsonism. Also, the negative symptoms are recalcitrant to these typical treatments. Follow up studies have shown that positive symptoms can be decreased within a year, whereas negative symptoms persist

over five years even when treatment is applied. Additionally, they also fail to improve cognitive impairment in patients (Hoff et al., 1999).

In current clinical practice, atypical treatments that co-target the dopaminergic and serotonergic system are being used, these include clozapine, risperidone/escitalopram and fluoxetine, which have been shown to be effective in treating both the positive and negative symptoms (Kahn et al., 2015; Lally and MacCabe, 2015; Spina et al., 1994). Nonetheless, the efficacy of these treatments is still low, and little is known about how they act.

1.5 Aetiology of schizophrenia

Schizophrenia is a complex condition, associated with genetic and environmental factors (Selemon and Zecevic, 2015). As mentioned before, its aetiology is still not clear. Strong evidence supports the notion that neurodevelopmental impairments are an important part underlying the disorder (Insel, 2010). To understand the progression and onset of schizophrenia, many studies focusing on the factor that affect normal neurodevelopment have been conducted. Different elements have been linked to higher risk of schizophrenia through neurodevelopment and are divided into environmental and genetic factors (Schizophrenia Working Group of the Psychiatric Genomics Consortium, 2014).

1.5.1 Environmental factors

The nervous system is continuously developing in humans since gestation, through childhood and into early phases of adolescence (Selemon and Zecevic, 2015). Environmental factors affect this process and shape, through multiple mechanisms, the neuronal network that underlie some of the schizophrenia-related behaviours. In the context of this disorder, environmental factors have been found to play an important role in every step of neurodevelopment.

During gestation, maternal exposure to different environmental cues have been associated with an increased risk of schizophrenia later in new-born. For instance, a link between maternal infections and schizophrenia has been proposed (Brown, 2012). Studies that have been conducted in different birth cohorts have shown that maternal infection in early to mid-term pregnancy with the parasite *Toxoplasma gondii,* is associated with a two-fold increase in the risk for schizophrenia in humans (Brown, 2012). Supporting this notion, similar results are found in animal models of maternal immune activation (MIA) (Bauman et al., 2019). In non-human

primates, MIA offspring showed increased striatal dopamine, similar to what is observed in patients with schizophrenia (Bauman et al., 2019).

Maternal malnutrition has also been associated with schizophrenia (Xu et al., 2009). Evidence from studies conducted after famine periods have shown that the population risk for schizophrenia can increase up to two-times under these conditions. For instance, studies carried out in the Dutch population that suffered a time-limited famine between 1944 and 1945 after the Nazi blockade was analysed. An association was found between maternal food deprivation during the first trimester (under 4700 kJ average daily ration) and an increase of schizophrenia hospitalizations in their corresponding birth cohorts (Susser, 2011). Similar results were found in a Chinese population that underwent a period famine between the years 1959 and 1961 due to the bad weather that affected agriculture and the economic crisis. These studies not only report a decrease in the birth rate over this period, but also the they had an increased risk of developing schizophrenia later in life of about 2% or more (St Clair et al., 2005; Xu et al., 2009).

At postnatal stages, several environmental factors can modulate the risk for schizophrenia. For instance, some social and cultural changes in adolescence have been associated with increased risk of schizophrenia in later life stages. Recent findings suggest that migration processes and the minority status of groups are associated with an increase in schizophrenia risk. Meta-analysis from studies published in the topic between the years 1977 and 2003 revealed convergent evidence of increased risk of schizophrenia (around 2.7 to 4.5 times) in first- and second-generation migrants (Selten et al., 2019). New evidence suggest that this effect could be related to social exclusion derived from the migrant status and dependent on the economic status of host country (Van Der Ven and Selten, 2018).

1.5.2 Genetic factors: genome-wide and family-based association studies

As introduced before, the genetic component contributing to this schizophrenia is another hallmark of this disorder. Schizophrenia shows high heritability, in the range of 65-80%, and is inherited in a non-Mendelian fashion, suggesting that it cannot be associated with changes in a single gene, making its aetiology complex (Harrison, 2015; Schizophrenia Working Group of the Psychiatric Genomics Consortium, 2014). Over the years, a number linkage-association studies have identified risk alleles in families and some of them have subsequently been also

associated in an unbiased fashion with schizophrenia in different populations by genome-wide association studies (GWAS) (Harrison, 2015; Ripke et al., 2013)

1.5.2.1 Synaptic hypothesis of schizophrenia

Throughout the years, a number of genes encoding for synaptic proteins have been found to be associated with schizophrenia, which lead to the proposal that a synaptic imbalance may be a major contribution to the pathology of schizophrenia. (Ganapathiraju et al. 2016; Harrison 2015; Ripke et al. 2013). Moreover, changes in the expression of some of these proteins have been found in *post mortem* samples, further agreeing with this notion (Matosin et al., 2016; Talbot et al., 2004; Wang et al., 2017). These include known components of presynaptic terminals (e.g. the dopamine transporter, calcium channels, active zone proteins, etc) and molecules associated with the postsynaptic regions like N-methyl-D-aspartate (NMDA) and α-amino-3-hydroxy-5-methyl-4-isoxazolepropionic acid (AMPA) ionotropic glutamate receptors (Harrison, 2015).

There are several genes for whose function is not completely known but they are strongly associated with this disorder. For instance, the gene *Disrupted-in-schizophrenia 1* (*DISC1*) (Niwa et al. 2016; Owen et al. 2004), which encodes the pre and postsynaptic protein DISC-1, who by sequence homology is thought to be a scaffolding protein (Farrell et al., 2015). While, the *Dystrobrevin-binding protein 1* (*DTNBP1*) gene which encoding for the Dysbindin-1 protein has several suggested neuronal roles including neurotransmission and synaptic plasticity (Chen et al., 2008; Feng et al., 2008). Lastly *Neuregulin-1* (*NRG1)* is another risk gene that encode a protein of the same name that has been suggested to be involved in the neuronal specialization, growth and synapse formation (Harrison and Law, 2006; Owen et al., 2004).

1.5.2.2 Calcium channels

The most over-represented genes associated with schizophrenia are related to Calcium (Ca^{2+}) channels and calcium signalling pathways (Schizophrenia Working Group of the Psychiatric Genomics Consortium, 2014). Within these genes, voltage-gated Ca^{2+} channels (VGCCs) genes have been found to be enriched.

VGCCs are major mediators of calcium influx in excitable cells in response to membrane depolarization. They are composed by a Cavα1 subunit, plus ancillary Cavβ and Cavα2δ subunits, from which the Cavα1 is determinant to define the

VGCC type. Based on their properties, the VGCCs can be divided in L-, P-/Q-, N-, R- and T-type. They all have different localizations, which is briefly summarize in Table 1.1.

Table 1.1 Calcium channels types *

Channel Type	Pore subunit	Gene name	Localization	Function
L-Type	Cav1.1	*CACNA1S*	Skeletal Muscle	Neurotransmission, cell cycle, muscular contraction, cardiac action potential, gene expression, and protein modulation
	Cav1.2	*CACNA1C*	Heart, neurons (somatodendritic) and endocrine cells	
	Cav1.3	*CACNA1D*	Heart, endocrine cells and neurons (somatodendritic)	
	Cav1.4	*CACNA1F*	Retina	
P/Q-Type	Cav2.1	*CACNA1A*	Neurons and endocrine cells	Fast-synaptic neurotransmitter release
N-Type	Cav2.2	*CACNA1B*	Neurons and endocrine cells	
R-Type	Cav2.3	*CACNA1E*	Cardiac, endocrine cells and neurons	
T-Type	Cav3.1	*CACNA1G*	Neurons and cardiac	Low voltage activated channels. Role in cellular excitability and development
	Cav3.2	*CACNA1H*	Cardiac, kidney and liver	
	Cav3.3	*CACNA1I*	Neurons	

*Modified from (Striessnig et al., 2014).

The *Ca^{2+} channel subunit α1C* (*CACNA1C*) gene, important in neuronal depolarization, was associated with schizophrenia (Curtis et al., 2011; Ripke et al., 2013). Moreover, recent studies have shown that more polymorphisms within this gene are associated with schizophrenia in different populations (Eckart et al., 2016; Zhang et al., 2017). These and other genes were also associated with bipolar disorder, another neuropsychiatric disorder that shares many of the negative symptoms of schizophrenia (Green et al., 2010; Moskvina et al., 2009; Ripke et al., 2013).

A recently published GWAS have identified about 108 new loci associated with this disorder (Harrison, 2015; Ripke et al., 2013; Schizophrenia Working Group of the Psychiatric Genomics Consortium, 2014). Interestingly, some of these loci are related with genes highly expressed in the brain and which mediate neurotransmission (Schizophrenia Working Group of the Psychiatric Genomics Consortium, 2014). Furthermore, most of the genes found were clustered by gene

ontology within the group of Ca^{2+} signalling genes (Schizophrenia Working Group of the Psychiatric Genomics Consortium, 2014). Among the new associations, the gene *CACNA1I* encoding the Cav3.3 channel important in synaptic plasticity (Leresche and Lambert, 2017), and the *Rab-3 interactor molecule 1* (*RIM1*) gene, appeared highlighted (Schizophrenia Working Group of the Psychiatric Genomics Consortium, 2014). Overall, this broaden the evidence supporting the notion that a synaptic calcium imbalance might contribute to the molecular underpinning of schizophrenia.

1.6 Animal models of schizophrenia

Most of what we know about the pathophysiology of schizophrenia arise from studies in animal models. It has been proposed that a valuable animal model should have validity in three main categories; traits, construct and predictive value (Jones et al., 2011). Therefore, animal models should be able to recapitulate some of the traits observed in schizophrenia, in terms of positive, negative and cognitive symptoms, among others, in order to be useful. For negative and cognitive symptoms, behavioural tasks can be easily assessed for instance by evaluation of social interactions or by measuring associative memory (Carpenter and Koenig, 2008). However, positive symptoms are a special case, as psychosis or hallucinations are tricky to model, and are perhaps specific to human or require language to diagnose. To overcome these issues, researchers have used different approaches to trace indirect outputs of psychosis. The most commonly used is to measure pre-pulse inhibition (PPI), which assesses the normal reduction in responses to startle with subsequent stimuli, a characteristic form of brain plasticity analogous to habituation (Blundell et al., 2010; Clapcote et al., 2007; Jones et al., 2011). In the case of rats, an acoustic stimulus, ranging from 4 to 16 decibels, is used to generate a startle response, which is followed by a second stimulus with the same characteristic. In healthy animals, the startle response generated by the second pulse is significatively reduced compared to the first stimulus presentation, whereas in schizophrenia models the difference in the startle response between the first and the second is unchanged. As discussed previously, the schizophrenia positive symptoms might arise because of a highly rigid model of perceived reality, that cannot be easily updated by new information or error-based information

(Fletcher and Frith, 2009). Hence, PPI has been proposed as a useful proxy to analyse positive symptoms.

In addition, animals models should be able to replicate some of the neuronal and physiological landmarks of schizophrenia, for instance, changes in the main neurotransmission system related with this disorder and structural changes (Grace, 2017, 2016). Finally, a valuable animal model should be able to have a predictive value, this is, give more information about what we currently know.

Several organisms, mostly mammalian models, have been used to explore this disorder and fulfil these criteria. Here I summarise the rat and mouse models of schizophrenia and their behavioural and physiological characteristics.

1.6.1 Drug-induced models

Drug-induced animal models of schizophrenia were the first to be described and some of them are still used nowadays. They recapitulate some of the positive symptoms of this disorder, however, some of them do not show traits related to negative symptoms (Carpenter and Koenig, 2008).

Chronic amphetamine exposure is one of them. It started to be used based on the observations previously described on LSD, and the potential to cause psychosis. Animals treated with chronic amphetamine also display long-lasting PPI and hyperexcitation to acute amphetamine challenges (Tenn et al., 2005). However, this manipulation fails to impair social interactions and cognitive function (Sams-Dodd, 1998). On the other hand, the model obtained by chronic administration of phencyclidine (PCP), an NMDA receptor antagonist, does display these features (Jones et al., 2011). For instance, rats under chronic PCP, unlike the amphetamine model, do display impaired social interactions. In addition, reduced PPI is also found in the chronic PCP rat model, although this effect disappear as soon the PCP administrations is reduced (Egerton et al., 2008; Mansbach and Geyer, 1989; Sams-Dodd, 1995).

Finally, treatments to induce schizophrenia traits in animals can also be obtained at the gestational stage, like in the methylazoxymethanol (MAM) model. Due to its role in DNA replication, MAM model is characterized by neurodevelopmental defects (Carpenter and Koenig, 2008; Jones et al., 2011). Moreover, animals generated by this treatment display disrupted PPI, impaired social interactions and reduced cognitive abilities. These traits are accompanied by changes in the PFC

structure and hyperdopaminergia, currently one of the most complete drug-induced models (Grace, 2017).

1.6.2 Genetic models

With the introduction of linkage-association studies, GWAS and new technologies in transgenic manipulation, genetic animal models of schizophrenia started to appear. Many of the genetic animal models have been proven to be useful, giving interesting information about the genetic component of schizophrenia (Tuathaigh et al., 2013). One common feature of these models is that they are all based on a knock-out of the responsible gene, which is almost certainly not the case for human SNPs etc associated with schizophrenia. As there are considerably more genetic models than drug-induced ones, I summarised some of the main genetic rodent models based on the genes described in section 1.5.2 (Table 1.2).

Table 1.2 Genetic models of schizophrenia and behavioural features

Gene	Pre-pulse inhibition	Social interaction	Cognitive phenotypes
DISC1	Disrupted (Hikida et al., 2007)	Impaired (Pletnikov et al., 2008)	Impaired working memory (Pletnikov et al., 2008)
DTBNP1	Increased (Papaleo et al., 2012)	Impaired (Feng et al., 2008; Hattori et al., 2008)	Impaired spatial memory (Papaleo et al., 2012)
NRG1 *	Disrupted (Savonenko et al., 2008)	Impaired/Normal (Savonenko et al., 2008)	Impaired contextual fear conditioning (Harrison and Law, 2006; Savonenko et al., 2008)
NMDA NRI +*	Disrupted (Fradley et al., 2005)	Impaired (Mohn et al., 1999)	Normal (Ramsey, 2009)

+NMDA NRI: NMDA receptor subunit 1. * NKO not viable. Data presented for hypomorphic mutants.

1.7 *Drosophila melanogaster* as animal model

Drosophila, with more than 100 years of research, has proven to be a particularly useful model for understanding biology and especially genetics. Many biological questions have been addressed using this model and discoveries have yielded the award of at least five Nobel prizes. There are several benefits of working with *Drosophila*, for instance, its lower maintenance cost, the wide range of genetic tools available, simple and highly tractable neural circuits and short generation

time. Under standard conditions of temperature and humidity, *Drosophila* embryos takes around 10 days to generate an adult fly and a single male-female cross can generate ~100 offspring (Vosshall, 2007).

One of the main features of *Drosophila* as animal model is its highly tractable and well annotated genome. The *Drosophila* chromosomal arrangement consist of four pairs of chromosomes; one pair of XX or XY sex chromosomes and three autosomal chromosomes, usually referred as X(Y), II, III and IV, respectively. Moreover, the *Drosophila* genome is non-duplicated containing around 14,000 genes compared to the 25,000 genes in mammals (Hales et al., 2015; Roberts, 2006), with many orthologs of the same gene and therefore displaying genetic redundancy. Despite this difference, it is estimated that approximately 75% of known human disease-associated genes have close orthologues in the fly (Alphen and Swinderen, 2013).

The human brain has around 80 billion neurons and each of them can stablish connections with around 10,000 neurons. *Drosophila* brain, instead, comprise around 90,000 neurons, that connect with approximately 1000 neurons, making this brain complex enough to show memory, sleep, courtship and addictive behaviours mediated by simplified and tractable neural circuits. Although the whole fly nervous system is simpler than mammals, each *Drosophila* neuron is very similar to a mammalian neuron with many of the same characteristics including action potentials and chemical neurotransmission and express many of the same ion channels, receptors, neuropeptides, neurotransmitters and pumps.

1.7.1 Genetic tools

Drosophila has a highly characterized and manipulatable genome. Throughout the years, a number of systems have been used to manipulate genes and their expression. Here, I introduce the two main tools that I have exploited in this thesis: the GAL4/UAS system and P-element mutagenesis.

1.7.1 GAL4/UAS binary system

The GAL4/UAS system was first introduced to *Drosophila* research by Drs Andrea Brand and Norbert Perrimon in 1993 (Brand and Perrimon, 1993). By using components of the galactose-induced expression system from yeast, the GAL4/UAS system allows the spatial-specific expression of transgenes in *Drosophila.* The mechanisms behind its function involves two elements, the trans-

activating GAL4 protein and the cis-acting DNA responsive sequence named Upstream Activating Sequences (UAS) (Fig. 1.1). The GAL4 protein is a transcription factor, that binds to the UAS site and promotes the transcription of genes placed downstream of its sequence. These components are not normally expressed in the *Drosophila* genome, therefore, transgenic manipulations using this system do not usually interact with any of the fly's endogenous transcription activity, so only drives transgenes artificially introduced into the fly genome (Duffy, 2002). In order to get transgenic expression, both elements (e.g. GAL4 and UAS) must be present in the same fly (e.g. in heterozygote offspring, who got one GAL4 chromosome from one homozygous parent and the other UAS chromosome from the other homozygous parent), otherwise they are inert on their own. Given that the UAS sequence is a DNA sequence present in all cells, the spatial specificity is given by the promoter sequences upstream of the GAL4 sequence. This is either achieved by fusing the GAL4 sequence downstream of promotors known to drive expression in specific tissues or cells or by randomly inserting Gal4 into the genome and screening with *UAS-GFP* expression in the required cells of interest. By crossing a transgenic fly bearing the *promoter-GAL4* transgene with another fly containing the UAS-*gene-of-interest*, it is possible to obtain heterozygous offspring, that contain the promoter of interest which drives expression of the *gene-of-interest* in the pattern required. This *gene-of-interest* can be DNA for a mutant or wildtype fly or human gene or one that encodes a fluorescent protein. In addition to this, this system can be used to express RNA molecules than can cause specific gene knock-down. This RNA-mediated know-down is known as RNA-interference (RNAi) and is achieved by the cleavage of the targeted messenger-RNA (mRNA) through an evolutionary-conserved machinery. The specificity is achieved by generating RNA molecules with a complementary sequence to the targeted mRNA. Different molecules can be generated as short-hairpin RNA (shRNA) or double stranded RNA (dsRNA), that will be processed first to produce small-interference RNA (siRNA) molecules, which are the ones that prime to the mRNA to mediate the cleavage (Fig 1.1) (Heigwer et al., 2018; Scialo et al., 2016).

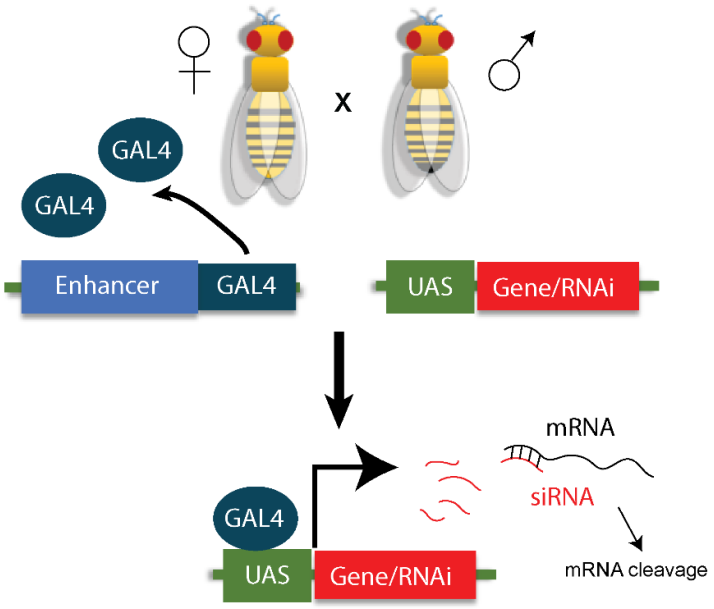

Figure 1.1 The GAL4/UAS system. When males carrying an element downstream UAS sequence (e.g. Gene/RNAi) are mated to females bearing a GAL4 driver, the progeny will bear both elements of the system (bottom panel). The GAL4 binds to the UAS sequence promoting the expression of an element of interest, in the pattern of expression of the enhancer used. In this case, siRNA molecules are generated, promoting the cleavage of the mRNA.

1.7.2 P-elements mutagenesis

Transposable *P*-elements are fragments of DNA characterized by their ability to 'jump' from one place in the genome to another. These elements encode for a transposase, an enzyme that allows its own excision from one DNA location, be mobilised and then to insert pseudo-randomly in to another site (Robertson et al., 1988). The nature of the modified *P*-elements can vary, however, they usually carry an external marker gene, such as gene that turns the colour of the fly's eye from white to red when the transgenes is present in the genome, allowing the researcher to easily check for the presence of the transgene. When *P*-elements insert pseudo-randomly into the genome they may enter directly into a gene disrupting it expression or function (Hummel and Klämbt, 2008). In addition, it is also possible to express transposase and cause the *P*-element to become mobile and to generate for what is called an imprecise excision of the *P*-element. This is generated by the tendency of *P*-elements to jump out the genome removing flanking sequence to its insertion site hence *P*-element can be used to delete whole

genes, e.g. generate knock-outs, nulls, partial loss-of-function alleles or whole regions of a chromosome called a deficiency or Df (Metaxakis et al., 2005).

1.8 Exploring behaviours and circuits in *Drosophila*

Drosophila has been used to explore the neuronal and genetic basis of behaviour, both in health and disease. Although these animals have a simple brain compared to mammals, they display a wide repertoire of behaviours that can be homologous to many mammalian behaviours (Dubowy and Sehgal, 2017; Hoopfer, 2016; Kacsoh et al., 2019; Malik and Hodge, 2014). Here I introduce some those that will be assessed in this work and mention the neural circuits involved.

1.8.1 Olfactory behaviour

Odorants are received by the olfactory receptor neurons (ORN), located in the antenna and maxillary palps, which send their projection to a primary olfactory centre, the antennal lobe (AL). ORN projections express only one specific type of olfactory receptor, and they converge onto one specific glomerulus within the AL based on which receptor they expressed. Therefore, defined responses of each glomeruli to specific signals can be found. In the AL, the ORN make synapse with two types of neurons, the local neurons (LNs) and the AL projection neurons (AL PNs). The LNs modulate the information within and between glomerulus, and the AL PNs send the output information to secondary processing centres, such as the mushroom bodies (MBs) and the lateral horn (LH; Fig. 1.2) (Hubland, 2008; Vosshall and Laissue, 2008; Vosshall and Stocker, 2007) .

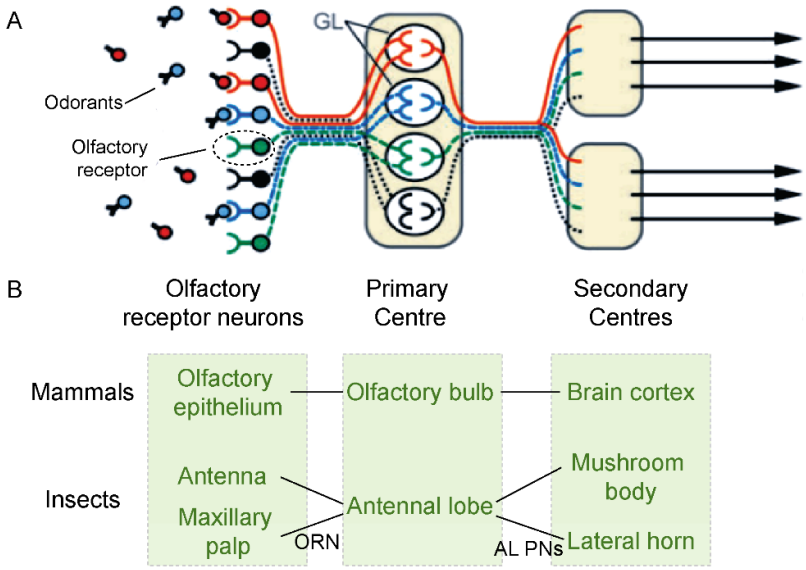

Figure 1.2 Olfactory processing in mammals and insects. (A) Odorants are received in the olfactory receptor neurons (ORNs) which send the information to a primary processing centre. Here, the terminals from different ORNs are clustered in glomerulus (GL), where they contact with projection neurons. These neurons send projections to secondary centres that will define a specific behavioural output (e.g. attraction/avoidance). (B) The organization of olfactory system of mammals and insects are presented. The processing relies in similar pathways, which mediates the odorant reception to higher brain structures. Modified from (Vosshall and Stocker, 2007)

Many neuroanatomical and functional characteristics are evolutionarily conserved, and similarities between the fly and mammalian olfactory system can be found. For example, the presence of ORN in the olfactory epithelium and the convergence to glomerular organization within the olfactory bulb (Hildebrand and Shepherd, 1997; Vosshall and Stocker, 2007). Because of this, the olfactory system of *Drosophila* serves as a useful proxy to understand the olfactory processing in mammals (Fig. 1.2).

As in many other insects, the fly display robust odorant-evoked behaviours and olfactory discrimination can be easily assessed in these animals. For instance, the T-maze apparatus, introduces flies at a choice point in a maze with two arms containing two odours (or concentrations or odour v air) allowing measurement of olfactory avoidance (Suh et al., 2004). This is a robust test, however, require hundreds of flies. New assays can be used to study olfactory discriminations. We have recently described a new olfactory assay using single-fly video tracking to presentation of an olfactory stimulus (Appendix A), this has the advantage of giving

information about locomotion as well as olfactory performance of flies (Hidalgo et al., 2017).

1.8.2 Learning and memory

Pavlovian conditioning has been used to generate aversive and appetitive memories in *Drosophila*. Starting with seminal studies by Tim Tully and William Quinn in 1974, this form of conditioning has been used to untangle the molecular and circuit mechanisms of memory processing in *Drosophila* (Heisenberg, 2003; Tully and Quinn, 1985). Moreover, it has been used to test schizophrenia-associated genes in this model, proposing this as proxy to model cognitive symptoms of this disorder (Alphen and Swinderen, 2013; Shao et al., 2011).

Aversive olfactory conditioning is commonly used, in which an odorant is paired with an electric shock to form an aversive memory in flies (Malik and Hodge, 2014). The retention of the memories can be assess by giving the flies a choice in the T-maze between the shock and non-shocked odour, the fly showing learning by avoiding the odour previously paired with shock (More detailed in 2.2.4) (Cavaliere et al., 2013; Higham et al., 2019; Malik et al., 2013). Alternatively, a sugar reward can substitute the electric shock to explore appetitive memories (Burke et al., 2012; Waddell, 2013).

The MBs have proven to be fundamental for the display of learning and memory, as affecting MBs neurotransmission or structure, has been shown to remove or implant memories (Busto et al., 2016; Davis, 2004; Heisenberg, 2003). Different dopaminergic neurons contacting the MBs relay either reward or punishment when a specific olfactory projection neuron excites a MB neuron (Fig. 1.3) (Waddell, 2016, 2013).

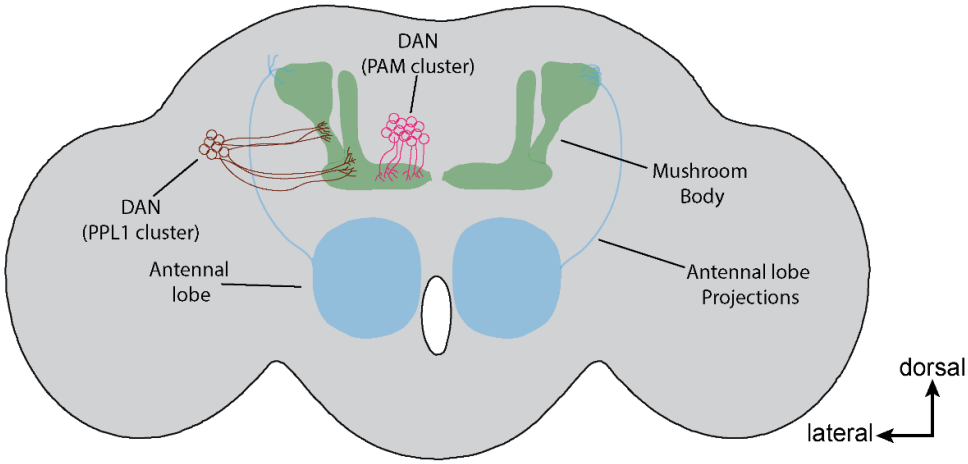

Figure 1.3 Mushroom body and dopaminergic innervations in *Drosophila*. The olfactory information conveys into the mushroom bodies (MBs) with the information of shock or sugar rewards processed by dopaminergic neurons (DAN). The DAN connects with the MBs through two major pathways, the posterior inferiorlateral protocerebrum (PPL1) cluster and the protocerebral anterior medial (PAM) cluster, which mediates the shock (negative) and sugar/water (positive) reinforcement, respectively.

1.8.3 Social interactions

Drosophila display many social interaction behaviours. From complex behaviours such as courtship to most simpler ones like grouping or clustering. However, the most studied social behaviours in flies are aggression and mating behaviours (Hoopfer, 2016).

A new form of social behaviour has been described in *Drosophila*, the social space interaction. It is based on the principle of local enhancement, an ancient and well conserved characteristic of animals that tends to cause individuals to group together with members of their own species (McNeil et al., 2015; Simon et al., 2012). In recent years, several publications have measured this behaviour, one of them modelling autism-like behaviour in flies (Ueoka et al., 2018; Xie et al., 2018). Aggression and mating behaviours are highly dependent on the olfactory circuit. It has been established that pheromones, like 11-cis-vaccenyl acetate (cVA) or methyl laurate (ML) secreted by male and females respectively, can modulate these behaviours (Dweck et al., 2015; Pitts et al., 2016; Svetec and Ferveur, 2005). The neuronal pathways mediating social space behaviour in flies are still unknown,

however, it has been suggested that dopamine can be a modulator of this behaviour (Fernandez et al., 2017).

1.8.4 Circadian rhythms and sleep behaviour

Circadian rhythms have been studied in *Drosophila* from almost 60 years, and started to gain attention when the first mutants affecting these behaviours were discovered (Dubowy and Sehgal, 2017). Since then, considerable amount of work has been conducted aiming to describe the molecular and physiological underpinnings that underly these behaviours. This ultimately led to the award in 2017 of a Nobel Prize to Drs Jeffrey C. Hall, Michael Rosbash and Michael W. Young, for their discoveries of molecular mechanisms controlling the circadian rhythm in flies that are conserved with humans, and which are fundamental for health.

Many circadian rhythms can be monitored as the periodicity of adult emergence from pupal case (eclosion rhythms) or locomotor activity, the latter, being the most commonly used and the one used in this thesis (Dubowy and Sehgal, 2017; Palacios-Muñoz and Ewer, 2018). Under 12 h light: 12 h dark cycles (LD), flies display a typical locomotor activity that is characterized by a peak of activity at morning and one at the evening. An increase in the activity can be observed prior the lights-on and lights-off transition, which is described as anticipatory behaviour. This activity pattern is also characterised by a reduction in locomotion during the night and during the middle of the day, which is known as ‘siesta’ much more pronounced in male flies than in females. These rhythms can be entrained by external cues, such as light and temperature, but they are able to persist in the absence of these signals under constant conditions, following a free-running period close to 24 h. The main external environmental input or entraining signal is called ‘zeitgeber’ (ZT), from the German, meaning ‘time giver’, such that when lights come on say at 9am in a 12 h : 12 h LD cycle this ZT0 and lights off will be ZT12 (i.e. 9pm). When entering into constant darkness (DD) condition, flies express a circadian rhythm, displaying the entrained activity pattern, so will be active in subjective day (circadian time CT0-12), even though it is dark in the incubator and will be inactive in the dark phase, subjective night, CT12-24.

The neural circuits involved in regulating circadian locomotion in flies are well described and defined by the activity of a central clock network. This is the so called

anatomical or central clock that consists of a dispersed network of groups of clock neurons which rhythmically express clock genes or the so-called molecular clock or rhythm. The central clock is composed of dorsal and ventral groups of clock neurons, of which the ventral lateral neurons (LNvs), are the key pacemakers of the circadian rhythms (Blanchardon et al., 2001; Grima et al., 2004; Nitabach et al., 2002). The LNvs can be divided into the small-LNvs (s-LNvs) and the large-LNvs (l-LNvs) with the s-LNvs being the most important in maintaining the molecular rhythm under DD (Nitabach et al., 2002; Rieger et al., 2006). The s-LNv neurons send projections to the dorsal part of the brain, where they connect with dorsal clock neurons and to outputs of clock, for instance the central complex which actually controls locomotion (Fig. 1.4) (Taghert and Shafer, 2006).

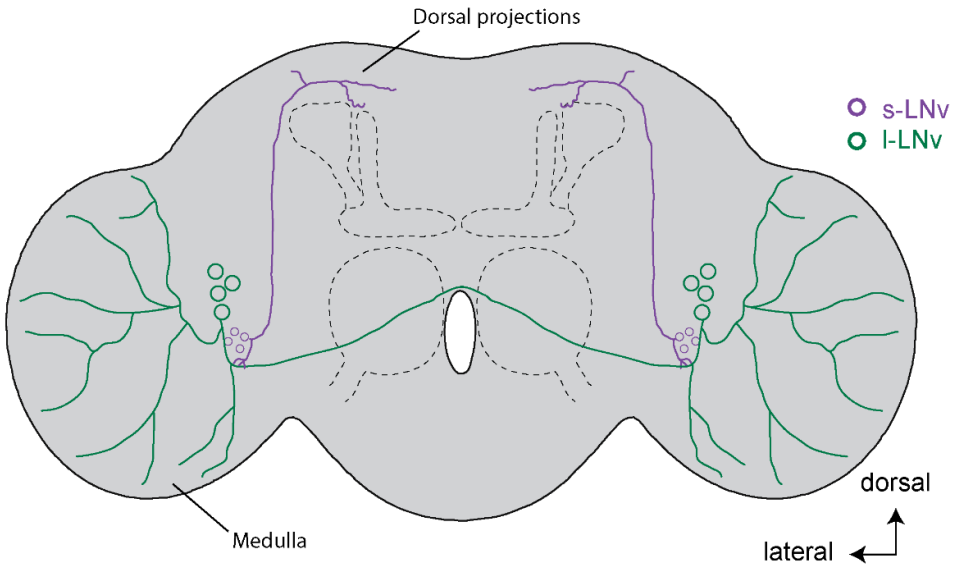

Figure 1.4 The distribution and projections of the ventral lateral neurons in *Drosophila.* The ventral lateral neurons (LNvs), part of the central clock, are major mediators of circadian rhythms in constant conditions. The large-LNvs (l-LNvs; green) projects to the medulla, where visual information arrives, and the small-LNvs (s-LNvs; purple) projects to the dorsal part of the brain, connecting with outputs of the clock.

Sleep studies in *Drosophila* are relatively new, compared to their circadian counterpart. The first studies defined sleep in flies as when individuals were inactive for longer than five minutes and displayed a state of low responsiveness to a sensory stimulus. These studies also shown that fly sleep, like in mammals, has both a circadian and homeostatic component. Flies that are sleep deprived show sleep rebound, so subsequently catch up on the lost sleep (Dissel and Shaw,

2016; Shaw et al., 2000). Both, circadian and sleep behaviours in flies have been proposed as a way to model the behavioural deficiencies observed in neuropsychiatric disorders such as in schizophrenia (Alphen and Swinderen, 2013).

1.9 Thesis aims and structure

The principal aim of my PhD project was to model schizophrenia symptoms in *Drosophila* by characterising fly mutants in orthologues of schizophrenia-associated genes. I focused on the effect of these genetic manipulations on locomotion, olfaction, learning and memory, circadian rhythms and sleep behaviours based on their known involvement in schizophrenia symptoms.

After this introduction, Chapter 2 displays all the materials and methods used in the course of the thesis. Then chapters 3-5 report the behavioural characterization of three individual genes associated with schizophrenia: *DTNBP1* (chapter 3), *RIM1* (chapter 4) and *CACNA1B* (chapter 5), giving background information on each. Chapter 6 is an overall discussion of the role of all the genes in schizophrenia and the suitability of flies as a model, followed by a brief conclusion and future experiments. After this is an appendix of work I contributed to other related projects during my PhD.

Chapter 2: Materials and Methods

2.1 Fly husbandry

Flies were raised under a LD cycle in plastic vials and bottles containing a standard cornmeal yeast diet, composed of a mix of 10% yeast extract, 8% glucose, 5% all-purpose flour, 1.1% agar, 0.6% propionic acid (to attract egg laying) and 1.2% nipagin (used as an anti-fungal). Flies stocks were kept at 19ºC, while flies used for the experiments and crosses were maintained at 25ºC. For the crosses, ~10 virgin flies and ~10 young males from the desired genotypes were collected using CO_2 anaesthesia and placed in one bottle or vial. Males and females can be differentiated by anatomical differences (females are bigger than males and have an extra abdominal stripe), and primary sexual characteristics, including the presence of the sex comb and large black reproductive apparatus at the end of the abdomen in males. Newly eclosed virgin females were recognized by the lack of pigmentation and by the presence of meconium (the first faecal material after eclosion is bright green). After ~4 days, parents from a cross were transferred to a new vial, while the offspring continued developing in the original vial. Parental strains are used again to obtain a new offspring and discarded after that.

2.1.1 Fly strains and genetics

The strains used throughout the thesis are summarised in the Table 2.1, with comments on their use and source. There are several wild type strains available, similar in terms of biological features, but with different origins. Here I described the ones that I used for each mutant, being the best option given the genetic background of each fly. The strain w^{1118} was used as genetic control for the $dysb^{1}$ and Rim^{Ex98}/Df, flies, both generated from w^{1118} flies. For the cac^{H18}, the strain *Canton-S* (*CS*) was used as genetic control as was the genetic background of this fly. The Rim^{Ex98}/Df flies were generated by crossing flies bearing the Rim^{Ex98} allele with flies containing the *Df(3R)ED5785* (henceforth *Df*) chromosome deletion in the *Rim* region in the genome, and selecting the Rim^{Ex98}/Df flies from the offspring for the experiments; these flies completely lacked *Rim*. The Rim^{Ex98} is a genomic deletion spanning 19.4 kb of the *Rim* gene, generated by imprecise excision of a

P-element. The *Df(3R)ED5785* is a chromosomal deletion of the third chromosome that also lacks the *Rim* gene. Both, Rim^{Ex98} and *Df* were homozygotic lethal.

For the *GAL4/UAS* experiments, strains containing either GAL4 or UAS were selected and crossed with the *Canton-S white minus* (CS^{w-}) strain that was used as control. *w-*, is a mutation which gives the flies white eyes, allowing to easily assess the presence or absence of a transgene in the flies following the presence of a red eye marker on the transgene. This generated heterozygotic offspring with the transgene on one chromosome over a wild-type chromosome (e.g. *PDF-GAL4* flies crossed with CSw^{-} flies generated *PDF-GAL4 /* + control flies). For the purpose of simplicity in this thesis, '*GAL4*' and '*UAS*' were omitted from the genotypes and only stated the name of the driver or the gene/RNAi downstream of UAS (e.g. *GH146-GAL4* is referred as *GH146* and *UAS-eGFP* is referred as *eGFP*).

Table 2.1 The *Drosophila* strains used, characteristics and source

	Fly name	Comment	Source*
Controls	w^{1118}	Wild type control	Dr Jorge Campusano, Pontificia Universidad Católica de Chile
	CS	Wild type control	Dr Scott Waddell, University of Oxford
	CS^{w-}	Wild type control	Dr Scott Waddell, University of Oxford
P-element derived mutants	$dysb^{1}$	Flies bearing a *P*-element within the 3' UTR sequence of the *dysbindin* gene, that results in a 40% reduction in the Dysb protein level (Shao et al., 2011)	BDSC (17918) (Mullin et al., 2015; Shao et al., 2011)
	Rim^{Ex98}/Df	Flies bearing the Rim^{Ex98} allele and *Df(3R)ED5785* allele	BDSC (78047) and (9207), respectively. (Graf et al., 2012; Muller et al., 2012)
	$Rim^{MI03470}$	Transposon insertion at the start of 3' UTR of the *Rim* gene	BDSC (37056)
	cac^{H18}	Flies bearing a point mutation in the *cac* gene causing incomplete *cac* products, generating a *loss-of-function* mutant	BDSC (42245) (Kulkarni and Hall, 1987; Smith et al., 1998)

Drivers (*GAL4* elements)	*GH146-GAL4*	Drives expression in a subset of AL PNs	BDSC (30026)
	C309-GAL4	Drives expression in the MBs	BDSC (6906)
	OK107-GAL4	Drives expression throughout the MBs	Dr James Hodge, University of Bristol (Higham et al., 2019; Malik et al., 2013)
	Tim-GAL4	Drives expression throughout the clock as Gal4 is placed downstream of the *timeless* clock gene promoter	Dr James Hodge, University of Bristol (Buhl et al., 2019; Julienne et al., 2017)
	PDF-GAL4	Drives expression in LNv clock neurons as Gal4 is placed downstream of the *PDF* clock gene promoter	Dr James Hodge, University of Bristol (Buhl et al., 2019)
	PDF-GAL4; UAS-tub:GFP	Expresses a GFP-tagged version of tubulin in the LNvs	Dr Herman Wijnen, University of Southampton
UAS constructs	*UAS-eGFP*	Expresses the enhanced green fluorescent protein (eGFP) under UAS control	BDSC (5431)
	UAS-GCaMP6f	Expresses the genetically encoded improved version of calcium indicator 6f (*GCaMP6f*) under *UAS* control	Dr James Hodge, University of Bristol (Higham et al., 2019)
	UAS-Rim-RNAi (II)	Expresses a *dsRNA* for *RNAi* under UAS control, located on chromosome 2	BDSC (44541)
	UAS-Rim-RNAi (III)	Expresses a *dsRNA* for *RNAi* under UAS control, located on chromosome 3	BDSC (27300)
	UAS-Rim:GFP	Expresses a GFP-tagged version of *Rim* under *UAS* control, located on chromosome 3	BDSC (78051) (Graf et al., 2012)
	UAS-cac-RNAi	Expresses a *shRNA* for *RNAi* under *UAS* control	VDRC (KK101468)

*****BDSC: Bloomington *Drosophila* Stock Center; VDRC: Vienna *Drosophila* Resource Center. The stock number is provided in brackets.

2.2 Behavioural Assays

All the behavioural assays were conducted at 25ºC, using three to five-day old male flies, except for the aversive olfactory conditioning to test learning and memory, where both sex flies were used. For single fly assays, anaesthetic was required to separate the flies; I used ice-induced quiescence to avoid any potential

long-lasting effect of the commonly used fly anaesthesia, CO_2. Any anaesthesia was avoided prior to memory assays.

2.2.1 Single fly video tracking

2.2.1.1 Odour induced locomotor activity

Male flies of the desired genotype were collected 24 h before the start of the experiment and kept at 25ºC in fresh food. On the day of the experiment, animals were anesthetized by placing the vial in the fridge for two minutes (min) and then transferred to a petri dish, similar to the one used for the experiments. The flies were allowed to acclimatize for 45 min prior the beginning of the experiments.

Single flies were then isolated from the group and placed in an arena where their behaviour was recorded for three min using a webcam connected to a computer running the Buritrack software (Fig. 2.1A) (Colomb et al., 2012). The arena consisted in a 39 millimetre (mm)-diameter and five mm-high Petri dish lid. Also, the arena had two three-mm openings in the walls, placed in opposite sides, that were covered with cotton swabs tips. The Buritrack software uses the live tracking of the flies to generate a spreadsheet of the position of the fly within the arena in each frame captured using x and y coordinates (Fig. 2.1B). This information is then analysed using the Centroid Trajectory Analysis application, based on R language which was run in R-Studio (Colomb et al., 2012). This allowed the calculation of the following motor parameters: basal total distance travelled, mean instantaneous speed and the centrophobism index. The mean instantaneous speed is an average of each fly's average instantaneous speed within the three min recording period. The centrophobism index is obtained by comparing the preference of flies to be in the periphery as opposed to the centre of the arena (Hidalgo et al., 2017).

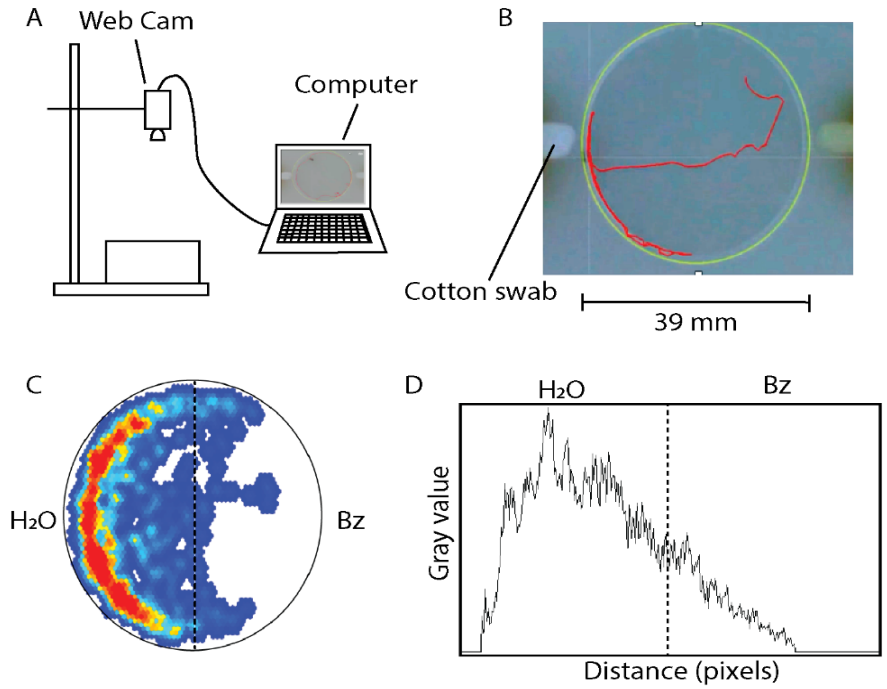

Figure 2.1 Single fly video tracking set up. (A) A camera, connected to a computer, was placed above the arena to video track the position of the fly. (B) The arena used was a Petri dish lid, with two openings on opposite sides, blocked by two cotton wool swabs. The trace that the fly made (red line) during three min is recorded. (C) A heat map of the time that the fly spent during the three-min recordings when the fly was exposed to the aversive odour, benzaldehyde (Bz). Warmer colours (red) to colder colours (blue) indicate the preference from more to less for the flies, respectively, while white indicates absence of fly or 0 preference. (D) Preference was assessed by graphing the grey intensity values within the arena and calculating the area under the curve (AUC) of each half.

2.2.1.2 Olfactory assay

The same arena was also used to assess the behavioural response to an aversive odorant (benzaldehyde, Bz, Sigma) (Hidalgo et al., 2017). Immediately after the three-min recording period of naïve locomotion, 100 μL H_2O was placed in one of the cotton wool swab tips and 100 μL of a 1% Bz solution (in water), on the other. Again, locomotor activity was assessed for three-min. The Buridan tracker software was used to obtain the positioning of the fly during this time and the centroid trajectory analysis application was used to generate a heat plot of fly's preferred position within the arena (Fig. 2.1C). The Fiji software (NIH, Bethesda, MD) was used to address the aversive response towards the odorant (Fuenzalida-Uribe and Campusano, 2018; Hidalgo et al., 2017; Molina-Mateo et al., 2017). Briefly, the heat plot was divided in half, and the pixel intensity was quantified in each half (Fig.

2.1D). This information was used to calculate an olfactory index (OI) according to the following formula:

$$OI = \frac{(AUC\ H_2O - AUC\ Bz)}{(AUC\ H_2O + AUC\ Bz)}$$

where; AUC means area under the curve in the pixel profile. AUC_{H_2O}= time spent on the water side and AUC_{Bz}= time spent on the Bz side.

This protocol was described in a recent article that we published, were I contributed to setting up of the behavioural assay and conducted electrochemical recordings (Appendix A) (Hidalgo et al., 2017).

2.2.2 Social space paradigm

For this behavioural assay, a previously reported social space paradigm was used (McNeil et al., 2015; Simon et al., 2012). Groups of 30-40 male flies were collected two days post eclosion and then kept on fresh food at 25ºC for 24 h. The animals were then transferred into fresh food vials and allowed to acclimatize for 2 h in the room where the experiment would take place. Using a mouth aspirator, the flies were transferred into a triangular arena formed by two transparent acrylics separated by 0.3 centimetre (cm)-thick acrylic spacers and a ruler attached to measure the distance between flies (McNeil et al., 2015). To start the experiment, the entire setup was tapped down three times to the base of the triangle and then the arena was placed vertically. After 30 min, a single photo was taken to measure the distribution of the flies in the chamber (Fig. 2.2A).

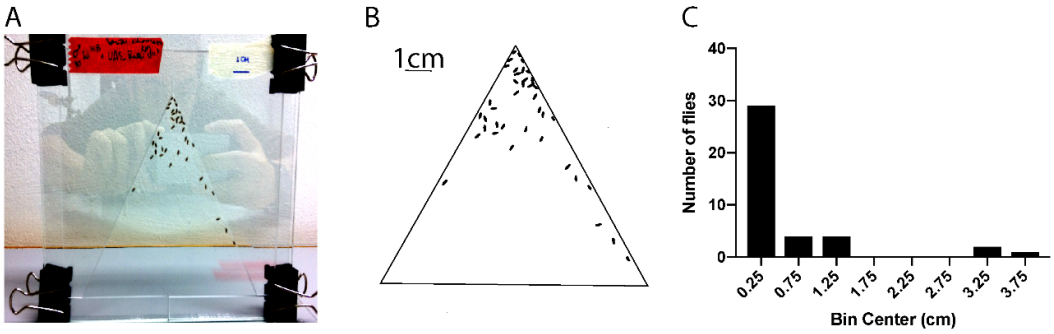

Figure 2.2 Social space behaviour set up. (A) A photograph of the triangular arena with a group of 40 flies. In the top right is shown a label indicating the distance of 1 cm which was used in image processing. In the top left is shown a label indicating the genotype of the fly and the number of animals. (B) After image processing, the distribution of the flies can be assessed by the measure of the distance between each fly to its closest neighbour. (C) A histogram of the distance preference of the flies observed in the example given in A.

The Fiji software was used to calculate the distances between each fly and all the other flies within the arena (Fig. 2.2B) (McNeil et al., 2015; Simon et al., 2012). The closest neighbour of each fly was then obtained based on the distance compared to all the other flies. This was also used to calculate the social space index (SSI), as a measure of local enhancement, which is defined as the natural tendency of the animals of the same species to congregate and form groups (Fernandez et al., 2017; McNeil et al., 2015). This was calculated by quantifying the number of flies that were within 0 to 0.5 cm to their closest neighbour (as percentage of the total) over the percentage of flies that prefer to stay in distances from 0.51 to 1 cm (Fig. 2.2C).

2.2.3 Startle-induced negative geotaxis assay

The startle-induced negative geotaxis assay was adapted from previously published protocols and it is based in the natural tendency of the flies to go against gravity (Ali et al., 2011; Fuenzalida-Uribe et al., 2013; Sun et al., 2018). Groups of 30-50 male flies collected were placed in 50 millilitres (mL) plastic graduated cylinders (height: 17 cm; diameter: 3 cm) with a mark 5 cm from the top. Flies were gently tapped down to the bottom of the tube and a 10 s period was allowed for the flies to climb to the top of the tube. A digital image was taken to quantify the number of flies above and below the 5-cm mark. This cycle was repeated with the same group of flies for 15 consecutive trials, with 30 s rest periods between each trial which allowed the animals to recover. An activity index was calculated which represents the ratio of flies above the 5-cm mark compared to the total number of flies, per trial.

A climbing index was also calculated which shows the change in negative geotaxis response between the first and last trials and was calculated by using the following formula:

$$Climbing\ index = \frac{(Average\ activity\ index\ for\ trials\ 13-15)}{(Average\ activity\ index\ for\ trials\ 1-3)}$$

2.2.4 Aversive olfactory conditioning

Aversive olfactory conditioning has been used extensively in *Drosophila* as a mean to study learning and memory (Cavaliere et al., 2013; Higham et al., 2019; Julienne et al., 2017; Malik et al., 2013). Briefly, groups of 20-50 flies were collected and

kept at 25ºC and 70% relative humidity under 12hr:12hr LD cycle in the behaviour room overnight. This is done prior to testing to allow acclimatisation of flies to control conditions. Experiments were conducted using a T-maze apparatus, consisting on an acrylic two-choice maze connected to a constant air flow (3 litres/min) to provide flies with either fresh air or a given odorant. This is done by means of an air flow passing through bubbling mineral oil or a solution of the odorant dissolved in mineral oil (Fig. 2.3A). The experiments were conducted under dim red light to prevent the confounding visual effects on olfactory memory formation and between ZT3 and ZT9 to avoid any confounding effect of circadian differences in olfactory acuity (Krishnan et al., 1999; Tanoue et al., 2004; Tully and Quinn, 1985).

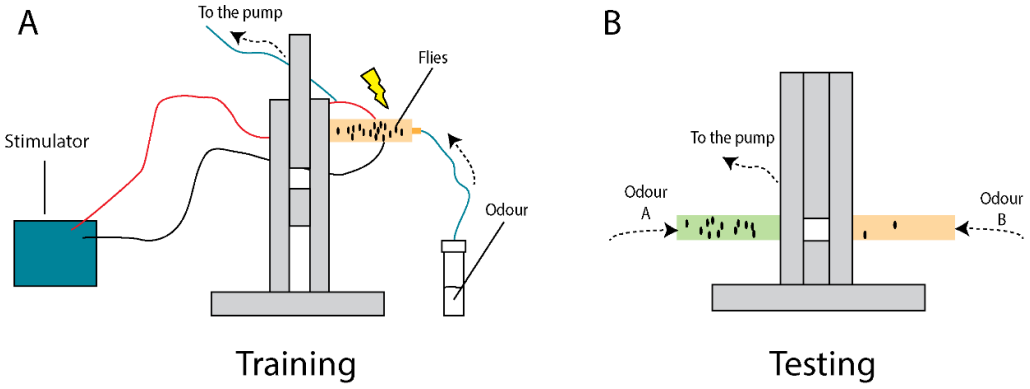

Figure 2.3 A diagram of the T-maze apparatus used for aversive olfactory conditioning assay. (A) During the training phase, flies were placed in a training tube while an odour e.g. B was presented paired with an electric shock which was provided by a stimulator and delivered via a copy grid lining the inside of the training tube. After that, flies were exposed to an odour A without shock (not shown). (B) During the test phase, the flies were exposed to both odours and they were free to decide to move into either direction, learning was demonstrated by flies avoiding the shock paired odour i.e. distributing in the green odour A tube.

The day of the experiment, flies were transferred into a training tube lined with an electrifiable grid. After 90 s acclimatization, flies were exposed to either 3-octanol (OCT, Sigma) or 4-methylcyclohexanol (MCH, Sigma) (conditioned stimulus, CS^{+}) paired with twelve 70 V DC electric shocks (unconditioned stimulus, US) over 60 s (Fig. 2.3A). This was followed by a 45 s rest period with fresh air. Flies were then exposed to the reciprocal odour (CS^{-}), which is not paired to electric shock. Memory was evaluated 2 min or 1 h post-conditioning to test short-term memory (STM) or intermediate-term memory (ITM), respectively. For this, flies are exposed

to both odorants and it is recorded the number of flies that chose each tube (Fig. 2.3B).

A performance index (PI) is calculated as:

$$PI = \frac{(correct\ flies - incorrect\ flies)}{(correct\ flies + \ incorrect\ flies)}$$

The OCT and MCH concentrations were carefully calibrated to allow a 50/50 distribution of naïve flies towards the odorants. However, the CS^{+} odour was reversed in alternate groups of flies to account for innate bias toward one odorant and a n = 1 was calculated as the average of the PI of two alternated groups. Sensory motor controls were performed to assess if electric shock and odorants avoidance were comparable between different strains. Briefly, for olfactory acuity, the odorant and air were pumped through opposite arms of the T-maze and the flies were let to decide for 2 min. For electric shock avoidance, flies were let to decide between two training tubes, one of them connected to the stimulator giving electric shock. The flies that were correct over the total are quantified and responses reported as percentage of avoidance.

2.2.5 Drosophila activity monitoring system

Locomotor activity of the flies was quantified by using the *Drosophila* Activity Monitoring (DAM) system (DAM2, TriKinetics Inc), to assess circadian rhythms and sleep (Curran et al., 2019; Julienne et al., 2017).

Flies were transferred into DAM tubes containing food at one end and a cotton wool plug at the other end (Fig. 2.4A) and were then loaded into DAM monitors (Fig. 2.4B), which contained up to 32 tubes each. These monitors contained infrared beams in each of the 32 channels and whenever a fly interrupted a beam, this was recorded and processed as a count of activity for that fly. Monitors are placed into incubators at 25ºC and connected to a computer running the DAMSystem3 data collection software (TriKinetics Inc). The host computer recorded the activity of the flies every min, writing the information as DAM files for each monitor. Flies were maintained in this system for five days under LD (with lights-on at 9 am and light-off at 9 pm) followed by five days in DD, to assess sleep and circadian rhythms, respectively.

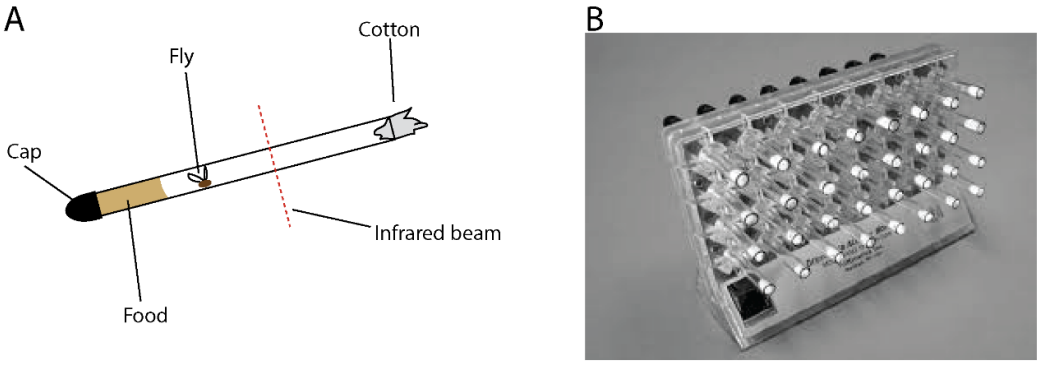

Figure 2.4 Monitoring locomotor activity using the *Drosophila* Activity Monitoring system. (A) Single flies were placed in a tube that contained food at one end and a cotton wool plug at the other end, in the middle of the tube is an infrared beam, which when the fly crosses, the computer records an activity count. (B) Up to 32 of these fly containing tubes can be placed in a monitor that is connected to a computer. The monitor records the number of beam cross of each tube across 24 h periods.

The raw data was first processed using the DAMFileScan software (DAM_2, TriKinetics Inc), allowing trimming of the data to the period of interest, i.e. the first bin of activity on the first day in LD and the last bin of activity of the last day in DD. All data were then analysed in MATLAB using the sleep and circadian analysis MATLAB program, SCAMP (Donelson et al., 2012). Only the flies that survived until the last day of DD were used for the analysis.

2.2.5.1 Circadian rhythm analysis

Circadian locomotor rhythms are usually observed in actograms, activity plots where the activity of two consecutive days are plotted horizontally. For instance, the activity of the second day will appear in the first row next to the activity of the first day but also in the second row, next to the activity of the third day and so on (Fig. 2.5A).

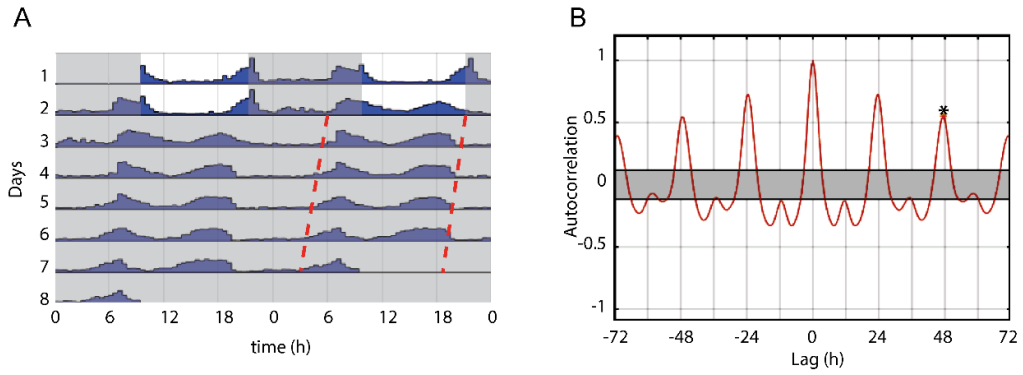

Figure 2.5 Visualization of the circadian locomotor activity. (A) Double-plotted actograms are used to visualize the locomotor activity of the flies on consecutive days, which are plotted both horizontally and vertically i.e. the right end of day 1 line is repeated at the left hand beginning of the day 2 line. Grey shading indicates where lights were turned off and the red lines highlight the trend in the activity, indicating the free-running period of rhythmicity. (B) An autocorrelation analysis of the activity allows a measure of the strength with which the recording correlates with itself in time. It also allows to calculate the rhythmicity statistic, as a measure of rhythmicity strength (calculate at the third peak; black asterisk).

To assess the rhythm strength, an autocorrelation analysis was used obtained using the SCAMP software (Donelson et al., 2012). In this analysis, the activity of each fly is compared to its own activity in time, therefore, obtaining a measure of how well the rhythm activity is sustained (Fig. 2.5B). From this autocorrelation it is possible to obtain a rhythmicity statistic (RS) value which is calculated as a ratio between the rhythmicity index at the third peak (height of the third peak in the correlogram; black asterisk in Fig. 2.5B) and the absolute value of the 95% confidence interval for the correlogram obtained for each fly (Levine et al., 2002a, 2002b). By convention, RS values > 1.5 indicate strong rhythmicity characteristic of a normal wild type fly (Buhl et al., 2019; Julienne et al., 2017). Additionally, an estimated period length under free-running conditions (i.e. DD which is without external circadian cues) can be calculated from the distance between the autocorrelation peaks (i.e. lag between the peaks). Flies with RS < 1.5 were excluded from the period calculation (Buhl et al., 2019; Julienne et al., 2017; Levine et al., 2002a).

2.2.5.2 Sleep analysis

Sleep information can also be obtained from the locomotor activity data acquired through the DAM system. The SCAMP software (Donelson et al., 2012), allowed

identification of sleep periods, which were defined as periods of inactivity longer than five min. Sleep is usually visualised by plots exhibiting the mean amount of sleep in 30-minute bin against the time of day. This is averaged across all the days of the experiment, generating an averaged sleep profile (Fig. 2.6). Throughout this thesis, only data obtained in the last two days of LD were used, as the first three days were used to entrain (or synchronise) the flies to the LD cycle. From the raw data it is possible to obtain the total sleep amount and the sleep during the day and during the night.

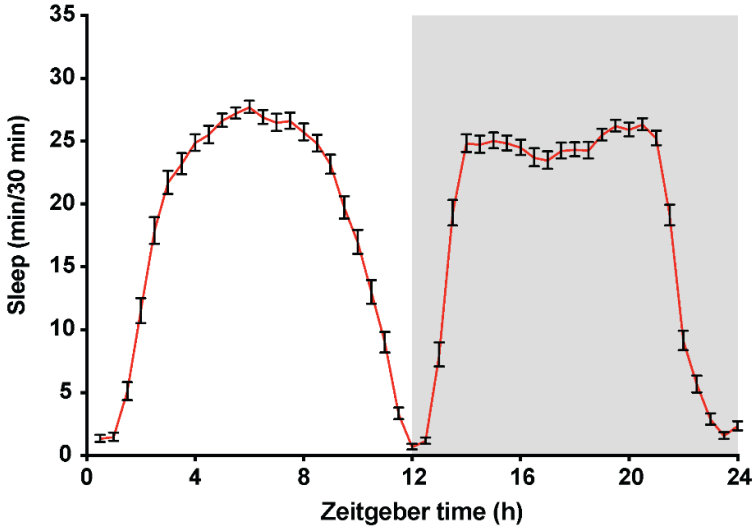

Figure 2.6 A representative sleep profile. Sleep is graphed as the amount of sleep in 30 min bins, against the time of day. This is also averaged for a group of flies over two days of LD. Time is given as zeitgeber time, meaning that ZT0 is when the lights were switch on (09:00) and ZT12 will be when the lights were switched off. A sleep known as 'siesta' is observed at the middle of the day. Data plotted as mean with SEM.

2.3 Imaging

2.3.1 Calcium imaging

Flies were anaesthetized under CO_2, decapitated and their brains were dissected in extracellular saline containing (in mM): 101 NaCl, 1 $CaCl_2$, 4 $MgCl_2$, 3 KCl, 5 D-glucose, 1.25 NaH_2PO_4, and 20.7 $NaHCO_3$ adjusted to a final pH of 7.2. Brains were held down using a custom-made anchor, with the dorsal part facing up for measuring the AL PNs terminals reaching the LH or front up for imaging the MBs. A 40x water-immersion lens was used, on an upright microscope (Zeiss Examiner Z1). Extracellular saline (3 mL/min) was used to perfuse the brains and transient

bath application of 100 mM potassium chloride (KCl) in extracellular solution for 12 s was used to depolarize the neurons (Higham et al., 2019; Malik et al., 2013). Images were acquired with Micro-manager software at 4 frames/s with 100 ms exposure using a CCD camera (Zeiss Axiocam) and a 470 nm light-emitting diode (LED) light source (Thor Labs). The baseline fluorescence (F0) was calculated as the mean fluorescence during the first 20 s of recordings (80 images), prior to the start of KCl perfusion. The change in fluorescence relative to baseline [(F-F0)/F0, where F is fluorescence at any given time] was recorded, and the change in the peak amplitude following high KCl exposure was used as a metric of transient Ca^{2+} increase (Higham et al., 2019; Malik et al., 2013). Data were processed and analysed using RStudio version 1.1.463 (RStudio, Inc., Boston, MA URL http://www.rstudio.com/).

2.3.2 Immunohistochemistry

Flies were anesthetized using CO_2 and brains were dissected at two day-points; 2 h after lights on (ZT2) and 2 h after lights off (ZT14). Phosphate-buffered saline (PBS) containing 4% paraformaldehyde and 0.1% Triton X-100 (Sigma) was used to fix and permeabilise the brains for 45 min at room temperature avoiding samples being exposed to light. Brains were washed and blocked in 5% normal goat serum (NGS, Thermo Fisher Scientific) for 30 min at room temperature. Brains were incubated with primary antibodies in 5% NGS at 4^{o}C for 2 days. To detect pigment dispersing factor (PDF) peptide a monoclonal antibody was used (1:200; developmental studies hybridoma bank, #PDF-C7) and green fluorescent protein (GFP) detection was enhanced by using an anti-GFP antibody (1:1000; Life Technologies # A11122). Vectashield hard set medium (Vector Laboratories) was used as mounting media for confocal visualization. Images were acquired using a Leica TCS SP8 AOBS confocal laser scanning microscope attached to a Leica DMi8 inverted epifluorescence microscope, which was equipped with “hybrid” GaAsP to improve sensitivity. A 40x oil immersion objective (40x HC PL APO CS2; Leica) was used and stacks of confocal images at 2 μm step size were taken.

2.3.2.1 Image processing

To quantify the axonal arborization of the dorsal projections of the s-LNvs, we used Sholl analysis (Curran et al., 2019; Gorostiza et al., 2014; Herrero et al., 2017; Sholl, 1953). First, images were adjusted by brightness and contrast to obtain a

clear view of all the terminal branches. Then, arborization was manually traced to produce a 'skeleton' of the neuronal terminals using the simple neurite tracer plugin on Fiji (Fig 2.7). Using this image, 10 evenly spaced (5 μm) concentric rings centred at the first branching of the dorsal projections were drawn and the number of intersections of each projection with the rings was quantified. To assess PDF intensity within each PDF signal a home-made Fiji macro was used using a Brightness/Contrast corrected copy of the PDF channel and applying an auto threshold function using IsoData method to define each cluster. Scoring of both, axonal arborization and PDF intensity were done automatized and blind to avoid bias.

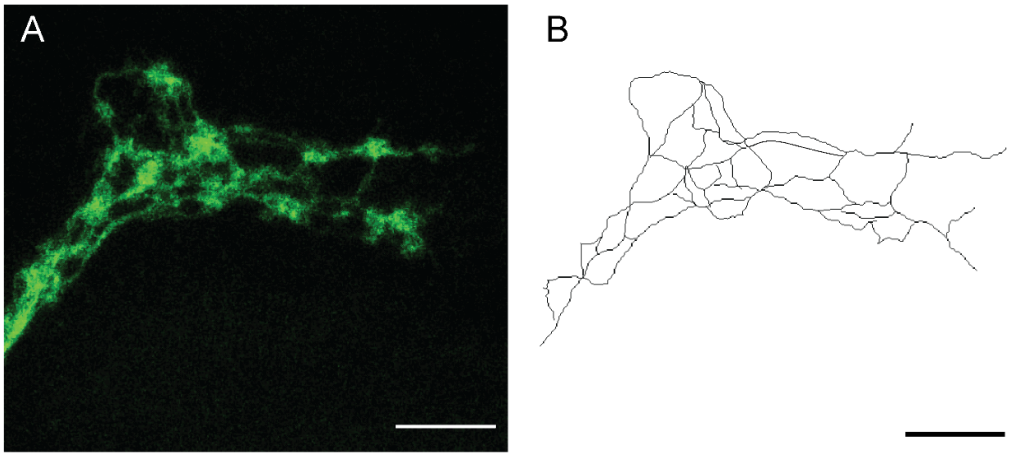

Figure 2.7 Neurite trace of a s-LNvs dorsal terminals. (A) A representative image of a dorsal arborization of a s-LNv neuron at ZT2 (i.e. 11 am) visualized by expressing a GFP-tagged version of tubulin in the LNvs (*PDF; tub:GFP*). (B) Each branch is traced and a 'skeletonised' representation of the terminal is used to quantify the arborization using Sholl analysis (Sholl, 1953). Scale bars are 10 μm.

2.4 Semi-quantitative Reverse Transcription Polymerase Chain Reactions

Semi-quantitative Reverse Transcription Polymerase Chain Reactions (RT-PCR) were used to assess expression of the *Drosophila serotonin transporter* (*dSERT*) gene in control and mutant flies adapting previously published protocols (Molina-Mateo et al., 2017). Briefly, total RNA from about 50 adult heads was obtained using a TRIzol (Invitrogen, Thermo Fisher Scientific) and a chloroform-isopropanol extraction (Hidalgo et al., 2017; Molina-Mateo et al., 2017). RNA quantification was evaluated using an Epoch Multi-volume Spectrophotometer (Bio Tek Instruments). RNA integrity was assessed by loading 1 μl of total RNA extract (~ 800 ng) onto an ethidium bromide-stained 1% agarose gel with 1x Tris-acetate-EDTA (TAE)

buffer composed by (in mM): 40 tris base, 20 acetic acid and 1 EDTA. Two major bands corresponding to the 18S and 28S ribosomal RNA (rRNA), the most abundant RNA within a cell, should be observed at the expected 2.0 kilobases (kb) and at 4.1 kb. Otherwise, a single band within the expected 18S size could be observed, as a product of the reported 28S rRNA break in two fragments of similar sizes to the one of the 18S (Winnebeck et al., 2010). If a sample showed RNAs of lower sizes than the 18S band with no 18S band, this sample was discarded as the RNA might have degraded.

Reverse transcription was carried out with 1 µg of total RNA (First strand cDNA synthesis kit, Thermo Scientific), using oligo-dT as primers and by following manufacturer's instructions. cDNA was then amplified using GoTaq G2 Flexi DNA polymerase (Promega). The PCR program used was; a first cycle of 15 min at 95°C, followed by 15 s at 95°C, 20 s at 59°C and 30 s at 72°C for 40 cycles. The final step was at 72°C, 30 s. The PCR products from each experiment were loaded onto an ethidium bromide-stained 1% agarose gel which was scanned for digitalization and the bands quantified using Fiji software (Molina-Mateo et al., 2017; Shao et al., 2011). A ratio of intensities for *dSERT* versus a *GAPDH2* control PCR amplicon was calculated for control and mutant animals. The primers used to amplify a sequence corresponded to exons 7 and 8 of the mRNA of *dSERT* and were: *dSERT* forward primer 5′- TGCTGGTCAACTTCCTGAAT-3′ and *dSERT* reverse primer 5′-ATGAATATGGTCAGCAGGAACA-3′. The PCR product was 200 bp. The PCR reaction conditions for the *GAPDH2* gene were as indicated above, with the exception that 150 ng of RNA was used. Primers for *GAPDH2* were as follows: *GAPDH2* forward primer, 5′-CGTTCATGCCACCACCGCTA-3′ and *GAPDH2* reverse primer, 5′-CCACGTCCATCACGCCACAA-3′ amplifying a PCR product of 72 bp.

2.5 High-performance liquid chromatography

Experiments of serotonin measurements were conducted in collaboration with Rafaella V. Zárate (Pontificia Universidad Católica de Chile) using previously published protocols (Molina-Mateo et al., 2017). For each independent measurement, five adult *Drosophila* brains were dissected and homogenized in 100 µl of 0.2 M perchloric acid (PCA) by sonication. The samples were passed through a Whatman PES 0.2 µm filter and endogenous serotonin tissue levels were

quantified using 5 µL of the sample which was injected into the high-performance liquid chromatography (HPLC) system (BAS, West Lafayette, IN) which was coupled to electrochemical detection. The HPLC mobile phase, consisted of 0.1 M sodium phosphate monobasic, 1.8 mM 1-octanesulfonic acid and 1 mM EDTA (pH 2.5) which was pumped at a flow rate of 60 µl/minute which yielded a retention time of 22.0 min for serotonin. The potential of the amperometry detector was set at 0.650 V. Samples were analysed by comparing the peak area of the biogenic amine and its elution time to a reference standard.

2.6 Drug exposure

The protocol for drug feeding was adapted from a previously published study (Hidalgo et al., 2017). Male flies (3-5 days old) were kept in fresh food vials, and then fed 100 µM 4-methylthioamphetamine (4-MTA) (Hidalgo et al., 2017; Matsumoto et al., 2014) in vehicle (5% sucrose in water) presented to them on filter paper circles for 45 minutes prior to the beginning of the experiment.

2.7 Statistical analysis

All statistical analyses were performed using GraphPad Prism (version 7.00 for Windows, GraphPad Software). Datasets were scrutinized for normal distribution in order for appropriate selection of parametric or non-parametric test use. Data is presented as Mean ± Standard error of the Mean (SEM). Statistical tests used for each comparison are detailed in figure legends. Statistical levels are denoted as following *$p < 0.05$, **$p < 0.01$, ***$p < 0.001$ and not significant (ns) $p > 0.05$.

Chapter 3: The behavioural and neurochemical characterization of the *Drosophila dysb*^{1} mutant suggests changes in serotonin signalling contribute to the negative symptoms of schizophrenia

This chapter describe the outcomes of experiments assessing the effect of the *dysb*^{1} mutation, on schizophrenia-related behaviours and neurochemistry in *Drosophila*. The section 3.1 gives an introduction on Dysbindin-1 function and its association with schizophrenia. Aims of this chapter are presented later. Results of *dysb*^{1} performance on olfaction, social interaction and in basal and stimulus-gated locomotor behaviour are presented in the Section 3.3. Furthermore, a brief characterization of changes in the serotonergic system in *dysb*^{1} flies is presented. Finally, a discussion of the results of this chapter and conclusions are presented in the Section 3.4 and 3.5, respectively.

3.1 Introduction

3.1.1 Dysbindin-1 association with schizophrenia

The human *Dysbindin-1* gene, called *DTNBP1* has been strongly associated with schizophrenia (Farrell et al., 2015; Tuathaigh et al., 2013; Wang et al., 2017). Since its first description in an Irish family by linkage-association studies (Straub et al., 2002), several SNPs within this gene have been found to be associated with schizophrenia in other populations (Ayalew et al., 2012; Fanous et al., 2005; Funke et al., 2004). In addition, studies in *post mortem* samples show that the expression of Dysbindin-1 is decreased by 73% to 93% in the brains of schizophrenia patients (Talbot et al., 2004).

Several studies have shown that subjects carrying the schizophrenia-linked high-risk alleles of *DTNBP1* exhibit a higher incidence of negative symptoms than those without these alleles (DeRosse et al., 2006; Fanous et al., 2005; Fanous and Kendler, 2005; Wessman et al., 2009).

In recent years, several animal models have been used to describe Dysbindin-1 function in neurons providing remarkable insights into schizophrenia pathophysiology (Wang et al., 2017). For instance, a *Dysbindin-1* mutant mice called *Sandy*, *Sdy* was generated by a large deletion of the gene, leading to a total loss of *Dysbindin-1* expression (Li et al., 2003). *Sdy* mice display some schizophrenia-like behaviours including decreased locomotor activity and impaired social behaviour, as reduced number of contacts with other animals was found (Hattori et al., 2008). Moreover, the same deletion in a C57BL/6J genetic background (referred to as *Dysb*$^{-/-}$) led to impaired spatial learning and higher acoustic startle reactivity to a 120-dB stimulus. This is reminiscent of what has been observed in individuals diagnosed with schizophrenia, which show impaired pre-pulse inhibition to an acoustic startle stimulus and it has been linked to the psychomotor symptoms related with psychosis (Papaleo et al., 2012; Wang et al., 2017).

3.1.2 Dysbindin-1 role in neurons

Dysbindin-1 protein contributes to a variety of processes, from membrane stability in skeletal muscle to dendritic spine formation in neurons (Chen et al., 2008; Shao et al., 2011; Wang et al., 2017). In humans, Dysbindin-1 protein has 3 isoforms, generated by alternative splicing, Dysbindin-1A, B and C, of which 1A product is localised in the post-synaptic density, 1B in synaptic vesicles and 1C is in both (Xu et al., 2015). Dysbindin-1 contains coil-coil domains and a PEST domain, thought to be involved in the interaction with a wide range of molecules at the pre- and post-synaptic terminals like Snapin and DISC1 (Kurita et al., 2016; Talbot et al., 2006).

Several studies have shown that the dysbindin-1 protein contributes to neuronal structure and synaptic function. *DTNBP1* knock-down affected primary hippocampal neurons leading to abnormally enlarged dendritic spines (Ito et al., 1998) and descriptions in a *DTNBP1* mutant mice (Chapter 1) have shown that it is also required for neurotransmitter release, possibly through its interaction with others presynaptic molecules (Chen et al., 2008).

3.1.3 Dysbindin-1 studies in Drosophila

In *Drosophila* the dysbindin-1 protein is encoded by *DTNBP1* orthologue, *Dysb*. This gene was found to be expressed in neurons and glia, where it regulates

synaptic functions and neurotransmitter release (Lu et al., 2014; Mullin et al., 2015; Shao et al., 2011). The characterization of a *Drosophila Dysbindin-1* hypomorphic mutation (*dysb*^{1}) has revealed a number of neurophysiological defects, that show some schizophrenia-related features (Shao et al., 2011). This mutant was generated by a transposon insertion in the 3' UTR end region of the *Dysb* gene, which lead to an approximate 40% reduction in the expression of the protein (Shao et al., 2011). The *dysb*^{1} mutant show altered presynaptic homeostasis potentiation (i.e. PHP, the increase of neurotransmitter release upon blockage of postsynaptic receptors) at the glutamatergic neuromuscular junction (NMJ) and a reduction in amplitude of excitatory junctional currents.

On the other hand, Dysb function in the neurons was shown to be essential (Dickman and Davis, 2009; Shao et al., 2011). *dysb*^{1} mutants have been shown to have defective short- and long-term memory, impaired olfactory habituation and mating preferences (Mullin et al., 2015; Shao et al., 2011). Because of this, *dysb*^{1} has been proposed as a *Drosophila* model of schizophrenia (Shao et al., 2011). Moreover, Shao et al. (2011) demonstrated that *dysb*^{1} flies have decreased glutamatergic (hypoglutamatergia) transmission and increase dopaminergic transmission (hyperdopaminergia), both characteristic changes observed in schizophrenia (Grace, 2017).

Although these reports have provided important insights into the cellular and molecular function of *dysbindin-1*, there are still open questions regarding the behavioural consequences of the loss-of-function of this gene.

3.2 Aims

As introduced in Chapter 1, *Dysbindin-1* mutants have been used as an animal model to study some of the events underlying the progression of schizophrenia. Therefore, building on its extensive functional characterization we used the *Drosophila dysb*^{1} mutant as a proof of principle model of schizophrenia-related behaviours in flies. This mutant also offers a good model to explore changes in other neuronal systems underlying schizophrenia pathophysiology, for instance, the serotonergic system (Chapter 1). Consequently, the aim of this chapter was to characterize *dysb*^{1} performance in olfactory, locomotor and social interaction behavioural tasks, relevant to schizophrenia symptomatology. We also aimed to characterize changes in the serotonergic system in these animals.

3.3 Results

3.3.1 Olfactory performance and social space are impaired in dysb[1]

As discussed in Chapter 1, olfactory dysfunctions are found in schizophrenia patients and is well-stablished now that they form part of the symptomatology of this disorder (Nguyen et al., 2010; Rupp, 2010). In order to test whether olfactory responses are affected in *dysb[1]* mutant flies, we used single-fly video tracking of flies exposed to an aversive odorant, Bz. Examples of heat maps before (Fig. 3.1A, left panel) and after (Fig. 3.1A, right panel) the Bz exposure showed that the flies avoid that side of the arena.

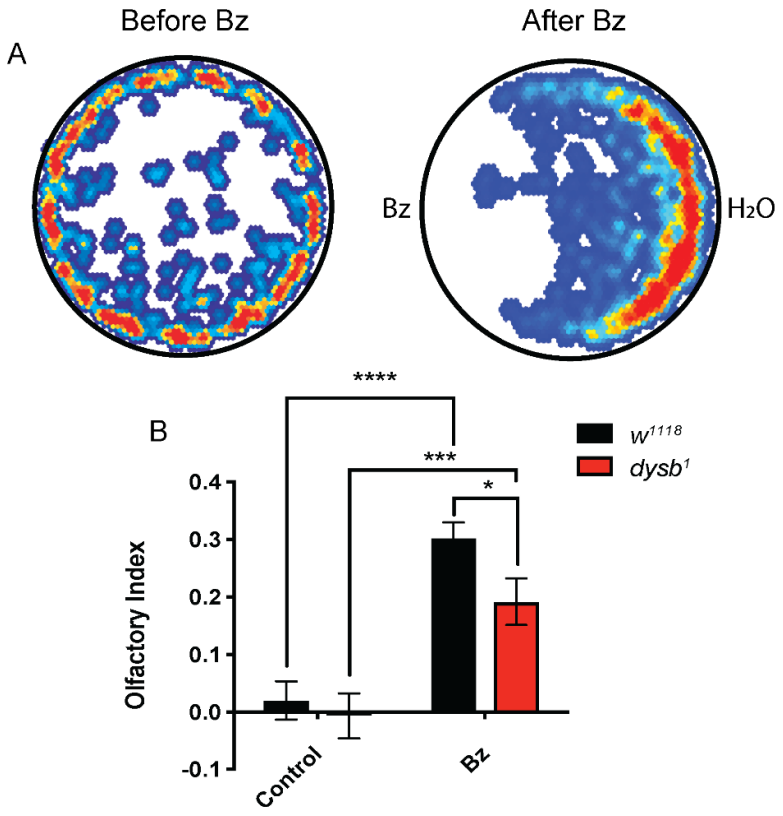

Figure 3.1 Olfactory acuity to an aversive stimulus is decreased in *dysb[1]* mutants. (A) Heat maps showing the preference position of a fly within the behavioural arena before (left panel) and after (right panel) Bz exposure to the left side. (B) *dysb[1]* mutant showed a decreased avoidance to the Bz compared to control flies. Two-way ANOVA followed by Fisher's LSD *post hoc* test. n(*w[1118]*) = 34, n(*dysb[1]*) = 21 flies.

The quantification of heat maps for control and *dysb[1]* mutant flies, show that both strains exhibited a strong aversive reaction to 1% benzaldehyde ($F_{1, 105} = 46.66$, $p < 0.0001$, Fig. 3.1). However, *dysb[1]* flies show a significant reduction in the

magnitude of the aversion to the odorant (0.192 ± 0.039, $p < 0.05$, Fig. 3.1), compared to control flies (0.302 ± 0.027).

To assess social impairments in the *dysb*^{1} mutant, we used a social space paradigm which evaluates social clustering in flies. While control flies seem to form groups in the arena, *dysb*^{1} mutants failed to do so (Fig. 3.2A; left and right panel, respectively). Control flies exhibited 0.56 ± 0.039 cm distance to their closest neighbour as opposed to 0.74 ± 0.038 cm distribution for *dysb*^{1} flies ($p < 0.001$, Fig. 3.2B). Similar observations were obtained when comparing the social space index suggesting social interactions are altered in *dysb*^{1} mutants ($p < 0.01$, Fig. 3.2C). To test if this observation could be explained by a defect in centrophobism, we measured the centrophobism index, a measure of the preference of flies to be in the periphery as opposed to the centre in the arena. No difference was found when comparing centrophobism between mutant and control flies ($p = 0.71$, Fig.3.2D). This suggests that the social space differences observed in *dysb*^{1} mutants arise from defects in social interactions rather than from a centrophobism defect.

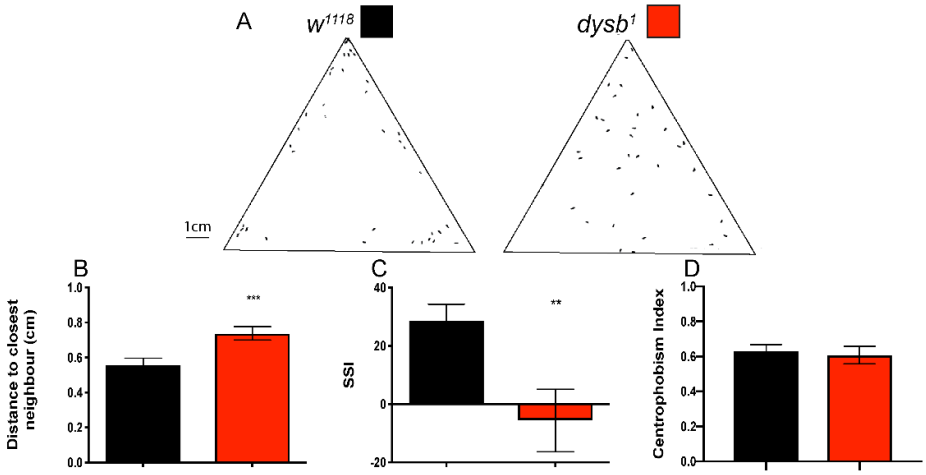

Figure 3.2 *dysb*^{1} flies showed defects in social interaction. (A) A contrast photograph of the social chamber shows a representative image of the preferred distribution of control (*w*^{1118}, left panel, black bars) and mutant flies (*dysb*^{1}, right panel, red bars). Clustering is observed in control flies, a behaviour that is reduced in *dysb*^{1} mutant flies. (B) *dysb*^{1} flies present an increase in social spacing compared to control flies. (C) Social space index (SSI), as a measure of local enhancement (i.e. clustering in of animals within groups), is significantly reduced in *dysb*^{1} mutant flies. (D) Centrophobism index was unchanged in the *dysb1* mutant compared to control flies. Data was analysed with Mann-Whitney test for data in B and Unpaired t-test in C and D. n(*w*^{1118}) = 8 and n(*dysb*^{1}) = 5 groups, ~ 40 flies each (B-C) and n(*w*^{1118}) = 28 and n(*dysb*^{1}) = 35 flies (D).

3.3.2 dysb[1] mutants displayed reduced basal locomotor activity and impaired stimulus-gated locomotor activity

Motor dysfunction can be observed in schizophrenia patients and this can range from impaired eye movement to Parkinsonism, however, the mechanisms underlying this dysfunctions are unclear (Hirjak et al., 2018; Manschreck et al., 1981; Walther and Strik, 2012; Wolff and O'Driscoll, 1999). To further characterize the behavioural deficits of the *dysb[1]* mutant, we measured basal and startle-induced locomotion. The single-fly tracking assay was used again to measure locomotion in these flies before and after Bz exposure. Examples of traces of a single control (Fig. 3.3A, left panel) and *dysb[1]* fly (Fig. 3.3A, right panel) evidenced a reduction in motor activity in mutant animals. The quantification of traces in different flies further supports this notion. Two-way ANOVA analysis showed an influence of genotype ($F_{1, 91}$ = 12.16, p < 0,0001) and Bz exposure ($F_{1, 91}$ = 4.911, p < 0.05) to the distance that the flies travelled. Under control conditions, *dysb[1]* flies (395.7 ± 59.3 mm) showed reduced distance travelled compared to control flies (811.5 ± 105.5 mm, p < 0.0001, Fig. 3.3B). Moreover, the mean of the instantaneous speed was also affected by the genotype and Bz exposure. *dysb1* showed reduced locomotion under basal conditions (10.25 ± 0.12 mm/s), compared to the control flies (11.55 ± 0.26 mm/s, p < 0.001, Fig. 3.3C). Interestingly, the influence of benzaldehyde could only been observed in control flies who exhibited a reduction in both distance travelled (811.53 ± 105.48 mm; Fig. 3B) and mean of instantaneous speed (11.55 ± 0.23 mm/s) upon benzaldehyde exposure (distance travelled; 484.33 ± 61.23 mm, p < 0.001, Fig. 3.3B; speed; 10.78 ± 0.17 mm/s, p < 0.0001, Fig. 3.3C). These parameters are not affected in *dysb[1]* mutant flies exposed to the odorant (distance travelled: $Control_{dysb1}$ = 395.71 ± 59.26 mm vs Bz_{dysb1} = 413.77 ± 43.23 mm, p = 0.9977, Fig. 3.3B; speed: $Control_{dysb1}$ = 10.25 ± 0.12 mm/s vs Bz_{dysb1} = 10.02 ± 0.13 mm/s, p = 0.7361, Fig. 3.3C).

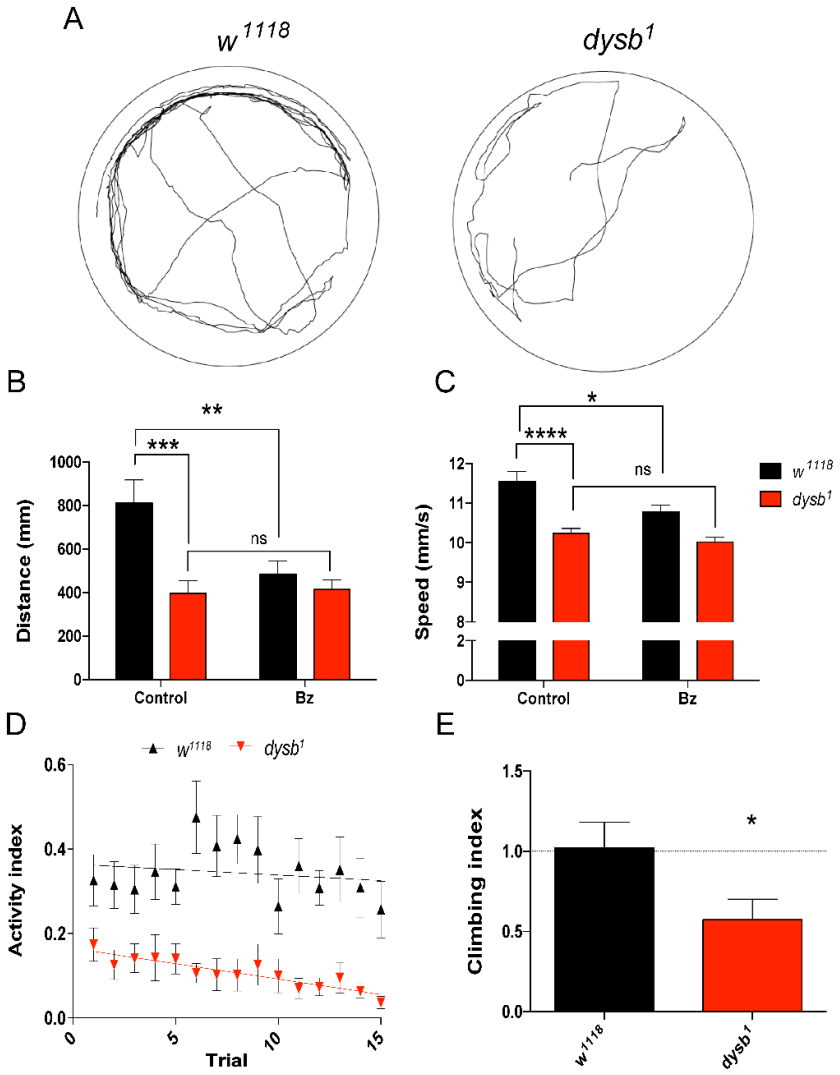

Figure 3.3 Basal and induced-locomotor responses are reduced in *dysb*^{1} mutants. (A) Representative experiments in which tracking was carried out in single *w*^{1118} (left) and *dysb*^{1} (right) flies for three min, to assess basal locomotion. (B) The total distance travelled and the Instantaneous speed (C) were measured before (control) and after benzaldehyde (Bz) exposure. (D) The climbing assay was conducted in 15 consecutive trials to test induced-locomotor activity of flies. Linear regression is represented by solid lines. (E) The change in locomotor activity was quantified and calculated as a climbing index, defined as the ratio between activity in the last 12-15 trials and the first 1-3 trials. A decrement in climbing response is represented as activity values < 1. Data was analysed using two-way ANOVA with Tukey's post hoc test in B or followed by a Sidak's *post hoc* test in D. The unpaired t-test was conducted in E. n(*w*^{1118}) = 23 and n(*dysb*^{1}) = 22 flies in B and C. n(*w*^{1118}) = 9 and n(*dysb*^{1}) = 10 groups of flies, ~40 flies each in D and E.

Startle-induced locomotor responses were assessed by using the climbing assay described in Chapter 2. Briefly, this assay quantifies locomotor activity by assessing the response of the fly to being tapped to the bottom of a tube. This manipulation causes a negative geotaxis response, where the flies climb up the

inside of a tube wall opposite to gravity. The number of flies that got to the top tube in a defined period of time was counted. Afterwards, an activity index is calculated comparing the number of flies that reach the top of the tube over the total number of flies assessed. The same climbing assay is repeated on the same set of flies a number of times (e.g. 15 trials). In the first trials, induced locomotion was not different in *dysb*^{1} mutants compared to controls (Trial 1_{w1118} = 0.326 ± 0.061 vs. Trial 1_{dysb1} = 0.174 ± 0.040, p = 0.4658). However, *dysb*^{1} flies showed reduced performance in latter trials (Trial 15_{w1118} = 0.257 ± 0.067 vs. Trial 15_{dysb1} = 0.037 ± 0.015, p = 0.049, Fig. 3.3D). Comparison of the activity index of flies over 15 consecutive trials showed that the control flies sustain their score over time, while *dysb*^{1} flies decrease their performance (as determined by a linear regression slope which was different from hypothetical zero, F test, w^{1118} p = 0.5055 and *dysb*^{1} p < 0.001). To quantify this decrement, a climbing index was calculated: an index value of 1 indicates that performance in the first and last trials were not different, whereas an index value smaller than 1 indicates a reduction in performance. This analysis revealed a 40% reduction in the startle-induced response of *dysb*^{1} flies compared to control (w^{1118} = 1.02 ± 0.16 vs. *dysb*^{1} = 0.57 ± 0.13, p < 0.05, Fig. 3.3E).

3.3.3 dysb^{1} *mutants exhibit alterations in the serotonergic system*

It has been argued that negative symptoms of schizophrenia are linked to changes in the serotonergic system. I sought to determine if changes in this system (Fig. 3.4A) were observed in *dysb*^{1} mutants. Quantification of serotonin levels by HPLC in *Drosophila* brains showed a reduction in the total brain content of this neurotransmitter in *dysb*^{1} flies compared to control flies (w^{1118} = 61.19 ± 3.57 fmol/brain vs *dysb*^{1} = 40.71 ± 9.54 fmol/brain, p < 0.05, Fig. 3.4B n=4). Interestingly, an increase in the expression of the *dSERT* was also found in *dysb*^{1} mutants compared to control flies (w^{1118} = 0.73 vs *dysb*^{1} = 1.39, p < 0.05, Fig. 3.4C-D). These data support the idea that the *dysb*^{1} mutants have an imbalance in their serotonergic system.

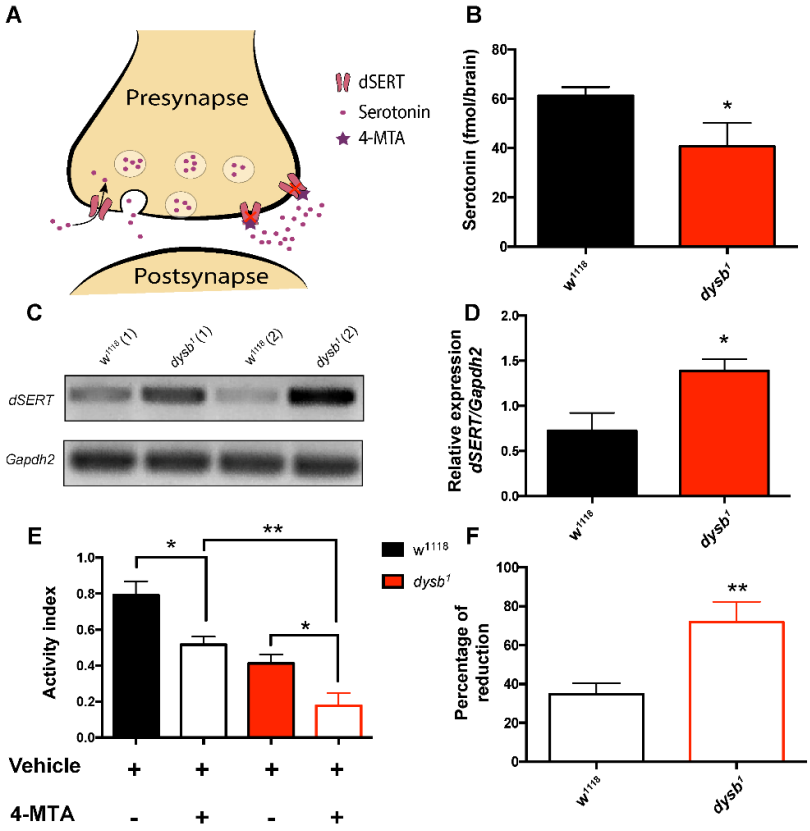

Figure 3.4 Components of the serotonergic system were altered in *dysb*^{1} mutant. (A) Representation of 4-MTA action in the terminals of serotonergic neurons. The *Drosophila serotonin transporter* (dSERT) is localised to the presynaptic terminals of serotonergic neurons, where it mediates the reuptake of serotonin. 4-MTA, an amphetamine-derived releasing agent, binds to the dSERT increasing 5-HT levels in the synaptic cleft. (B) Quantification of brain serotonin by HPLC showed a reduction in levels of the neurotransmitter in *dysb*^{1} compared to control flies. (C) Semi-quantitative RT-PCR showed an increase in *dSERT* expression in *dysb*^{1} heads compared to control flies as seen in two independent samples. (D) Quantification of four independent experiments indicates a two-fold increase. (E) Feeding flies 100 µM 4-MTA, caused a reduction in locomotion in control and mutant flies. (F) While 4-MTA induced a reduction in the activity index in control flies, a bigger reduction in activity was observed in *dysb*^{1} as compared to control flies. Data analysed with an unpaired t-test in B and D and F and two-way ANOVA followed by a Holm-Sidak's *post hoc* test in E. n(w^{1118}) = 5 and n(*dysb*^{1}) = 5 brains in B. n(w^{1118}) = 4 and n(*dysb*^{1}) = 4 samples, 50 heads each in D. n(w^{1118}) = 6 and n(*dysb*^{1}) = 8 groups, ~40 flies each, in E and F.

To further assess changes in serotonergic signalling in *dysb*^{1} mutants, flies were fed 4-MTA, a serotonin releasing drug targeting SERT similar to fluoxetine (used to treat schizophrenia as discussed in Chapter 1) (Spina et al., 1994) and then induced-locomotor responses were measured. 4-MTA reduced the climbing activity index in both *dysb*^{1} and control flies (Vehicle$_{w1118}$ = 0.79 ± 0.08 vs. 4-MTA$_{w1118}$ = 0.52 ± 0.05; Vehicle$_{dysb1}$ = 0.41 ± 0.05 vs. 4-MTA$_{dysb1}$ = 0.18 ± 0.07, $p < 0.0157$ and $p < 0.0286$ respectively, Fig. 3.4E). A two-way ANOVA showed a

genotype ($F_{1,24}$ = 32,29, $p < 0.0001$) and a drug effect ($F_{1,24}$ = 16,30, $p < 0.001$). However, this analysis shows that these factors did not interact to explain the variation observed ($F_{1,24}$ = 0.0932, $p = 0.7628$). The reduction as a percentage of the control condition (vehicle) was compared for each strain with the effect of 4-MTA being greater for *dysb*^{1} than control flies (*w*^{1118} = 34.67 ± 5.718 vs *dysb*^{1}= 71.75 ± 10.56, $p = 0.007$, Fig. 3.4F).

3.4 Discussion

Several animal models of schizophrenia have begun to elucidate the pathophysiology of the disorder (Sigurdsson, 2016), although much remains to be understood, including the missing heritability of this complex disease. In this regard, animal models based on the genetic alterations recently identified by GWAS may provide an important source of new information (Carpenter and Koenig, 2008; Jones et al., 2011). Here, we characterized the *dysbindin* hypomorphic mutant, *dysb*^{1}, the fly ortholog of the *DTNBP1* gene, in which mutations have been associated with increased risk of schizophrenia (Ayalew et al., 2012; Funke et al., 2004). We extended previous behavioural and cellular pathological descriptions of the *dysb*^{1} mutant (Dickman and Davis, 2009; Larimore et al., 2017; Mullin et al., 2015) to include behaviours related to negative symptoms, revealing a contribution of the serotonergic system to mutant pathology.

3.4.1 Social space and olfactory alterations in dysb^{1} *mutant flies*

Altered social interaction has been described in schizophrenia and constitutes a classical negative symptom, which is one of the hallmarks of the disorder. Social interaction defects are also a characteristic observed in animal models of the disease (Jones et al., 2011; Sigurdsson, 2016; Tuathaigh et al., 2013). Previous descriptions of *dysbindin* mutants, both in mice and flies, showed a wide range of alterations in social behaviours. While *sdy* mice showed reduced social contact in an open field paradigm (Feng et al., 2008; Hattori et al., 2008), *dysb*^{1} flies showed defective mating orientation (Shao et al., 2011).

Here, we evaluated the performance of *dysb*^{1} flies in a new paradigm to study social space. The new setup addresses a specific aspect of social interactions observed in humans, namely social space, which relies on the interaction between

a person and his surrounding environment through their personal space (Fernandez et al., 2017; McNeil et al., 2015; Simon et al., 2012; Ueoka et al., 2018). This assay has been previously used to evaluate how dopamine affects social behaviour in flies (Fernandez et al., 2017), how the progeny of older animals exhibit increased asociality (Brenman-Suttner et al., 2018) and to study alterations in social behaviours associated with neurodevelopmental disorders (Kaur et al., 2015; Wise et al., 2015). Using this assay, I show that *dysb*^{1} display altered social space behaviour, consistent with the importance of Dysbindin in pathways that regulate social behaviours in mammals and flies. Specifically, I showed an increased social spacing in *dysb*^{1} flies compared to control flies. Interestingly, my observations are consistent with several behavioural studies in schizophrenia patients including those that show similar defects assessed by stop-distance techniques in natural environments or similar measures performed in virtual reality. For instance, highly enlarged changes in personal space have been reported by people diagnosed with schizophrenia when they report at what distance they start to feel discomfort from another subject approaching (Deuš and Jokiá-Begić, 2006; Di Cosmo et al., 2018; Holt et al., 2015; Park et al., 2009).

Although the neural circuits involved in the modulation of social space distance in mammals and insects remains to be fully elucidated, it has been suggested that social space in invertebrates is highly dependent of the olfactory system. For instance, It was shown that nesting behaviours, similar to the grouping behaviours described here, depends on the ability to recognize other members of a community via olfactory cues in ants (Trible et al., 2017). Moreover, as in other neuropsychiatric and neurodegenerative disorders, olfactory acuity is decreased in schizophrenia (Auster et al., 2014; Nguyen et al., 2010; Robabeh et al., 2015; Rupp, 2010). Thus, we decided to assess whether *dysb*^{1} mutants exhibit olfactory alterations. Our results indicate that *dysb*^{1} mutants exhibit an intrinsic olfactory processing deficit, namely a reduction in aversion to benzaldehyde. Interestingly, it has been reported that dysbindin is important in the modulation of short-term olfactory habituation in flies (Mullin et al., 2015) as well as a similar phenotype in mouse (Petit et al., 2017). Further experiments would be required to assess olfaction and social space phenotypes are linked in the *dysb*^{1}, as they may arise independently. Knocking down *Dysb* in the olfactory circuit could be a suitable next step to test this.

3.4.2 Basal locomotion and induced startle locomotor responses are altered in dysb[1] mutants

Motor impairment is another feature in patients diagnosed with schizophrenia (Hirjak et al., 2018; Manschreck et al., 1982; Wolff and O'Driscoll, 1999). These motor defects are highly correlated with the negative symptoms of the disease and, therefore, have received attention as clinical markers of this disorder (Walther and Strik, 2012).

Interestingly, *DTNBP1* mutations result in motor deficits that have been associated with a higher severity of schizophrenia negative symptoms (DeRosse et al., 2006; Walther and Strik, 2012). Since previous observation in *sdy* mice have shown a significant reduction in locomotion in an open field test (Hattori et al., 2008), I decided to evaluate the basal locomotor activity in a three-cm circular arena, in *dysb[1]* flies. The single-fly tracking analysis showed that the *dysb[1]* mutant displayed decreased speed and distance travelled during the three-minute interval. Strikingly, the mouse and our fly model data are in line with clinical descriptions of motor dysfunction seen in patients with schizophrenia. It has been suggested that the motor phenotype observed in both mice and flies could be partially explained by poor motor coordination which is supported by early studies that have established that there is generalized incoordination in schizophrenics (Abboud et al., 2017; Manschreck et al., 1982, 1981). *Dysbindin* expression and function is prominent in skeletal muscle cells, where it forms part of the dystrophin-associated protein complex (DPC) which is involved in the stabilization of the muscle fibers (Talbot et al., 2004). Therefore, it is possible that the phenotype observed in *dysb[1]* mutants arise from a sum of a muscular and neuronal dysfunction. Further experiments assessing the role of neuronal versus the muscular role of *Dysb* in the phenotypes I observed would be of outstanding interest. For instance, overexpressing the wild-type version of *Dysb* either in all neurons or muscles in a *dysb[1]* fly, and testing if this rescues mutant behaviour to wild type.

Interestingly, while benzaldehyde triggers a reduction in locomotor responses in control flies, it did not have an effect in *dysb[1]* mutants; this suggests an olfactory deficit in the mutant similar to what has been reported in other animal models (Mullin et al., 2015).

To further characterize the role of Dysbindin in stimulated locomotor responses in flies, we conducted a negative geotaxis assay (Ali et al., 2011). We found that

dysb^{1} mutants behave as control flies in initial trails, while they decreased their response to mechanical stimuli in later trails. These findings are intriguing as others have presented conflicting evidence (Mullin et al., 2015; Shao et al., 2011). While Shao et al. reported a near 50% increase in the startle-induced locomotion in the *dysb*^{1} mutants, Mullin et al. were unable to find any locomotor defect at all (Mullin et al., 2015; Shao et al., 2011). Although the underlying causes of such contradictory results are unknown, we believe that the genetic background and/or the genetic dosage of the *dysb*^{1} expression could be differentially contributing to these discrepancies (Mullin et al., 2015).

Nevertheless, our results obtained using both, the negative geotaxis and the single-tracking assays, are consistent on their own, agreeing with a primary locomotor defect found in *dysb*^{1} mutants. Moreover, the reduction over time in the activity index here reported for this flies could be explained by fatigue after repetitive tasks, which it has been observed in other flies models that also exhibited impaired locomotion (Bazzell et al., 2013; Gargano et al., 2005).

3.4.3 Serotonergic dysregulation in schizophrenia

Several studies have described changes in the serotonergic system, involving the serotonin receptors 1A and 2A, serotonin transporter and serotonin levels, which might be important in the pathology of schizophrenia (Li et al., 2019; Takano, 2018).

Analysis of post-mortem brain samples have provided some insights into the involvement of the serotonergic system in this disorder, although with some contradictory and inconsistent results. When direct measurements of serotonin concentrations have been obtained, some reports indicate that the levels are increased in patients with schizophrenia, while others report the opposite (Crow et al., 1979; Farley et al., 1980; Winblad et al., 1979). We find serotonin levels are reduced in the *dysb*^{1} mutants, suggesting impaired serotonergic neurotransmission in these flies. A previous study also suggested a role of neuronal serotonin in adult *Drosophila* locomotion and showed reduced serotonin resulted in a reduction in locomotion (Neckameyer et al., 2007). Therefore, it is possible that the differences observed in *dysb*^{1} locomotion compared to controls arose from reduced levels of brain serotonin.

Also, recent studies have established associations between polymorphisms in genes involved in serotonergic neurotransmission and schizophrenia. One of these genes is *SLC6A4*, which encodes for a plasma membrane serotonin transporter (Dubertret et al., 2005; Fan and Sklar, 2005; Xu et al., 2019). Moreover, early studies in humans suggest that *SERT* mRNA levels and serotonin reuptake are increased in schizophrenia patients (Hernandez and Sokolov, 1997; Joyce et al., 1993). In line with these reports, we observed a two-fold increase in *dSERT* expression in $dysb^{1}$ flies. It is possible that the reduced serotonin levels in the $dysb^{1}$ flies we measured using HPLC, might be explained by compensatory mechanisms that result in the increased *dSERT* expression, allowing more amine reuptake from the extracellular space.

We also show a stronger reduction in locomotion in $dysb^{1}$ flies that were fed the *dSERT* substrate 4-MTA, compared to control flies, an effect likely due to the overexpression of the transporter (Hidalgo et al., 2017). Although the effect of 4-MTA on startle-induced motor responses has not been studied before, one study using fluoxetine, has shown a decreased locomotor response in *Drosophila* larvae (Majeed et al., 2016). Together with our data, this suggests differences in *dSERT* expression could explain the locomotor defects observed in $dysb^{1}$ mutants. Further experiments should be conducted to explore *Dysb* function in serotonergic neurons. Knock-down of *Dysb* in these neurons would help the assessment of the phenotypes that we observed here and whether they are associated with a direct role in these neurons or whether they are affected by some compensatory mechanisms. The later might be addressed by using inducible mutants.

3.5 Conclusions of the chapter

- $dysb^{1}$ flies displayed reduced olfactory performances and impaired social interaction behaviours.
- Basal and induce startle locomotor responses are decreased in $dysb^{1}$.
- Reduced serotonin levels and increased expression of *SERT* are observed in $dysb^{1}$.
- The behavioural phenotypes of $dysb^{1}$ mutant show schizophrenia-relevant pathology allowing further modelling of the role of this gene in this disorder

including screening new serotonergic treatments to reverse the *dysb*^{1} mutant defects.

Given that the *dysb*^{1} showed relevant schizophrenia-related behaviours in the tasks that we used, the next question is whether is possible to observe similar phenotypes in other genes associated with schizophrenia. This is addressed in Chapter 4 and 5.

Chapter 4: Differential contribution of Rim to schizophrenia-related behaviours in *Drosophila*

This chapter describes the results of experiments investigating the effect of genetic manipulation of the *Drosophila* orthologue of *RIM1* gene, *Rim*, on different sets of neurons in *Drosophila*. A brief introduction to *RIM1* association with schizophrenia and role in neurons are illustrated in the initial sections. After that, the results of *Rim*'s contribution to olfactory performance, social behaviour and memory are presented. First, exploring the effects of *Rim* knock-down in behaviours and then the underlying structural and functional changes in the targeted neurons. Additionally, this chapter provides an insight on *Rim* role on circadian locomotion and sleep, with a subsequent section illustrating the underlying mechanisms including neuron plasticity and PDF release. Finally, the discussion of the observations gathered across this chapter and conclusions are presented in the last sections.

4.1 Introduction

4.1.1 The association of RIM with schizophrenia

RIM1 genetic association with schizophrenia is relatively new, when in 2014 it appeared in a large GWAS, in the highly enriched category of calcium signalling genes. (Schizophrenia Working Group of the Psychiatric Genomics Consortium, 2014). However, the peculiarity around this gene is that it was first associated with schizophrenia through behavioural studies, as opposite to genetic association study, four years before this GWAS was published (Blundell et al., 2010).

Blundell et al. (2010), sought to analyse the role of RIM1 on schizophrenia-related behaviours, motivated by the observations of genetics and physiological changes in synaptic proteins on this disorder. The authors showed that a *RIM1*α homozygotic knock-out mouse (*RIM1*$\alpha^{-/-}$), displayed altered schizophrenia-related behaviours, including reduced PPI and enhanced effect of psychotomimetic drugs.

Other behavioural studies have shown RIM1 contribution to other behaviours using the same mutant. For instance, *RIM1*$\alpha^{-/-}$ mutants displayed reduced performance in a fear conditioning memory task, suggesting a critical role of RIM1 in learning and memory. Moreover, social impairments where found in this mutant, as the time spend engaged in social interactions and performing maternal behaviour were shown to be reduced in these animals (Blundell et al., 2010; Schoch et al., 2002). Interestingly, another study has shown that only some of these behavioural features can be observed in conditional *RIM1* knock-out mice, suggesting a specialized role and contribution of RIM in adult neuronal circuits and behaviour (Haws et al., 2012). Finally, a recent study has also shown a contribution of RIM1 to action control and habit formation, through its contribution to corticostriatal neurotransmission, increasing the amount of information about RIM1 function in behaviours (Hidalgo, 2019; Kupferschmidt et al., 2019).

4.1.2 Rab-3 interacting molecules definition and physiological roles

RIMs are a family of scaffolding proteins with function in neurotransmitter release. In vertebrates, RIMs proteins are encoded by four independent genes: *RIM1, RIM2, RIM3* and *RIM4,* that give rise to seven isoforms by alternative splicing, which are RIM1α, RIM1β, RIM2α, RIM2β, RIM2ɣ, RIM3γ and RIM4γ, of which the first two, are the most studied (Kupferschmidt et al., 2019; Wang and Südhof, 2003). Full-length isoforms have a Zn^{2+}-finger domain, PDZ domain and two C_2 domains, specialized protein-protein interaction domains that allow RIMs to interact with several proteins such as Munc-13, SNAP25, Synaptotagmin I, Rab-3 and VGCC (Gandini and Felix, 2012; Kaeser et al., 2011; Kaeser and Südhof, 2005; Tang et al., 2016).

RIMs are expressed in the brain and localize at the highly intricate active zone (AZ), a specialization of the presynaptic membrane composed of dozens of different proteins, contributing to vesicle cycle and neurotransmitter release (Ackermann et al., 2015). It has been shown that RIMs at the AZ contribute to vesicle priming and docking (Deng et al., 2011; Han et al., 2011; Kaeser et al., 2011; Wang and Südhof, 2003). Furthermore RIMs play an important role in clustering VGCC at the AZ, specifically N- and P/Q-types, which mediate fast neurotransmitter release (Graf et al., 2012; Luebke et al., 1993). This function is possible by a direct interaction of RIMs with these Ca^{2+} channels, through the PDZ

domain of RIM, as impaired neurotransmission observed in *RIM1* conditional knock-out mice is only restored when expressing a RIM construct bearing this site (Kaeser et al., 2011). The functional importance of RIM is evident as deleting *RIM* in several synapses impair spontaneous and evoked neurotransmission (Castillo et al., 2002; Han et al., 2011; Kaeser et al., 2011; Kupferschmidt et al., 2019; Schoch et al., 2002).

4.1.3 Characterisation of Rim functions using Drosophila

In *Drosophila*, the RIMs are encoded by a single gene, *Rim* (Graf et al., 2012; Wang and Südhof, 2003). The invertebrate gene is unusually large compare to the mammalian *RIM1* gene (i.e. 11.7 kb of genomic DNA) with the longest splicing variant encoding a protein of approximately 300 kDa (Wang and Südhof, 2003). The general identity and similarity between the human RIM1 and the *Drosophila* Rim is relatively low at 21% and 31% respectively, however, all functional protein-protein interaction domains are highly conserved (Gandini and Felix, 2012; Kaeser and Südhof, 2005; Wang and Südhof, 2003).

The study of Rim in *Drosophila* has focused on its role in synaptic plasticity and neurotransmission, mostly at the highly tractable NMJ. Lack of *Rim* from the developing NMJ spares gross-morphology of the terminals, although subtle differences in the number of AZ are observed (Graf et al., 2012). As described above, positioning of VGCC at the presynaptic terminals is a key role of RIM (Kaeser et al., 2011). In *Drosophila*, Rim was required for the positioning of the main orthologue of the synaptic P/Q- and N-type VGCC in flies, cacophony (cac), in the AZ at the NMJ (Graf et al., 2012). A role in PHP was also shown at the NMJ, with *Rim* mutant flies failing to increase neurotransmitter release after postsynaptic glutamate-receptor blockage (Muller et al., 2012). To our knowledge, there are no studies of Rim function in adult *Drosophila* central nervous system, as oppose to the description in rodents. Moreover, there is no information of Rim contribution to behaviours in flies, even though, *Rim* has appeared in a number of fly screens for instance for courtship conditioning memory and clock neuron gene expression (Jones et al., 2018; Kula-Eversole et al., 2010; Wang et al., 2018).

4.2 Aims

The evidence described above on Rim's function in neurotransmitter release and VGCC function, suggests that it may be important in regulating behaviour, especially those affected in schizophrenia. Hence, I explored the structural and functional effects of manipulating *Rim* expression in neurons that regulate olfaction, memory and circadian rhythms in order to assess some of the schizophrenia-related behaviours highlighted in Chapter 1.

4.3 Results

4.3.1 Knock-down of Rim in the antennal lobe projection neurons, but not in the mushroom bodies, affected olfaction

To start Rim characterization, a previously described *Rim* null mutant, Rim^{Ex98}/Df (Graf et al., 2012), was used to see if lack of *Rim* had any effect on olfactory behaviour.

Control flies actively avoided the Bz side of the arena as exemplified by the averaged heat map plot of positioning (Fig. 4.1A, left panel). Rim^{Ex98}/Df flies showed slightly less reactivity to the odorant (Fig. 4.1A, right panel). Quantification of the effect showed a reduction in the OI in this mutant ($t = 2.654$, $p < 0.05$, Fig. 4.1B). A transposon insertion in the *Rim* gene (*Mi{MIC}* insertion; $Rim^{MI03407}$) also caused a reduction in olfaction ($t = 2.481$, $p < 0.05$, Fig. 4.1C). The effect observed is similar to that seen for the *Rim* null. Flies expressing a *RNAi* against *Rim* in the AL-PNs (*GH146 > Rim-RNAi (II)*) displayed around 70% reduction in the OI compared to controls ($F_{2, 57} = 3.399$, $p < 0.05$, Fig. 4.1D). Moreover, results were confirmed using a different *RNAi* line against *Rim*, further agreeing with this notion (*GH146 > Rim-RNAi (III)*, $F_{2, 58} = 11.75$, $p < 0.0001$, Fig. 4.1E). In sharp contrast, knocking-down *Rim* in the MBs did not influence the olfactory performance of flies with neither of the two RNAi lines tested (*c309 > Rim-RNAi (II)*, $q = 1.004$, $p > 0.05$; *c309 > Rim-RNAi (III)*, $q = 2.232$, $p > 0.05$).

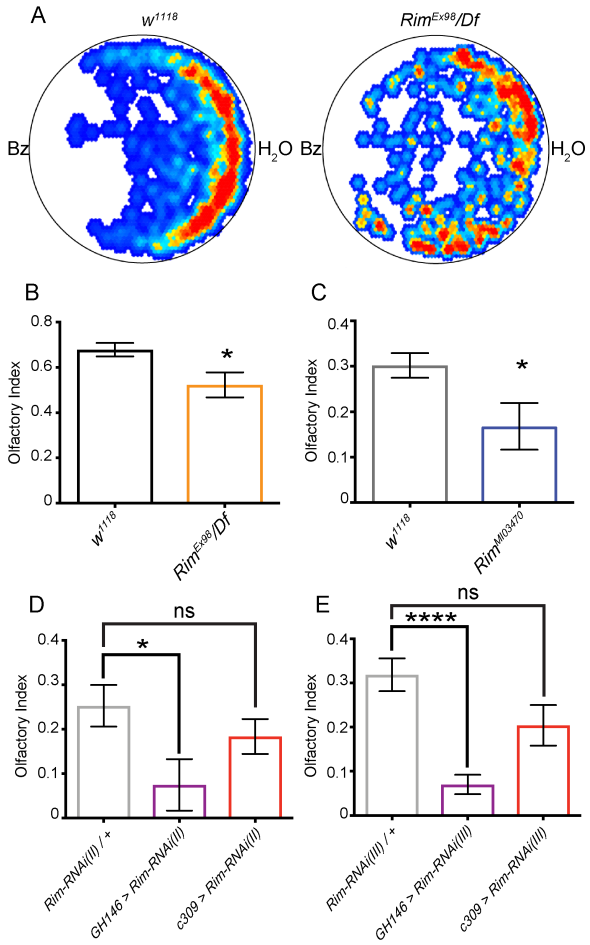

Figure 4.1 *Rim* mutants displayed impaired olfaction. Averaged heat-maps showing the position of control (A, left plot) and Rim^{Ex98}/Df mutant (A, right plot) flies upon benzaldehyde (Bz) exposure are shown. (B) A reduction in the olfactory index was observed in the mutants (orange open bar) compared to control flies (black open bar) (Unpaired t-test). (C) $Rim^{MI03470}$ flies also showed reduced olfactory index compared to control flies (Unpaired t-test). (D) Targeted knock down of *Rim* in antennal lobe (GH146; purple bars) but not mushroom body (c309; red bars) neurons caused a reduced olfaction compared to the control (grey bars). (E) Similar results were observed using an independent RNAi transgene to *Rim* (one-way ANOVA with Dunnett's *post-hoc* test). Data is presented as mean ± SEM (henceforward in all figures), n (w^{1118}) = 12 and n (Rim^{Ex98}/Df) = 10, n (w^{1118}) = 34 and n ($Rim^{MI03470}$) = 13, n (*Rim-RNAi (II) / +*) = 20, n (*Rim-RNAi (III) / +*) = 21, n (*GH146 > Rim-RNAi (II)*) = 20, n (*GH146 > Rim-RNAi (III)*) = 20, n (*c309 > Rim-RNAi (II)*) = 20, n (*c309 > Rim-RNAi (III)*) = 20 flies.

4.3.2 Rim expression in the antennal lobe projection neurons, but not in the mushroom bodies, was important for social space behaviour

Altered social behaviour has been described as a symptom of schizophrenia patients (Kohler et al., 2001; Moberg and Turetsky, 2003; Robabeh et al., 2015; Rupp, 2010). As the olfactory system has been shown to be a key component in social outcomes in different organisms, I decided to test if flies that displayed

impaired olfaction are also deficient in social behaviours. Social space in *Drosophila*, was used as a proxy to model a role of schizophrenia-associated gene in personal space in humans, also affected in schizophrenia (Park et al., 2009). While control animals formed groups within the arena, $Rim^{MI03407}$ flies failed to do so (Fig. 4.2A). This is translated in an increased distance of each fly to its closest neighbour ($U = 21418$, $p < 0.0001$, Fig. 4.2B). Knocking-down *Rim* in the AL PNs yielded to a similar defect in clustering behaviours as $Rim^{MI03407}$ (Fig. 4.2C), confirming the importance of the olfactory system and the role of Rim in social behaviour. A 1.9-fold increase in social distance was observed in *GH146 > Rim-RNAi* (II) flies compared to control ($H = 7.929$, $p < 0.05$, Fig. 4.2D). The effect was similar to that observed in Rim^{MI0340} and reproducible with another RNAi line ($H = 12.99$, $p < 0.01$, Fig. 4.2E). Consistent with our olfactory data, knocking-down *Rim* in the MBs did not have an effect on the distance to the closest neighbour compared to control flies (*c309 > Rim-RNAi (II)*, $Z = 0.5387$, $p > 0.05$; *c309 > Rim-RNAi (III)*, $Z = 0.8442$, $p > 0.05$).

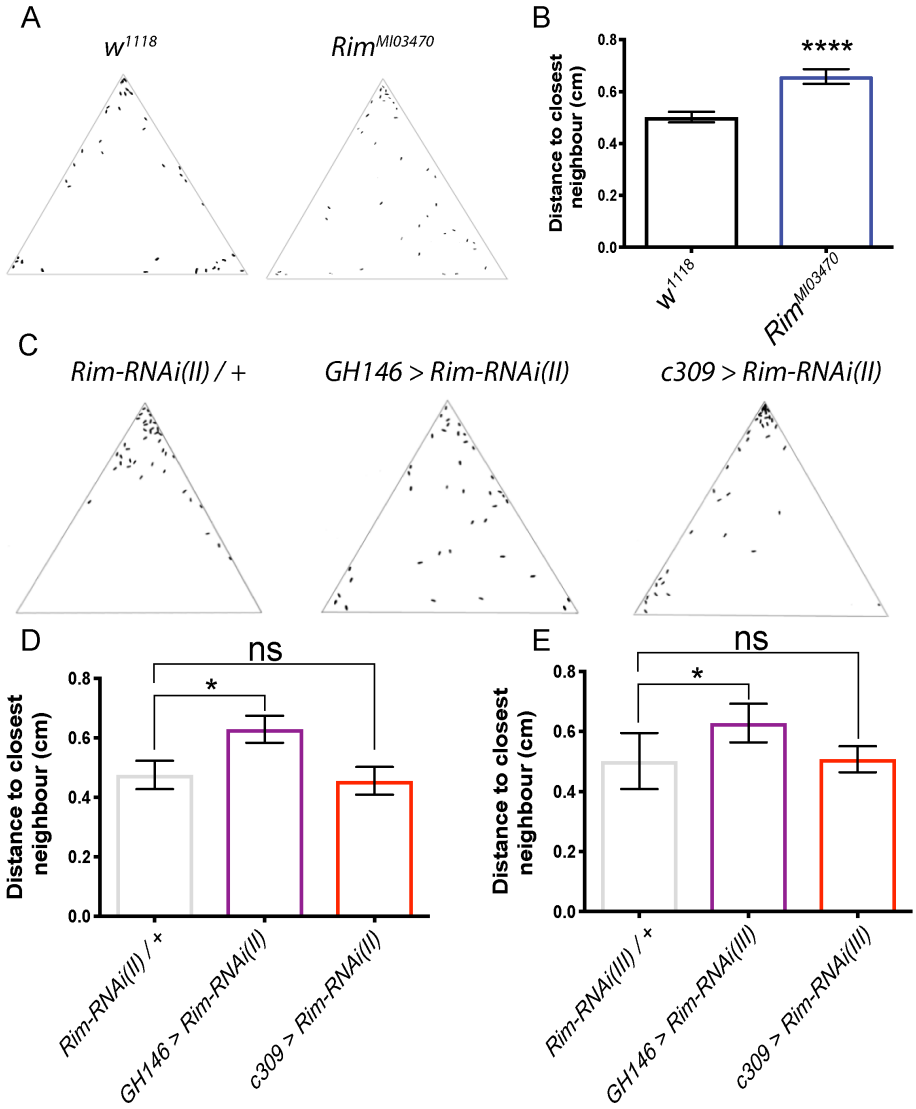

Figure 4.2 *Rim* expression in the antennal lobe is involved in social space behaviour. (A) Representative results for control (left) and $Rim^{MI03470}$ flies (right) are shown. (B) Quantification of the social distance in $Rim^{MI03470}$ mutants (blue open bar) and control flies (black open bar). (C) Representative results are shown for control flies (left) and for antennal lobe (*GH146*, middle) or mushroom body (*c309*, right) neuron specific knock-down of *Rim*, this revealed only a change in social clustering in *GH146 > Rim-RNAi* flies. Quantification of the distance to closest neighbour are shown in for two RNAi lines against *Rim* (D) and (E). (A) and by a Kruskal-Wallis test followed by Dunn's Multiple comparisons test. N = 5 repetitions in each condition with 34-40 flies for each.

As differences observed might arise from locomotor defects or changes in centrophobism, I recorded the flies' behaviour, to address total locomotion during three minutes and centrophobism. No differences were found upon knock-down of *Rim* in the antennal lobe or mushroom body, suggesting that the differences observed arise from social impairments (Fig. 4.3).

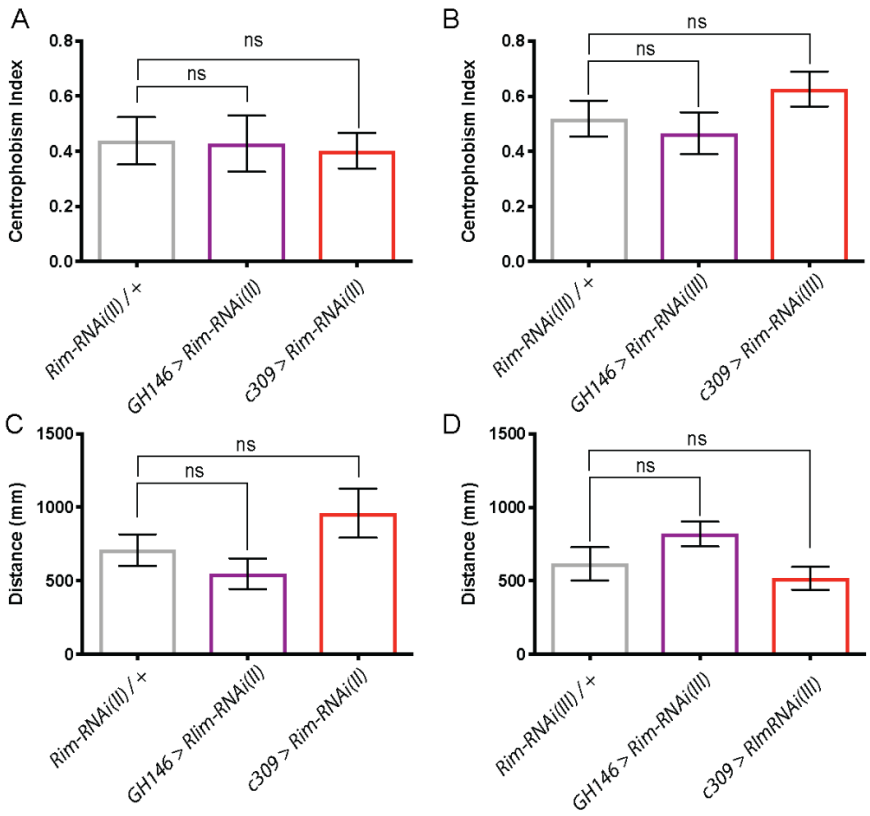

Figure 4.3 Reduced *Rim* expression in antennal lobe or mushroom body does not alter centrophobism or motor performance. The fly's behaviour was recorded for a 3-minute period and a centrophobism index and the total distance travelled were assessed. (A) Centrophobism was unchanged in *GH146 > Rim-RNAi (II)* (open purple bars) and in *c309 > Rim-RNAi* (III) (open red bars), compared to control flies (open grey bars). The same findings were replicated when using a second RNAi line (B). (C) Total distance travelled during the 3 min recording also appeared unchanged in GH146 > *Rim*-RNAi (II) (open purple bars) and in c309 > *Rim*-RNAi (III) (open red bars), compared to control flies (open grey bars). Again, similar results were obtained using the *Rim*-RNAi (III) line (D). Data were analysed using one-way ANOVA with Dunn's *post hoc* test. n (*Rim-RNAi (II) /* +) = 20, n (*Rim*-RNAi (III) / +) = 21, n (GH146 > *Rim-RNAi (II)*) = 20, n (GH146 > *Rim*-RNAi (III)) = 20, n (*c309 > Rim-RNAi (II)*) = 20, n (*c309 > Rim-RNAi (III))* = 20 flies.

4.3.3 Loss of Rim altered the structure and function of the antennal lobe projection neuron terminals on to the lateral horn

Given the effect of *Rim* knock-down in the AL PNs on olfaction and social behaviour, I sought to determine if these were accompanied by changes in structure or function of these neurons. Expression of enhanced green fluorescent protein (eGFP) in the AL PNs visualised their somas, projections and terminals. The majority of the AL PNs send projections to the MB (Fig. 4.4, dark pink arrowhead) and LH (Fig. 4.4, light blue arrowhead) through the inner antenno-cerebral tract (iACT, Fig. 4.4, dark pink arrow), while others project directly to the

LH through the median antenno-cerebral tract (mACT, Fig. 4.4, light blue arrowhead).

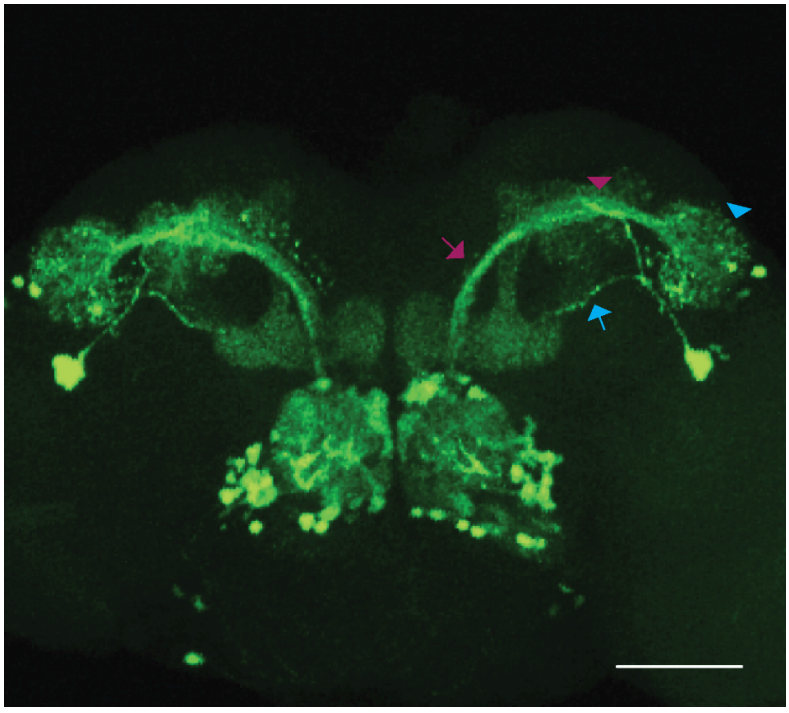

Figure 4.4 The expression pattern of the GH146-GAL4 driver. Enhanced green fluorescent protein (eGFP) was expressed in the antennal lobe projection neurons (AL PNs) using the GH146-GAL4 driver. AL PNs send projections to the mushroom bodies (dark pink arrowhead) and lateral horn (light blue arrowhead), through the inner antenno-cerebral tract (iACT, dark pink arrow) as well as directly to the lateral horn through the median antenno-cerebral tract (mACT, light blue arrowhead). Scale bar is 50 μm.

It was possible to observe intact iACT and mACT pathways in controls and in knock-down animals and no gross-morphology changes were found (Fig. 4.5).

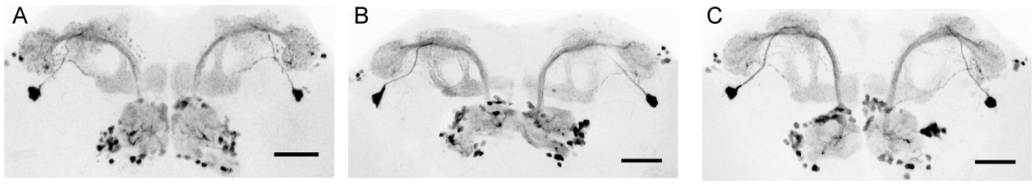

Figure 4.5 *Rim* knock-down did not appear to cause gross-morphological changes in the antennal lobe projection neurons. Representative images of GFP expression in the antennal lobe projection neurons of (A) control (*GH146, eGFP /* +), (B) *GH146, eGFP > Rim-RNAi (II)* (C) *GH146, eGFP > Rim-RNAi (III)* showed no apparent gross morphological difference. Scale bar is 50 μm.

Similar antennal lobe diameter ($F_{2, 33}$ = 0.9314, p = 0.40, Fig. 4.6A) and equal numbers of labelled cells were observed (U = 21, p = 0.73, Fig. 4.6B). Nonetheless, close inspection of the presynaptic terminals reaching the LH (Fig. 4.6C) uncovered an approximate 50% reduction in the area covered by these AL PNs terminals in *Rim* knock-downs compared to control flies ($F_{2, 21}$ = 50.03, p < 0.0001, Fig. 4.6D). Given the role of Rim in positioning VGCC at the presynaptic terminals (Kaeser et al., 2011), I sought to analyse the effect of *Rim* knock-down in evoked calcium responses in the area of the AL PNs terminals reaching the LH.

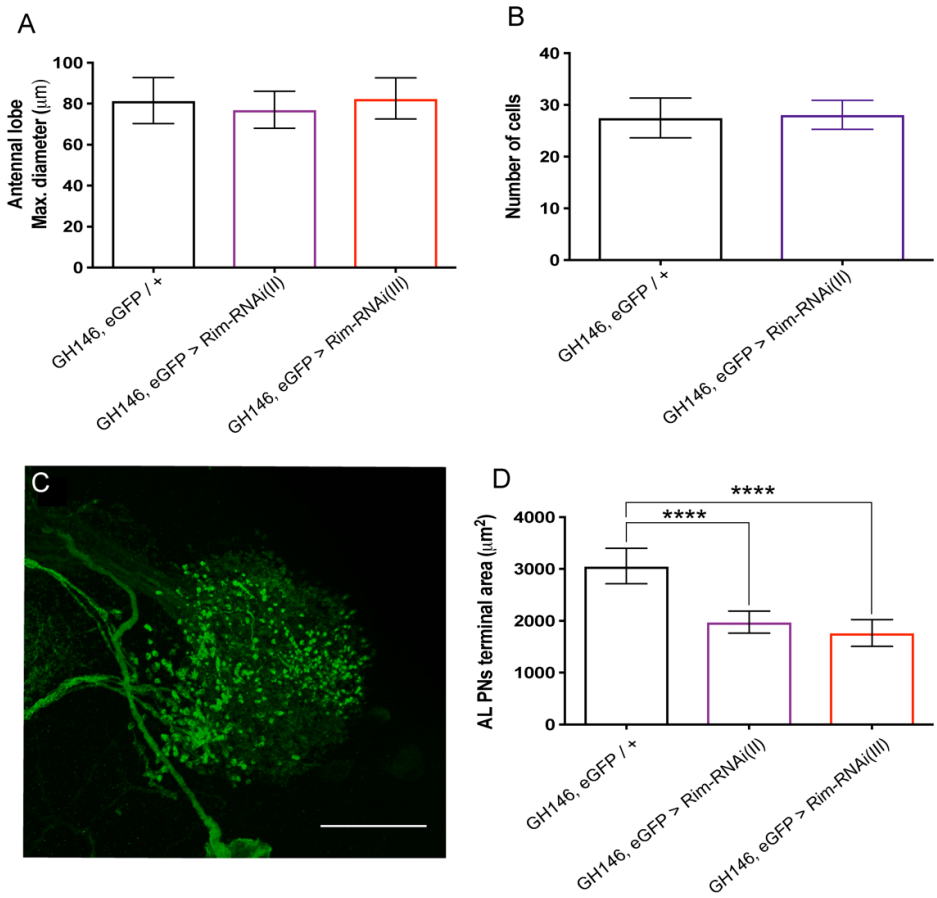

Figure 4.6 *Rim* knock-down altered the antennal lobe projection neuron terminals on to the lateral horn. (A) Knocking down *Rim* in the projection neurons did not affect the antennal lobe structure as maximum diameter remained unchanged compare to control flies. (B) The total number of eGFP positive neurons labelled with the GH146 driver was quantified per lobe. No differences were found when comparing GH146, eGFP / + control flies (black open bar) compared to GH146, eGFP > *Rim*-RNAi (II) (purple open bar) (Mann-Whitney test). n (GH146, eGFP / +) = 6 and n (GH146, eGFP > *Rim*-RNAi (II)) = 8 brains each. (C) A representative confocal image of the terminals reaching the lateral horn from AL-PN labelled by *GH146, eGFP*. Scale bar 20 μm. (D) AL-PN *Rim* knock-down caused a reduction in the area covered by these terminals to about half that of controls. Data were analysed with one-way ANOVA with a Dunnett's post hoc test. n (GH146, eGFP / +) = 16, n (GH146, eGFP > *Rim*-RNAi (II)) = 14 and n (GH146, eGFP > *Rim*-RNAi (III)) = 6 brain hemispheres.

The genetically-encoded calcium sensor, GCaMP6f, was expressed in the AL PNs and the calcium transients evoked by high [KCl] were assessed at these terminals (Fig. 4.7A-B). Bath application of KCl evoked a robust increase in the normalized fluorescence, that decayed once KCl was washed out (Fig. 4.7C). In response to this depolarizing activation treatment, a small but significant decrease in the amplitude of the peak signal was found to result from *Rim* knock-down ($U = 6.5$, $p < 0.05$, Fig. 4.7D).

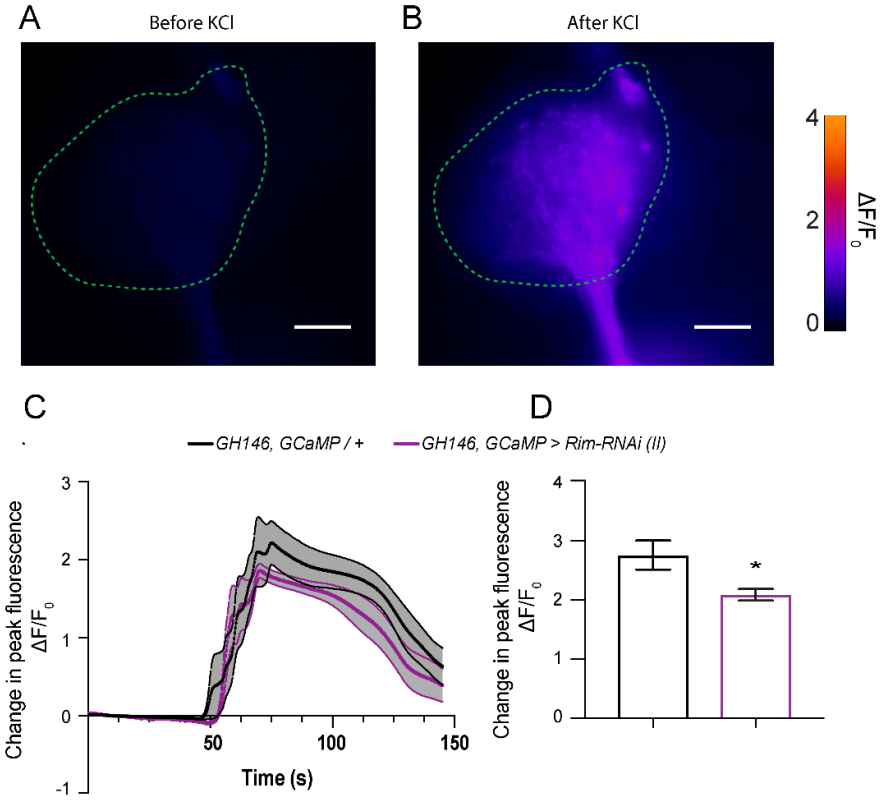

Figure 4.7 *Rim* knock-down reduced evoked calcium transients of antennal lobe projection neuron terminals. The genetically encoded calcium sensor, GCaMP6f, was expressed in the antennal lobe projection neurons and its fluorescence was measured. (A) Basal fluorescence was low under basal conditions, (B) while addition of depolarizing high concentration of potassium chloride (KCl) cause an increase in calcium evoked fluorescence. Calibration bar showing the changes in fluorescence can be observed to the right. Scale bar 10 μm. (C) Transients were observed in controls and a reduction was seen in *Rim* knock-down flies both responses eventually returned to baseline after KCl was washed out (mean fluorescence as solid lines ± SEM in grey) (D) A reduction in the amplitude of the peak fluorescence was found upon *Rim* knock-down (Mann Whitney test. n (*GH146; GCaMP /* +) = 7 and n (*GH146; GCaMP* > *Rim-RNAi (II)*) = 8 brains.

4.3.4 Rim expression in the mushroom bodies was dispensable for memory performance

Another well described symptom of schizophrenia are the cognitive and memory impairments observed frequently in patients (Kahn et al., 2015). Moreover, RIM function in learning and memory was demonstrated in the *RIM* knock-out mouse (Powell et al., 2004; Takano, 2018; Topolov and Getova, 2016). Because of this, I decided to further investigate the role of this protein in this process in *Drosophila*, assessing its contribution in the MBs.

To check the localization and distribution of Rim in the MBs, I expressed a GFP-tagged version of Rim to assess its distribution within this structure (*c309* > *Rim:GFP*). Rim:GFP was widely distributed in the MB neurons including the lobes which consist of axons and presynaptic terminals of the MBs' neurons (Fig. 4.8A). To test for a role of Rim in MB mediated memory I used aversive olfactory conditioning and assessed STM at 2 min and ITM at 1 h (Malik et al., 2013; Malik and Hodge, 2014). No effect was seen in STM ($F_{4, 27}$ = 1.382, p = 0.27, Fig. 4.8B) or ITM ($F_{4, 23}$ = 1.492, p = 0.24, Fig. 4.8C) as *c309* > *Rim-RNAi* flies displayed normal memory, compared to control flies. To further confirm this result, I used a second MB GAL4 line and saw a similar result (STM: $F_{4, 18}$ = 2.725, p = 0.06, ITM: H = 2.035, p = 0.36, Fig. 4.8D-E).

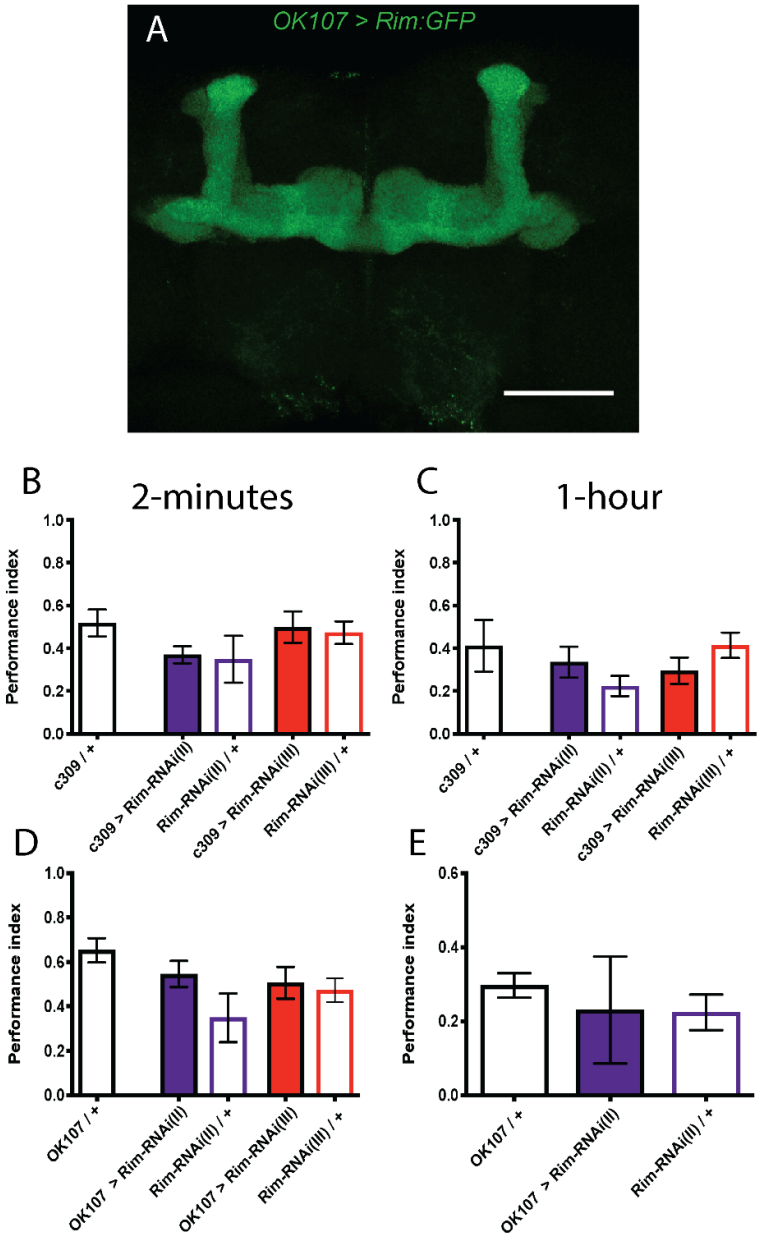

Figure 4.8 *Rim* knockdown in the mushroom bodies did not affect aversive olfactory learning and memory. (A) Expression of a Rim:GFP fusion construct throughout the mushroom body using *OK107-GAL4* showed localisation in the lobes that include axons and presynaptic terminals of these neurons. Scale bar is 50 μm. Olfactory aversive conditioning was used to test memory in flies with reduced *Rim* expression in the mushroom body which had no effect on 2-minutes memory (short-term memory; B) or 1-hour memory (middle-term memory; C) using the *c309-GAL4* driver (One-way ANOVA with Sidak's *post hoc* test). Similar results were yielded with the driver OK107-GAL4 in STM (D) and ITM (E) (Kruskal-Wallis test with Dunn's *post hoc* test. n > 4 repetitions (each n consisted of ~100 flies) for each genotype and condition.

4.3.5 Rim manipulations differentially impacted locomotor activity and sleep under light-dark cycles

Sleep and circadian rhythms disruption are observed in schizophrenia, with abnormal sleep patterns (Chan et al., 2017; Waters and Manoach, 2012), arrhythmic behaviours (Wulff et al., 2012; Yates, 2016) and circadian misalignment (Wulff et al., 2012). *Drosophila* has been proved as a useful model to study circadian rhythms and sleep (Chapter 1). In order to assess the role of *Rim* in sleep I monitored locomotor activity using the DAM system. Sleep was analysed by measuring locomotor activity of flies during 2 days of LD cycles, where inactivation periods larger than five minutes are considered sleep episodes (Donelson et al., 2012; Dubowy and Sehgal, 2017).

Under these conditions, Rim^{Ex98}/Df flies exhibited a strong reduction in the total locomotor activity (i.e. activity during the 24 h period) compared to control flies (Fig. 4.9A), that was caused by a reduction in activity during the night (Fig. 4.9B). Total sleep time was increased in Rim^{Ex98}/Df mutants compared to control animals (Fig. 4.9C) due to increased night sleep (Fig. 4.9D).

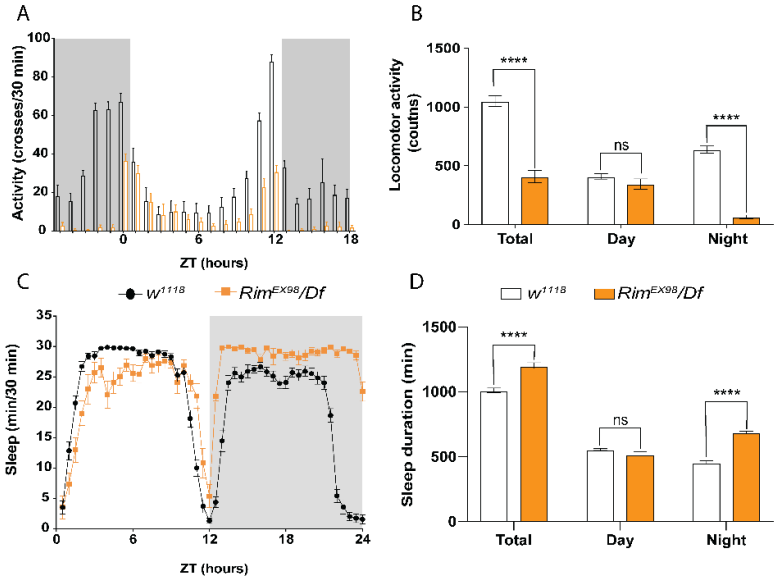

Figure 4.9 Rim^{Ex98}/Df mutants displayed reduced night locomotion and increased sleep. (A) Average of activity across 2 day of LD revealed Rim^{Ex98}/Df mutants were less active than control flies at night. (B) The total activity of the flies across 24hrs was reduced in Rim^{Ex98}/Df and this was due to reduction in night-time activity (Two-way ANOVA with Sidak's *post hoc* test). (C) Sleep profile showed impaired sleeping patterns in Rim^{Ex98}/Df (yellow line) compared to controls (black line). (D) Total sleep time was increased due to an increase in the night sleep (Two-way ANOVA with Sidak's *post hoc* test). n (w^{1118}) = 29, n (Rim^{Ex98}/Df) = 10 flies.

Sleep has circadian and homeostatic components. To determine the contribution of the clock to sleep, *Rim* was knocked down throughout the clock using *Tim-Gal4* as well as just in the PDF-expressing LNvs using the *PDF-GAL4* driver (Guo et al., 2014; Nitabach et al., 2002). Experiments yielded to inconsistent results in both, locomotor activity (Fig. 4.10) and sleep (Fig. 4.11). Total activity was reduced in the *Tim > Rim-RNAi (II)* compared to *Tim / +* control flies but no such difference was found when comparing with the *Rim-RNAi (II) / +* control flies, while activity in *Tim > Rim-RNAi (III)* flies was unchanged (Fig. 4.10B). *PDF > Rim-RNAi (II)* flies showed reduced total locomotor activity only when comparing to *Rim-RNAi (II) / +*. Again, no differences were found using the second RNAi line (*PDF > Rim-RNAi (III)*) (Fig. 4.10D).

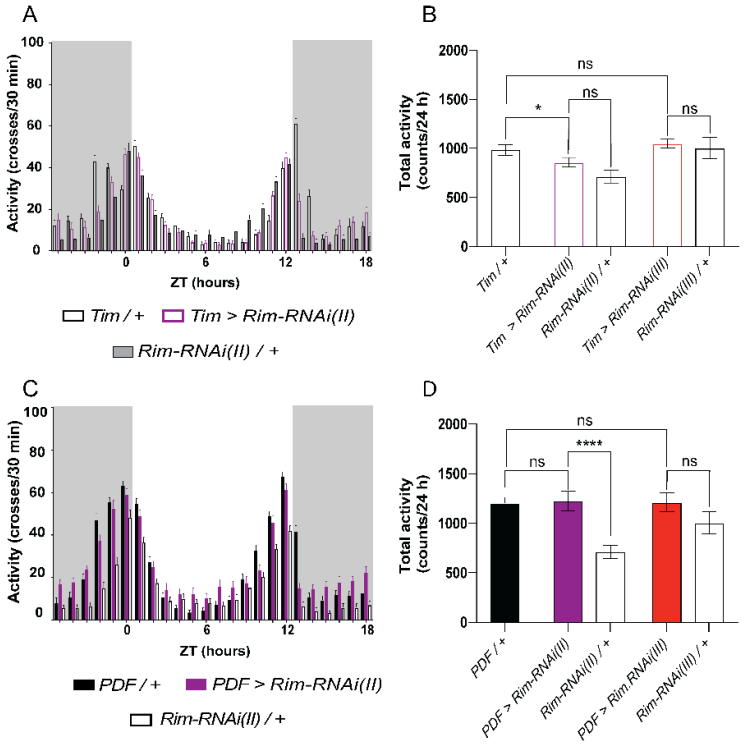

Figure 4.10 Contribution of *Rim* knock-down in the clock network to locomotor activity under light-dark conditions. Average activity profiles show *Tim* > *Rim*-RNAi activity under LD (A; purple open bars) (B) Comparison of total activity levels between different genotypes of flies. (C) The average distribution of activity across the day and night in *PDF > Rim-RNAi (II)* is shown with the respective comparison between genotypes shown in (D) Data in B and D were analysed with Kruskal-Wallis test with Dunn's *post hoc* test. n (*Tim / +)* = 95 , n (Tim > *Rim-RNAi(II))* = 92, n (*Tim > Rim-RNAi(III))* = 114, n (*PDF / +)* = 61, n (*PDF > Rim-RNAi(II))* = 94, n (*PDF > Rim-RNAi(III))* = 63, n (*Rim-RNAi(II) / +)* = 32 and n (*Rim-RNAi(II) / +)* = 29 flies.

Additionally, total sleep was increased in *Tim* > *Rim-RNAi* compared to *Tim* / + flies but no with Rim-RNAi flies in both RNAi lines tested (Fig. 4.11A, lower panel). While, the only difference found in total sleep using the PDF-GAL4 driver was found between the PDF / + and *PDF* > *Rim-RNAi* (II) (Fig. 4.11B, lower panel).

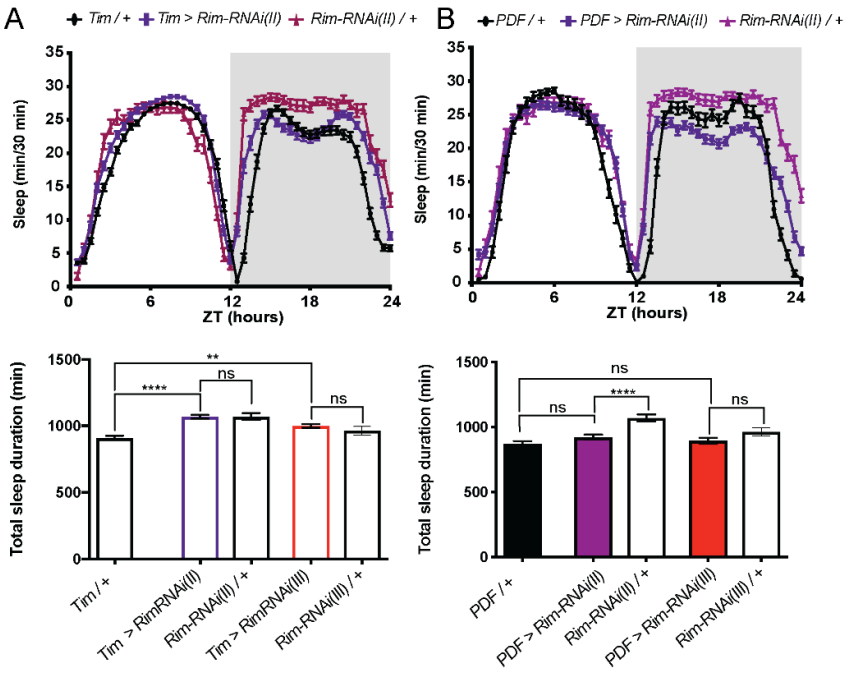

Figure 4.11 Effect of *Rim* knock-down in sleep. Averaged sleep profiles of *Tim* > *Rim-RNAi* flies (A, upper panel) and *PDF* > *Rim-RNAi* flies (B, upper panel) are shown. (A, lower panel) Multiple comparison showed *Tim* > *Rim-RNAi* total sleep was increased compared to GAL4 flies (*Tim* / +) but no such differences were observed when comparing to UAS control flies (*Rim-RNAi* / +). (B, lower panel) Total sleep duration is decreased in *PDF* > *Rim-RNAi (II)* compared to *Rim-RNAi (II)* / + but no difference was found when comparing to *PDF* / +. n (*Tim* / +) = 95 , n (*Tim* > *Rim-RNAi(II))* = 92, n (*Tim* > *Rim-RNAi(III))* = 114, n (*PDF* / +) = 61, n (*PDF* > *Rim-RNAi(II))* = 94, n (*PDF* > *Rim-RNAi(III))* = 63, n (*Rim-RNAi(II)* / +) = 32 and n (*Rim-RNAi(II)* / +) = 29 flies.

4.3.6 Rim is required in the LNvs to maintain circadian locomotor activity under constant darkness

In order to determine role of Rim in circadian rhythms, locomotor activity was measured in DD. As opposed to control flies whose behaviour appeared rhythmic under constant conditions (Fig. 4.12A), Rim^{Ex98}/*Df* flies appeared less rhythmic in DD (Fig. 4.12B). Similar arrhythmic behaviour appeared in *Tim* > *Rim-RNAi* (Fig. 4.12D-E) and *PDF* > *Rim-RNAi* (Fig. 4.12G-H) flies compared to their respective controls.

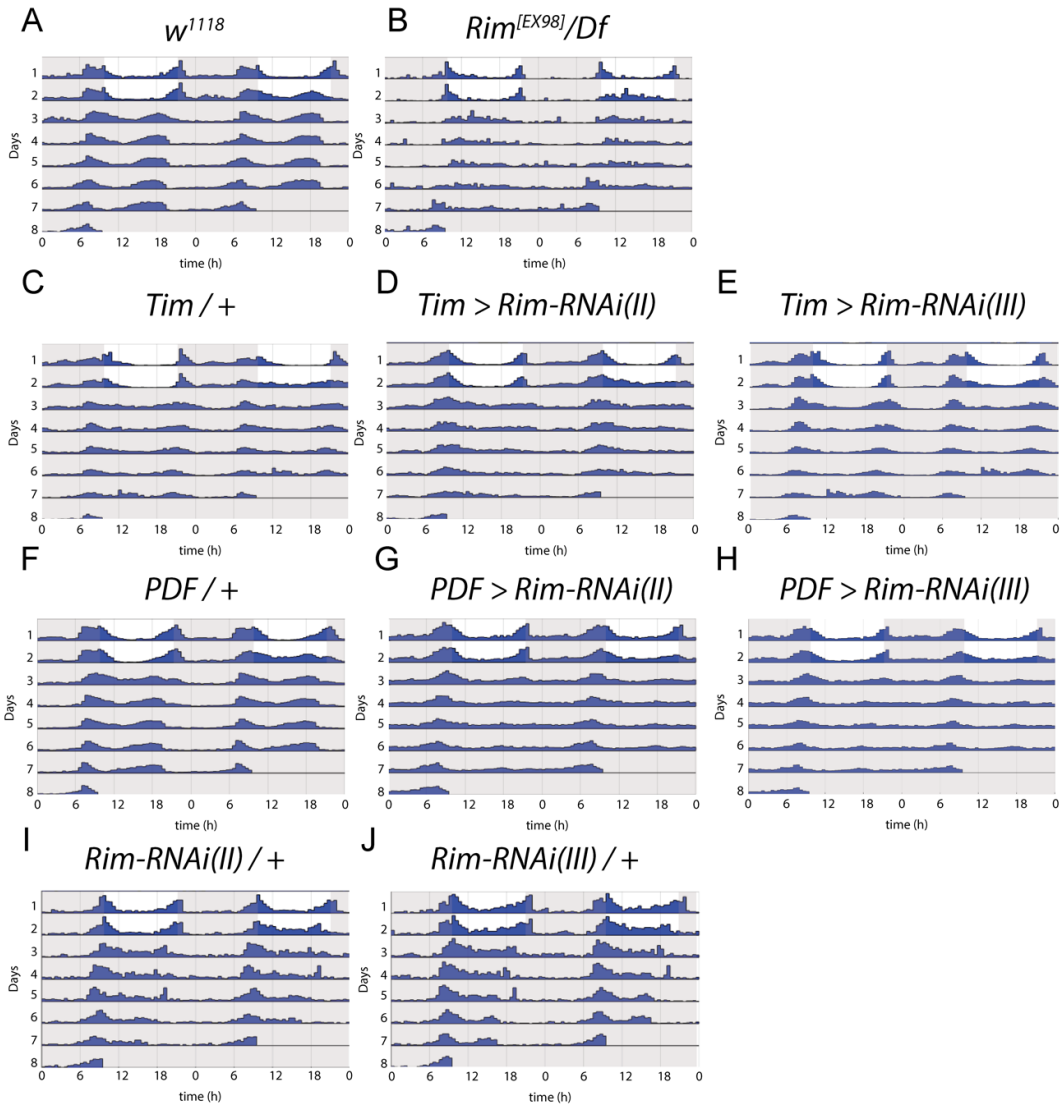

Figure 4.12 *Rim* knock-down in the clock affected rhythmic behaviour under constant darkness. Averaged double-plotted actograms of single flies of the following genotypes: (A) w^{1118}, (B) Rim^{Ex98}/Df, (C)*Tim* / +, (D) *Tim* > *Rim-RNAi* (II), (E) *Tim* > *Rim-RNAi (III)*, (F) *PDF* / +, (G) *PDF* > *Rim-RNAi (II)* , (H) *PDF* > *Rim-RNAi (III)* (I) *Rim-RNAi (II) /* + and (J) *Rim-RNAi (III) /* + for 2 days in LD (alternated white and grey) followed by 5 days in DD. The activity patterns of Rim^{Ex98}/Df, *Tim* > *Rim-RNAi* and *PDF* > *Rim-RNAi* flies appeared less rhythmic under DD than controls.

Autocorrelation analysis revealed a reduction in RS, which is a metric of strength of the circadian rhythm, which was 3-times less in Rim^{Ex98}/Df mutants than control flies (Fig. 4.13A). Flies are normally considered to be rhythmic if they have a RS greater than 1.5 (Buhl et al., 2019; Hodge and Stanewsky, 2008; Julienne et al., 2017). By using this measure, 100% of control flies showed the expected wildtype

rhythmic behaviour. In contrast only 58% percent of *Rim^{Ex98}/Df* mutant were rhythmic (Table 4.1).

Table 4.1 Circadian behaviour of *Rim* flies in constant darkness (DD).

genotype	RS	% rhythmic	period (h)	n
w^{1118}	3.68 ± 0.09	100	23.53 ± 0.03	29
Rim^{Ex98}/Df	1.29 ± 0.12	42	23.25 ± 0.14	12
Tim / +	2.45 ± 0.09	85	24.04 ± 0.05	82
Tim >Rim-RNAi (II)	1.93 ± 0.10	54	23.82 ± 0.07	22
Tim >Rim-RNAi (III)	2.07± 0.10	57	23.69 ± 0.04	32
PDF / +	3.14 ± 0.11	100	23.71 ± 0.03	61
PDF > Rim-RNAi (II)	1.99 ± 0.11	66	23.62 ± 0.06	94
PDF > Rim-RNAi (III)	1.71 ± 0.13	51	23.29 ± 0.05	63
Rim-RNAi (II) / +	2.76 ± 0.14	90	23.62 ± 0.06	32
Rim-RNAi (III) / +	2.78 ± 0.11	100	23.52 ± 0.08	29

This table is related to Figure 4.12 - 4.13. Data are mean ± SEM.

This change was accompanied by a modest reduction in the period length in rhythmic flies, further supporting a circadian defect in this mutant (Fig. 4.13B). A similar reduction in the RS was shown in *Tim > Rim-RNAi* (54% and 57% for the respective knock-down genotypes) compared to controls (100%, 90% and 85%) (Fig. 4.13C) (Table 4.1). There appeared to be a reduction in the period length in *Tim > Rim-RNAi* compared to *Tim /* + control, but not to the UAS / + controls (Fig. 4.13D). These conflicting results may arise from the fact that changes in circadian behaviours are highly dependent on the genetic background of the animal tested (i.e. the original flies from which the transgenic flies were made) or by opposite roles of different neurons in the control of periodicity, as it has been shown (Rieger et al., 2012; Schlichting et al., 2019; Yao and Shafer, 2014; Zimmerman et al., 2012). In order to try to clarify the potential inconsistency between genotypes as well as to map the *Rim* circadian phenotypes to more restricted number of neurons in the clock circuit*, Rim-RNAi* was just expressed in the pacemaker LNvs. Again, consistent with the *Rim^{Ex98}/Df* and *Tim > Rim-RNAi* arrhythmic behaviour, *Rim* knock-down in just the LNvs reduced rhythm strength (Fig. 4.13E), with only 66% and 51% of the *PDF > Rim-RNAi* flies being rhythmic compared to a 100% and 90% for controls (Table 4.1). Moreover, comparison of the period of the rhythmic

flies in each group again unveiled a reduction in period length in *PDF > Rim-RNAi* flies (Fig. 4.13F).

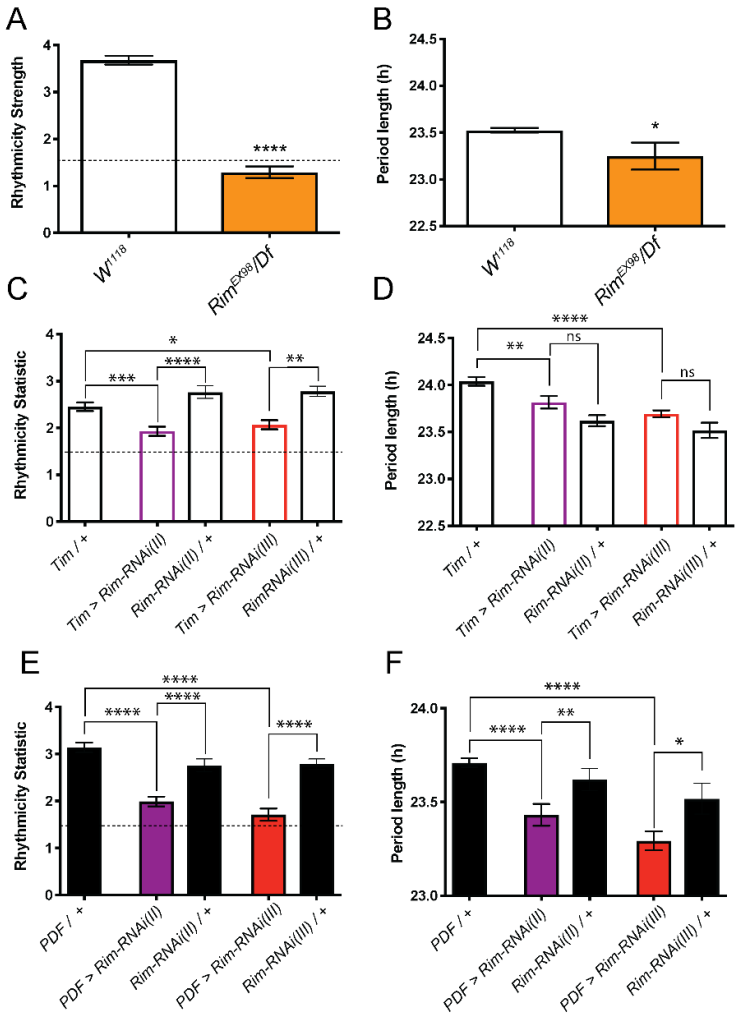

Figure 4.13 *Rim* knock-down in the clock network reduced rhythmicity and shortened period length under constant darkness. The Rhythmicity Statistic was used as a measure of rhythm strength after 5 days of DD, which was when period length of the circadian rhythm was also measured. Rim^{Ex98}/Df mutants showed a reduction in RS (A, orange bar) and shorter period (B, orange bar) compared to control flies (open black bars). (C) In order to localize this phenotype, *Rim* was knocked down throughout the clock again leading to a significant reduction in rhythm strength and (D) shortening of period compared to *Tim* / + control. (E) Further restricted expression of *Rim*-RNAi just to the PDF positive LNvs caused an even more reduction in rhythm strength and (F) lengthening of period in PDF > *Rim*-RNAi compared to control flies. Unpaired t-test were conducted for data in A and B. Kruskal-Wallis test were conducted for data in C, D and F with Dunn's *post hoc* test. One-way ANOVA with Holm-Sidak's *post hoc* test. n (w^{1118}) = 29, n (Rim^{Ex98}/Df) = 10 flies, n (*Tim / +)* = 95 , n (*Tim > Rim-RNAi(II))* = 92, n (*Tim > Rim-RNAi(III))* = 114, n (*PDF / +)* = 61, n (*PDF > Rim-RNAi(II))* = 94, n (*PDF > Rim-RNAi(III))* = 63, n (*Rim-RNAi(II) / +)* = 32 and n (*Rim-RNAi(II) / +)* = 29

4.3.7 Rim knock-down disrupted day/night remodelling of the s-LNvs dorsal terminals and PDF cycling

Previous works have described circadian remodelling of the dorsal projections of the s-LNvs, going from an open state in the morning to a more simple state at night (Curran et al., 2019; Gorostiza et al., 2014). Furthermore, the amount of PDF neuropeptide in s-LNvs synaptic terminals is greater in the day than at night (Park et al., 2000). Given the rhythmic changes in behaviour of *Rim* mutants that I described above and the role of Rim in presynaptic terminals, I sought to analyse whether *Rim* knock-down had an effect in these clock outputs.

A GFP-tagged version of tubulin was expressed in the LNvs, using the *PDF-Gal4* promoter, revealing GFP localisation through the l-LNvs projections to the medulla and the s-LNvs dorsal and ventral projections, which co-localized with the PDF peptide assessed by immunohistochemistry (Fig. 4.14A). During the day (ZT2) wild type s-LNv dorsal terminals appeared more branched than at night (ZT14) (Fig. 4.14B) as was quantified by Sholl analysis (Fig 4.15B, right upper panel) (Sholl, 1953). In contrast, *Rim* knock-down in the LNv removed this day/night remodelling with the dorsal terminals appearing to be in an intermediate level of complexity between wild type day and night levels (Fig. 4.14C).

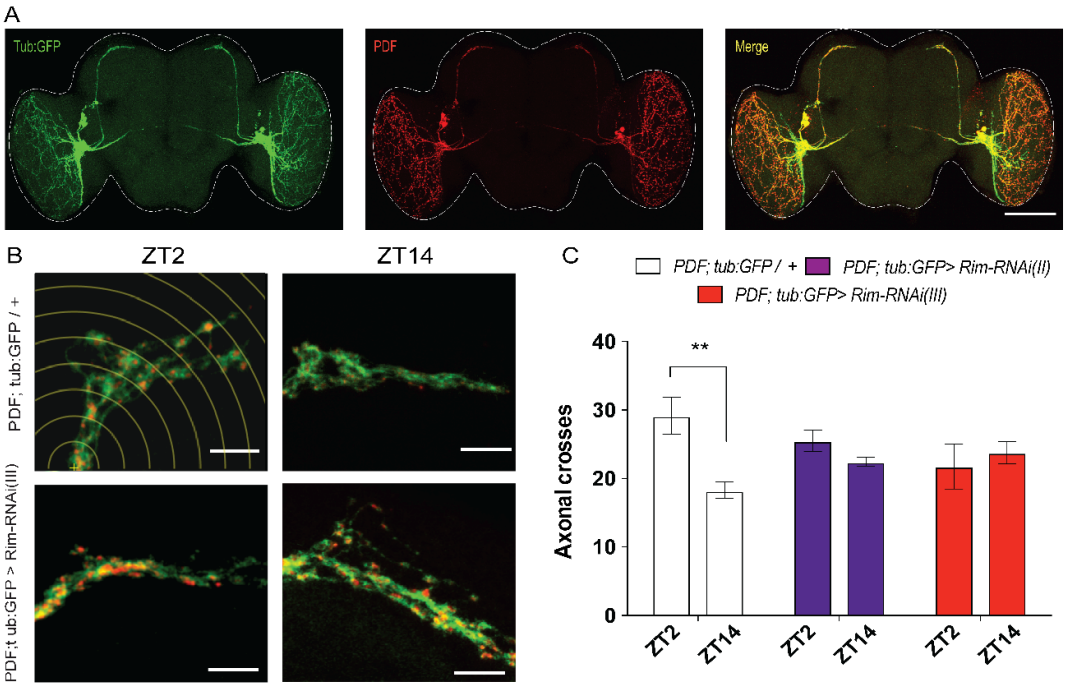

Figure 4.14 Day/night differences in dorsal s-LNvs terminal complexity was removed by *Rim* knock-down. (A) *PDF-GAL4* driven expression of a GFP-tagged version of tubulin (tub:GFP) was used to label LNvs. Tub:GFP (green) can be observed in the terminals, axons and somas of LNvs. Immunodetection of PDF is shown in red. Scale bar 50 μm (B) Dorsal terminals of the s-LNvs during day-time (ZT2 e.g. 11am) and night (ZT14 e.g. 11pm) in control flies (top panels) and *PDF; tub:GFP > Rim-RNAi* (bottom panels). Scale bar 10 μm. Yellow lines in upper left panel in B represent the circles used for Sholl analysis. (C) This analysis revealed that there were significantly more axonal crosses for controls in day than night (open white bars). This day/night difference in terminal complexity was abolished in the PDF > *Rim*-RNAi flies (purple and red bars), two-way ANOVA with Tukey's *post hoc* test). Mean ± SEM, (*PDF; tub:GFP / +)* = 18, n (*PDF; tub:GFP > Rim-RNAi (II))* = 29, n (*PDF; tub:GFP > Rim-RNAi (III))* = 13 hemispheres.

In order to assess if *Rim* is involved in the rhythmic accumulation of PDF in s-LNv terminals, I quantified PDF levels at ZT2 and ZT14. In order to avoid any potential confound of appearing less PDF at night due to the terminals just being smaller at night, PDF signal intensity was measured in each PDF marked area within the dorsal terminals of the s-LNvs. This would make structural remodelling and changes in PDF accumulation independent of each other (Fig. 4.15A-B). PDF was clearly seen to cycle in control flies, with high levels of PDF at ZT2 and lower levels at ZT14. In contrast, PDF accumulated to similar levels at ZT2 and ZT14 in *PDF > Rim-RNAi* (Fig. 4.15C), values intermediate between wild type day and night levels.

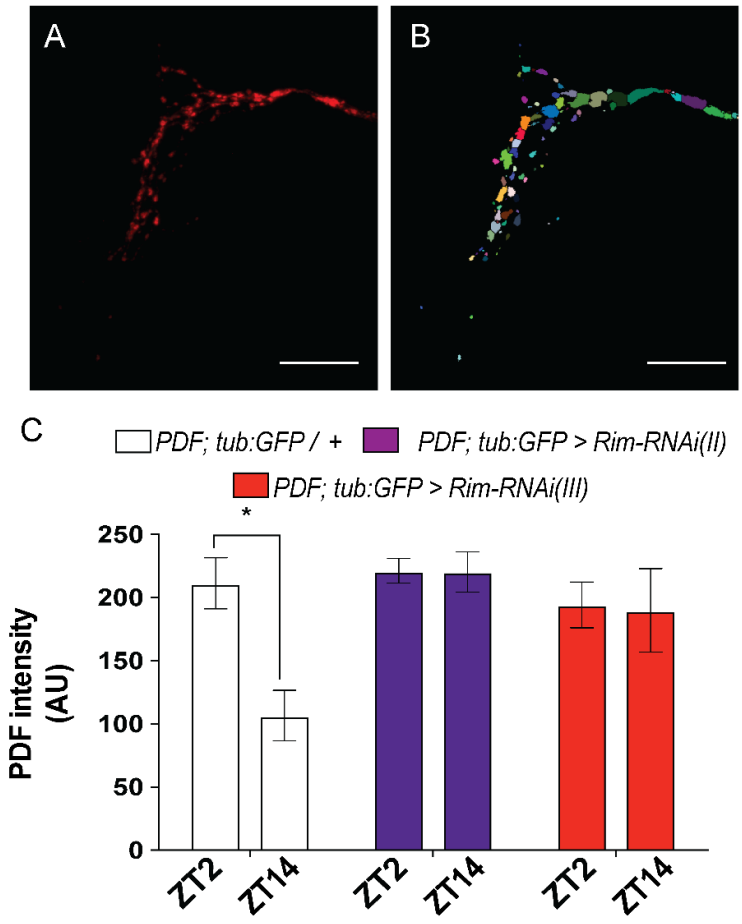

Figure 4.15 Day/night differences in PDF accumulation of dorsal s-LNvs terminals are removed in *Rim* knock-down. Representative confocal images showing (A) PDF immunohistochemical signal in the dorsal terminals of the s-LNvs and (B) potential localised aggregates of PDF that were highlighted in different colours by an automatized image processing tool which obtained separation of each from its neighbours. Scale bar 20 μm. (C) PDF was also found to be cycling in control flies (open white bars), with high levels during the day (ZT2) and reduced levels at night (ZT14) as measured by the mean intensity of each PDF cluster. This day/night difference in PDF accumulation was missing in the *PDF > Rim-RNAi* flies (purple and red bars, two-way ANOVA with Tukey's *post hoc* test), which remained in a perpetually high, day state. (*PDF; tub:GFP / +)* = 18, n (*PDF; tub:GFP > Rim-RNAi (II))* = 29, n (*PDF; tub:GFP > Rim-RNAi (III))* = 13 hemispheres.

Rhythmic PDF accumulation, high in the day and low at night, has been proposed as clock output phenotype which could result from disrupted PDF neuropeptide vesicle release (Park et al., 2000). Therefore, the high levels of PDF in the dorsal terminals of the s-LNvs in *PDF > Rim-RNAi* could be explained by a potential role of Rim in vesicular release of PDF, leading the accumulation of perpetually high levels of PDF. Rim is known to regulate neurotransmitter release including at developing *Drosophila* synapses (Graf et al., 2012; Muller et al., 2012), a specific

role in adults or during neuropeptide release has not been reported. In order to determine if Rim may play such a role, the distribution of Rim and PDF in the s-LNvs terminals was analysed. A GFP-tagged version of Rim was expressed under the *PDF* promoter and PDF was detected by immunohistochemistry, revealing Rim:GFP was preferentially localised in the s-LNvs terminals as well as in the soma, whereas it was appeared absent in the l-LNvs terminals terminating in the medulla (Fig. 4.16A). Interestingly, co-localisation images showed PDF was in close proximity to Rim:GFP, but were not directly co-localising (Fig. 4.16B). Higher magnification images of the terminals containing PDF showed that Rim:GFP formed aggregates around the sites where PDF might be released, suggesting that there may be some sort of functional organization of Rim and PDF in these areas (Fig. 4.16C).

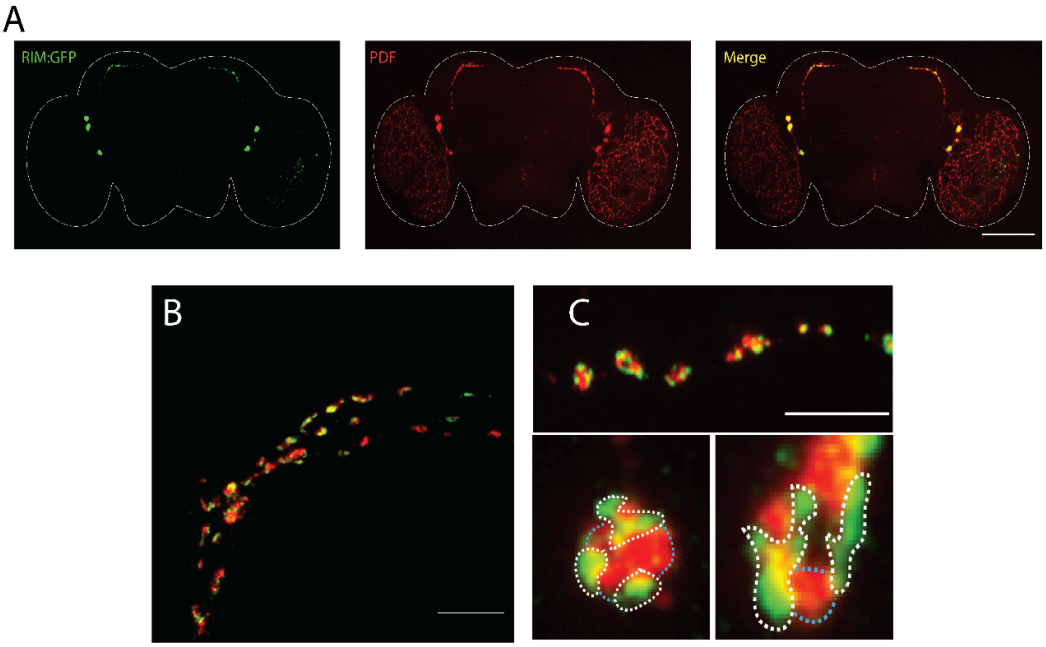

Figure 4.16 Rim:GFP was found near but not with PDF in s-LNvs dorsal terminals. (A) Expression of a GFP-tagged version of *Rim* was driven in the LNvs using the *PDF-GAL4* promoter (in green) while PDF was assessed by immunohistochemistry. Distribution of Rim:GFP was found to be mostly localized to the soma of the small and large LNvs while also appearing in the dorsal projection of the s-LNvs. (B) Higher magnification of the s-LNv terminals showed Rim:GFP and PDF were not completely colocalized. (C) Rim:GFP (green) was occasionally found to co-localise (yellow) with PDF (red). Closer inspection of high magnified images (bottom panels) revealed that Rim:GFP formed aggregates (white dotted line), mostly separated from where PDF was localized (light blue dotted line). Scale bar 50 μm (A) and 10μm (B-C).

4.4 Discussion

Schizophrenia is commonly diagnosed in clinical practice by a number of symptoms, including psychosis and asociality, however, little is known about the molecular mechanisms underlying these behaviours (Howes et al., 2017; Kahn et al., 2015). Current treatments are symptomatic and limited, as they only improve some symptoms in some people further highlighting the need to better understand the cellular underpinnings of these schizophrenia-related behaviours (Buoli et al., 2013; Yang and Tsai, 2017). This suggests the need for animal models based on the genetic component of schizophrenia in order to uncover the pathophysiology of these poorly understood disorder and to test new experimental drug (Carpenter and Koenig, 2008; Jones et al., 2011; Sigurdsson, 2016). In order to address this need, I generated a novel high-throughput genetic and behavioural model of schizophrenia based on *Drosophila* mutant for the orthologue of the schizophrenia-associated gene *RIM1*, *Rim*. I found *Rim* is required in a number of different central synapses to modulate schizophrenia-relevant phenotypes in flies. Also, this worked demonstrated *Rim* shows different functional roles in different types of neurons.

4.4.1 Olfactory function was impaired in Rim mutants

Rim mutants showed defects in olfactory processing with olfactory acuity to the normally highly aversive odorant benzaldehyde being impaired in these flies, this behaviour seemed to be regulated by Rim functioning in the AL PNs, as targeted inactivation of *Rim*, by expression of RNAi specifically in these neurons was sufficient to result in olfactory impairments (Fig. 4.1). Interestingly, similar changes in olfactory processing is also commonly observed in schizophrenia patients (Rupp, 2010). Several studies have shown that odour detection threshold sensitivity is reduced in patients and, moreover, these dysfunctions are independent of environmental factors such as neuroleptic use and smoking (Crespo-Facorro et al., 2001; Robabeh et al., 2015; Ugur et al., 2005). Although well documented, it is not fully understood how olfactory impairments arise in schizophrenia, however, it is seen in early stages of the disorder suggesting a role as a prodromal marker (Moberg and Turetsky, 2003; Rupp, 2010). This work demonstrated that the *Drosophila* olfactory system is a tractable system to evaluate these questions with the similarities between olfactory dysfunctions in patients with

schizophrenia and *Rim* mutant phenotypes here potentially validating this approach.

A previous study have shown that transgenic mice carrying the schizophrenia-associated G72/G30 genomic region, display schizophrenia-like pathology, including impaired smell (Otte et al., 2009). Moreover, a study in *Drosophila* using a null mutant *dysb*^{1}, showed impaired olfactory habituation, which was phenocopied by downregulated *Dysb* expression in the AL PNs (Mullin et al., 2015). Interestingly RIM is highly expressed in the olfactory bulb suggesting RIM may have a similar function in mammalian olfactory function as in flies. It would be interesting to know if people with *RIM1* SNPs associated with schizophrenia also have olfactory symptoms.

4.4.2 Social impairments and their possible olfactory origins in Rim mutants

Impaired social behaviour is a hallmark of schizophrenia therefore it might be expected that models of this disorder may show some form of analogous deficit (Jones et al., 2011). I found social behaviour was also affected in *Rim* mutant flies (Fig. 4.2), specifically, social space was increased in these animals, in a manner reminiscent of people with schizophrenia. In line with these results, social impairments where found in a *RIM1*$\alpha^{-/-}$ mutant mouse, suggesting the role of RIM, in olfaction and social behaviour is evolutionarily ancient. One study showed that the *RIM1* mutants displayed decreased time engaging in social recognition of a novel mouse (Blundell et al., 2010). Other study suggested that deficiencies in maternal behaviour can be observed in *RIM1*$\alpha^{-/-}$ mice, further suggesting an imbalance in social behaviour associated with RIM dysfunction (Schoch et al., 2002). The social space defect was also observed when knocking-down *Rim* in the AL PNs, again consistent with a role of olfaction in this social behaviour (Fig. 4.2). Recent evidence in ants suggested that nesting behaviour (Depickère et al., 2004), a similar grouping behaviour than the one described here, relies on analogous olfactory processing (Martin et al., 2019; Takeichi et al., 2018; Trible et al., 2017; Yan et al., 2017). CRISPR deletion of the olfactory co-receptor, *orco*, significatively reduced the ability of mutant ants to interact with unaffected animals by a mechanism involving impaired olfactory processing (Trible et al., 2017; Yan et al., 2017). My behavioural and functional data is consistent with this being the case for

social space in *Drosophila.* Future work will be required to address further genes contributing in this response and the neuronal circuits involved in this behaviour.

4.4.3 Rim contributed to structure and function of the antennal lobe projection neuron terminals on to the lateral horn

My data demonstrated that both, the structure and the function of the AL PNs are affected by knock-down of *Rim* (Fig. 4.6-4.7). Several studies have suggested that Rim is dispensable for the development of synapses, in *Drosophila*. It was shown that *Rim* mutations did not have any gross-synaptic morphology defects at the NMJ, however, modest reductions in the number of release sites was observed (Graf et al., 2012; Muller et al., 2012). Consistent with these findings I also found that in adults there is no gross-morphological changes at *Rim* knock-down synapses with no change in AL PNs numbers and its projections were found. However, I did find a smaller presynaptic terminal area of the AL PNs reaching the LH (Fig. 4.6). The AL PN axonal arborization on to the LH are likely synaptic sites (Jefferis et al., 2007), with the smaller size of this area that I described in my results, being similar to the reduction in AZ/releasing sites observed at the NMJ (Graf et al., 2012). It is well known that RIMs act as scaffolding molecules, clustering calcium channels at the presynaptic terminals of different synapses in different organisms (Böhme et al., 2016; Graf et al., 2012; Schoch et al., 2002). Here I show that *Rim* is required at the presynaptic terminals of the AL PNs onto the LH with a role in regulating calcium handling (Fig. 4.7). *Rim* knock-down decreased the amplitude of peak Ca^{2+} signals in response to a depolarising stimulus, which is consistent with the role of RIM clustering calcium channels at active zones, ready for calcium-dependent vesicle release from synapses.

The olfactory defects observed in *Rim* mutants therefore appear to be caused by both functional and structural deficits of olfactory structures. It is possible that this may also be the case for individuals with schizophrenia. For instance, it was shown that patients displayed reduced cortical volume in brain areas that receive direct inputs from olfactory afferents (Turetsky et al., 2003). Using MRI, a reduction in the anterior ventromedial temporal lobe volume was present in schizophrenia patients, a decrement that correlates with decreased olfactory acuity (Turetsky et al., 2003). It was also shown using MRI that some schizophrenia patients present a 23% reduction in olfactory bulb volume, however surprisingly in this study there was not a clear correlation between this decrement and the changes in odour detection

sensitivity of schizophrenia patients (Turetsky et al., 2000). This portrait how difficult structure/function studies are to perform in humans and particularly schizophrenics, reiterating the need for new animal models. Additionally, a recent functional study has shown a dysconnectivity of olfactory regions in schizophrenia, that may contribute to the olfactory behaviours observed in the disorder (Kiparizoska and Ikuta, 2017).

Altogether, our results on olfaction show good alignment between animal models including flies and humans, validating *Drosophila Rim* as a highly tractable model to assess these phenotypes. Additionally, future experiments are needed to investigate the role of *Rim* in these phenotypes, dissecting its contribution to neural development versus neuronal function. This would be possible by affecting *Rim* expression in the AL PNs in a time-dependent fashion, e.g. using the TARGET system, which by changing the temperature, would allow the expression of the RNAi only in adult flies (McGuire et al., 2004).

4.4.4 Loss of Rim in mushroom body neurons had no effect on memory, consistent with Rim having differential contribution to different synapses and behaviours

The lack of olfactory or social dysfunction resulting from *Rim* knock-down in the MBs might be explained by a number of options for instance: *Rim* expression in the MBs is dispensable for the behavioural outputs tested, *Rim* is not expressed in MB or it is expressed at such a level, that enough remains in the mutants to perform the behaviours. Also, because I used constitutive Gal4 promoters that express throughout development into adulthood, there could be some form of compensation occurring whereby Rim or a Rim-like proteins, like the recently described Fife, is upregulated in MB synapses (Bruckner et al., 2017, 2012). Alternatively, Rim could have differential roles in different subsets of MB neurons or output neurons, for instance Rim may mediate memory in some of MB lobe neurons, while in others it regulates forgetting, therefore pan-MB expression would cancel each other's effects out (Guven-Ozkan and Davis, 2014). Future work to address this further could be by misexpression of *Rim* in subsets of MB neurons or MB output neurons (Higham et al., 2019) as well as using inducible MB promoters (Scialo et al., 2016).

Because *Rim* knock-down in the MB did not yield any STM or ITM impairment it would appealing to suggest that Rim is dispensable for MB function (Fig. 4.8),

however, I did not test other types of memory like 3 h memory, anaesthesia-resistant memory, long-term memory, or memories formed by appetitive conditioning, all of these dependent of the MBs, which could have been effected (Burke et al., 2012; Davis, 2015; Malik et al., 2013; Tully and Quinn, 1985; Waddell, 2013). Interestingly, assessing mushroom bodies-specific transcriptomic before and after different conditioning assays in *Drosophila* can give some insights. Recent studies have shown that *Rim* expression increased after courtship conditioning (Jones et al., 2018) but no differential changes were found after appetitive olfactory conditioning (Widmer et al., 2018). Therefore, I would expect that knocking-down *Rim* would have an effect in courtship conditioning-dependent memory if this increment is important for the display of this behaviour. Future experiments addressing other types of memory such as the ones described, could be tested to dissect Rim contribution to MB functioning.

Working memory impairments are another feature observed in schizophrenia, and studies using *RIM* knock-out mice have addressed this with inconsistent results (Selemon and Zecevic, 2015; Takano, 2018; Tripathi et al., 2018; Zhou et al., 2018). While *RIM1*$\alpha^{-/-}$ mice showed impaired memory in a fear conditioning test (Powell et al., 2004), deletion of *RIM1* from the dentate gyrus or pyramidal neurons of the CA3 regions yielded normal memory in similar conditions, even though the hippocampus is critical for learning and memory (Haws et al., 2012). A possible explanation may emerge from the differential contribution of RIM that has been described at different synapses in mammals, that others and myself (Appendix B) have reviewed (Hidalgo, 2019; Lonart, 2002). For instance, deletion of *RIM1* from the Schaffer collateral fibers and pyramidal cell synapse increased short-term plasticity (Schoch et al., 2002), while deletion of *RIM1* from the hippocampal mossy fiber and pyramidal cell synapse spared this form of plasticity (Castillo et al., 2002). In contrast, deleting *RIM1* from the cortico-striatal synapses did not have an effect either on long or short-term plasticity (Hidalgo, 2019; Kupferschmidt et al., 2019), this again highlights the fact that RIM may have differential roles in different synapses. Hence, the lack of effect observed in *Rim* MB knock-down experiments could be explained by Rim having synapse-specific roles in *Drosophila* as described in mice.

4.4.5 Rim function in locomotion and sleep under light-dark conditions and its relationship with the clock

Locomotor activity levels measurements across the day, revealed that locomotor activity levels were lower in Rim^{Ex98}/Df in LD across the whole 24 h period and specifically caused by decreased activity during the night. However, this appeared not to be due to Rim functioning in the clock, as knocking-down *Rim* in the clock was wild type (Fig. 4.9-4.10). A possible explanation is that this effect arise from a defective neuron-muscle synapse. The role of *Rim* in the NMJ of *Drosophila* might suggests that the reduction in locomotor activity observed in Rim^{Ex98}/Df mutant may arise from a purely peripheral dysfunction, although it was not tested in flies (Muller et al., 2012). Though, it has been shown in the worm *Caenorhabditis elegans*, that mutants in the *RIM1* orthologous gene, *unc-10*, caused incoordination and locomotor defects (Koushika et al., 2001). To assess if the decrease levels in locomotion observed in Rim^{Ex98}/Df mutants arise from a general incoordination phenotype in these flies, future experiments should be conducted like the roll over assay in larvae or startle-induced negative geotaxis assay in adult flies (Lowe et al., 2019; Sun et al., 2018). This would be consistent with observations in schizophrenia, as motor dysfunctions are observed in patients, which can range from impaired eye movement to Parkinsonism which has also been observed in other genetic models (Hirjak et al., 2018; Jones et al., 2011; Otte et al., 2009).

Sleep phenotypes observed in schizophrenia vary between individuals. Some studies have shown insomnia in some patients, while others may present increased night-time sleep (Cosgrave et al., 2018; Wulff et al., 2012). Rim^{Ex98}/Df flies showed increased night sleep which is in line with these findings (Fig. 4.9). Wulff et al. (2012) showed that schizophrenia patients could be divided by the sleep time into a subgroup that showed increased sleep time while the other showed decreased sleep time.

Our inconsistent results when addressing *Rim* contributions to the circadian component of locomotor activity and sleep, might arise from various reasons. For instances, it has been shown that, although useful, the GAL4-UAS system is not perfect. Elements downstream the UAS sequences can be transcribed in the absence of the GAL4 element, and this is different for all the UAS transgene (which is known as ‘leak’ expression) (Akmammedov et al., 2017; Scialo et al., 2016).

Though, this expression should be minimal, this could also be influencing the results obtained. Consistent with this, in most of the cases I was able to find differences between the GAL4 and experimental flies (i.e. *GAL4 > Rim-RNAi*), but not with the UAS control flies. If the phenotypes observed are sensible to small changes in *Rim* expression, leaky expression should be enough to manifest in behaviour. This also highlight the importance of using different RNAi lines to confirm the results. Future experiments should be conducted to dissect this, like test the leaky expression by quantitative RT-PCR.

Additionally, the *tim-GAL4* line here used, was made by using the timeless promotor, which it is known to be regulated in a circadian manner (Stanewsky et al., 1998). This driver has been used to infer timeless cycling throughout the day and, therefore, variations in the GAL4 production and, consequently, dsRNA production could be happening affecting the temporality of the knock-down. Nonetheless, this is unlike as it has been shown that reporter proteins such as GFP can be found constantly expressed throughout the entire time, due to its stability (Kaneko and Hall, 2000). For the dsRNA, this would also be the case and although if only transient expression of this RNA molecules is achieved, the potency of the manipulation would lead to persistent changes in the knock-down activity (Bosch et al., 2016).

4.4.6 Rim was required, particularly in the LNvs, to maintain circadian locomotion rhythmicity under continuous darkness

Circadian rhythmicity under constant darkness showed a clear dependence on *Rim* expression in the clock network (Fig. 4.12). Rim^{Ex98}/Df flies showed reduce rhythmicity and shorter free-running period length, phenotypes also seen when *Rim* was just knocked down in the LNvs, suggesting a specific role of Rim in these neurons for these circadian behaviours. These neurons have been described as the major pacemakers under DD, contributing to locomotor rhythmicity (Guo et al., 2014; Nitabach et al., 2002). It has been shown that flies lacking PDF-neurons have abnormal locomotor activity under DD, as seen by the display of shorter periods and lack of rhythmicity (Lin et al., 2004). Furthermore, it has been shown that lack of PDF can cause similar abnormalities in PDF-null flies which display arrhythmicity and changes in anticipation under the same conditions (Renn et al., 1999). Hence, our results agree with the notion that Rim and the LNvs are

important in maintaining rhythmicity under DD (Buhl et al., 2019; Guo et al., 2014; Nitabach et al., 2002; Taghert and Shafer, 2006).

Accompanying the changes in rhythmicity in *PDF > Rim-RNAi* flies, I found a removal of day/night remodelling of the dorsal s-LNvs terminals (Fig. 4.14). The dorsal projections of these neurons undergo changes in their branching state which go from being in a more open and complex state during day, to a simple and closed state at night (Arnes et al., 2019; Curran et al., 2019; Gorostiza et al., 2014; Herrero et al., 2017; Mehnert and Cantera, 2011). This is observed in control flies, however, was removed in *PDF > Rim-RNAi* flies whose terminals were intermediate in complexity between wild type day and night levels. This structural reorganization has been shown to be accompanied by changes in the number of active zones, allowing the s-LNv to potentially change how they interact with postsynaptic clock neurons during different times of the day (Gorostiza et al., 2014). Because of this, it is proposed that this clock output is fundamental to the accurate display of circadian activity as I described here. Interestingly, my results are reminiscent of those found in aged animals or in flies that have the *period* and *timeless* clock genes knocked down in the clock suggesting that *Rim* might be one of the genes downstream of the molecular clock that allows this remodelling (Curran et al., 2019; Herrero et al., 2017). In line with this, *Rim* has been found to be cycling in the s-LNvs neurons, further supporting this idea (Kula-Eversole et al., 2010). In future it would be interesting to see if *Rim* changes the day/night differences in active zones using endogenous GFP-tagged versions of active zone proteins or calcium channels like the Rim-interacting cacophony (Scholz et al., 2019; Sugie et al., 2015).

4.4.7 Rim was required for day/night differences in PDF accumulation suggesting that Rim maybe involved in neuropeptide release

The abundance of PDF in s-LNv terminals cycles during day and night with higher levels in the morning and low levels in the evening (Herrero et al., 2017; Park et al., 2000). These PDF variations are not associated with transcriptionally or translationally rhythmic patterns, but instead arise from changes in its release (Park et al., 2000; Taghert and Shafer, 2006). Hence, it is believed that PDF release cycle begins in the morning and finishes at night, therefore its accumulation in neuronal terminals would be inversely correlated to its release. Consistent with this idea, I found PDF is highly accumulated in the morning, whereas low levels were

found at night in control flies (Fig. 4.15) and as seen by others (Herrero et al., 2017; Park et al., 2000) . Such day/night fluctuation in PDF accumulation was not seen in *PDF* > *Rim-RNAi* s-LNv terminals, with PDF being found at high levels during both day and night, suggesting that loss of *Rim* was preventing the normal day/night differences in PDF neuropeptide release.

Little is known about the molecular machinery behind PDF release. Two studies have indirectly shown that PDF release is independent of the SNARE protein synaptobrevin, as overexpression of tetanus toxin (that partially cleaves it), failed to induced abnormal circadian phenotypes (Blanchardon et al., 2001; Kaneko et al., 2000). Nonetheless, other study has shown that eclosion hormone (EH) release in *Drosophila* required this mechanism as flies overexpressing the tetanus toxin in the EH-producing cells failed to release the peptide (McNabb and Truman, 2008). Here I show that PDF release depends on *Rim* expression in the LNvs. Moreover, I observed that PDF and Rim are localized in largely distinct zones within the dorsal s-LNvs projections (Fig. 4.14). Remarkably, similar organization of peptidergic vesicles has also been observed in a number of different neuronal types, where dense vesicles are loaded with peptides that are in close proximity to the presynaptic releasing site, possibly using some of the machinery for the fast synaptic release of small neurotransmitters (van den Pol, 2012).

4.5 Conclusions of the chapter

- *Rim* was required in central synapses of *Drosophila* to modulate behaviours such as olfaction, social interaction, circadian rhythms and sleep.
- Social space behaviour, similar to other species, relied on olfaction in *Drosophila,* with Rim-mediated olfactory defects likely causing the social space phenotypes.
- *Rim* expression in the MBs was dispensable for olfaction, social interaction and memory, suggesting differential contribution of Rim to central synapses in *Drosophila*.
- Knock-down of *Rim* in AL PN caused both structural and calcium handling defects on to the lateral horn.
- Circadian rhythm and sleep phenotypes caused by *Rim* knock-down in clock neurons were underlain by a loss of day/night differences in s-LNvs terminal

complexity and PDF cycling, which went into a perpetual day state of high PDF accumulation suggesting lack of *Rim* blocked neuropeptide vesicle release.

- Rim distribution in s-LNvs terminals also suggest a function in PDF release.

Chapter 5: The role of the *Drosophila* calcium channel *cacophony* in memory, circadian rhythms and sleep

This chapter explores the effects of knocking-down *cacophony (cac)*, the *Drosophila* orthologue of the human *Calcium Channel Subunit* α*1B* (*CACNA1B)* gene*,* on schizophrenia related behaviours. The chapter gives a brief introduction to the *CACNA1B*, its association with schizophrenia and its role in behaviour and neuronal physiology. The results of the behavioural characterization of *cac* in learning and memory are shown first, accompanied by experiments exploring the effect of *cac* knock-down in calcium handling. The circadian locomotor activity and sleep data obtained with different *cac* manipulations are also shown in this chapter. The discussion and conclusions related to the results found in this chapter are presented in the last sections.

5.1 Introduction

5.1.1 The association of CACNA1B with schizophrenia

The *CACNA1B* gene has been associated with schizophrenia in a number of independent studies, and by different approaches. The first study dates from 2009, where Moskvina et al. (2009) used a previously published GWAS dataset of schizophrenia cases (Moskvina et al., 2009; O'Donovan et al., 2008). By running a different analysis on the data set published by O'Donovan et al., the authors unveiled new hits that were enriched for calcium channels (Moskvina et al., 2009). With these results, the authors suggested a link between schizophrenia and channelopathies, as in other neuropsychiatric disorders like bipolar disorder (Green et al., 2010; Moskvina et al., 2009). Supporting this, another study using whole-genome copy number variation (CNV) analysis demonstrated that several synaptic transmission genes were strongly associated with schizophrenia. Among them, CACNA1B was one of the strongest associations, including 16 cases where it was possible to identify deletions in the *CACNA1B* gene (Glessner et al., 2010).

Additionally, population-based exome sequencing in other cohorts showed that a disruptive nonsense mutation in the *CACNA1B* gene was part of a group of mutations associated with this disorder (Purcell et al., 2014). After correcting for multiple comparisons, it was possible to determine that none of the genes (including the *CACNA1B*) achieved significance individually. Based on this, the authors suggested that these mutations correspond to a polygenic burden associated with schizophrenia, in which the VGCC channels genes play a fundamental role (Curtis et al., 2011; Li et al., 2018; O'Connell et al., 2019; Purcell et al., 2014).

Behavioural studies have shown that CACNA1B plays a role in learning and memory, locomotion and sensory processing, all schizophrenia-related behaviours as discussed previously in this thesis. The *CACNA1B* homozygotic knock-out mutant mouse ($Ca_v2.2^{-/-}$) displays reduced PPI and increased locomotion (Beuckmann et al., 2003; Nakagawasai et al., 2010). Moreover, $Ca_v2.2^{-/-}$ mutants have impaired memory, as shown by reduced scores in spatial memory and decreased long-term memory in social transmission of food preferences (Jeon et al., 2007). Also, $Ca_v2.2^{-/-}$ mice showed difference in their vigilance state, measured by the time spent in REM, NREM sleep and awake states (Beuckmann et al., 2003).

5.1.2 CACNA1B role in synaptic transmission

CACNA1B encodes the α-1B subunit of the Cav2.2 Ca^{2+} channels and constitutes the selective pore of this N-type channel (Qian and Noebels, 2001; Simms and Zamponi, 2014). $Ca_v2.2$, together with the $Ca_v2.1$ or P/Q-type Ca^{2+} channels, are the main mediators of fast synaptic neurotransmission in synapses of the central nervous system. Both, $Ca_v2.1$ and 2.2 channels are localised to the active zone and have specialized domains that allow them to interact with synaptic proteins like RIM, SNAP-25 and syntaxin 1 (Kaeser et al., 2011; Simms and Zamponi, 2014; Xie et al., 2017).

Because of its presynaptic role, several studies have shown that Cav2.2 channels play a fundamental role in synaptic plasticity (Ackermann et al., 2015; Lübbert et al., 2019; Wu et al., 2005). In the hippocampal CA3-CA1 synapses, Cav2.2 contribute to basal synaptic neurotransmission and to long-term potentiation of neurotransmitter release (Jeon et al., 2007). Moreover, it was shown that N-type

calcium channels also play a role in the hippocampal medial perforant pathway when measuring presynaptic cortical neurotransmitter release onto the dental gyrus (Qian and Noebels, 2001).

5.1.3 Studies of *cacophony* in *Drosophila*

In *Drosophila*, Cav2.1, Cav2.2 and Cav2.3 channels are encoded by just one gene, *cac*, and the protein corresponding protein cacophony behaves as a P/Q- and N-type Ca^{2+} channel (Kawasaki et al., 2002; Peng and Wu, 2007). cacophony localizes at the active zone playing a fundamental role mediating fast neurotransmitter release (Gu et al., 2009; Muller et al., 2012).

Studies using cultured *Drosophila* neurons have shown that cac mediate the frequency of the spontaneous cholinergic excitatory postsynaptic currents (Gu et al., 2009). This is similar to what is found at the NMJ, where cac regulates the evoked neurotransmitter release and is also required for synaptic homeostasis (Kawasaki et al., 2004; Lee et al., 2014). It was also suggested that cac mediates the frequency of these events in the antennal lobe projection neurons *ex vivo*, suggesting similar functions of cac in peripheral and central synapses (Gu et al., 2009).

Null mutants of this gene die at larval stages, suggesting a crucial role in development (Kulkarni and Hall, 1987). Because of this, many hypomorphic *cac* alleles have been described, displaying different behavioural features. For instance, the cac^{H18} mutant was found to have defective vision accompanied by impaired visual physiology, while cac^{S} mutants failed to effectively produce courtship behaviours and only have subtle visual phenotypes (Chan et al., 2002; Smith et al., 1998, 1996). Other studies have shown that the temperature sensitive cac^{TS2} mutant mimic the defective courtship behaviours of the cac^{s} mutant but also displays seizure-like phenotypes (Chan et al., 2002).

Due to its high expression in the CNS, assessing the specific contribution of cac in different synapses using these mutants is a difficult task.

5.2 Aims

CACNA1B is a schizophrenia related gene and the corresponding *cac* gene has been described as a major contributor to fast neurotransmitter release in different synapses. Although some behavioural characterization has been performed using

different *cac* alleles, a description of *cac* contribution to neuronal physiology and behaviours is still missing Therefore, I performed behavioural analysis of flies with *cac* knockdown in central neuronal populations as a means to assess the role of cac in schizophrenia symptomatology. Specifically, I assessed learning and memory and circadian and sleep phenotypes which have been linked to the disorder.

5.3 Results

5.3.1 Knock-down of cac in the mushroom bodies impaired short- and intermediate-term memory

Cognitive functions and working memory are impaired in schizophrenia (Petit et al., 2017; Pogue-Geile and Harrow, 1984; Štrac et al., 2016). Moreover, the role of N-type calcium channels in this process has been shown using $Ca_V2.2^{-/-}$ mutants (Jeon et al., 2007). Here the contribution of *cac* in learning and memory was assessed by knocking-down *cac* in the MBs.

Aversive olfactory conditioning was used to train flies and then STM and ITM was measured. Knocking-down *cac* in the mushroom bodies using *OK107-GAL4* (*OK107* > *cac-RNAi*) caused a reduction in both, STM (Fig. 5.1A) and ITM (Fig. 5.1B). To confirm these findings, I replicated the effect by using a second independent MB GAL4 driver to knock-down *cac* (*c309* > *cac-RNAi*; Fig. 5.1C-D), which resulted in reduced STM and ITM.

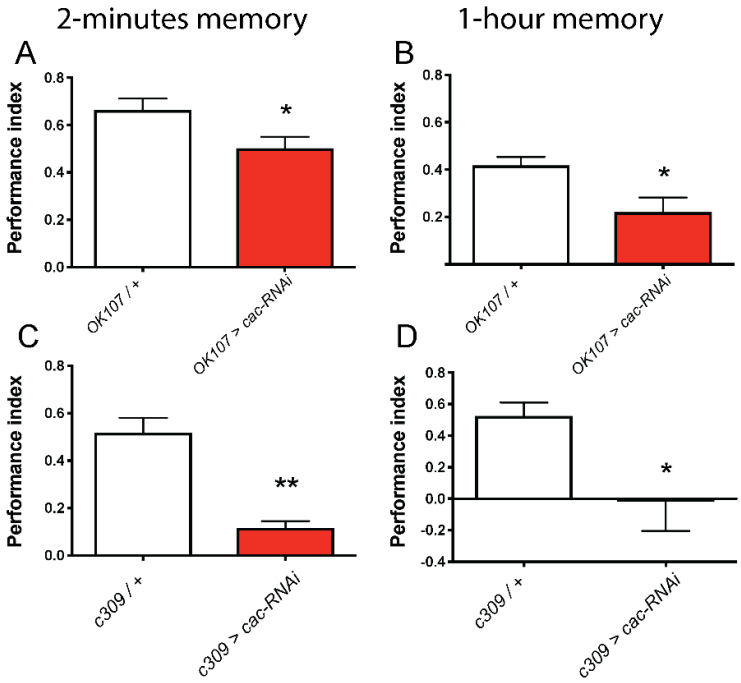

Figure 5.1 *cac* knockdown in the mushroom bodies impaired aversive olfactory learning and memory. Olfactory aversive conditioning was used to test memory in flies with reduced *cac* expression in the mushroom body. Knocking-down *cac* using the *OK107-GAL4* driver impaired two-minutes memory (short-term memory; STM; A) and 1-hour memory (intermediate-time memory; ITM; B). A reduction in performance index was also found using the c309-GAL4 driver in both STM (C) and ITM (D). Data in all datasets was analysed using unpaired t-test. n > 4 repetitions (each n consisted of ~100 flies) for each genotype and condition.

5.3.2 cac knock-down in the mushroom bodies impaired calcium handling

Given the role of *cac* in mediating calcium influx at the active zone, I sought to analyse the effect of *cac* knock-down on evoked calcium responses in the area where most of the presynaptic terminals of the MB are placed, the lobes. The genetically-encoded calcium sensor, GCaMP6f, was expressed in the MB and the calcium transients evoked by high [KCl] were assessed at these areas (Fig. 5.2A-B). Bath application of KCl evoked a robust increase in the normalized fluorescence, that decayed once KCl was washed out (Fig. 5.2C). Quantification of the peak normalized fluorescence reached by this stimulation in *GCaMP6f; OK107 > cac-RNAi* flies was reduced by about 40% compared to the control flies ($p < 0.05$, Fig. 5.2D).

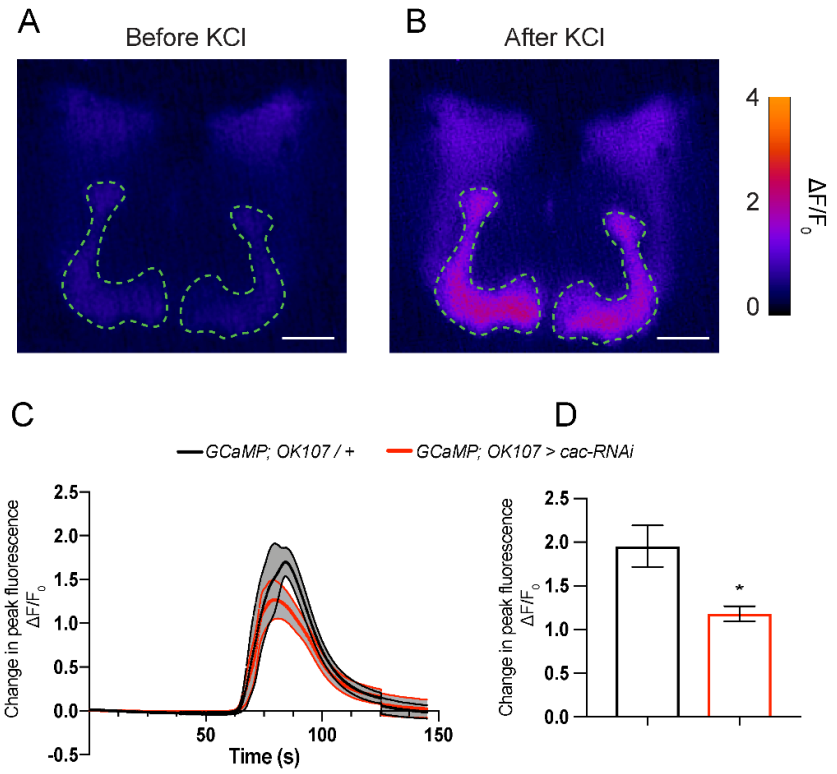

Figure 5.2 *cac* knock-down reduced evoked calcium transients of mushroom body lobes. The genetically encoded calcium sensor, GCaMP6f, was expressed in the antennal lobe projection neurons and its fluorescence was measured. Example images showing the (A) basal fluorescence and (B) fluorescence after the addition of depolarizing high concentration of potassium chloride (KCl). Calibration bar showing the changes in fluorescence can be observed to the right. Scale bar 20 μm. (C) Transients were observed in controls (black) and in the *cac* knock-down condition (red), however, the changes in the peak was lower in the *GCaMP; OK107 > cac-RNAi* flies (mean fluorescence as solid lines ± SEM in grey) (D) A reduction in the amplitude of the peak fluorescence was found upon *cac* knock-down (Unpaired t-test). n (*GCaMP; OK107 /* +) = 4 and n (*GCaMP; OK107 > cac-RNAi*) = 4 brains.

5.3.3 cac^{H18} mutants displayed increased locomotor activity and reduced sleep at night

As discussed, sleep phenotypes are widely observed in schizophrenia patients (Benson, 2006; Wulff et al., 2012). Additionally, changes in locomotion have been observed in the *$Ca_V2.2^{-/-}$* mouse (Beuckmann et al., 2003). To assess the contribution of cac in these behaviours I sought to analyse the locomotor activity of the cac^{H18} mutant flies under LD.

cac^{H18} flies displayed increased locomotor activity under LD conditions (Fig. 5.3A). The overall increase in total locomotion was explained by an increase in the night-time locomotion activity (Fig. 5.3B). As *cac^{H18}* mutants have been shown to have

a defective visual system (Smith et al., 1998), I wanted to further dissect this LD phenotype by knocking-down *cac* in the clock without affecting the visual inputs. *Tim > cac-RNAi* flies displayed no changes in total locomotor activity compared to control flies (Fig. 5.3C). However, analysis of the locomotor activity in day and night unveiled a decrease in day locomotion and an increase in night activity (Fig. 5.3D).

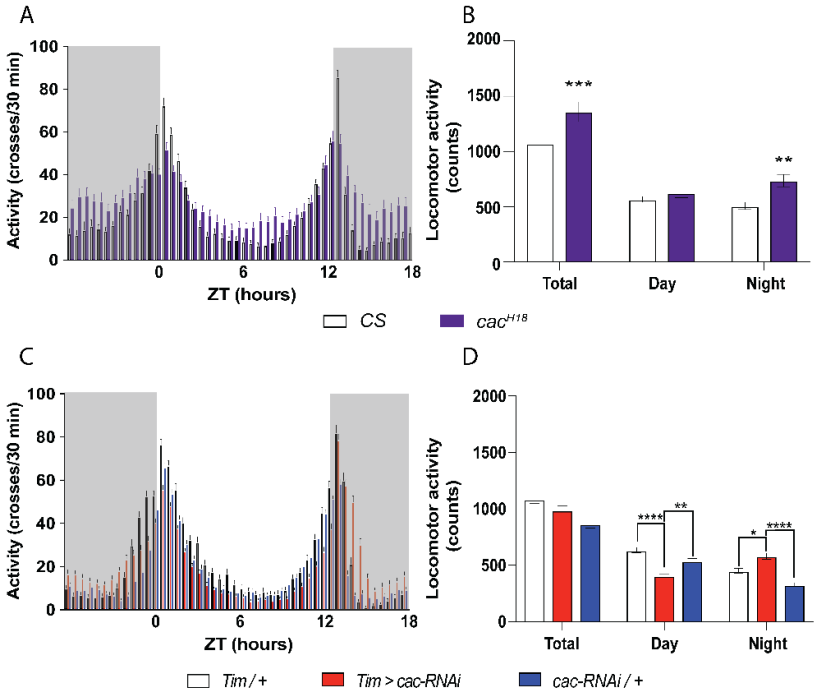

Figure 5.3 Effect of *cac* manipulations displayed different effects in locomotion under day and night. (A) Average of activity across 2 day of LD revealed cac^{H18} mutants were more active than control flies at night. (B) The total activity of the flies across 24 h was increased in cac^{H18} mutants and this was explained by an increased activity during the night (Two-way ANOVA with Holm-Sidak's *post hoc* test). (C) Average activity profiles show *Tim > cac-RNAi* activity under LD (red bars). (D) Close inspection of day and night locomotion showed a reduction in day activity and an increase in night activity (Two-way ANOVA with Dunnett's *post hoc* test). n (*CS*) = 62, n (cac^{H18}) = 26, n (*Tim / +)* = 46, n (*Tim > cac-RNAi)* = 112 and n (*cac-RNAi / +)* = 64 flies.

The changes in locomotor activity observed in cac^{H18} flies were accompanied by a reduction in the total sleep time (Fig. 5.4A, left panel), with both day and night sleep time being decreased (Fig. 5.4B). Analysis of the sleep time in the *Tim > cac-RNAi* flies revealed an increase in the day sleep while night sleep was reduced (Fig. 5.4A, right panel). As observed in the locomotor activity analysis, effects of day and night cancelled each other out, therefore, showing no changes in the total sleep or total locomotor activity in these flies (Fig. 5.4C).

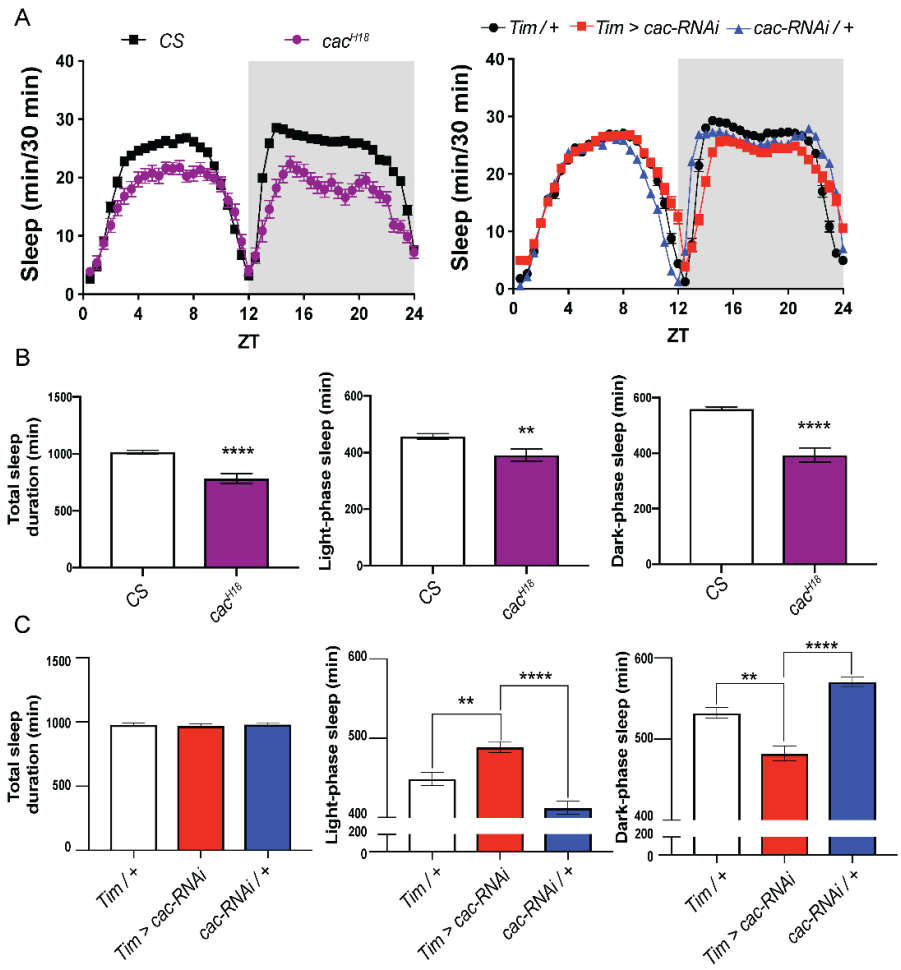

Figure 5.4 Effect of *cac* knock-down in sleep. Averaged sleep profiles of cac^{H18} and control flies (A, left panel) and *Tim* > *cac-RNAi* flies (B, right panel) are shown. Total sleep (B, left), day sleep (B, middle) and night sleep (B, right panel) are reduced in mutant flies compared to controls (Unpaired t-test). Multiple comparisons showed *Tim* > *cac-RNAi* flies displayed unchanged total sleep (B, left), however, the sleep during the day was increased (B, middle). While sleep during night-time was reduced (B, right) (One-way ANOVA with Dunnett's *post hoc* test). n (*CS*) = 62, n (cac^{H18}) = 26, n (*Tim / +)* = 46, n (Tim > *cac-RNAi)* = 112 and n (*cac-RNAi / +)* = 64 flies.

5.3.4 cac^{H18} and knocking-down cac in the clock circuit caused arrhythmic behaviour under constant darkness

To assess circadian locomotor rhythms of these animals, I analysed the locomotor activity patterns after five days of DD. In sharp contrast to the control flies, cac^{H18} flies showed arrhythmicity after entering the DD phase, with the normal morning and evening peaks disappearing as a result of the hyperactivity of these flies (Fig. 5.5).

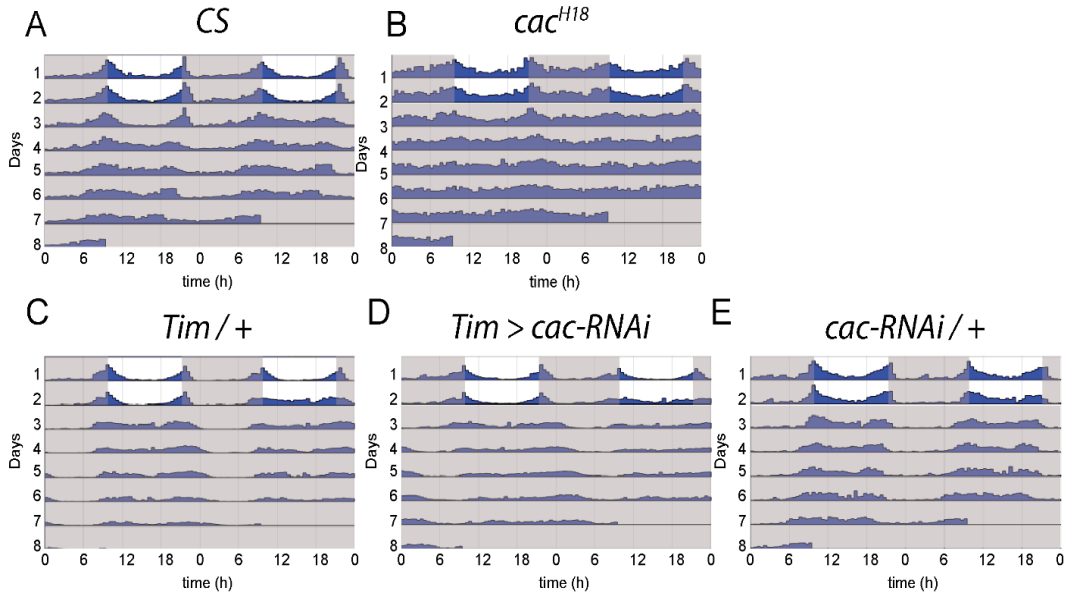

Figure 5.5 *cac* knock-down in the clock affected rhythmic behaviour under constant darkness. Averaged double-plotted actograms of single flies of the following genotypes: (A) *CSw*$^{-}$, (B) *cac*^{H18}, (C)*Tim* / +, (D) *Tim* > *cac-RNAi* and (E) *cac-RNAi* / + for two days in LD (white depicts day and grey night, actograms are double plotted to high light rhythm) followed by 5 days in DD. The activity patterns of *cac*^{H18} and *Tim* > *cac-RNAi* flies becomes arrhythmic under DD compared to controls.

Only 46% of the *cac*^{H18} flies were rhythmic, compared with 77% of the control flies (Table 5.1). Knocking-down *cac* in the clock circuit leads to similar results with 64% of the *Tim* > *cac-RNAi* flies being rhythmic compared to 96% and 92% of the control flies (*Tim* / + and *cac-RNAi* / +, respectively; Table 5.1).

Table 5.1 Circadian behaviour of *cac* flies in constant darkness (DD).

genotype	RS	% rhythmic	period (h)	n
CS	2.15 ± 0.09	77	23.64 ± 0.07	62
cac^{H18}	1.49 ± 0.14	46	23.58 ± 0.25	26
Tim / +	2.75 ± 0.10	96	24.15 ± 0.08	46
Tim > *cac-RNAi*	1.92 ± 0.11	64	24.56 ± 0.15	112
cac-RNAi / +	3.00 ± 0.11	92	23.40 ± 0.03	64

This table is related to Figure 5.5 – 5.6. Data are mean ± SEM

Using autocorrelation analysis, we found that both *cac*^{H18} and *Tim* > *cac-RNAi* produced a reduction in the RS compared to control flies (Fig. 5.6A and C). Nonetheless, only the knock-down produced an increase in the period length while *cac*^{H18} period was indistinguishable from controls (Fig. 5.6 B and D).

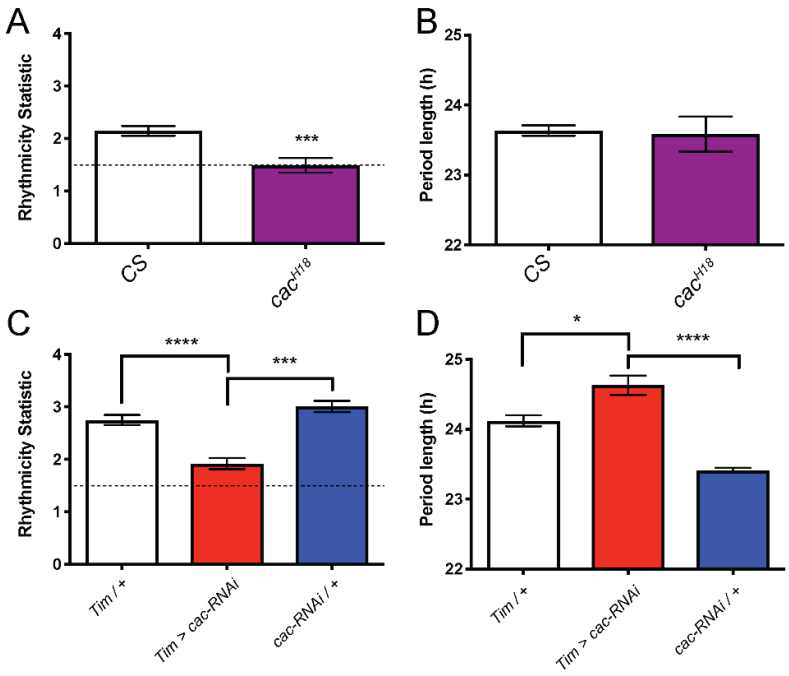

Figure 5.6 *cac* knock-down in the clock network reduced rhythmicity and increased period length under constant darkness. Rhythmicity Statistic was used as a measure of rhythm strength after five days of DD and the period length of the circadian rhythm was also measured at this time point. *cac*^{H18} mutants showed a reduction in RS (A, purple bar) without a change in the period (B, purple bar) compared to control flies (open black bars) (Mann-Whitney test). (C) In order to map this phenotype, *cac* was knocked down throughout the clock again leading to a reduction in rhythmicity (D) while increasing the period length compared to *Tim* / + and *cac-RNAi* / + control flies (E). Data was analysed using a Kruskal-Wallis test with Dunn's *post hoc* test. n (*CS*) = 62, n (*cac*^{H18}) = 26, n (*Tim / +)* = 46, n (*Tim > cac-RNAi)* = 112 and n (*cac-RNAi / +)* = 64 flies.

5.4 Discussion

5.4.1 cac knock-down impaired learning and memory and mushroom body calcium handling

Several studies have shown that cacophony is required for wide variety of behaviours, from production of the courtship song in males to the visual-dependent phototactic response (Chan et al., 2002; Kulkarni and Hall, 1987; Smith et al., 1998). The role of *cac* in learning and memory has yet to be fully explored, although a previous study has shown cac levels change in the MBs after a form of memory training called courtship conditioning (Jones et al., 2018). Based on this and the link between Cav2 and memory in mammals (Jeon et al., 2007), I evaluated the role of cac in the MBs in aversive olfactory memory (Fig. 5.1). Data show both STM and ITM were impaired after *cac* knock-down in the MBs. Moreover, the results were confirmed by using two different well-described MBs drivers further agreeing

with the notion of the importance of cac in this memory centre. Therefore, the role of Cav2.2 in memory appears conserved between flies and mammals. Additionally, those changes were reminiscent of what is observed in schizophrenia patients. Several reports have unveiled deficient working memory in individuals with this disorder and moreover, treatments now consider this as one of the important targets to be addressed with new drugs (Dollfus and Lyne, 2017; Topolov and Getova, 2016; Yang and Tsai, 2017).

Little is known about the physiological relevance of cac in Kenyon cells (KCs) which constitute the MB. One report has shown that the spontaneous calcium transients are generated in cultured KCs, and these transients are sensitive to Plectreurys toxin (PLTX), a VGCC blocker (Jiang et al., 2005). Together with observations of N-type calcium channels being PLTX-sensitive, suggests that cac might be regulating the spontaneous activity in KCs (Gu et al., 2009). Here I show that cac knock-down in the MBs was sufficient to reduce around 40% of the calcium influx into MBs lobes upon a depolarizing high [KCl] stimulus (Fig. 5.2). This would also suggest that cac might be important for evoked calcium influx at presynaptic terminals, possibly via increasing neurotransmitter release (Simms and Zamponi, 2014). Further experiments should be conducted to test this, like electrophysiological recordings on the mushroom body output neurons, while activating the mushroom bodies with optogenetics.

There is a requirement for increased calcium influx in the presynaptic terminals as a substrate for long-term potentiation (LTP) (Kaeser and Südhof, 2005; Kavalali, 2015; Leresche and Lambert, 2017). *$Ca_v2.2^{-/-}$* mutants displayed reduced forms of LTP, suggesting the involvement of N-type Ca^{2+} channels in this process (Jeon et al., 2007). In *Drosophila*, *cac* mediates PHP at the NMJ synapse (Davis and Müller, 2014; Lee et al., 2014; Ortega et al., 2018; Peng and Wu, 2007). It was shown that mutants of other genes involved in PHP (e.g. *unc-13*) showed impaired STM (Böhme et al., 2019). Therefore, it is possible that the decreased STM and ITM observed upon *cac* knock-down might arise from its role in PHP.

Interestingly, my results show that knocking-down the *Drosophila* orthologue of the schizophrenia-related gene *CACNA1C, Caα1D (L-type Calcium channel)*, in the MBs resulted in reduced STM and ITM (Appendix C). Nonetheless, no differences in the peak Ca^{2+} signals were found, using the same manipulation as described

here, suggesting that cac and Caα1D differentially contribute to calcium handling in the MBs (Higham et al., 2019).

5.4.2 Locomotor activity and sleep under light-dark conditions are caused by cac loss of function

Locomotor activity was shown to be impaired in the cac^{H18} mutant (Fig 5.3) resulting from an overall increase in the total activity observed in these flies, explained by a night-time hyperactivity. Interestingly, these results are in line with observations in $Ca_V2.2^{-/-}$ mutant mice that displayed increased night-time activity with unchanged day activity when in an habituated environment (Beuckmann et al., 2003). The changes in locomotor activity under LD, were accompanied by an overall decrease in the total sleep time, however, this was accounted for a reduction in both day and night sleep (Fig. 5.4). Insomnia has been reported in schizophrenia patients, and also disrupted activity patterns throughout the day and night, with hyperactivity under night-time being widely observed (Cosgrave et al., 2018; Wulff et al., 2012). My observations match these descriptions and would suggest that monitoring the activity of these flies can serve as a good behavioural output to test schizophrenia-associated genes.

Because cac^{H18} mutants were shown to be defective in visual processing as manifested by reduced phototactic activity (Smith et al., 1998), I specifically knocked down *cac* in the clock network independent of the visual system, and measured the locomotion of these flies. Results from these experiments unveiled an important function of *cac* in the clock circuit, contributing to the modulation of day/night locomotion. Interestingly, differences in total activity and total sleep time were masked, as opposite effects were found in the day versus night. While knocking-down *cac* in the clock (*Tim* > *cac-RNAi*) resulted in reduced day locomotor activity, activity during the night was increased, as in cac^{H18} flies. Similar results were found in a study when knock-down of *cac* in the MBs decreased sleep time during the night with no apparent effect in daytime sleep (Tong et al., 2016).

Although activity phenotypes were similar for cac^{H18} and *Tim* > *cac-RNAi* flies during the night (when comparing with their respective controls), the changes in daytime were not. A possible explanation could arise from the nature of the genetic manipulations. cac^{H18} mutation is affecting all the animal, therefore, effects out of the clock network regulating locomotion might be occurring. Thus, phenotypes

observed here are the sum of the individual contributions of clock and non-clock structures. Considering this, the effects observed at night in the mutant might be driven principally by the clock network, whereas the effects observed during the day are not. Further experiments to dissect which are the components contributing to the hyperactivity observed in the cac^{H18} should be conducted, like restoring the expression of *cac* in the clock and non-clock circuits in the mutant background and evaluating whether day and night-time phenotypes are restored.

5.4.3 Rhythmicity under constant darkness required cac expression in the clock network

The contribution of *cac* in the clock to modulate locomotor activity in DD was recently described. In 2018, Palacios et al. showed that knocking-down *cac* in the clock caused arrhythmicity, an effect that was mimicked by *cac* ablation in the LNvs (Palacios-Muñoz and Ewer, 2018). I obtained similar results by using the cac^{H18} mutant and the *Tim-GAL4* driver, were rhythmicity was highly compromised (Fig. 5.5). Nonetheless, no differences in the free-running period were found by Palacios et al. compared to control flies. I observed an increase in the period when knocking-down *cac* in the clock (Fig. 5.6). A simple explanation might arise from the number of animals used in my experiments compared to the published study. While in the published study they only used 16 animals as GAL4 control (*Tim /* +), 17 as UAS control (*cac-RNAi /* +) and 49 flies in the experimental set (*Tim > cac-RNAi*), I used a more conventional range of n which was 46, 64 and 113, respectively. This difference in the number of animals will considerably increase the power of any statistical analysis, turning even small differences to be significant.

Nonetheless, the effect on rhythmicity was clear in the published study (Palacios-Muñoz and Ewer, 2018), and this study. Knowing the role of *cac* calcium channels in other neurons, it is possible that cac is not mediating changes in excitability in the clock neurons as predicted (Buhl et al., 2019; Julienne et al., 2017). Instead, it is possible that knocking-down *cac* decoupled the components of the clock, leading to the phenotypes reported. Although the effect on rhythmicity is not as drastic as results from completely blocking chemical neurotransmission in the clock using tetanus toxin-light chain, it is possible that the mechanism is the same (Kaneko et al., 2000).

5.5 Conclusions of the chapter

- cac is important in the MBs in modulating aversive olfactory STM and ITM, possible through its function in presynaptic calcium handling and plasticity.
- Locomotor activity is increased, and sleep is reduced during the night in cac^{H18} mutants, effects that are likely due to the role of *cac* in the clock neurons.
- As previously described, *cac* expression in the clock is fundamental for the maintenance of rhythmicity under constant darkness.

Chapter 6: General discussion

There is a current lack of information about the aetiology of schizophrenia and its symptoms, which is hindering the rationale design of more efficacious treatments for all symptoms of the disease (Jones et al., 2011; Meltzer, 2017). One way to help determine the underlying molecular, physiological and circuit level mechanisms underlying the disorder, is the use of animal models which allow the testing of novel experimental drugs. This thesis reports the behavioural and physiological characterization of a number of *Drosophila* models of schizophrenia, supporting the use of this highly genetically tractable animal as a model for this disorder. This work particularly addresses the need for new models of the non-classical symptoms of schizophrenia, which are particularly poorly understood and treated.

6.1 New *Drosophila* models for schizophrenia-associated symptoms

This thesis characterised three models of schizophrenia based on loss of function mutations in fly orthologues of the schizophrenia genes: *Dysb*, *Rim* and *cac.* These mutants displayed a number of schizophrenia relevant defects including impaired olfaction, reduced social interaction, locomotor dysfunctions, memory impairments, sleep disruption and circadian perturbations. The $dysb^{1}$ mutant has previously been used as a fly model of schizophrenia (Shao et al., 2011), so was used as an initial proof-of-principle to replicate and then extend characterisation of a broad range of phenotypes. The battery of behavioural and cell-based assays was then extended to *Rim* and *cac* mutants, which have not been previously used to model schizophrenia-related behaviours in flies. Therefore, this work provides new evidence for the use of this high-throughput and non-protected species as model to explore schizophrenia symptoms and treatments.

6.2 Olfactory performance is reduced in fly models of schizophrenia

In Chapter 2 and 3, behavioural experiments demonstrated *Dysb* and *Rim* mutants had significatively reduced olfactory performance (Fig. 3.1 and 4.1). These results

complement the findings in different models of schizophrenia, where olfactory identification and sensitivity threshold were found to be impaired (Otte et al., 2009; Shan et al., 2018). Consistent with these observations, olfactory acuity was shown to be reduced in patients with schizophrenia (Kohler et al., 2001; Robabeh et al., 2015; Turetsky et al., 2003). The nature of this olfactory dysfunction is unknown. Studies in humans have suggested that structural changes in brain areas that contribute to olfactory processing, like the olfactory bulb and the ventromedial temporal lobe, may underlie these features (Kohler et al., 2001; Turetsky et al., 2003). However, there is somewhat conflicting evidence suggesting that it is possible to get changes in the structure of areas associated with olfactory processing without changes in the olfactory function (Turetsky et al., 2000). I found that knocking-down *Rim* in the fly olfactory AL PNs caused olfactory, structural and functional defects that appeared to be mediated by changes in presynaptic terminals. Likewise, similar neurodevelopmental structural changes have been seen in rodent pharmacological and genetic models of schizophrenia (Jones et al., 2011; Selemon and Zecevic, 2015; Sigurdsson, 2016). However, the nature of these olfactory dysfunctions are not fully understood and require further study (Shan et al., 2018). Future experiments using conditional *Drosophila* mutants could help tease apart the role of schizophrenia genes in development and adult pathology. By using gene rescue experiments it could be possible to ask whether the behavioural or functional effects are reversible.

6.3 Social space, a readout of social interactions, is increased in the schizophrenia gene mutants

Social withdrawal is one of the hallmarks of schizophrenia and has previously been studied in animal models of this disorder (Jones et al., 2011; Tuathaigh et al., 2013). There are many levels at which social impairments can manifest in humans, including changes in social space (Holt et al., 2015). Monitoring social behaviours, by adapting a novel social space paradigm in flies (McNeil et al., 2015; Simon et al., 2012), showed that *dysb*^{1} and *Rim* flies displayed increased social space distance (Fig. 3.2 and 4.2). These findings are in line with studies showing increased social space in individuals with schizophrenia (Holt et al., 2015; Park et al., 2009). Although the neuronal circuits that govern social space in *Drosophila* are not known, a recent study showed that dopamine levels might be involved in

modulating this behaviour. Therefore its mis-regulation may contribute to the pathology of the disease and manipulations that correct dopaminergic signalling might have potential as a treatment for this disorder (Fernandez et al., 2017). Likewise, differences in dopamine levels were also found in *dysb*^{1} flies, which may contribute to the phenotype observed in these animals (Shao et al., 2011). It is not known what is causing the changes in dopamine levels, or whether they occur in *Rim* flies, although it is intriguing that RIM has been shown to be required for dopamine release in the mouse brain (Liu et al., 2018). Future work could test if dopamine levels are changed in *Rim* flies and by which mechanisms. Moreover, it could be possible to assess whether manipulations that restore dopaminergic levels rescue the cellular and behavioural pathology to normal. It might also be possible that the effect observed in mutant flies is due to a neurodevelopmental effect as discussed for the olfactory performance. This would be consistent with observations where neurodevelopmental manipulations in *Drosophila* resulted in social space behaviour deficits as the one here observed (Kaur et al., 2015; Ueoka et al., 2018; Wise et al., 2015). Again, this could be explored through conditional expression of mutant versions of the genes at different stages of life course. Rescue experiments where wildtype versions of Rim are expressed in different spatio-temporal patterns in the *Rim* null flies, looking for recovery of normal physiology and behaviour would also provide very important information on this issue.

6.4 Relationship between the olfactory system and social space

The performance of *dysb*^{1} and *Rim* mutants in the olfactory and social tests together with the vast body of literature in a range of animals showing that several social behaviours depend on the olfactory system, supported the notion that social space in *Drosophila* might rely on the operation of the olfactory system (Hoopfer, 2016). Consistent with this idea, knocking-down *Rim* in the AL PNs, major contributors of olfaction in insects, had profound effects on both, olfaction and social space (Fig. 4.1 and Fig. 4.2). This suggests that social space, as other behaviours, depends on the olfactory performance in flies. It is known that olfactory information is sent by the AL PNs to two major areas: the MB and the LH (Vosshall and Stocker, 2007). It has been proposed that the LH mediates innate olfactory

behaviours while the MB participates in odour-mediated learning (Schultzhaus et al., 2017; Vosshall and Laissue, 2008). *Rim* knock-down in the AL PNs, had the most prominent structural and functional changes in the terminals reaching the LH. These terminals where smaller and displayed reduced calcium responses upon depolarising high [KCl] stimulation (Fig. 4.6 and 4.7). Therefore, consistent with this view, it is possible that social space information is being processed through the olfactory system mediated by the LH. This is also supported by the lack of effect of *Rim* knocked down in the MB (Fig. 4.2).

6.5 *Rim* and *cac* manipulation differentially contributes to learning and memory

Cognitive impairments have been observed in 98% of first-episode schizophrenia patients (Tripathi et al., 2018). Animal models have addressed these impairments by assessing memory in different tasks like fear-conditioning or spatial memory (Jaholkowski et al., 2009; Jones et al., 2011). I used the aversive olfactory conditioning test in flies, which has been extensively used to describe memory processing including impairments displayed by the $dysb^{1}$ mutant (Malik and Hodge, 2014; Shao et al., 2011).

Although we failed to observe any defects in STM and ITM when *Rim* was knocked down in the MB, a clear reduction in memory was found with MB *cac* knockdown (Fig. 4.8 and 5.2). Since it is known that Rim is involved in localization and clustering of cac, this opposite results were a rather unexpected finding (Graf et al., 2012; Kaeser et al., 2011). Several reasons for these results were previously discussed in Chapter 4. The lack of effect with *Rim* but the strong effect with *cac* manipulations suggest that there might be other proteins supplying the function of Rim in the MB. Although in *Drosophila Rim* has the strongest homology with mammal *RIM1*, there is another gene that shares similarities with *RIM1*, *Fife.* Lack of *Fife* in the NMJ caused phenotypic defects like those described in *Rim* mutants in terms of synaptic vesicle docking and priming. This suggests that Fife and Rim might share some functions in *Drosophila* (Bruckner et al., 2012). Furthermore, Fife also drives the accumulation of cac channels to the AZ (Bruckner et al., 2017). Hence, it is possible to think that either Fife is important in the MB while Rim is dispensable, or that the two proteins maybe functionally redundant, such that if one is missing the other is sufficient to drive cac localization to the AZ. Thus, I would

like to propose to characterise *Fife* mutants' MB memory and presynaptic structure and function and as well as perform double mutant analysis on *Rim/Fife, Rim/cac* and *Fife/cac,* to try and determine who is redundant or clustering whom.

6.6 Day/night locomotor activity and sleep phenotypes differs between genes

Sleep and circadian disruptions are observed in up to 80% of schizophrenia patients (Waters and Manoach, 2012). Moreover, they have been linked to the onset and development of psychosis (Cosgrave et al., 2018). *Rim* and *cac* flies displayed altered sleep profiles (Fig. 4.9 and 5.4). The most prominent phenotypes were observed during sleep in the night, with *Rim* flies displaying increased sleep while *cac* flies displayed reduced sleep during the night. Furthermore, *cac* knock-down in the clock was sufficient to cause disrupted night sleep, whereas clock knockdown of *Rim* failed to reproduce the increased night sleep observed in the Rim^{Ex98}/Df mutant (Fig. 4.11 and 5.4). This could be because *Rim* in the clock is not regulating sleep, and in the global knock out, loss of *Rim* in a downstream brain region controlling sleep amount is occurring. Given time I would test the effect of knocking-down Rim in different regions of the brain known to affect sleep. Differences in sleep amount during the night have been reported in schizophrenia, with both increased or reduced sleep, observed in patients (Wulff et al., 2012).

Although Rim and cac are thought to be in the same pathway, the results of this thesis suggest they may function separately and/or in different tissues. One study has shown that RIM1 might have postsynaptic function at cortical synapses (Liu et al., 2018). Hence, it is possible that the phenotypes observed in the *Rim* mutants arise from roles of Rim beyond its canonical function in neurotransmitter release from presynaptic terminals.

6.7 Disruption of rhythmic circadian behaviour is observed in *Drosophila* mutants of schizophrenia genes

Circadian locomotor activity was affected in *Rim* and *cac* mutants (Fig. 4.13 and 5.6). Moreover, these changes were mapped to the fly clock circuit. Both, the *Rim* and *cac* genetic manipulations showed reduced rhythmicity. Nonetheless, the period length was differentially changed in *Rim* and *cac* mutants. Whereas *Rim* knock-down in the clock reduced the free-running period length, the *cac* knock-

down increased the length. As was discussed previously this could be possible if Rim had postsynaptic roles separate to cac. As the major neuronal mediators of rhythmicity under constant darkness are the s-LNvs neurons (Grima et al., 2004; Nitabach et al., 2002), *Rim* and *cac* were knocked down in the LNv and was demonstrated to be sufficient to cause the locomotor arrhythmia (Fig. 4.13). This was accompanied by a loss of the day/night remodelling of the s-LNvs dorsal terminals as well as a loss of day/night difference in PDF accumulation, further suggesting a role of these neurons in the behaviours observed (Fig. 4.14 and 4.15). Possibly, the effects of *cac* knock-down in the clock was through a similar s-LNv remodelling and PDF accumulation mechanism, however, future experiments are needed to confirm this.

6.8 Future directions

6.8.1 To determine if the behavioural and physiological effects observed product of neurodevelopmental and/or functional problems

Schizophrenia has been proposed as a neurodevelopmental disorder (Kahn et al., 2015). The constitutive mutants I characterised would cause loss of function of the schizophrenia genes in development and result in some neuronal structural defects, somewhat consistent with this. As mentioned earlier it is also likely Rim, Dysb and cac have post-developmental roles in adult synapses and the contribution of both, neurodevelopmental and functional effects may underlie the behavioural and physiological changes observed. To test this hypothesis, I propose to knock-down the expression of these genes just in development or just in adult flies thereby separating neurodevelopmental and physiological contributions of these genes to the pathology.

6.8.2 What is the role of Fife and Rim in flies?

As suggested earlier, Fife could be replacing or adding to the function of Rim in the MB. This could potentially explain the lack of effect of *Rim* knocked down in the MB. It is not known if *Fife* is expressed in the MB or whether it influences learning and memory. I would like to test if *Fife* knock-down in this structure or the double mutant experiments suggested above effect MB presynaptic structure and function as well as memory.

6.8.3 Are the effects of *Rim* and *cac* on sleep due to changes in neural excitability of the l-LNvs?

The l-LNvs are wake promoting neurons, and differences in day/night electrical properties of these cells are proposed to drive the sleep-wake cycle in flies (Curran et al., 2019; Parisky et al., 2008; Shang et al., 2008; Sheeba et al., 2008). It is possible that the differences in sleep amount during the night are explained by changes in the properties of these neurons in *Rim* and *cac* mutants. To test this hypothesis whole-cell patch clamp recordings from the l-LNvs during the day and night should be conducted and the effect of clock knockdown of *Rim* or *cac* measured.

6.8.4 Are changes in the dopaminergic and/or serotonergic system observed in *Rim* and *cac* mutants?

Previous publications have shown that dopaminergic levels are increased in $dysb^{1}$ mutants (Shao et al., 2011). Additionally, I have helped to show that the serotonergic levels are reduced in flies with mutations in schizophrenia genes, particularly $dysb^{1}$ mutant (Fig. 3.4). Similar observations have been found in schizophrenia cases in humans (Blelch et al., 1988; Eggers, 2013; Stahl, 2018). I would like to test if this is a general characteristic of the schizophrenia models in *Drosophila* such as in *Rim* and *cac* mutants by measuring dopamine and serotonin levels in these mutants. This could be accompanied by assessing the levels of the biosynthetic enzymes of these neurotransmitters by quantitative RT-PCR. Lastly as alluded to earlier it would be interesting to know if the pharmacological treatments targeting these systems influence the behaviours observed. For instance, by treating the flies with anti-psychotic drugs and testing to see if it corrects their behaviour.

6.9 Final conclusions

Manipulating the expression of schizophrenia-associated genes in flies resulted in a number of interesting behavioural deficits reminiscent of some schizophrenia-relevant behaviours. These included disruption in olfaction, social interactions, locomotion, sleep and circadian locomotor rhythms. Moreover, these where accompanied by both structural and functional properties of the neurons mediating the behavioural changes. As in other models of social interaction, social space

deficits were mediated by the olfactory system, possibly through the AL PNs-LH connections. The results of this thesis add more information to the role of synaptic proteins in circuits mediating behaviour in flies and supports the use of *Drosophila* as a simple genetic model to study schizophrenia.

References

Abboud, R., Noronha, C., Diwadkar, V.A., 2017. Motor system dysfunction in the schizophrenia diathesis: Neural systems to neurotransmitters. Eur. Psychiatry 44, 125–133. https://doi.org/10.1016/j.eurpsy.2017.04.004

Ackermann, F., Waites, C.L., Garner, C.C., 2015. Presynaptic active zones in invertebrates and vertebrates. EMBO Rep. 16, 1–16. https://doi.org/10.15252/embr.201540434

Akmammedov, A., Geigges, M., Paro, R., 2017. Single vector non-leaky gene expression system for *Drosophila melanogaster*. Sci. Rep. 7. https://doi.org/10.1038/s41598-017-07282-w

Ali, Y.O., Escala, W., Ruan, K., Zhai, R.G., 2011. Assaying Locomotor, Learning, and Memory Deficits in *Drosophila* Models of Neurodegeneration. J. Vis. Exp. 1–6. https://doi.org/10.3791/2504

Alphen, B. Van, Swinderen, B. Van, 2013. *Drosophila* strategies to study psychiatric disorders. Brain Res. Bull. 92, 1–11. https://doi.org/10.1016/j.brainresbull.2011.09.007

Andrew, A., Knapp, M., McCrone, P., Parsonage, M., Trachtenberg, M., 2012. Effective interventions in schizophrenia. The economic case: A report prepared for the Schizophrenia Commission. London Rethink Ment. Illn. 1–44.

Arnes, M., Alaniz, M.E., Karam, C.S., Cho, J.D., Lopez, G., Javitch, J.A., Santa-Maria, I., 2019. Role of Tau Protein in Remodeling of Circadian Neuronal Circuits and Sleep. Front. Aging Neurosci. 11, 1–11. https://doi.org/10.3389/fnagi.2019.00320

Auster, T.L., Cohen, A.S., Callaway, D.A., Brown, L.A., 2014. Objective and subjective olfaction across the schizophrenia spectrum. Psychiatry (New York) 77, 57–66. https://doi.org/10.1521/psyc.2014.77.1.57

Ayalew, M., Le-Niculescu, H., Levey, D.F., Jain, N., Changala, B., Patel, S.D., Winiger, E., Breier, A., Shekhar, A., Amdur, R., Koller, D., Nurnberger, J.I., Corvin, A., Geyer, M., Tsuang, M.T., Salomon, D., Schork, N.J., Fanous, A.H., O'Donovan, M.C., Niculescu, A.B., 2012. Convergent functional genomics of schizophrenia: from comprehensive understanding to genetic risk prediction. Mol. Psychiatry 17, 887–905. https://doi.org/10.1038/mp.2012.37

Bauman, M.D., Lesh, T.A., Rowland, D.J., Schumann, C.M., Smucny, J., Kukis, D.L., Cherry, S.R., McAllister, A.K., Carter, C.S., 2019. Preliminary evidence of increased striatal dopamine in a nonhuman primate model of maternal immune activation. Transl. Psychiatry 9. https://doi.org/10.1038/s41398-019-0449-y

Bazzell, B., Ginzberg, S., Healy, L., Wessells, R.J., 2013. Dietary composition regulates *Drosophila* mobility and cardiac physiology. J. Exp. Biol. 216, 859–868. https://doi.org/10.1242/jeb.078758

Benson, K.L., 2006. Sleep in Schizophrenia: Impairments, Correlates, and Treatment. Psychiatr. Clin. North Am. https://doi.org/10.1016/j.psc.2006.08.002

Berrios, G., 1985. Positive and Negative Symptoms and Jackson. Arch Gen Psychiatry. 42, 95–97. https://doi.org/10.1097/00001504-199701000-00007

Beuckmann, C.T., Sinton, C.M., Miyamoto, N., Ino, M., Yanagisawa, M., 2003. N-

Type Calcium Channel α 1B Subunit (Ca V 2.2) Knock-Out Mice Display Hyperactivity and Vigilance State Differences. J. Neurosci. 23, 6793–6797. https://doi.org/10.1523/JNEUROSCI.23-17-06793.2003
Blanchardon, E., Grima, B., Klarsfeld, A., Chélot, E., Hardin, P.E., Préat, T., Rouyer, F., 2001. Defining the role of *Drosophila* lateral neurons in the control of circadian rhythms in motor activity and eclosion by targeted genetic ablation and PERIOD protein overexpression. Eur. J. Neurosci. https://doi.org/10.1046/j.0953-816X.2000.01450.x
Blelch, A., Brown, S.-L., Kahn, R., van Praag, H.M., 1988. The role of serotonin in schizophrenia. Eur. Neuropsychopharmacol. 14, 297–315. https://doi.org/10.1016/0924-977X(95)00027-M
Blundell, J., Kaeser, P.S., Sudhof, T.C., Powell, C.M., 2010. RIM1 and Interacting Proteins Involved in Presynaptic Plasticity Mediate Prepulse Inhibition and Additional Behaviors Linked to Schizophrenia. J. Neurosci. 30, 5326–5333. https://doi.org/10.1523/JNEUROSCI.0328-10.2010
Böhme, M.A., Beis, C., Reddy-Alla, S., Reynolds, E., Mampell, M.M., Grasskamp, A.T., Lützkendorf, J., Bergeron, D.D., Driller, J.H., Babikir, H., Göttfert, F., Robinson, I.M., O'Kane, C.J., Hell, S.W., Wahl, M.C., Stelzl, U., Loll, B., Walter, A.M., Sigrist, S.J., 2016. Active zone scaffolds differentially accumulate Unc13 isoforms to tune Ca2+channel-vesicle coupling. Nat. Neurosci. 19, 1311–1320. https://doi.org/10.1038/nn.4364
Böhme, M.A., McCarthy, A.W., Grasskamp, A.T., Beuschel, C.B., Goel, P., Jusyte, M., Laber, D., Huang, S., Rey, U., Petzoldt, A.G., Lehmann, M., Göttfert, F., Haghighi, P., Hell, S.W., Owald, D., Dickman, D., Sigrist, S.J., Walter, A.M., 2019. Rapid active zone remodeling consolidates presynaptic potentiation. Nat. Commun. 10, 1–16. https://doi.org/10.1038/s41467-019-08977-6
Bosch, J.A., Sumabat, T.M., Hariharan, I.K., 2016. Persistence of RNAi-mediated knockdown in *Drosophila* complicates mosaic analysis yet enables highly sensitive lineage tracing. Genetics 203, 109–118. https://doi.org/10.1534/genetics.116.187062
Brand, A.H., Perrimon, N., 1993. Targeted gene expression as a means of altering cell fates and generating dominant phenotypes. Development 118, 401–415.
Brenman-Suttner, D.B., Long, S.Q., Kamesan, V., De Belle, J.N., Yost, R.T., Kanippayoor, R.L., Simon, A.F., 2018. Progeny of old parents have increased social space in *Drosophila melanogaster*. Sci. Rep. 8, 1–13. https://doi.org/10.1038/s41598-018-21731-0
Brown, A.S., 2012. Epidemiologic studies of exposure to prenatal infection and risk of schizophrenia and autism. Dev. Neurobiol. 72, 1272–1276. https://doi.org/10.1002/dneu.22024
Browne, S., Clarke, M., Gervin, M., Lane, A., Waddington, J.L., Larkin, C., O'Callaghan, E., 2000. Determinants of neurological dysfunction in first episode schizophrenia. Psychol. Med. https://doi.org/10.1017/S003329179900286X
Bruckner, J.J., Gratz, S.J., Slind, J.K., Geske, R.R., Cummings, A.M., Galindo, S.E., Donohue, L.K., O'Connor-Giles, K.M., 2012. Fife, a *Drosophila* Piccolo-RIM homolog, promotes active zone organization and neurotransmitter release. J. Neurosci. 32, 17048–17058. https://doi.org/10.1523/JNEUROSCI.3267-12.2012

Bruckner, J.J., Zhan, H., Gratz, S.J., Rao, M., Ukken, F., Zilberg, G., O'Connor-Giles, K.M., 2017. Fife organizes synaptic vesicles and calcium channels for high-probability neurotransmitter release. J. Cell Biol. 216, 231–246. https://doi.org/10.1083/jcb.201601098

Buhl, E., Higham, J.P., Hodge, J.J.L., 2019. Alzheimer's disease-associated tau alters *Drosophila* circadian activity, sleep and clock neuron electrophysiology. Neurobiol. Dis. 130, 104507. https://doi.org/10.1016/j.nbd.2019.104507

Buoli, M., Caldiroli, A., Panza, G., Altamura, A.C., 2013. Prominent clinical dimension, duration of illness and treatment response in schizophrenia: A naturalistic study. Psychiatry Investig. 10, 354–360.

Burke, C.J., Huetteroth, W., Owald, D., Perisse, E., Krashes, M.J., Das, G., Gohl, D., Silies, M., Certel, S., Waddell, S., 2012. Layered reward signalling through octopamine and dopamine in *Drosophila*. Nature 492, 433–437. https://doi.org/10.1038/nature11614

Busto, G.U., Cervantes-sandoval, I., Davis, R.L., 2016. Olfactory Learning in *Drosophila*. Physiology 25, 338–346. https://doi.org/10.1152/physiol.00026.2010

Campanella, S., Montedoro, C., Streel, E., Verbanck, P., Rosier, V., 2006. Early visual components (P100, N170) are disrupted in chronic schizophrenic patients: an event-related potentials study. Neurophysiol. Clin. 36, 71–78. https://doi.org/10.1016/j.neucli.2006.04.005

Cannon, T.D., Chung, Y., He, G., Sun, D., Jacobson, A., Van, T.G.M., Mcewen, S., Addington, J., Bearden, C.E., Cadenhead, K., Cornblatt, B., Mathalon, D.H., Mcglashan, T., Perkins, D., Jeffries, C., Seidman, L.J., Tsuang, M., Walker, E., Woods, S.W., Heinssen, R., 2014. Progressive Reduction in Cortical Thickness as Psychosis Develops: A Multisite Longitudinal Neuroimaging Study of Youth at Elevated Clinical Risk. Biol. Psychiatry 1–10. https://doi.org/10.1016/j.biopsych.2014.05.023

Carpenter, W.T., Koenig, J.I., 2008. The evolution of drug development in schizophrenia: Past issues and future opportunities. Neuropsychopharmacology. https://doi.org/10.1038/sj.npp.1301639

Castillo, P.E., Schoch, S., Schmitz, F., Südhof, T.C., Malenka, R.C., 2002. RIM1α is required for presynaptic long-term potentiation. Nature 415, 327–330. https://doi.org/10.1038/415327a

Cavaco, S., Goncalves, A., Mendes, A., Vila-Cha, N., Moreira, I., Fernandes, J., Damasio, J., Teixeira-Pinto, A., Bastos Lima, A., 2015. Abnormal Olfaction in Parkinson's Disease Is Related to Faster Disease Progression. Behav. Neurol. 2015, 976589. https://doi.org/10.1155/2015/976589

Cavaliere, S., Malik, B.R., Hodge, J.J.L., 2013. KCNQ Channels Regulate Age-Related Memory Impairment. PLoS One 8. https://doi.org/10.1371/journal.pone.0062445

Chan, B., Villella, A., Funes, P., Hall, J.C., 2002. Courtship and other behaviors affected by a heat-sensitive, molecularly novel mutation in the cacophony calcium-channel gene of *Drosophila*. Genetics 162, 135–153.

Chan, M.-S., Chung, K.-F., Yung, K.-P., Yeung, W.-F., 2017. Sleep in schizophrenia: A systematic review and meta-analysis of polysomnographic findings in case-control studies. Sleep Med. Rev. 32, 69–84. https://doi.org/10.1016/j.smrv.2016.03.001

Chen, X.W., Feng, Y.Q., Hao, C.J., Guo, X.L., He, X., Zhou, Z.Y., Guo, N.,

Huang, H.P., Xiong, W., Zheng, H., Zuo, P.L., Zhang, C.X., Li, W., Zhou, Z., 2008. DTNBP1, a schizophrenia susceptibility gene, affects kinetics of transmitter release. J. Cell Biol. 181, 791–801. https://doi.org/10.1083/jcb.200711021

Clapcote, S.J., Lipina, T. V., Millar, J.K., Mackie, S., Christie, S., Ogawa, F., Lerch, J.P., Trimble, K., Uchiyama, M., Sakuraba, Y., Kaneda, H., Shiroishi, T., Houslay, M.D., Henkelman, R.M., Sled, J.G., Gondo, Y., Porteous, D.J., Roder, J.C.C., 2007. Behavioral Phenotypes of Disc1 Missense Mutations in Mice. Neuron. https://doi.org/10.1016/j.neuron.2007.04.015

Cohrs, S., 2008. Sleep disturbances in patients with schizophrenia : impact and effect of antipsychotics. CNS Drugs 22, 939–962. https://doi.org/10.2165/00023210-200822110-00004

Colomb, J., Reiter, L., Blaszkiewicz, J., Wessnitzer, J., Brembs, B., 2012. Open source tracking and analysis of adult *Drosophila* locomotion in Buridan's paradigm with and without visual targets. PLoS One 7, e42247. https://doi.org/10.1371/journal.pone.0042247

Cornblatt, B. a, Lenzenweger, M.F., Dworkin, R.H., Erlenmeyer-Kimling, L., 1985. Positive and negative schizophrenic symptoms, attention, and information processing. Schizophr. Bull. 11, 397–408. https://doi.org/10.1093/schbul/11.3.397

Cortese, L., Caligiuri, M.P., Malla, A.K., Manchanda, R., Takhar, J., Haricharan, R., 2005. Relationship of neuromotor disturbances to psychosis symptoms in first-episode neuroleptic-naïve schizophrenia patients. Schizophr. Res. https://doi.org/10.1016/j.schres.2004.08.003

Cosgrave, J., Wulff, K., Gehrman, P., 2018. Sleep, circadian rhythms, and schizophrenia: Where we are and where we need to go. Curr. Opin. Psychiatry 31, 176–182. https://doi.org/10.1097/YCO.0000000000000419

Crespo-Facorro, B., Paradiso, S., Andreasen, N.C., O'Leary, D.S., Watkins, G.L., Ponto, L.L., Hichwa, R.D., 2001. Neural mechanisms of anhedonia in schizophrenia: a PET study of response to unpleasant and pleasant odors. JAMA 286, 427–435.

Crow, T.J., 1985. The Two-syndrome Concept: Origins and Current Status. Schizophr. Bull. https://doi.org/10.1093/schbul/11.3.471

Crow, T.J., 1980. Molecular pathology of schizophrenia: more than one disease process? Br. Med. J. 66–68.

Crow, T.J., Baker, H.F., Cross, A.J., Joseph, M.H., Lofthouse, R., Longden, A., Owen, F., Riley, G.J., Glover, V., Killpack, W.S., 1979. Monoamine mechanisms in chronic schizophrenia: post-mortem neurochemical findings. Br. J. Psychiatry 134, 249–256. https://doi.org/10.1192/bjp.134.3.249

Curran, J.A., Buhl, E., Tsaneva-Atanasova, K., Hodge, J.J.L., 2019. Age-dependent changes in clock neuron structural plasticity and excitability are associated with a decrease in circadian output behavior and sleep. Neurobiol. Aging 77, 158–168. https://doi.org/10.1016/j.neurobiolaging.2019.01.025

Curtis, D., Vine, A.E., McQuillin, A., Bass, N.J., Pereira, A., Kandaswamy, R., Lawrence, J., Anjorin, A., Choudhury, K., Datta, S.R., Puri, V., Krasucki, R., Pimm, J., Thirumalai, S., Quested, D., Gurling, H.M.D., 2011. Case-case genome-wide association analysis shows markers differentially associated with schizophrenia and bipolar disorder and implicates calcium channel genes. Psychiatr. Genet. 21, 1–4.

https://doi.org/10.1097/YPG.0b013e3283413382
Darke, H., Peterman, J.S., Park, S., Sundram, S., Carter, O., 2013. Are patients with schizophrenia impaired in processing non-emotional features of human faces? Front. Psychol. https://doi.org/10.3389/fpsyg.2013.00529
Davis, G.W., Müller, M., 2014. Homeostatic Control of Presynaptic Neurotransmitter Release. Annu. Rev. Physiol. 1–20. https://doi.org/10.1146/annurev-physiol-021014-071740
Davis, R.L., 2015. SnapShot : Olfactory Classical Conditioning of *Drosophila*. Cell 163, 524-524.e1. https://doi.org/10.1016/j.cell.2015.09.043
Davis, R.L., 2004. Olfactory Learning. Neuron 44, 31–48.
Dazzan, P., Murray, R.M., 2002. Neurological soft signs in first-episode psychosis: A systematic review. Br. J. Psychiatry. https://doi.org/10.1192/bjp.181.43.s50
Deng, L., Kaeser, P.S., Xu, W., Su, T.C., 2011. RIM Proteins Activate Vesicle Priming by Reversing Autoinhibitory Homodimerization of Munc13. Neuron 317–331. https://doi.org/10.1016/j.neuron.2011.01.005
Depickère, S., Fresneau, D., Deneubourg, J.L., 2004. A basis for spatial and social patterns in ant species: Dynamics and mechanisms of aggregation. J. Insect Behav. 17, 81–97. https://doi.org/10.1023/B:JOIR.0000025134.06111.be
DeRosse, P., Funke, B., Burdick, K.E., Lencz, T., Ekholm, J.M., Kane, J.M., Kucherlapati, R., Malhotra, A.K., 2006. Dysbindin genotype and negative symptoms in schizophrenia. Am. J. Psychiatry 163, 532–534. https://doi.org/10.1176/appi.ajp.163.3.532
Deuš, V., Jokiá-Begić, N., 2006. Personal space in schizophrenic patients. Psychiatr. Danub.
Di Cosmo, G., Costantini, M., Salone, A., Martinotti, G., Di Iorio, G., Di Giannantonio, M., Ferri, F., 2018. Peripersonal space boundary in schizotypy and schizophrenia. Schizophr. Res. https://doi.org/10.1016/j.schres.2017.12.003
Dickman, D.K., Davis, G.W., 2009. The schizophrenia susceptibility gene dysbindin controls synaptic homeostasis. Science (80-.). 326, 1127–1130. https://doi.org/10.1126/science.1179685
Dissel, S., Shaw, P.J., 2016. Sleep Switch. Nature 536, 278–280.
Dollfus, S., Lyne, J., 2017. Negative symptoms: History of the concept and their position in diagnosis of schizophrenia. Schizophr. Res. 186, 3–7. https://doi.org/10.1016/j.schres.2016.06.024
Donelson, N., Kim, E.Z., Slawson, J.B., Vecsey, C.G., Huber, R., Griffith, L.C., 2012. High-resolution positional tracking for long-term analysis of *Drosophila* sleep and locomotion using the “tracker” program. PLoS One 7, e37250. https://doi.org/10.1371/journal.pone.0037250
Dubertret, C., Hanoun, N., Adès, J., Hamon, M., Gorwood, P., 2005. Family-based association study of the 5-HT transporter gene and schizophrenia. Int. J. Neuropsychopharmacol. 87–92.
Dubowy, C., Sehgal, A., 2017. Circadian rhythms and sleep in *Drosophila melanogaster*. Genetics 205, 1373–1397. https://doi.org/10.1534/genetics.115.185157
Duffy, J.B., 2002. GAL4 system in *Drosophila*: A fly geneticist’s swiss army knife. genesis 34, 1–15. https://doi.org/10.1002/gene.10150
Dweck, H.K.M., Ebrahim, S.A.M., Thoma, M., Mohamed, A.A.M., Keesey, I.W.,

Trona, F., Lavista-Llanos, S., Svatos, A., Sachse, S., Knaden, M., Hansson, B.S., 2015. Pheromones mediating copulation and attraction in *Drosophila*. Proc. Natl. Acad. Sci. U. S. A. 112, E2829-35. https://doi.org/10.1073/pnas.1504527112

Eckart, N., Song, Q., Yang, R., Wang, R., Zhu, H., McCallion, A.S., Avramopoulos, D., 2016. Functional Characterization of Schizophrenia-Associated Variation in CACNA1C. PLoS One 11, e0157086. https://doi.org/10.1371/journal.pone.0157086

Egerton, A., Reid, L., McGregor, S., Cochran, S.M., Morris, B.J., Pratt, J.A., 2008. Subchronic and chronic PCP treatment produces temporally distinct deficits in attentional set shifting and prepulse inhibition in rats. Psychopharmacology (Berl). https://doi.org/10.1007/s00213-008-1071-5

Eggers, A.E., 2013. A serotonin hypothesis of schizophrenia. Med. Hypotheses 80, 791–794. https://doi.org/10.1016/j.mehy.2013.03.013

Evensen, S., Wisløff, T., Lystad, J.U., Bull, H., Ueland, T., Falkum, E., 2016. Prevalence, Employment Rate, and Cost of Schizophrenia in a High-Income Welfare Society: A Population-Based Study Using Comprehensive Health and Welfare Registers. Schizophr. Bull. 42, 476–483. https://doi.org/10.1093/schbul/sbv141

Fan, J.B., Sklar, P., 2005. Meta-analysis reveals association between serotonin transporter gene STin2 VNTR polymorphism and schizophrenia. Mol. Psychiatry 10, 928–938. https://doi.org/10.1038/sj.mp.4001690

Fanous, A.H., Kendler, K.S., 2005. Genetic heterogeneity, modifier genes, and quantitative phenotypes in psychiatric illness: Searching for a framework. Mol. Psychiatry 10, 6–13. https://doi.org/10.1038/sj.mp.4001571

Fanous, A.H., Van Den Oord, E.J., Riley, B.P., Aggen, S.H., Neale, M.C., O'Neill, F.A., Walsh, D., Kendler, K.S., 2005. Relationship between a high-risk haplotype in the DTNBP1 (dysbindin) gene and clinical features of schizophrenia. Am. J. Psychiatry 162, 1824–1832. https://doi.org/10.1176/appi.ajp.162.10.1824

Farley, I.J., Shannak, K.S., Hornykiewicz, O., 1980. Brain monoamine changes in chronic paranoid schizophrenia and their possible relation to increased dopamine receptor sensitivity. Adv. Biochem. Psychopharmacol. 21, 427–433.

Farrell, M.S., Werge, T., Sklar, P., Owen, M.J., Ophoff, R.A., O'donovan, M.C., Corvin, A., Cichon, S., Sullivan, P.F., 2015. Evaluating historical candidate genes for schizophrenia. Mol. Psychiatry 20, 555–562. https://doi.org/10.1038/mp.2015.16

Feng, Y.Q., Zhou, Z.Y., He, X., Wang, H., Guo, X.L., Hao, C.J., Guo, Y., Zhen, X.C., Li, W., 2008. Dysbindin deficiency in sandy mice causes reduction of snapin and displays behaviors related to schizophrenia. Schizophr. Res. 106, 218–228. https://doi.org/10.1016/j.schres.2008.07.018

Fernandez, R.W., Akinleye, A.A., Nurilov, M., Feliciano, O., Lollar, M., Aijuri, R.R., O'Donnell, J.M., Simon, A.F., 2017. Modulation of social space by dopamine in *Drosophila melanogaster*, but no effect on the avoidance of the *Drosophila* stress odorant. Biol. Lett. 13, 20170369. https://doi.org/10.1098/rsbl.2017.0369

Ferrarelli, F., Huber, R., Peterson, M.J., Massimini, M., Murphy, M., Riedner, B.A., Watson, A., Bria, P., Tononi, G., 2007. Reduced Sleep Spindle Activity in Schizophrenia Patients. Am. J. Psychiatry 164, 483–492.

Ferrarelli, F., Tononi, G., 2017. Reduced sleep spindle activity point to a TRN-MD thalamus-PFC circuit dysfunction in schizophrenia. Schizophr. Res. 180, 36–43. https://doi.org/10.1016/j.schres.2016.05.023
Fletcher, P.C., Frith, C.D., 2009. Perceiving is believing: A Bayesian approach to explaining the positive symptoms of schizophrenia. Nat. Rev. Neurosci. https://doi.org/10.1038/nrn2536
Fradley, R.L., O'Meara, G.F., Newman, R.J., Andrieux, A., Job, D., Reynolds, D.S., 2005. STOP knockout and NMDA NR1 hypomorphic mice exhibit deficits in sensorimotor gating. Behav. Brain Res. https://doi.org/10.1016/j.bbr.2005.05.012
Fuenzalida-Uribe, N., Campusano, J.M., 2018. Unveiling the Dual Role of the Dopaminergic System on Locomotion and the Innate Value for an Aversive Olfactory Stimulus in *Drosophila*. Neuroscience 371, 433–444. https://doi.org/10.1016/j.neuroscience.2017.12.032
Fuenzalida-Uribe, N., Meza, R.C., Hoffmann, H.A., Varas, R., Campusano, J.M., 2013. NAChR-induced octopamine release mediates the effect of nicotine on a startle response in *Drosophila melanogaster*. J. Neurochem. 125, 281–290. https://doi.org/10.1111/jnc.12161
Funke, B., Finn, C.T., Plocik, A.M., Lake, S., DeRosse, P., Kane, J.M., Kucherlapati, R., Malhotra, A.K., 2004. Association of the DTNBP1 Locus with Schizophrenia in a U.S. Population. Am. J. Hum. Genet. 75, 891–898. https://doi.org/10.1086/425279
Ganapathiraju, M.K., Thahir, M., Handen, A., Sarkar, S.N., Sweet, R.A., Nimgaonkar, V.L., Loscher, C.E., Bauer, E.M., Chaparala, S., 2016. Schizophrenia interactome with 504 novel protein – protein interactions. Nat. Publ. Gr. https://doi.org/10.1038/npjschz.2016.12
Gandini, M.A., Felix, R., 2012. Functional interactions between voltage-gated Ca 2 + channels and Rab3-interacting molecules (RIMs): New insights into stimulus-secretion coupling. Biochim. Biophys. Acta - Biomembr. 1818, 551–558. https://doi.org/10.1016/j.bbamem.2011.12.011
Gargano, J.W., Martin, I., Bhandari, P., Grotewiel, M.S., 2005. Rapid iterative negative geotaxis (RING): A new method for assessing age-related locomotor decline in *Drosophila*. Exp. Gerontol. 40, 386–395. https://doi.org/10.1016/j.exger.2005.02.005
Glessner, J.T., Reilly, M.P., Kim, C.E., Takahashi, N., Albano, A., Hou, C., Bradfield, J.P., Zhang, H., Sleiman, P.M.A., Flory, J.H., Imielinski, M., Frackelton, E.C., Chiavacci, R., Thomas, K.A., Garris, M., Otieno, F.G., Davidson, M., Weiser, M., Reichenberg, A., Davis, K.L., Friedman, J.I., Cappola, T.P., Margulies, K.B., Rader, D.J., Grant, S.F.A., Buxbaum, J.D., Gur, R.E., Hakonarson, H., 2010. Strong synaptic transmission impact by copy number variations in schizophrenia. Proc. Natl. Acad. Sci. U. S. A. 107, 10584–10589. https://doi.org/10.1073/pnas.1000274107
Gorostiza, E.A., Depetris-Chauvin, A., Frenkel, L., Pírez, N., Ceriani, M.F., 2014. Circadian pacemaker neurons change synaptic contacts across the day. Curr. Biol. 24, 2161–2167. https://doi.org/10.1016/j.cub.2014.07.063
Goto, Y., Grace, A.A., 2007. The Dopamine System and the Pathophysiology of Schizophrenia: A Basic Science Perspective. Int. Rev. Neurobiol. 78, 41–68. https://doi.org/10.1016/S0074-7742(06)78002-3
Grace, A.A., 2017. Dopamine System Dysregulation and the Pathophysiology of Schizophrenia: Insights From the Methylazoxymethanol Acetate Model. Biol.

Psychiatry 81, 5–8. https://doi.org/10.1016/j.biopsych.2015.11.007
Grace, A.A., 2016. Dysregulation of the dopamine system in the pathophysiology of schizophrenia and depression. Nat. Rev. Neurosci. 17, 524–532. https://doi.org/10.1038/nrn.2016.57
Graf, E.R., Valakh, V., Wright, C.M., Wu, C., Liu, Z., Zhang, Y.Q., DiAntonio, A., 2012. RIM promotes calcium channel accumulation at active zones of the *Drosophila* neuromuscular junction. J. Neurosci. 32, 16586–96. https://doi.org/10.1523/JNEUROSCI.0965-12.2012
Green, E.K., Grozeva, D., Jones, I., Jones, L., Kirov, G., Caesar, S., Gordon-Smith, K., Fraser, C., Forty, L., Russell, E., Hamshere, M.L., Moskvina, V., Nikolov, I., Farmer, A., McGuffin, P., Holmans, P.A., Owen, M.J., O'Donovan, M.C., Craddock, N., 2010. The bipolar disorder risk allele at CACNA1C also confers risk of recurrent major depression and of schizophrenia. Mol. Psychiatry 15, 1016–1022. https://doi.org/10.1038/mp.2009.49
Grima, B., Chélot, E., Xia, R., Rouyer, F., 2004. Morning and evening peaks of activity rely on different clock neurons of the *Drosophila* brain. Nature 431, 869–873. https://doi.org/10.1038/nature02935
Gu, H., Jiang, S.A., Campusano, J.M., Iniguez, J., Su, H., Hoang, A.A., Lavian, M., Sun, X., O'Dowd, D.K., 2009. Cav2-type calcium channels encoded by cac regulate AP-independent neurotransmitter release at cholinergic synapses in adult *Drosophila* brain. J. Neurophysiol. 101, 42–53. https://doi.org/10.1152/jn.91103.2008
Guo, F., Cerullo, I., Chen, X., Rosbash, M., 2014. PDF neuron firing phase-shifts key circadian activity neurons in *Drosophila*. Elife 2014, 1–21. https://doi.org/10.7554/eLife.02780
Guven-Ozkan, T., Davis, R.L., 2014. Functional neuroanatomy of *Drosophila* olfactory memory formation. Learn. Mem. https://doi.org/10.1101/lm.034363.114
Hales, K.G., Korey, C.A., Larracuente, A.M., Roberts, D.M., 2015. Genetics on the fly: A primer on the *Drosophila* model system. Genetics 201, 815–842. https://doi.org/10.1534/genetics.115.183392
Ham, J.H., Lee, J.J., Sunwoo, M.K., Hong, J.Y., Sohn, Y.H., Lee, P.H., 2016. Effect of olfactory impairment and white matter hyperintensities on cognition in Parkinson's disease. Park. Relat. Disord. 24, 95–99. https://doi.org/10.1016/j.parkreldis.2015.12.017
Han, Y., Kaeser, P.S., Südhof, T.C., Schneggenburger, R., 2011. RIM determines Ca2+ channel density and vesicle docking at the presynaptic active zone. Neuron 69, 304–316. https://doi.org/10.1016/j.neuron.2010.12.014
Harrison, P.J., 2015. Recent genetic findings in schizophrenia and their therapeutic relevance. J. Psychopharmacol. 29, 85–96. https://doi.org/10.1177/0269881114553647
Harrison, P.J., Law, A.J., 2006. Neuregulin 1 and Schizophrenia: Genetics, Gene Expression, and Neurobiology. Biol. Psychiatry 60, 132–140. https://doi.org/10.1016/j.biopsych.2005.11.002
Hattori, S., Murotani, T., Matsuzaki, S., Ishizuka, T., Kumamoto, N., Takeda, M., Tohyama, M., Yamatodani, A., Kunugi, H., Hashimoto, R., 2008. Behavioral abnormalities and dopamine reductions in sdy mutant mice with a deletion in Dtnbp1, a susceptibility gene for schizophrenia. Biochem. Biophys. Res.

Commun. 373, 298–302. https://doi.org/10.1016/j.bbrc.2008.06.016
Haws, M.E., Kaeser, P.S., Jarvis, D.L., Südhof, T.C., Powell, C.M., 2012. Region-specific deletions of RIM1 reproduce a subset of global RIM1α -/- phenotypes. Genes, Brain Behav. 11, 201–213. https://doi.org/10.1111/j.1601-183X.2011.00755.x
Heigwer, F., Port, F., Boutros, M., 2018. RNA Interference (RNAi) Screening in *Drosophila*. https://doi.org/10.1534/genetics.117.300077
Heisenberg, M., 2003. Mushroom body memoir: from maps to models. Nat. Rev. Neurosci. 4, 266–275. https://doi.org/10.1038/nrn1074
Hernandez, I., Sokolov, B.P., 1997. Abnormal expression of serotonin transporter mRNA in the frontal and temporal cortex of schizophrenics 57–64.
Herrero, A., Duhart, J.M., Ceriani, M.F., 2017. Neuronal and glial clocks underlying structural remodeling of pacemaker neurons in *Drosophila*. Front. Physiol. 8, 1–10. https://doi.org/10.3389/fphys.2017.00918
Hidalgo, S., 2019. RIM1αβ Are Required at the Corticostriatal Synapses for Habit Formation. J. Neurosci. https://doi.org/10.1523/JNEUROSCI.0896-19.2019
Hidalgo, S., Molina-Mateo, D., Escobedo, P., Zarate, R. V, Fritz, E., Fierro, A., Perez, E.G., Iturriaga-Vasquez, P., Reyes-Parada, M., Varas, R., Fuenzalida-Uribe, N., Campusano, J.M., 2017. Characterization of a Novel *Drosophila* SERT Mutant: Insights on the Contribution of the Serotonin Neural System to Behaviors. ACS Chem. Neurosci. https://doi.org/10.1021/acschemneuro.7b00089
Higham, J.P., Hidalgo, S., Buhl, E., Hodge, J.J.L., 2019. Restoration of Olfactory Memory in *Drosophila* Overexpressing Human Alzheimer's Disease Associated Tau by Manipulation of L-Type Ca2+ Channels. Front. Cell. Neurosci. 13. https://doi.org/10.3389/fncel.2019.00409
Hikida, T., Jaaro-Peled, H., Seshadri, S., Oishi, K., Hookway, C., Kong, S., Wu, D., Xue, R., Andradé, M., Tankou, S., Mori, S., Gallagher, M., Ishizuka, K., Pletnikov, M., Kida, S., Sawa, A., 2007. Dominant-negative DISC1 transgenic mice display schizophrenia-associated phenotypes detected by measures translatable to humans. Proc. Natl. Acad. Sci. U. S. A. https://doi.org/10.1073/pnas.0704774104
Hildebrand, J.G., Shepherd, G.M., 1997. MECHANISMS OF OLFACTORY DISCRIMINATION:Converging Evidence for Common Principles Across Phyla. Annu. Rev. Neurosci. https://doi.org/10.1146/annurev.neuro.20.1.595
Hirjak, D., Meyer-Lindenberg, A., Kubera, K.M., Thomann, P.A., Wolf, R.C., 2018. Motor dysfunction as research domain in the period preceding manifest schizophrenia: A systematic review. Neurosci. Biobehav. Rev. 87, 87–105. https://doi.org/10.1016/j.neubiorev.2018.01.011
Hodge, J.J., Stanewsky, R., 2008. Function of the Shaw potassium channel within the *Drosophila* circadian clock. PLoS One 3. https://doi.org/10.1371/journal.pone.0002274
Hoff, A.L., Sakuma, M., Wieneke, M., Horon, R., Kushner, M., DeLisi, L.E., 1999. Longitudinal neuropsychological follow-up study of patients with first-episode schizophrenia. Am. J. Psychiatry 156, 1336–1341.
Holt, D.J., Boeke, E.A., Coombs, G., Decross, S.N., Cassidy, B.S., Stufflebeam, S., Rauch, S.L., Tootell, R.B.H., 2015. Abnormalities in personal space and parietal-frontal function in schizophrenia. NeuroImage Clin. 9, 233–243. https://doi.org/10.1016/j.nicl.2015.07.008
Honer, W.G., Kopala, L.C., Rabinowitz, J., 2005. Extrapyramidal symptoms and

signs in first-episode, antipsychotic exposed and non-exposed patients with schizophrenia or related psychotic illness. J. Psychopharmacol. https://doi.org/10.1177/0269881105051539
Hoopfer, E.D., 2016. Neural control of aggression in *Drosophila*. Curr. Opin. Neurobiol. https://doi.org/10.1016/j.conb.2016.04.007
Howes, O.D., McCutcheon, R., Owen, M.J., Murray, R.M., 2017. The Role of Genes, Stress, and Dopamine in the Development of Schizophrenia. Biol. Psychiatry. https://doi.org/10.1016/j.biopsych.2016.07.014
Hubland, A., 2008. Olfaction and olfactory learning in *Drosophila* : recent progress 720–726. https://doi.org/10.1016/j.conb.2007.11.009
Hummel, T., Klämbt, C., 2008. P-element mutagenesis. Methods Mol. Biol. https://doi.org/10.1007/978-1-59745-583-1_6
Insel, T.R., 2010. Rethinking schizophrenia. Nature 468, 187–193. https://doi.org/10.1038/nature09552
Ismail, B., Cantor-Graae, E., McNeil, T.F., 2001. Neurodevelopmental Origins of Tardivelike Dyskinesia in Schizophrenia Patients and Their Siblings. Schizophr. Bull. https://doi.org/10.1093/oxfordjournals.schbul.a006902
Ito, K., Suzuki, K., Estes, P., Ramaswami, M., Yamamoto, D., Strausfeld, N.J., 1998. The Organization of Extrinsic Neurons and Their Implications in the Functional Roles of the Mushroom Bodies in *Drosophila melanogaster* Meigen. Learn. Mem. 5, 52–78.
Jablensky, A., 2010. The diagnostic concept of schizophrenia: its history, evolution, and future prospects. Dialogues Clin. Neurosci. 12, 271–87.
Jaholkowski, P., Kiryk, A., Jedynak, P., Ben Abdallah, N.M., Knapska, E., Kowalczyk, A., Piechal, A., Blecharz-Klin, K., Figiel, I., Lioudyno, V., Widy-Tyszkiewicz, E., Wilczynski, G.M., Lipp, H.P., Kaczmarek, L., Filipkowski, R.K., 2009. New hippocampal neurons are not obligatory for memory formation; cyclin D2 knockout mice with no adult brain neurogenesis show learning. Learn. Mem. 16, 439–451. https://doi.org/10.1101/lm.1459709
Jefferis, G.S.X.E., Potter, C.J., Chan, A.M., Marin, E.C., Rohlfing, T., Maurer, C.R., Luo, L., 2007. Comprehensive Maps of *Drosophila* Higher Olfactory Centers: Spatially Segregated Fruit and Pheromone Representation. Cell 128, 1187–1203. https://doi.org/10.1016/j.cell.2007.01.040
Jeon, D., Kim, C., Yang, Y.M., Rhim, H., Yim, E., Oh, U., Shin, H.S., 2007. Impaired long-term memory and long-term potentiation in N-type Ca 2+ channel-deficient mice. Genes, Brain Behav. 6, 375–388. https://doi.org/10.1111/j.1601-183X.2006.00267.x
Jiang, S.A., Campusano, J.M., Su, H., O'Dowd, D.K., 2005. *Drosophila* mushroom body Kenyon cells generate spontaneous calcium transients mediated by PLTX-sensitive calcium channels. J. Neurophysiol. 94, 491–500. https://doi.org/10.1152/jn.00096.2005
Jones, C., Watson, D., Fone, K., 2011. Animal models of schizophrenia. Br. J. Pharmacol. 1162–1194. https://doi.org/10.1111/j.1476-5381.2011.01386.x
Jones, S.G., Nixon, K.C.J., Chubak, M.C., Kramer, J.M., 2018. Mushroom body specific transcriptome analysis reveals dynamic regulation of learning and memory genes after acquisition of long-term courtship memory in *Drosophila*. G3 Genes, Genomes, Genet. 8, 3433–3446. https://doi.org/10.1534/g3.118.200560
Joyce, J., Shane, A., Lexow, N., Winokur, A., Casanova, M., JE., K., 1993. Serotonin Uptake Sites and Serotonin Receptors Are Altered in the Limbic

System of Schizophrenics. Neuropsychopharmacology 8, 315–336.
Julienne, H., Buhl, E., Leslie, D.S., Hodge, J.J.L., 2017. *Drosophila* PINK1 and parkin loss-of-function mutants display a range of non-motor Parkinson's disease phenotypes. Neurobiol. Dis. 104, 15–23. https://doi.org/10.1016/j.nbd.2017.04.014
Kacsoh, B.Z., Bozler, J., Hodge, S., Bosco, G., 2019. Neural circuitry of social learning in *Drosophila* requires multiple inputs to facilitate inter-species communication. Commun. Biol. 2. https://doi.org/10.1038/s42003-019-0557-5
Kaeser, P.S., Deng, L., Wang, Y., Dulubova, I., Liu, X., Rizo, J., Südhof, T.C., 2011. RIM proteins tether Ca2+ channels to presynaptic active zones via a direct PDZ-domain interaction. Cell 144, 282–295. https://doi.org/10.1016/j.cell.2010.12.029
Kaeser, P.S., Südhof, T.C., 2005. RIM function in short- and long-term synaptic plasticity. Biochem. Soc. Trans. 33, 1345. https://doi.org/10.1042/BST20051345
Kahn, R.S., Sommer, I.E., Murray, R.M., Meyer-Lindenberg, A., Weinberger, D.R., Cannon, T.D., O'Donovan, M., Correll, C.U., Kane, J.M., van Os, J., Insel, T.R., 2015. Schizophrenia. Nat. Rev. Dis. Prim. 1, 15067. https://doi.org/10.1038/nrdp.2015.67
Kaneko, M., Hall, J.C., 2000. Neuroanatomy of cells expressing clock genes in *Drosophila*: Transgenic manipulation of the period and timeless genes to mark the perikarya of circadian pacemaker neurons and their projections. J. Comp. Neurol. 422, 66–94. https://doi.org/10.1002/(SICI)1096-9861(20000619)422:1<66::AID-CNE5>3.0.CO;2-2
Kaneko, M., Park, J.H., Cheng, Y., Hardin, P.E., Hall, J.C., 2000. Disruption of synaptic transmission or clock-gene-product oscillations in circadian pacemaker cells of *Drosophila* cause abnormal behavioral rhythms. J. Neurobiol. 43, 207–233. https://doi.org/10.1002/(SICI)1097-4695(20000605)43:3<207::AID-NEU1>3.0.CO;2-0
Kaur, K., Simon, A.F., Chauhan, V., Chauhan, A., 2015. Effect of bisphenol A on *Drosophila melanogaster* behavior - A new model for the studies on neurodevelopmental disorders. Behav. Brain Res. 284, 77–84. https://doi.org/10.1016/j.bbr.2015.02.001
Kavalali, E.T., 2015. The mechanisms and functions of spontaneous neurotransmitter release. Nat. Rev. Neurosci. 16, 5–16. https://doi.org/10.1038/nrn3875
Kawasaki, F., Collins, S.C., Ordway, R.W., 2002. Synaptic calcium-channel function in *Drosophila*: Analysis and transformation rescue of temperature-sensitive paralytic and lethal mutations of Cacophony. J. Neurosci. 22, 5856–5864. https://doi.org/10.1523/jneurosci.22-14-05856.2002
Kawasaki, F., Zou, B., Xu, X., Ordway W., R., 2004. Active Zone Localization of Presynaptic Calcium Channels Encoded by the cacophony Locus of *Drosophila*. J. Neurosci. 24, 282–285. https://doi.org/10.1523/JNEUROSCI.3553-03.2004
Keshavan, M.S., Reynolds, C.F., Miewald, J.M., Montrose, D.M., Sweeney, J.A., Vasko, R.C., Kupfer, D.J., 1998. Delta Sleep Deficits in Schizophrenia. Arch. Gen. Psychiatry 55, 443. https://doi.org/10.1001/archpsyc.55.5.443
Kiparizoska, S., Ikuta, T., 2017. Disrupted olfactory integration in schizophrenia: Functional connectivity study. Int. J. Neuropsychopharmacol. 20, 740–746.

https://doi.org/10.1093/ijnp/pyx045
Kohler, C.G., Moberg, P.J., Gur, R.E., O'Connor, M.J., Sperling, M.R., Doty, R.L., 2001. Olfactory dysfunction in schizophrenia and temporal lobe epilepsy. Neuropsychiatry. Neuropsychol. Behav. Neurol. 14, 83–88.
Koushika, S.P., Richmond, J.E., Hadwiger, G., Weimer, R.M., Jorgensen, E.M., Nonet, M.L., 2001. A post-docking role for active zone protein Rim. Nat. Neurosci. 4, 997–1005. https://doi.org/10.1038/nn732
Krishnan, B., Dryer, S.E., Hardin, P.E., 1999. Circadian rhythms in olfactory responses of *Drosophila melanogaster*. Nature 400, 375–378. https://doi.org/10.1038/22566
Kula-Eversole, E., Nagoshi, E., Shang, Y., Rodriguez, J., Allada, R., Rosbash, M., 2010. Surprising gene expression patterns within and between PDF-containing circadian neurons in *Drosophila*. Proc. Natl. Acad. Sci. 107, 13497–13502. https://doi.org/10.1073/pnas.1002081107
Kulkarni, S.J., Hall, J.C., 1987. Behavioral and Cytogenetic Analysis of the cacophony Courtship Song Mutant and Interacting Genetic Variants in *Drosophila melanogaster*.
Kuperberg, G., Broome, M., McGuire, P., David, A., Eddy, M., Ozawa, F., Goff, D., West, W., Williams, S., van der Kouwe, A., Salat, D., Dale, A., Fischl, B., 2010. Regionally Localized Thinning of the Cerebral Cortex in Schizophrenia. Schizophrenia 60.
Kupferschmidt, D.A., Augustin, S.M., Johnson, K.A., Lovinger, D.M., 2019. Active Zone Proteins RIM1αβ Are Required for Normal Corticostriatal Transmission and Action Control. J. Neurosci. 39, 1457–1470. https://doi.org/10.1523/jneurosci.1940-18.2018
Kurita, K., Honjo, K., Pandey, H., Ando, T., Takayama, K., Arai, Y., Mochizuki, H., Ando, M., Kamiya, A., 2016. DISC1 causes associative memory and neurodevelopmental defects in fruit flies. Mol. Psychiatry 21, 1232–1243. https://doi.org/10.1038/mp.2016.15
Lally, J., MacCabe, J.H., 2015. Antipsychotic medication in schizophrenia: A review. Br. Med. Bull. 114, 169–179. https://doi.org/10.1093/bmb/ldv017
Larimore, J., Zlatic, S.A., Arnold, M., Singleton, K.S., Cross, R., Rudolph, H., Bruegge, M. V., Sweetman, A., Garza, C., Whisnant, E., Faundez, V., 2017. Dysbindin deficiency modifies the expression of GABA neuron and ion permeation transcripts in the developing hippocampus. Front. Genet. 8, 1–14. https://doi.org/10.3389/fgene.2017.00028
Lee, J., Ueda, A., Wu, C.F., 2014. Distinct roles of *Drosophila* cacophony and Dmca1D Ca2+channels in synaptic homeostasis: Genetic interactions with slowpoke Ca2+-activated BK channels in presynaptic excitability and postsynaptic response. Dev. Neurobiol. 74, 1–15. https://doi.org/10.1002/dneu.22120
Lelan, F., Boyer, C., Thinard, R., Rémy, S., Usal, C., Tesson, L., Anegon, I., Neveu, I., Damier, P., Naveilhan, P., Lescaudron, L., 2011. Effects of Human Alpha-Synuclein A53T-A30P Mutations on SVZ and Local Olfactory Bulb Cell Proliferation in a Transgenic Rat Model of Parkinson Disease. Parkinsons. Dis. 2011, 987084. https://doi.org/10.4061/2011/987084
Leresche, N., Lambert, R.C., 2017. T-type calcium channels in synaptic plasticity. Channels 11, 121–139. https://doi.org/10.1080/19336950.2016.1238992
Levine, J.D., Funes, P., Dowse, H.B., Hall, J.C., 2002a. Advanced analysis of a cryptochrome mutation's effects on the robustness and phase of molecular

cycles in isolated peripheral tissues of *Drosophila*. BMC Neurosci. 3, 1–17. https://doi.org/10.1186/1471-2202-3-5
Levine, J.D., Funes, P., Dowse, H.B., Hall, J.C., 2002b. Signal analysis of behavioral and molecular cycles. BMC Neurosci. https://doi.org/10.1186/1471-2202-3-1
Li, J., Hashimoto, H., Meltzer, H.Y., 2019. Association of serotonin 2C receptor polymorphisms with antipsychotic drug response in schizophrenia. Front. Psychiatry 10. https://doi.org/10.3389/fpsyt.2019.00058
Li, W., Fan, C.C., Mäki-Marttunen, T., Thompson, W.K., Schork, A.J., Bettella, F., Djurovic, S., Dale, A.M., Andreassen, O.A., Wang, Y., 2018. A molecule-based genetic association approach implicates a range of voltage-gated calcium channels associated with schizophrenia. Am. J. Med. Genet. Part B Neuropsychiatr. Genet. 177, 454–467. https://doi.org/10.1002/ajmg.b.32634
Li, W., Zhang, Q., Oiso, N., Novak, E.K., Gautam, R., O'Brien, E.P., Tinsley, C.L., Blake, D.J., Spritz, R.A., Copeland, N.G., Jenkins, N.A., Amato, D., Roe, B.A., Starcevic, M., Dell'Angelica, E.C., Elliott, R.W., Mishra, V., Kingsmore, S.F., Paylor, R.E., Swank, R.T., 2003. Hermansky-Pudlak syndrome type 7 (HPS-7) results from mutant dysbindin, a member of the biogenesis of lysosome-related organelles complex 1 (BLOC-1). Nat. Genet. 35, 84–89. https://doi.org/10.1038/ng1229
Lin, Y., Stormo, G.D., Taghert, P.H., 2004. The neuropeptide pigment-dispersing factor coordinates pacemaker interactions in the *Drosophila* circadian system. J. Neurosci. 24, 7951–7957. https://doi.org/10.1523/JNEUROSCI.2370-04.2004
Liu, C., Kershberg, L., Wang, J., Schneeberger, S., Kaeser, P.S., 2018. Dopamine Secretion Is Mediated by Sparse Active Zone-like Release Sites. Cell 172, 706-718.e15. https://doi.org/10.1016/j.cell.2018.01.008
Lonart, G., 2002. RIM1: An edge for presynaptic plasticity. Trends Neurosci. https://doi.org/10.1016/S0166-2236(02)02193-8
Lowe, S.A., Usowicz, M.M., Hodge, J.J.L., 2019. Neuronal overexpression of Alzheimer's disease and down's syndrome associated DYRK1A/minibrain gene alters motor decline, neurodegeneration and synaptic plasticity in *Drosophila*. Neurobiol. Dis. 125, 107–114. https://doi.org/10.1016/j.nbd.2019.01.017
Lu, B., Shao, L., Feng, S., Wang, T., Zhong, Y., 2014. The beta-alanyl-monoamine synthase ebony is regulated by schizophrenia susceptibility gene dysbindin in *Drosophila*. Sci. China. Life Sci. 57, 46–51. https://doi.org/10.1007/s11427-013-4595-9
Lübbert, M., Goral, R.O., Keine, C., Thomas, C., Guerrero-Given, D., Putzke, T., Satterfield, R., Kamasawa, N., Young, S.M., 2019. Ca V 2.1 α 1 Subunit Expression Regulates Presynaptic Ca V 2.1 Abundance and Synaptic Strength at a Central Synapse. Neuron 101, 260-273.e6. https://doi.org/10.1016/j.neuron.2018.11.028
Luebke, J.I., Dunlap, K., Turner, T.J., 1993. Multiple calcium channel types control glutamatergic synaptic transmission in the hippocampus. Neuron 11, 895–902. https://doi.org/10.1016/0896-6273(93)90119-C
Majeed, Z.R., Abdeljaber, E., Soveland, R., Cornwell, K., Bankemper, A., Koch, F., Cooper, R.L., 2016. Modulatory Action by the Serotonergic System : Behavior and Neurophysiology in *Drosophila melanogaster* 2016. https://doi.org/10.1155/2016/7291438

Malik, B.R., Gillespie, J.M., Hodge, J.J.L., 2013. CASK and CaMKII function in the mushroom body α "/β" neurons during *Drosophila* memory formation. Front. Neural Circuits 7, 1–16. https://doi.org/10.3389/fncir.2013.00052
Malik, B.R., Hodge, J.J.L., 2014. *Drosophila* adult olfactory shock learning. J. Vis. Exp. https://doi.org/10.3791/50107
Mansbach, R.S., Geyer, M.A., 1989. Effects of phencyclidine and phencyclidine biologs on sensorimotor gating in the rat. Neuropsychopharmacology. https://doi.org/10.1016/0893-133x(89)90035-3
Manschreck, T., Maher, B., Rucklos, M., Vereen, D.J., Ader, D., 1981. Deficient motor synchrony in schizophrenia. J. Abnorm. Psychol. 90, 321–328. https://doi.org/10.1037/0021-843X.90.4.321
Manschreck, T., Maher, B., Rucklos, M., Vereen, D.R., 1982. Disturbed voluntary motor activity in schizophrenic disorder. Psychol. Med. 12, 73–84. https://doi.org/10.1017/S0033291700043300
Marosi, C., Fodor, Z., Csukly, G., 2019. From basic perception deficits to facial affect recognition impairments in schizophrenia. Sci. Rep. 9. https://doi.org/10.1038/s41598-019-45231-x
Martin, S.J., Drijfhout, F.P., Hart, A.G., 2019. Phenotypic Plasticity of Nest-Mate Recognition Cues in Formica exsecta Ants. J. Chem. Ecol. 45, 735–740. https://doi.org/10.1007/s10886-019-01103-2
Matosin, N., Fernandez-enright, F., Lum, J.S., Engel, M., Andrews, J.L., Gassen, N.C., Wagner, K. V, Schmidt, M. V, Newell, K.A., 2016. Molecular evidence of synaptic pathology in the CA1 region in schizophrenia. Nat. Publ. Gr. 1–8. https://doi.org/10.1038/npjschz.2016.22
Matsumoto, T., Maeno, Y., Kato, H., Seko-Nakamura, Y., Monma-Ohtaki, J., Ishiba, A., Nagao, M., Aoki, Y., 2014. 5-hydroxytryptamine- and dopamine-releasing effects of ring-substituted amphetamines on rat brain: A comparative study using in vivo microdialysis. Eur. Neuropsychopharmacol. 24, 1362–1370. https://doi.org/10.1016/j.euroneuro.2014.04.009
McGuire, S.E., Mao, Z., Davis, R.L., 2004. Spatiotemporal gene expression targeting with the TARGET and gene-switch systems in *Drosophila*. Sci. STKE 2004. https://doi.org/10.1126/stke.2202004pl6
McNabb, S.L., Truman, J.W., 2008. Light and peptidergic eclosion hormone neurons stimulate a rapid eclosion response that masks circadian emergence in *Drosophila*. J. Exp. Biol. 211, 2263–2274. https://doi.org/10.1242/jeb.015818
McNeil, A.R., Jolley, S.N., Akinleye, A.A., Nurilov, M., Rouzyi, Z., Milunovich, A.J., Chambers, M.C., Simon, A.F., 2015. Conditions Affecting Social Space in *Drosophila melanogaster*. J. Vis. Exp. e53242. https://doi.org/10.3791/53242
Mehnert, K.I., Cantera, R., 2011. Circadian rhythms in the morphology of neurons in *Drosophila*. Cell Tissue Res. https://doi.org/10.1007/s00441-011-1174-x
Meltzer, H.Y., 2017. New Trends in the Treatment of Schizophrenia. CNS Neurol. Disord. - Drug Targets 16. https://doi.org/10.2174/1871527316666170728165355
Metaxakis, A., Oehler, S., Klinakis, A., Savakis, C., 2005. Minos as a genetic and genomic tool in *Drosophila melanogaster*. Genetics. https://doi.org/10.1534/genetics.105.041848
Meyhofer, I., Kumari, V., Hill, A., Petrovsky, N., Ettinger, U., 2017. Sleep deprivation as an experimental model system for psychosis: Effects on

smooth pursuit, prosaccades, and antisaccades. J. Psychopharmacol. 31, 418–433. https://doi.org/10.1177/0269881116675511
Moberg, P.J., Turetsky, B.I., 2003. Scent of a disorder: olfactory functioning in schizophrenia. Curr. Psychiatry Rep. 5, 311–9.
Mohn, A.R., Gainetdinov, R.R., Caron, M.G., Koller, B.H., 1999. Mice with reduced NMDA receptor expression display behaviors related to schizophrenia. Cell. https://doi.org/10.1016/S0092-8674(00)81972-8
Molina-Mateo, D., Fuenzalida-Uribe, N., Hidalgo, S., Molina-Fernández, C., Abarca, J., Zárate, R. V., Escandón, M., Figueroa, R., Tevy, M.F., Campusano, J.M., 2017. Characterization of a presymptomatic stage in a *Drosophila* Parkinson's disease model: Unveiling dopaminergic compensatory mechanisms. Biochim. Biophys. Acta - Mol. Basis Dis. 1863, 2882–2890. https://doi.org/10.1016/j.bbadis.2017.07.013
Monti, J.M., Torterolo, P., Pandi Perumal, S.R., 2017. The effects of second generation antipsychotic drugs on sleep variables in healthy subjects and patients with schizophrenia. Sleep Med. Rev. 33, 51–57. https://doi.org/10.1016/j.smrv.2016.05.002
Moskvina, V., Craddock, N., Holmans, P., Nikolov, I., Pahwa, J.S., Green, E., Owen, M.J., O'Donovan, M.C., 2009. Gene-wide analyses of genome-wide association data sets: evidence for multiple common risk alleles for schizophrenia and bipolar disorder and for overlap in genetic risk. Mol. Psychiatry 14, 252–260. https://doi.org/10.1038/mp.2008.133
Muller, M., Liu, K.S.Y., Sigrist, S.J., Davis, G.W., 2012. RIM Controls Homeostatic Plasticity through Modulation of the Readily-Releasable Vesicle Pool. J. Neurosci. 32, 16574–16585. https://doi.org/10.1523/JNEUROSCI.0981-12.2012
Mullin, A.P., Sadanandappa, M.K., Ma, W., Dickman, D.K., Vijay Raghavan, K., Ramaswami, M., Sanyal, S., Faundez, V., 2015. Gene dosage in the dysbindin schizophrenia susceptibility network differentially affect synaptic function and plasticity. J. Neurosci. 35, 325–338. https://doi.org/10.1523/JNEUROSCI.3542-14.2015
Nakagawasai, O., Onogi, H., Mitazaki, S., Sato, A., Watanabe, K., Saito, H., Murai, S., Nakaya, K., Murakami, M., Takahashi, E., Tan-No, K., Tadano, T., 2010. Behavioral and neurochemical characterization of mice deficient in the N-type Ca 2+ channel α 1B subunit. Behav. Brain Res. 208, 224–230. https://doi.org/10.1016/j.bbr.2009.11.042
Neckameyer, W.S., Coleman, C.M., Eadie, S., Goodwin, S.F., 2007. Compartmentalization of neuronal and peripheral serotonin synthesis in *Drosophila melanogaster*. Genes, Brain Behav. 6, 756–769. https://doi.org/10.1111/j.1601-183X.2007.00307.x
Németh, G., Laszlovszky, I., Czobor, P., Szalai, E., Szatmári, B., Harsányi, J., Barabássy, Á., Debelle, M., Durgam, S., Bitter, I., Marder, S., Fleischhacker, W.W., 2017. Cariprazine versus risperidone monotherapy for treatment of predominant negative symptoms in patients with schizophrenia: a randomised, double-blind, controlled trial. Lancet 389, 1103–1113. https://doi.org/10.1016/S0140-6736(17)30060-0
Nguyen, A.D., Shenton, M.E., Levitt, J.J., 2010. Olfactory dysfunction in schizophrenia: a review of neuroanatomy and psychophysiological measurements. Harv. Rev. Psychiatry 18, 279–292. https://doi.org/10.3109/10673229.2010.511060

Nitabach, M.N., Blau, J., Holmes, T.C., 2002. Electrical Silencing of *Drosophila* Pacemaker Neurons Stops the Free-Running Circadian Clock An important area of circadian rhythm research is the relationship between the function of the molecular clock in pacemaker neurons and the central physiological. Cell 109, 485–495.

Niwa, M., Cash-Padgett, T., Kubo, K.-I., Saito, A., Ishii, K., Sumitomo, A., Taniguchi, Y., Ishizuka, K., Jaaro-Peled, H., Tomoda, T., Nakajima, K., Sawa, A., Kamiya, A., 2016. DISC1 a key molecular lead in psychiatry and neurodevelopment: No-More Disrupted-in-Schizophrenia 1. Mol. Psychiatry 21, 1488–1489. https://doi.org/10.1038/mp.2016.154

O'Connell, K.S., McGregor, N.W., Malhotra, A., Lencz, T., Emsley, R., Warnich, L., 2019. Variation within voltage-gated calcium channel genes and antipsychotic treatment response in a South African first episode schizophrenia cohort. Pharmacogenomics J. 19, 109–114. https://doi.org/10.1038/s41397-018-0033-5

O'Donovan, M.C., Craddock, N., Norton, N., Williams, H., Peirce, T., Moskvina, V., Nikolov, I., Hamshere, M., Carroll, L., Georgieva, L., Dwyer, S., Holmans, P., Marchini, J.L., Spencer, C.C.A., Howie, B., Leung, H.T., Hartmann, A.M., Möller, H.J., Morris, D.W., Shi, Y.Y., Feng, G.Y., Hoffmann, P., Propping, P., Vasilescu, C., Maier, W., Rietschel, M., Zammit, S., Schumacher, J., Quinn, E.M., Schulze, T.G., Williams, N.M., Giegling, I., Iwata, N., Ikeda, M., Darvasi, A., Shifman, S., He, L., Duan, J., Sanders, A.R., Levinson, D.F., Gejman, P. V., Buccola, N.G., Mowry, B.J., Freedman, R., Amin, F., Black, D.W., Silverman, J.M., Byerley, W.F., Cloninger, C.R., Cichon, S., Nöthen, M.M., Gill, M., Corvin, A., Rujescu, D., Kirov, G., Owen, M.J., 2008. Identification of loci associated with schizophrenia by genome-wide association and follow-up. Nat. Genet. 40, 1053–1055. https://doi.org/10.1038/ng.201

Ortega, J.M., Genç, Ö., Davis, G.W., 2018. Molecular mechanisms that stabilize short term synaptic plasticity during presynaptic homeostatic plasticity. Elife 7. https://doi.org/10.7554/eLife.40385

Otte, D.M., Bilkei-Gorzó, A., Filiou, M.D., Turck, C.W., Yilmaz, Ö., Holst, M.I., Schilling, K., Abou-Jamra, R., Schumacher, J., Benzel, I., Kunz, W.S., Beck, H., Zimmer, A., 2009. Behavioral changes in G72/G30 transgenic mice. Eur. Neuropsychopharmacol. https://doi.org/10.1016/j.euroneuro.2008.12.009

Owen, M.J., Williams, N.M., O'Donovan, M.C., 2004. The molecular genetics of schizophrenia: new findings promise new insights. Mol. Psychiatry 9, 14–27. https://doi.org/10.1038/sj.mp.4001444

Palacios-Muñoz, A., Ewer, J., 2018. Calcium and cAMP directly modulate the speed of the *Drosophila* circadian clock. PLoS Genet. 14, 1–21. https://doi.org/10.1371/journal.pgen.1007433

Papaleo, F., Yang, F., Garcia, S., Chen, J., Lu, B., Crawley, J., Weinberger, D.R., 2012. Dysbindin-1 modulates prefrontal cortical activity and schizophrenia-like behaviors via dopamine/D2 pathways. Mol. Psychiatry 17, 85–89. https://doi.org/10.1016/j.pain.2013.06.005.Re-Thinking

Parisky, K.M., Agosto, J., Pulver, S.R., Shang, Y., Kuklin, E., Hodge, J.J.L., Kang, K., Liu, X., Garrity, P.A., Rosbash, M., Griffith, L.C., 2008. PDF Cells Are a GABA-Responsive Wake-Promoting Component of the *Drosophila* Sleep Circuit. Neuron 60, 672–682. https://doi.org/10.1016/j.neuron.2008.10.042

Park, J.H., Helfrich-Förster, C., Lee, G., Liu, L., Rosbash, M., Hall, J.C., 2000. Differential regulation of circadian pacemaker output by separate clock genes in *Drosophila*. Proc. Natl. Acad. Sci. U. S. A. 97, 3608–13. https://doi.org/10.1073/pnas.070036197

Park, S.H., Ku, J., Kim, J.J., Jang, H.J., Kim, S.Y., Kim, S.H., Kim, C.H., Lee, H., Kim, I.Y., Kim, S.I., 2009. Increased personal space of patients with schizophrenia in a virtual social environment. Psychiatry Res. 169, 197–202. https://doi.org/10.1016/j.psychres.2008.06.039

Peng, I.-F., Wu, C.-F., 2007. *Drosophila* cacophony Channels: A Major Mediator of Neuronal Ca2+ Currents and a Trigger for K+ Channel Homeostatic Regulation. J. Neurosci. 27, 1072–1081. https://doi.org/10.1523/JNEUROSCI.4746-06.2007

Peralta, V., Campos, M.S., De Jalón, E.G., Cuesta, M.J., 2010. Motor behavior abnormalities in drug-naïve patients with schizophrenia spectrum disorders. Mov. Disord. https://doi.org/10.1002/mds.23050

Petit, E.I., Michalak, Z., Cox, R., O'Tuathaigh, C.M.P., Clarke, N., Tighe, O., Talbot, K., Blake, D., Joel, J., Shaw, A., Sheardown, S.A., Morrison, A.D., Wilson, S., Shapland, E.M., Henshall, D.C., Kew, J.N., Kirby, B.P., Waddington, J.L., 2017. Dysregulation of Specialized Delay/Interference-Dependent Working Memory Following Loss of Dysbindin-1A in Schizophrenia-Related Phenotypes. Neuropsychopharmacology 42, 1349–1360. https://doi.org/10.1038/npp.2016.282

Pitts, S., Pelser, E., Meeks, J., Smith, D., 2016. Odorant Responses and Courtship Behaviors Influenced by at4 Neurons in *Drosophila*. PLoS One 11, e0162761. https://doi.org/10.1371/journal.pone.0162761

Pletnikov, M. V., Ayhan, Y., Nikolskaia, O., Xu, Y., Ovanesov, M. V., Huang, H., Mori, S., Moran, T.H., Ross, C.A., 2008. Inducible expression of mutant human DISC1 in mice is associated with brain and behavioral abnormalities reminiscent of schizophrenia. Mol. Psychiatry. https://doi.org/10.1038/sj.mp.4002079

Pogue-Geile, M.F., Harrow, M., 1984. Negative and positive symptoms in schizophrenia and depression: a followup. Schizophr. Bull. 10, 371–387.

Poulin, J., Daoust, A.M., Forest, G., Stip, E., Godbout, R., 2003. Sleep architecture and its clinical correlates in first episode and neuroleptic-naive patients with schizophrenia. Schizophr. Res. 62, 147–153. https://doi.org/10.1016/S0920-9964(02)00346-8

Powell, C.M., Schoch, S., Monteggia, L., Barrot, M., Matos, M.F., Feldmann, N., Südhof, T.C., Nestler, E.J., 2004. The presynaptic active zone protein RIM1α is critical for normal learning and memory. Neuron 42, 143–153. https://doi.org/10.1016/S0896-6273(04)00146-1

Purcell, S.M., Moran, J.L., Fromer, M., Ruderfer, D., Solovieff, N., Roussos, P., O'Dushlaine, C., Chambert, K., Bergen, S.E., Kähler, A., Duncan, L., Stahl, E., Genovese, G., Fernández, E., Collins, M.O., Komiyama, N.H., Choudhary, J.S., Magnusson, P.K.E., Banks, E., Shakir, K., Garimella, K., Fennell, T., Depristo, M., Grant, S.G.N., Haggarty, S.J., Gabriel, S., Scolnick, E.M., Lander, E.S., Hultman, C.M., Sullivan, P.F., McCarroll, S.A., Sklar, P., 2014. A polygenic burden of rare disruptive mutations in schizophrenia. Nature 506, 185–190. https://doi.org/10.1038/nature12975

Purves, D., Augustine, G.J., Fitzpatrick, D., Hall, W.C., Lamantia, A.-S., Mcnamara, J.O., Willians, S.M., 2004. Neuroscience, Sunderland.

https://doi.org/978-0878937257
Qian, J., Noebels, J.L., 2001. Presynaptic CA2+ channels and neurotransmitter release at the terminal of a mouse cortical neuron. J. Neurosci. 21, 3721–3728. https://doi.org/10.1523/jneurosci.21-11-03721.2001
Ramsey, A.J., 2009. NR1 knockdown mice as a representative model of the glutamate hypothesis of schizophrenia. Prog. Brain Res. 179, 51–58. https://doi.org/10.1016/S0079-6123(09)17906-2
Renn, S.C.P., Park, J.H., Rosbash, M., Hall, J.C., Taghert, P.H., 1999. A pdf neuropeptide gene mutation and ablation of PDF neurons each cause severe abnormalities of behavioral circadian rhythms in *Drosophila*. Cell 99, 791–802. https://doi.org/10.1016/S0092-8674(00)81676-1
Rieger, D., Peschel, N., Dusik, V., Glotz, S., Helfrich-Förster, C., 2012. The ability to entrain to long photoperiods differs between 3 *Drosophila melanogaster* wild-type strains and is modified by twilight simulation. J. Biol. Rhythms 27, 37–47. https://doi.org/10.1177/0748730411420246
Rieger, D., Shafer, O.T., Tomioka, K., Helfrich-Förster, C., 2006. Functional analysis of circadian pacemaker neurons in *Drosophila melanogaster*. J. Neurosci. 26, 2531–2543. https://doi.org/10.1523/JNEUROSCI.1234-05.2006
Riehle, M., Lincoln, T.M., 2017. Social consequences of subclinical negative symptoms: An EMG study of facial expressions within a social interaction. J. Behav. Ther. Exp. Psychiatry 55, 90–98. https://doi.org/10.1016/j.jbtep.2017.01.003
Ripke, S., Dushlaine, C.O., Chambert, K., Moran, J.L., Anna, K., Akterin, S., Bergen, S., Collins, A.L., Crowley, J.J., Kim, Y., Lee, S.H., Magnusson, P.K.E., Sanchez, N., Eli, A., Williams, S., Wray, N.R., Xia, K., Bettella, F., Anders, D., Hougaard, D.M., Kendler, K.S., Lin, K., Morris, D.W., Milovancevic, M., Posthuma, D., Powell, J., Richards, A.L., Consortium, C., Bramon, E., Corvin, A.P., Donovan, M.C.O., Hultman, M., Sullivan, P.F., 2013. Genome-wide association analysis identifies 13 new risk loci for schizophrenia. Nat. Genet. 45, 1–26. https://doi.org/10.1038/ng.2742.Genome-wide
Robabeh, S., Mohammad, J.M., Reza, A., Mahan, B., 2015. The Evaluation of Olfactory Function in Patients With Schizophrenia. Glob. J. Health Sci. 7, 319–330. https://doi.org/10.5539/gjhs.v7n6p319
Roberts, D.B., 2006. *Drosophila melanogaster*: The model organism. Entomol. Exp. Appl. https://doi.org/10.1111/j.1570-8703.2006.00474.x
Robertson, H.M., Preston, C.R., Phillis, R.W., Johnson-Schlitz, D.M., Benz, W.K., Engels, W.R., 1988. A stable genomic source of P element transposase in *Drosophila melanogaster*. Genetics.
Rupp, C.I., 2010. Olfactory function and schizophrenia: an update. Curr. Opin. Psychiatry 23, 97–102. https://doi.org/10.1097/YCO.0b013e328336643f
Sams-Dodd, F., 1998. A test of the predictive validity of animal models of schizophrenia based on phencyclidine and d-amphetamine. Neuropsychopharmacology. https://doi.org/10.1016/S0893-133X(97)00161-9
Sams-Dodd, F., 1995. Distinct effects of d-amphetamine and phencyclidine on the social behaviour of rats. Behav. Pharmacol. https://doi.org/10.1097/00008877-199501000-00009
Savonenko, A. V., Melnikova, T., Laird, F.M., Stewart, K.A., Price, D.L., Wong, P.C., 2008. Alteration of BACE1-dependent NRG1/ErbB4 signaling and

schizophrenia-like phenotypes in BACE1-null mice. Proc. Natl. Acad. Sci. U. S. A. 105, 5585–5590. https://doi.org/10.1073/pnas.0710373105
Schizophrenia Working Group of the Psychiatric Genomics Consortium, 2014. Biological insights from 108 schizophrenia-associated genetic loci. Nature 511, 421–427. https://doi.org/10.1038/nature13595
Schlichting, M., Díaz, M.M., Xin, J., Rosbash, M., 2019. Neuron-specific knockouts indicate the importance of network communication to *Drosophila* rhythmicity. Elife 8. https://doi.org/10.7554/eLife.48301
Schoch, S., Castillo, P.E., Jo, T., Mukherjee, K., Geppert, M., Wang, Y., Schmitz, F., Malenka, R.C., Südhof, T.C., 2002. RIM1α forms a protein scaffold for regulating neurotransmitter release at the active zone. Nature 415, 321–326. https://doi.org/10.1038/415321a
Scholz, N., Ehmann, N., Sachidanandan, D., Imig, C., Cooper, B.H., Jahn, O., Reim, K., Brose, N., Meyer, J., Lamberty, M., Altrichter, S., Bormann, A., Hallermann, S., Pauli, M., Heckmann, M., Stigloher, C., Langenhan, T., Kittel, R.J., 2019. Complexin cooperates with Bruchpilot to tether synaptic vesicles to the active zone cytomatrix. J. Cell Biol. 218, 1011–1026. https://doi.org/10.1083/jcb.201806155
Schultzhaus, J.N., Saleem, S., Iftikhar, H., Carney, G.E., 2017. The role of the *Drosophila* lateral horn in olfactory information processing and behavioral response. J. Insect Physiol. 98, 29–37. https://doi.org/10.1016/j.jinsphys.2016.11.007
Scialo, F., Sriram, A., Stefanatos, R., Sanz, A., 2016. Practical recommendations for the use of the geneswitch Gal4 system to knock-down genes in *Drosophila melanogaster*. PLoS One 11. https://doi.org/10.1371/journal.pone.0161817
Selemon, L.D., Zecevic, N., 2015. Schizophrenia: a tale of two critical periods for prefrontal cortical development. Transl. Psychiatry 5, e623. https://doi.org/10.1038/tp.2015.115
Selten, J.P., Van Der Ven, E., Termorshuizen, F., 2019. Migration and psychosis: A meta-analysis of incidence studies. Psychol. Med. https://doi.org/10.1017/S0033291719000035
Shan, L., Liu, T., Zhang, Z., Liu, Q., Zhang, M., Zhao, X., Zhang, Y., Xu, F., Ma, Y., 2018. Schizophrenia-like olfactory dysfunction induced by acute and postnatal phencyclidine exposure in rats. Schizophr. Res. 199, 274–280. https://doi.org/10.1016/j.schres.2018.02.045
Shang, Y., Griffith, L.C., Rosbash, M., 2008. Light-arousal and circadian photoreception circuits intersect at the large PDF cells of the *Drosophila* brain. Proc. Natl. Acad. Sci. U. S. A. 105, 19587–19594. https://doi.org/10.1073/pnas.0809577105
Shao, L., Shuai, Y., Wang, J., Feng, S., Lu, B., Li, Z., Zhao, Y., Wang, L., Zhong, Y., 2011. Schizophrenia susceptibility gene dysbindin regulates glutamatergic and dopaminergic functions via distinctive mechanisms in *Drosophila*. Proc. Natl. Acad. Sci. U. S. A. 108, 18831–18836. https://doi.org/10.1073/pnas.1114569108
Shaw, P.J., Cirelli, C., Greenspan, R.J., Tononi, G., 2000. Correlates of Sleep and Waking in *Drosophila melanogaster*. Science (80-.). 287, 1834–1837. https://doi.org/10.1126/science.287.5459.1834
Sheeba, V., Fogle, K.J., Kaneko, M., Rashid, S., Chou, Y.T., Sharma, V.K., Holmes, T.C., 2008. Large Ventral Lateral Neurons Modulate Arousal and

Sleep in *Drosophila*. Curr. Biol. 18, 1537–1545. https://doi.org/10.1016/j.cub.2008.08.033
Sholl, D.A., 1953. Dendritic organization in the neurons of the visual and motor cortices of the cat. J. Anat. 87, 387–406.
Sigurdsson, T., 2016. Neural circuit dysfunction in schizophrenia: Insights from animal models. Neuroscience 321, 42–65. https://doi.org/10.1016/j.neuroscience.2015.06.059
Simms, B.A., Zamponi, G.W., 2014. Neuronal voltage-gated calcium channels: Structure, function, and dysfunction. Neuron 82, 24–45. https://doi.org/10.1016/j.neuron.2014.03.016
Simon, A.F., Chou, M.-T., Salazar, E.D., Nicholson, T., Saini, N., Metchev, S., Krantz, D.E., 2012. A simple assay to study social behavior in *Drosophila*: measurement of social space within a group. Genes. Brain. Behav. 11, 243–252. https://doi.org/10.1111/j.1601-183X.2011.00740.x
Smith, L.A., Peixoto, A.A., Kramer, E.M., Villella, A., Hall, J.C., 1998. Courtship and Visual Defects of cacophony Mutants Reveal Functional Complexity of a Calcium-Channel 1 Subunit in *Drosophila*.
Smith, L.A., Wang, X.J., Peixoto, A.A., Neumann, E.K., Hall, L.M., Hall, J.C., 1996. A *Drosophila* calcium channel α1 subunit gene maps to a genetic locus associated with behavioral and visual defects. J. Neurosci. 16, 7868–7879. https://doi.org/10.1523/jneurosci.16-24-07868.1996
Spina, E., De Domenico, P., Ruello, C., Longobardo, N., Gitto, C., Ancione, M., Di Rosa, A.E., Caputi, A.P., 1994. Adjunctive fluoxetine in the treatment of negative symptoms in chronic schizophrenic patients. Int. Clin. Psychopharmacol. 9, 281–285. https://doi.org/10.1097/00004850-199400940-00007
St Clair, D., Xu, M., Wang, P., Yu, Y., Fang, Y., Zhang, F., Zheng, X., Gu, N., Feng, G., Sham, P., He, L., 2005. Rates of Adult Schizophrenia Following Prenatal Exposure to the Chinese Famine of 1959-1961. JAMA 294, 557. https://doi.org/10.1001/jama.294.5.557
Stahl, S.M., 2018. Beyond the dopamine hypothesis of schizophrenia to three neural networks of psychosis: Dopamine, serotonin, and glutamate. CNS Spectr. 23, 187–191. https://doi.org/10.1017/S1092852918001013
Stanewsky, R., Kaneko, M., Emery, P., Beretta, B., Wager-Smith, K., Kay, S.A., Rosbash, M., Hall, J.C., 1998. The cry(b) mutation identifies cryptochrome as a circadian photoreceptor in *Drosophila*. Cell 95, 681–692. https://doi.org/10.1016/S0092-8674(00)81638-4
Steen, A.N.T., Mull, C., Mcclure, R., Hamer, R.M., Lieberman, J.A., 2004. Brain volume in first-episode schizophrenia Systematic review and meta-analysis of magnetic resonance imaging studies. Imaging i.
Štrac, D.Š., Pivac, N., Mück-Šeler, D., 2016. The serotonergic system and cognitive function. Transl. Neurosci. 7, 35–49. https://doi.org/10.1515/tnsci-2016-0007
Straub, R.E., Jiang, Y., MacLean, C.J., Ma, Y., Webb, B.T., Myakishev, M. V., Harris-Kerr, C., Wormley, B., Sadek, H., Kadambi, B., Cesare, A.J., Gibberman, A., Wang, X., O'Neill, F.A., Walsh, D., Kendler, K.S., 2002. Genetic Variation in the 6p22.3 Gene DTNBP1, the Human Ortholog of the Mouse Dysbindin Gene, Is Associated with Schizophrenia. Am. J. Hum. Genet. 71, 337–348. https://doi.org/10.1086/341750
Striessnig, J., Pinggera, A., Kaur, G., Bock, G., Tuluc, P., 2014. L-type Ca2+

channels in heart and brain. Wiley Interdiscip. Rev. Membr. Transp. Signal. 3, 15–38. https://doi.org/10.1002/wmts.102
Sugie, A., Hakeda-Suzuki, S., Suzuki, E., Silies, M., Shimozono, M., Möhl, C., Suzuki, T., Tavosanis, G., 2015. Molecular Remodeling of the Presynaptic Active Zone of *Drosophila* Photoreceptors via Activity-Dependent Feedback. Neuron 86, 711–726. https://doi.org/10.1016/j.neuron.2015.03.046
Suh, G.S.B., Wong, A.M., Hergarden, A.C., Wang, J.W., 2004. A single population of olfactory sensory neurons mediates an innate avoidance behaviour in *Drosophila*. Nature 431, 854–859.
Sun, J., Giraud, J., Poppinga, H., Riemensperger, T., Fiala, A., Birman, S., 2018. Neural Control of Startle-Induced Locomotion by the Mushroom Bodies and Associated Neurons in *Drosophila*. Front. Syst. Neurosci. 12, 1–18. https://doi.org/10.3389/fnsys.2018.00006
Susser, E.S., 2011. Schizophrenia After Prenatal Exposure to the Dutch Hunger Winter of 1944-1945. Arch. Gen. Psychiatry 49, 983. https://doi.org/10.1001/archpsyc.1992.01820120071010
Svetec, N., Ferveur, J.-F., 2005. Social experience and pheromonal perception can change male-male interactions in *Drosophila melanogaster*. J. Exp. Biol. 208, 891–898. https://doi.org/10.1242/jeb.01454
Taghert, P.H., Shafer, O.T., 2006. Mechanisms of clock output in the *Drosophila* circadian pacemaker system. J. Biol. Rhythms. https://doi.org/10.1177/0748730406293910
Tajima-Pozo, K., de Castro Oller, M.J., Lewczuk, A., Montañes-Rada, F., 2015. Understanding the direct and indirect costs of patients with schizophrenia. F1000Research 4, 182. https://doi.org/10.12688/f1000research.6699.2
Takano, H., 2018. Cognitive function and monoamine neurotransmission in schizophrenia: Evidence from positron emission tomography studies. Front. Psychiatry 9, 1–8. https://doi.org/10.3389/fpsyt.2018.00228
Takeichi, Y., Uebi, T., Miyazaki, N., Murata, K., Yasuyama, K., Inoue, K., Suzaki, T., Kubo, H., Kajimura, N., Takano, J., Omori, T., Yoshimura, R., Endo, Y., Hojo, M.K., Takaya, E., Kurihara, S., Tatsuta, K., Ozaki, K., Ozaki, M., 2018. Putative Neural Network Within an Olfactory Sensory Unit for Nestmate and Non-nestmate Discrimination in the Japanese Carpenter Ant: The Ultra-structures and Mathematical Simulation. Front. Cell. Neurosci. 12, 1–15. https://doi.org/10.3389/fncel.2018.00310
Talbot, K., Cho, D.S., Ong, W.Y., Benson, M.A., Han, L.Y., Kazi, H.A., Kamins, J., Hahn, C.G., Blake, D.J., Arnold, S.E., 2006. Dysbindin-1 is a synaptic and microtubular protein that binds brain snapin. Hum. Mol. Genet. 15, 3041–3054. https://doi.org/10.1093/hmg/ddl246
Talbot, K., Eidem, W.L., Tinsley, C.L., Benson, M.A., Thompson, E.W., Smith, R.J., Hahn, C.G., Siegel, S.J., Trojanowski, J.Q., Gur, R.E., Blake, D.J., Arnold, S.E., 2004. Dysbindin-1 is reduced in intrinsic, glutamatergic terminals of the hippocampal formation in schizophrenia. J. Clin. Invest. 113, 1353–1363. https://doi.org/10.1172/JCI200420425
Tang, A.H., Chen, H., Li, T.P., Metzbower, S.R., MacGillavry, H.D., Blanpied, T.A., 2016. A trans-synaptic nanocolumn aligns neurotransmitter release to receptors. Nature 536, 210–214. https://doi.org/10.1038/nature19058
Tanoue, S., Krishnan, P., Krishnan, B., Dryer, S.E., Hardin, P.E., 2004. Circadian Clocks in Antennal Neurons Are Necessary and Sufficient for Olfaction Rhythms in *Drosophila*. Curr. Biol. 14, 638–649.

https://doi.org/10.1016/j.cub.2004.04.009
Tenn, C.C., Kapur, S., Fletcher, P.J., 2005. Sensitization to amphetamine, but not phencyclidine, disrupts prepulse inhibition and latent inhibition. Psychopharmacology (Berl). https://doi.org/10.1007/s00213-005-2253-z
Tong, H., Li, Q., Zhang, Z.C., Li, Y., Han, J., 2016. Neurexin regulates nighttime sleep by modulating synaptic transmission. Sci. Rep. 6. https://doi.org/10.1038/srep38246
Topolov, M.K., Getova, D.P., 2016. Cognitive Impairment in Schizophrenia, Neurotransmitters and the New Atypical Antipsychotic Aripiprazole. Folia Med. (Plovdiv). 58, 12–18. https://doi.org/10.1515/folmed-2016-0002
Trible, W., Olivos-cisneros, L., Mckenzie, S.K., Matthews, B.J., Oxley, P.R., Kronauer, D.J.C., Trible, W., Olivos-cisneros, L., Mckenzie, S.K., Saragosti, J., Chang, N., 2017. orco Mutagenesis Causes Loss of Antennal Lobe Glomeruli and Impaired Social Behavior in Ants Article orco Mutagenesis Causes Loss of Antennal Lobe Glomeruli and Impaired Social Behavior in Ants. Cell 170, 727-732.e10. https://doi.org/10.1016/j.cell.2017.07.001
Tripathi, A., Kar, S.K., Shukla, R., 2018. Cognitive deficits in schizophrenia: Understanding the biological correlates and remediation strategies. Clin. Psychopharmacol. Neurosci. 16, 7–17. https://doi.org/10.9758/cpn.2018.16.1.7
Tuathaigh, C.M.P.O., Moran, P.M., Waddington, J.L., 2013. Genetic models of schizophrenia and related psychotic disorders : progress and pitfalls across the methodological " minefield ." Cell Tissue Res. 354, 247–257. https://doi.org/10.1007/s00441-013-1652-4
Tully, T., Quinn, W.G., 1985. Classical conditioning and retention in normal and mutant *Drosophila melanogaster*. J. Comp. Physiol. a-Neuroethology Sens. Neural Behav. Physiol. https://doi.org/10.1007/BF01350033
Turetsky, B.I., Moberg, P.J., Roalf, D.R., Arnold, S.E., Gur, R.E., 2003. Decrements in volume of anterior ventromedial temporal lobe and olfactory dysfunction in schizophrenia. Arch. Gen. Psychiatry 60, 1193–1200. https://doi.org/10.1001/archpsyc.60.12.1193
Turetsky, B.I., Moberg, P.J., Yousem, D.M., Doty, R.L., Arnold, S.E., Gur, R.E., 2000. Reduced olfactory bulb volume in patients with schizophrenia. Am. J. Psychiatry 157, 828–830. https://doi.org/10.1176/appi.ajp.157.5.828
Ueoka, I., Kawashima, H., Konishi, A., Aoki, M., Tanaka, R., Yoshida, H., Maeda, T., Ozaki, M., Yamaguchi, M., 2018. Novel *Drosophila* model for psychiatric disorders including autism spectrum disorder by targeting of ATP-binding cassette protein A. Exp. Neurol. 300, 51–59. https://doi.org/10.1016/j.expneurol.2017.10.027
Ugur, T., Weisbrod, M., Franzek, E., Pfuller, U., Sauer, H., 2005. Olfactory impairment in monozygotic twins discordant for schizophrenia. Eur. Arch. Psychiatry Clin. Neurosci. 255, 94–98. https://doi.org/10.1007/s00406-004-0536-8
Van den Pol, A.N., 2012. Neuropeptide Transmission in Brain Circuits. Neuron. https://doi.org/10.1016/j.neuron.2012.09.014
Van Der Ven, E., Selten, J.P., 2018. Migrant and ethnic minority status as risk indicators for schizophrenia: New findings. Curr. Opin. Psychiatry 31, 231–236. https://doi.org/10.1097/YCO.0000000000000405
Vosshall, L.B., 2007. Into the mind of a fly. Nature. https://doi.org/10.1038/nature06335

Vosshall, L.B., Laissue, P.P., 2008. The olfactory sensory map in *Drosophila*. Adv. Exp. Med. Biol. https://doi.org/10.1007/978-0-387-78261-4_7
Vosshall, L.B., Stocker, R.F., 2007. Molecular Architecture of Smell and Taste in *Drosophila*. Annu. Rev. Neurosci. 30, 505–533. https://doi.org/10.1146/annurev.neuro.30.051606.094306
Waddell, S., 2016. Neural Plasticity : Dopamine Tunes the Mushroom Body Output Network. Curr. Biol. 26, R109–R112. https://doi.org/10.1016/j.cub.2015.12.023
Waddell, S., 2013. Reinforcement signalling in *Drosophila*; dopamine does it all after all. Curr. Opin. Neurobiol. 23, 324–329. https://doi.org/10.1016/j.conb.2013.01.005
Walther, S., Strik, W., 2012. Motor symptoms and schizophrenia. Neuropsychobiology 66, 77–92. https://doi.org/10.1159/000339456
Wang, H., Xu, J., Lazarovici, P., Zheng, W., 2017. Dysbindin-1 involvement in the etiology of schizophrenia. Int. J. Mol. Sci. 18, 1–15. https://doi.org/10.3390/ijms18102044
Wang, Q., Abruzzi, K.C., Rosbash, M., Rio, D.C., 2018. Striking circadian neuron diversity and cycling of *Drosophila* alternative splicing. Elife 7, 1–24. https://doi.org/10.7554/eLife.35618
Wang, Y., Südhof, T.C., 2003. Genomic definition of RIM proteins: Evolutionary amplification of a family of synaptic regulatory proteins. Genomics 81, 126–137. https://doi.org/10.1016/S0888-7543(02)00024-1
Waters, F., Manoach, D.S., 2012. Sleep dysfunctions in schizophrenia: A practical review. Open J. Psychiatry 02, 384–392. https://doi.org/10.4236/ojpsych.2012.224054
Wessman, J., Paunio, T., Tuulio-Henriksson, A., Koivisto, M., Partonen, T., Suvisaari, J., Turunen, J.A., Wedenoja, J., Hennah, W., Pietiläinen, O.P.H., Lönnqvist, J., Mannila, H., Peltonen, L., 2009. Mixture Model Clustering of Phenotype Features Reveals Evidence for Association of DTNBP1 to a Specific Subtype of Schizophrenia. Biol. Psychiatry 66, 990–996. https://doi.org/10.1016/j.biopsych.2009.05.034
Widmer, Y.F., Bilican, A., Bruggmann, R., Sprecher, S.G., 2018. Regulators of Long-Term Memory Revealed by Mushroom Body-Specific Gene Expression Profiling in *Drosophila melanogaster*. Genetics 209, 1167–1181. https://doi.org/10.1534/genetics.118.301106
Winblad, B., Bucht, G., Gottfries, C.G., Roos, B. -E, 1979. Monoamines and monoamine metabolites in brains from demented schizophrenics. Acta Psychiatr. Scand. 60, 17–28. https://doi.org/10.1111/j.1600-0447.1979.tb00261.x
Winnebeck, E.C., Millar, C.D., Warman, G.R., 2010. Why Does Insect RNA Look Degraded? J. Insect Sci. 10, 1–7. https://doi.org/10.1673/031.010.14119
Wise, A., Tenezaca, L., Fernandez, R.W., Schatoff, E., Flores, J., Ueda, A., Zhong, X., Wu, C.-F., Simon, A.F., Venkatesh, T., 2015. *Drosophila* mutants of the autism candidate gene neurobeachin (rugose) exhibit neuro-developmental disorders, aberrant synaptic properties, altered locomotion, and impaired adult social behavior and activity patterns. J. Neurogenet. 29, 135–143. https://doi.org/10.3109/01677063.2015.1064916
Wolff, A.L., O'Driscoll, G.A., 1999. Motor deficits and schizophrenia: The evidence from neuroleptic-naïve patients and populations at risk. J. Psychiatry Neurosci. 24, 304.

Wu, Y., Kawasaki, F., Ordway, R.W., 2005. Properties of short-term synaptic depression at larval neuromuscular synapses in wild-type and temperature-sensitive paralytic mutants of *Drosophila*. J. Neurophysiol. 93, 2396–2405. https://doi.org/10.1152/jn.01108.2004

Wulff, K., Dijk, D.J., Middleton, B., Foster, R.G., Joyce, E.M., 2012. Sleep and circadian rhythm disruption in schizophrenia. Br. J. Psychiatry 200, 308–316. https://doi.org/10.1192/bjp.bp.111.096321

Xie, T., Ho, M.C.W., Liu, Q., Horiuchi, W., Lin, C.C., Task, D., Luan, H., White, B.H., Potter, C.J., Wu, M.N., 2018. A Genetic Toolkit for Dissecting Dopamine Circuit Function in *Drosophila*. Cell Rep. 23, 652–665. https://doi.org/10.1016/j.celrep.2018.03.068

Xie, Z., Long, J., Liu, J., Chai, Z., Kang, X., Wang, C., 2017. Molecular Mechanisms for the Coupling of Endocytosis to Exocytosis in Neurons. Front. Mol. Neurosci. 10, 1–8. https://doi.org/10.3389/fnmol.2017.00047

Xu, F.L., Wang, B.-J., Yao, J., 2019. Association between the SLC6A4 gene and schizophrenia: an updated meta-analysis. Neuropsychiatr. Dis. Treat. 15, 143–155. https://doi.org/10.2147/NDT.S190563

Xu, M.Q., Sun, W.S., Liu, B.X., Feng, G.Y., Yu, L., Yang, L., He, G., Sham, P., Susser, E., St. Clair, D., He, L., 2009. Prenatal malnutrition and adult Schizophrenia: Further evidence from the 1959-1961 chinese famine. Schizophr. Bull. 35, 568–576. https://doi.org/10.1093/schbul/sbn168

Xu, Y., Sun, Y., Ye, H., Zhu, L., Liu, J., Wu, X., Wang, L., He, T., Shen, Y., Wu, J.Y., Xu, Q., 2015. Increased dysbindin-1B isoform expression in schizophrenia and its propensity in aggresome formation. Cell Discov. 1, 1–17. https://doi.org/10.1038/celldisc.2015.32

Yan, H., Opachaloemphan, C., Mancini, G., Yang, H., Gallitto, M., Mlejnek, J., Leibholz, A., Haight, K., Ghaninia, M., Huo, L., Perry, M., Slone, J., Zhou, X., Traficante, M., Penick, C.A., Dolezal, K., Gokhale, K., Stevens, K., Fetter-Pruneda, I., Bonasio, R., Zwiebel, L.J., Berger, S.L., Liebig, J., Reinberg, D., Desplan, C., 2017. An Engineered orco Mutation Produces Aberrant Social Behavior and Defective Neural Development in Ants. Cell 170, 736-747.e9. https://doi.org/10.1016/j.cell.2017.06.051

Yang, A.C., Tsai, S.J., 2017. New targets for schizophrenia treatment beyond the dopamine hypothesis. Int. J. Mol. Sci. 18. https://doi.org/10.3390/ijms18081689

Yao, Z., Shafer, O.T., 2014. The *Drosophila* circadian clock is a variably coupled network of multiple peptidergic units. Science (80-.). 343, 1516–1520. https://doi.org/10.1126/science.1251285

Yates, N.J., 2016. Schizophrenia: The role of sleep and circadian rhythms in regulating dopamine and psychosis. Rev. Neurosci. 27, 669–687. https://doi.org/10.1515/revneuro-2016-0030

Zhang, S.-Y., Hu, Q., Tang, T., Liu, C., Li, C.-C., Yang, X.-G., Zang, Y.-Y., Cai, W.-X., 2017. Role of CACNA1C gene polymorphisms and protein expressions in the pathogenesis of schizophrenia: a case-control study in a Chinese population. Neurol. Sci. Off. J. Ital. Neurol. Soc. Ital. Soc. Clin. Neurophysiol. 38, 1393–1403. https://doi.org/10.1007/s10072-017-2963-0

Zhou, Y., Zeidman, P., Wu, S., Razi, A., Chen, C., Yang, L., Zou, J., Wang, G., Wang, H., Friston, K.J., 2018. Altered intrinsic and extrinsic connectivity in schizophrenia. NeuroImage Clin. 17, 704–716. https://doi.org/10.1016/j.nicl.2017.12.006

Zimmerman, J.E., Chan, M.T., Jackson, N., Maislin, G., Pack, A.I., 2012. Genetic Background Has a Major Impact on Differences in Sleep Resulting from Environmental Influences in *Drosophila*. Sleep 35, 545–557. https://doi.org/10.5665/sleep.1744

Appendix A: A published manuscript describing the setup of the single-fly olfactory test

This is a published manuscript in ACS Chemical Neuroscience, describing a characterization of a *Drosophila* Serotonin transporter hypomorphic mutant. In this work, the setup of the single-fly olfactory assay was first proposed. My contribution to this work, as first author, was to assess the behavioural activity of flies and to conduct the neurochemical experiments.

ACS Chemical Neuroscience
Cite This: ACS Chem. Neurosci. 2017, 8, 2168-2179
Research Article
pubs.acs.org/chemneuro

Characterization of a Novel *Drosophila* SERT Mutant: Insights on the Contribution of the Serotonin Neural System to Behaviors

Sergio Hidalgo,[†] Daniela Molina-Mateo,[†] Pía Escobedo,[†] Rafaella V. Zárate,[†] Elsa Fritz,[†] Angélica Fierro,[‡] Edwin G. Perez,[‡] Patricio Iturriaga-Vasquez,[§] Miguel Reyes-Parada,[∥,⊥] Rodrigo Varas,[⊥] Nicolás Fuenzalida-Uribe,[*,†] and Jorge M. Campusano[*,†]

[†]Laboratorio Neurogenética de la Conducta, Departamento de Biología Celular y Molecular, Facultad de Ciencias Biológicas, Pontificia Universidad Católica de Chile, Alameda #340, Santiago, Chile
[‡]Facultad de Química, Pontificia Universidad Católica de Chile, Alameda #340, Santiago, Chile
[§]Facultad de Ingeniería y Ciencias, Universidad de la Frontera, Temuco, Chile
[∥]Escuela de Medicina, Facultad de Ciencias Médicas, Universidad de Santiago de Chile, Santiago, Chile
[⊥]Facultad de Ciencias de la Salud, Universidad Autónoma de Chile, Talca, Chile

Supporting Information

ABSTRACT: A better comprehension on how different molecular components of the serotonergic system contribute to the adequate regulation of behaviors in animals is essential in the interpretation on how they are involved in neuropsychiatric and pathological disorders. It is possible to study these components in "simpler" animal models including the fly *Drosophila melanogaster*, given that most of the components of the serotonergic system are conserved between vertebrates and invertebrates. Here we decided to advance our understanding on how the serotonin plasma membrane transporter (SERT) contributes to serotonergic neurotransmission and behaviors in *Drosophila*. In doing this, we characterized for the first time a mutant for *Drosophila* SERT (dSERT) and additionally used a highly selective serotonin-releasing drug, 4-methylthioamphetamine (4-MTA), whose mechanism of action involves the SERT protein. Our results show that *dSERT* mutant animals exhibit an increased survival rate in stress conditions, increased basal motor behavior, and decreased levels in an anxiety-related parameter, centrophobism. We also show that 4-MTA increases the negative chemotaxis toward a strong aversive odorant, benzaldehyde. Our neurochemical data suggest that this effect is mediated by dSERT and depends on the 4-MTA-increased release of serotonin in the fly brain. Our in silico data support the idea that these effects are explained by specific interactions between 4-MTA and dSERT. In sum, our neurochemical, in silico, and behavioral analyses demonstrate the critical importance of the serotonergic system and particularly dSERT functioning in modulating several behaviors in *Drosophila*.

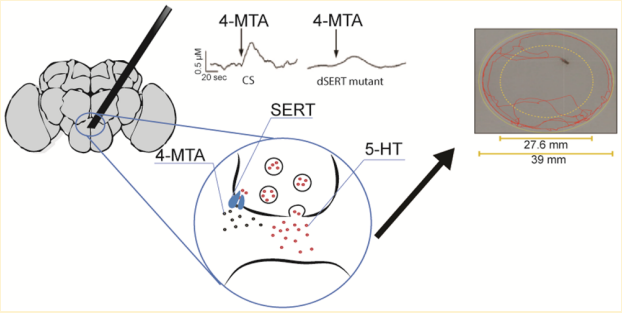

KEYWORDS: *SERT, Drosophila, amine release, olfaction, motor behavior, centrophobism*

INTRODUCTION

Biogenic amines (BAs) are a group of bioactive molecules that act as neurotransmitters/neuromodulators in the central nervous system. They are involved in the regulation of several brain functions, including motor control, learning and memory, mood and affection, motivation, and so forth. Their synthesis, release, and signaling are finely regulated, and it has been described that defects in the ability of aminergic neurons to communicate to other cell populations underlie a number of psychiatric disorders and neurodegenerative diseases. For instance, deregulation of the serotonergic system has been linked to depression, anxiety, and the effects of psychostimulants.[1] As with other classical neurotransmitters, high-affinity reuptake mediated by a plasma membrane transporter, i.e., the serotonin transporter (SERT), plays a key role in the regulation of neurotransmitter levels in the synapse.[2] An altered operation of SERT has been associated with different psychiatric diseases. In addition, SERT is the main molecular target of a broad spectrum of therapeutic and recreational drugs, including antidepressants, anxiolytics, psychostimulants, and anorectics.[3]

A better understanding on the proteins responsible for the adequate regulation of neural aminergic systems is essential for the comprehension of brain normal functioning and the molecular mechanisms responsible for neuropsychiatric diseases. Interestingly, aminergic systems and their cellular components are highly conserved between vertebrates and

Received: March 6, 2017
Accepted: June 30, 2017
Published: June 30, 2017

DOI: 10.1021/acschemneuro.7b00089
ACS Chem. Neurosci. 2017, 8, 2168−2179

invertebrates. Thus, work carried out in invertebrate animal models including the fly *Drosophila melanogaster* has shed some light on the operation of key proteins responsible for normal synaptic communication in vertebrates and their contribution to behaviors. The fly offers additional advantages as a genetic model to modify the function or expression of these proteins, in order to advance our understanding on how neurons communicate to each other, and also to generate models of different pathologies where synaptic proteins are involved.[4,5] Hence, using different pharmacological and genetic tools including mutant flies for different components of the serotonergic system, it has been possible to describe the contribution of this amine to several behaviors, including motor programs,[6] feeding,[7] sleep regulation,[8] and learning and memory.[9]

Interestingly, only a partial and rather scattered description on the functional properties of the serotonin neural system and its contribution to behaviors is available in animal models including *Drosophila*. In the present work, we focused our attention in the *Drosophila* SERT (dSERT) and tested the hypothesis that altering the operation of this protein affects several innate behaviors in flies. We characterized for the first time a mutation in dSERT and performed a neurochemical study to demonstrate that this is an actual mutant. By using this genetic tool and also a highly selective serotonin-releasing agent, 4-methylthioamphetamine (4-MTA[10]), we studied the functional and behavioral consequences of tampering the operation of this protein. A 3D model for dSERT and 4-MTA binding was generated to gain some structural insights on the binding of this protein to its ligands.

RESULTS AND DISCUSSION

Here we attempted to advance our comprehension on the contribution of neural serotonergic system to different behaviors, by pharmacological and genetic manipulations aimed at a particular molecular target, dSERT. In spite of its importance for an adequate regulation of serotonergic neurotransmission in fly brain and the advantages of *Drosophila* as a genetic model, there is no description of a mutant for dSERT, as recently reviewed.[4]

The *dSERT* Mutant Is a Hypomorph. The *dSERT* mutant was generated by the group of Bellen in the Gene Disruption Project.[11] This mutant was obtained by insertion of a transposable element in the intron that separates the exons 3 and 4 of the *Drosophila* SERT gene. This transposable element contains in its sequence a splice acceptor (SA) followed by three stop codons and a polyadenylation site downstream. Thus, it is expected to obtain a null mutant for the dSERT protein (a truncated protein that spans up to the second transmembrane domain) if the splicing machinery recognizes the SA of the transposon. However, it is possible that the splicing machinery bypasses the SA contained in the transposon and recognizes the endogenous SA present in the intron−exon boundary. This situation would generate an animal that is not different from a wildtype fly in terms of its phenotype. It is also possible that both SAs are recognized, to generate both the truncated and the wildtype transcripts and proteins, which phenotypically could behave as a hypomorph.

To evaluate these possibilities we carried out a qPCR with a set of primers that amplify a sequence downstream the insertion site (Figure 1A). Our data suggest a relative reduction of 46.5% of the wildtype PCR product (Figure 1B). This result is consistent with the idea that the *dSERT* mutant is a

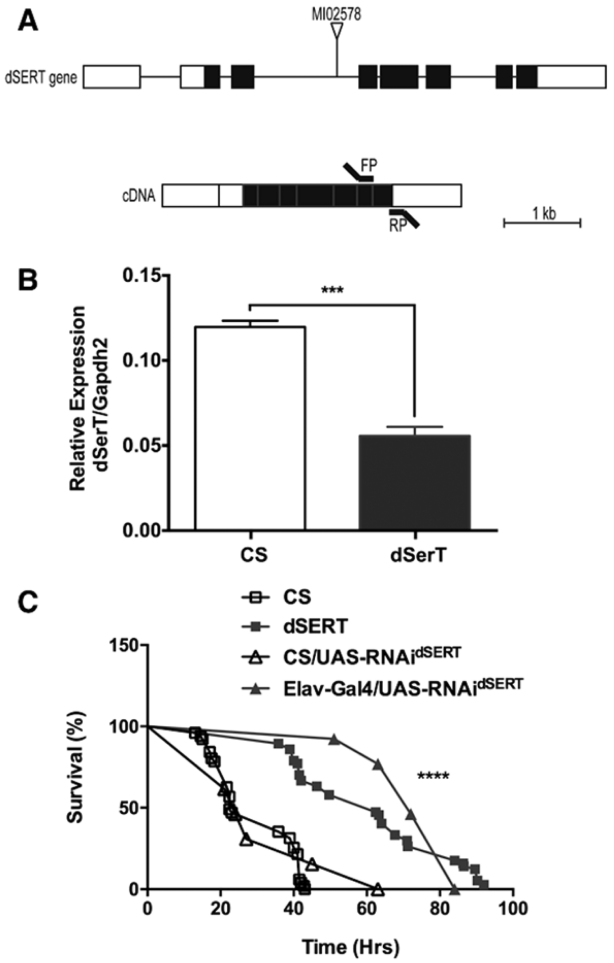

Figure 1. *dSERT* mutant is a hypomorph. (A) Top, schematic representation of the dSERT gene: in black boxes are indicated the exons joined together by the introns (black lines), while in white boxes the untranslated regions of the gene. It is also presented wherein the gene is inserted the P-element (MI0258). Bottom, schematic representation of the dSERT transcript. Primers were designed on exons 7−8 (FP and RP). (B) qPCR results showing a reduced expression of dSERT transcript in mutant flies as compared to controls. ***$p < 0.005$, one sample t test ($n = 3$ independent experiments, a single experiment consists of 100 fly heads from each genotype). (C) Fly survival under desiccation stress. Data shows an increased survival in *dSERT* mutants or in flies where RNAi for dSERT was expressed pan-neurally (elav-gal4/UAS-RNAi^{dSERT}), when compared to control groups (CS and CS/UAS-RNAi^{dSERT}, respectively). ****$p < 0.0001$ after Log-rank (Mantel-Cox) test, as compared to controls ($n = 3$ experiments; each experiment consisting of 20 flies).

hypomorph. Noteworthy, the genetic background of many neuropsychiatric disorders seems to be associated with a partial malfunction of a subset of gene products rather than a full loss of function. Therefore, the dSERT mutant fly described here might constitute a more realistic model for such disorders, similar to what has been proposed for heterozygous SERT mutant mice.[12,13]

To begin the characterization of the *dSERT* mutant, we carried out a fly survival assay under desiccation conditions. This is a study that asks whether a given manipulation affects fly fitness and life-span. Our data show an increase in survival in *dSERT* mutant flies (Figure 1C). Given the dramatic effect of the mutant on survival, we decided to carry out a different

DOI: 10.1021/acschemneuro.7b00089
ACS Chem. Neurosci. 2017, 8, 2168−2179

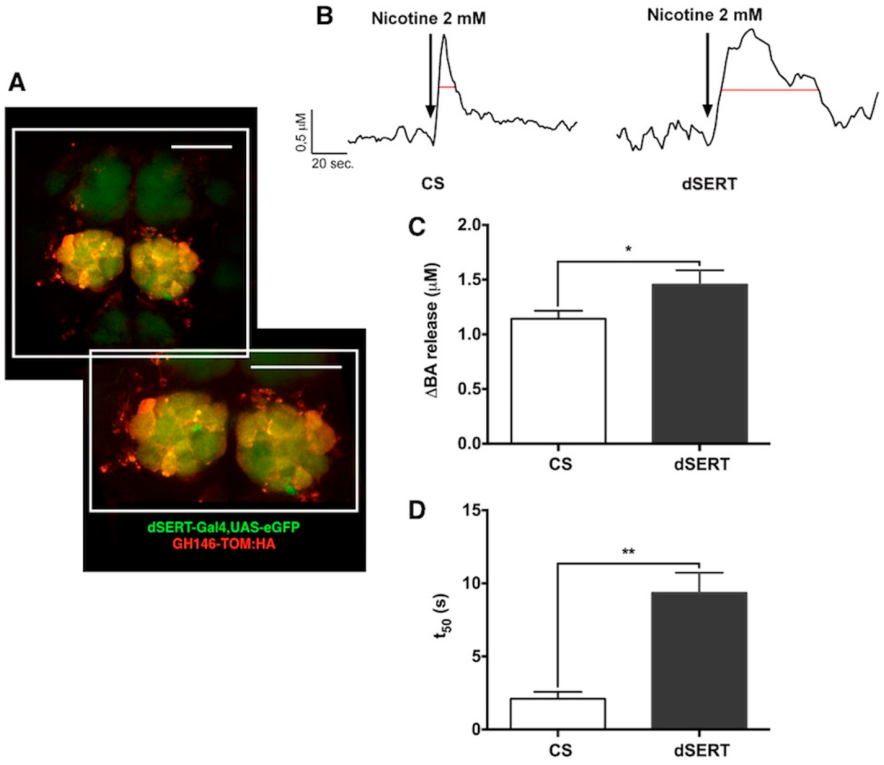

Figure 2. nAChR-evoked release of amines is increased in *dSERT* mutant flies. (A) Microphotograph of a *Drosophila* brain, focusing in the antennal lobe (AL) region. AL neurons expressing tomato fluorescent protein are shown in red, while GFP is detected in the expression pattern of the dSERT gene (in green). It is possible to detect high expression of dSERT in the AL region. Scale bar indicates 50 μm. (B) Representative traces of chronoamperometry recordings in brains of control (CS, left) and *dSERT* mutant (right) flies, in response to 2 mM nicotine. In red it is presented the time to half decay (t_{50}) in the representative experiments. (C) Nicotine-stimulated BAs release is increased in *dSERT* mutant flies (black bars) as compared to control animals (CS, white bars). Fly brains from control and mutant animals were exposed to nicotine and the amine efflux was measured as ΔBA release, which corresponds to the difference between peak amplitude in the presence of the stimulus minus the mean basal signal. (D) The t_{50} for the response after nicotine stimulus is larger in *dSERT* mutant flies (black bars) as compared to CS animals. Data shown in (C) and (D) were obtained in CS (n = 32) and *dSERT* mutant (n = 14) fly brains. *p < 0.05 and **p < 0.005 between experimental groups, unpaired t test.

manipulation to target the same molecular target: the panneural expression of a RNAi directed to dSERT ($RNAi^{dSERT}$), which is a genetic tool previously used to knock-down dSERT expression.[14] Our data show that knocking down dSERT induces the same dramatic effect as the mutant, a dramatic increase in fly survival. Thus, alteration of dSERT expression has a strong effect on survival of flies under desiccation conditions. This result agrees with a previous report that demonstrate that the serotonergic system activates $5HT_{1A}$ receptors to modulate survival of flies exposed to two stressful conditions, starvation and heat.[15] All these data support the idea that the serotoninergic system contributes to stress responses in *Drosophila*. Moreover, they support the idea that serotonin could play a role as a trophic signal in invertebrates, as in vertebrates.

Functional Characterization of *dSERT* Mutant. The generation of new neurochemical techniques has made possible to assess the release of neurotransmitters in different *Drosophila* brain preparations and to functionally characterize synaptic proteins. For instance, by using a new chronoamperometric system we generated[16,17] we recently described that nicotinic acetylcholine receptors (nAChRs) induce the release of BAs in fly brain. This is consistent with the idea that acetylcholine is the main excitatory neurotransmitter in fly brain and that nAChRs mediate fast synaptic excitatory neurotransmission in insects.[18] Here we used the chronoamperometry system to assess the functional properties of dSERT in control and mutant flies. In order to do this, we decided to carry out recordings in the *Drosophila* antennal lobe (AL) region, a fly brain center involved in processing olfactory information, where serotonergic innervation is strongly represented,[19,20] and where it has been previously reported the expression of dSERT (Figure 2A).[21] We hypothesized that *dSERT* mutant flies would show different kinetics of BA release and reuptake as compared to control animals after a nicotine challenge. To assess this, we exposed brains obtained from control and *dSERT* mutant animals to nicotine (2 mM) and the amplitude and the time for the signal to decay to 50% from its maximal amplitude (t_{50}) were calculated, as previously reported.[22,23]

Nicotine induced a significantly higher response in *dSERT* mutants as compared to control brains (Figure 2B,C). Furthermore, the t_{50} for the nicotine-induced response was larger in brains obtained from mutant animals as compared to the response observed in control tissue (Figure 2B,D). Thus, as hypothesized, chronoamperometry studies show that exposure to nicotine induces a fast increase in the extracellular levels of amines, both in control and *dSERT* mutant animals. Importantly, the t_{50}, a kinetic parameter that reflects the clearance of BA from the extracellular space and which is mainly due to the activity of plasma membrane transporter, is altered in mutant flies as compared to control animals (Figure 2). This is a feature that strongly supports the idea that this is a

DOI: 10.1021/acschemneuro.7b00089
ACS Chem. Neurosci. 2017, 8, 2168−2179

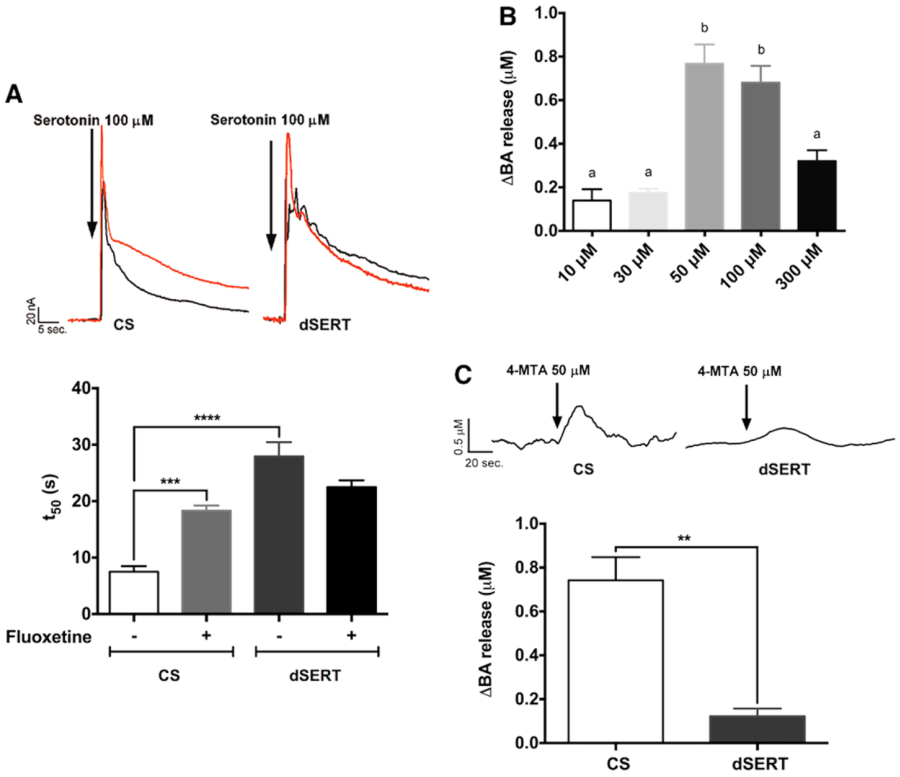

Figure 3. Characterization of *dSERT* mutants. (A) Effect of fluoxetine on serotonin uptake in control and dSERT mutant brains. Top: representative trace of the signal recorded in control (CS, left) or mutant (dSERT, right) brains exposed to a serotonin (100 μM) challenge in absence (black trace) or presence (red trace) of fluoxetine (100 μM). Fluoxetine induces a signal of bigger magnitude than control situation. In addition, the trace suggests that fluoxetine exposure results in a longer time to reach basal levels, consistent with the idea that this chemical blocks dSERT. The effect of fluoxetine is not observed in the representative trace for *dSERT* mutant animals, consistent with the idea that fluoxetine and the mutation are directed to the same molecular target, dSERT. Bottom: t_{50} measured in several brains under conditions indicated above. ***$p < 0.005$ and ****$p < 0.001$; two-way ANOVA followed by Tukey post test, between indicated experimental groups ($n = 10$ brains per condition). ANOVA analysis indicates that strain effect is significant, while drug treatment is not. In addition, interaction between these parameters is also significant. (B) Fly brain exposure to 4-MTA evoked responses that depend on the dose. Here 10 and 30 μM evoked small signals, while 50 and 100 μM induced larger responses. Exposure to 300 μM results in a middle size response ($n = 10$ or more recordings in each condition). ΔBAs values correspond to the difference between peak amplitude in the presence of the stimulus minus the mean basal signal. "a", indicates statistical differences as compared to basal release ($p < 0.05$); "b" indicates statistical differences when compared to basal release ($p < 0.001$), and also when compared to responses recorded when brain tissue is exposed to 4-MTA 10, 30, and 300 μM ($p < 0.05$); one-way ANOVA followed by Tukey post test. (C) Top: Representative traces of chronoamperometry recordings for control CS (left) and *dSERT* mutant (right) animals, in response to 50 μM 4-MTA. Bottom: 4-MTA-stimulated release of endogenous BAs is decreased in *dSERT* mutant flies (black bars) as compared to control CS animals (white bars). Bars correspond to mean ΔBA release in response to 50 μM 4-MTA. **$p < 0.005$, unpaired t test when comparing CS ($n = 32$) and *dSERT* mutant ($n = 15$) flies.

plasma membrane transporter mutant. Moreover, our results are consistent with those obtained in SERT KO mice either measuring the clearance of exogenously added serotonin or its stimulated release.[24,25]

To further support the idea that this is a *dSERT* mutant, we exposed fly brains obtained from control and mutant animals to a serotonin (100 μM) challenge. It would be expected that exposure to serotonin results in an increase in t_{50} in mutant animals as compared to control flies. The representative trace shown in Figure 3A (upper panel) demonstrates that this is what we observe. Moreover, the effect of the mutation on serotonin uptake is not statistically different from the t_{50} recorded when control flies are exposed to fluoxetine (100 μM), a chemical that binds and blocks dSERT (Figure 3A).[23] Exposure of *dSERT* mutant brains to fluoxetine does not have a further effect (Figure 3A). In addition, dopamine (100 μM) uptake is not affected by *dSERT* mutation ($t_{50} = 7.92 \pm 1.36$ in *dSERT* mutant and 6.41 ± 0.64 in control animals, $n = 10$ brains per genotype; $p > 0.05$, t test). All these data are consistent with the idea that fluoxetine and the mutation affect the same molecular target, dSERT.

To further characterize the mutant, we used the amphetamine derivative 4-MTA, a highly selective serotonin-releasing agent[10] whose action in mammals depends on SERT.[26] In our preparation, 4-MTA at 10 or 30 μM induced a small increase in the extracellular levels of amines from control fly brains, while at 50, 100, and 300 μM, a bigger response was observed (Figure 3B). Interestingly, the effect induced at 300 μM was smaller than that detected at 100 μM (Figure 3B), which suggests an inverted-U response curve. Data reported in heterologous systems show that 4-MTA inhibits uptake of serotonin uptake by dSERT with a K_i of 4.6 ± 0.2 μM.[27] We have previously reported that the concentration of the drug effectively reaching the brain in the recording chamber used in our experiments is about 1:200 of what is actually applied in the bolus.[16,17] Thus, the fact that at higher concentrations of 4-MTA smaller effects

DOI: 10.1021/acschemneuro.7b00089
ACS Chem. Neurosci. 2017, 8, 2168−2179

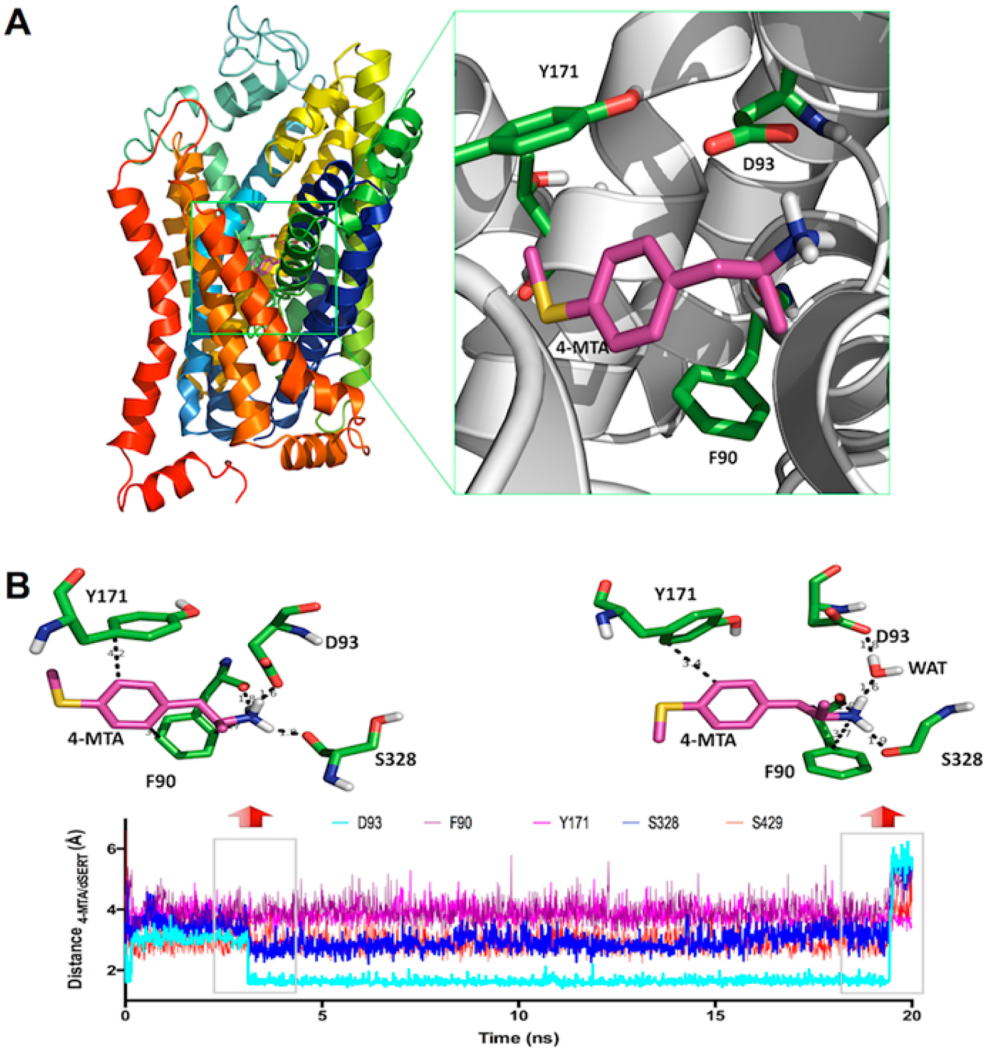

Figure 4. Three-dimensional structure model of dSERT generated by homology modeling. (A) It is shown the dSERT model generated. In close-up (right), it is shown the binding pocket of dSERT where it is possible to observe 4-MTA (purple) and dSERT amino acids D93, Y171 and F90 (green) interacting with the amphetamine derivative. (B) Atomic distances between 4-MTA and the indicated amino acids in the dSERT binding site during the 20 ns molecular dynamics simulations. Top left and right insets show specific interactions between 4-MTA and identified residues of dSERT, at 4 and 19 ns, respectively (indicated in boxes). Numbers represent distance (in Å) between the different groups of 4-MTA and dSERT residues. WAT at 19 ns indicates a water molecule.

is observed, which helps define the inverted U-shape for the response curve, might well be explained by 4-MTA inhibition of dSERT.

To evaluate whether the effect of 4-MTA on the release of amines in *Drosophila* brain depends on the activity of the dSERT protein, we exposed mutant flies to 50 μM 4-MTA, the concentration eliciting the maximal response on amine release in control flies. We observed an ~84% reduction in the response to 4-MTA in *dSERT* mutant flies as compared to control animals (Figure 3C), consistent with the idea that the target of this chemical is the transporter. Importantly, the response after the 4-MTA challenge in *dSERT* mutant animals is different from basal amine release ($p < 0.05$, t test), consistent with the idea that this is a hypomorph mutant. Overall, our neurochemical analysis indicates that the mutant flies show an impaired dSERT activity.

With our chronoamperometric system we are able to detect the release of endogenous BAs in the fly brain, including serotonin, dopamine, tyramine and octopamine. The detection method allows us to differentiate the first two amines from the last two. However, under the experimental conditions used it is not possible to discriminate between dopamine and serotonin.[16,17] Thus, the experiment shown in Figure 3A where it is demonstrated that serotonin uptake is affected in mutant animals supports the idea that we are describing a *dSERT* mutant. On the other hand, the other pharmacological tool used, 4-MTA, shows high selectivity toward mammalian SERT, but it also acts at two other targets, the Dopamine plasma membrane transporter DAT[26,28] and the monoamine oxidase type A (MAO-A).[29,30] Since there is no gene for MAOs in *Drosophila*,[31] the literature available suggests there are only two possible targets for 4-MTA in flies: *Drosophila* DAT (dDAT) and dSERT. Noteworthy, we recorded the efflux of amines in the AL region, a *Drosophila* brain area enriched in serotonergic terminals and where little or no dopaminergic innervation exists.[32−34] Overall, our data support the idea that the amine whose uptake is altered in the mutant animal is serotonin, and that the affected protein is dSERT.

DOI: 10.1021/acschemneuro.7b00089
ACS Chem. Neurosci. 2017, 8, 2168−2179

We would like to make an additional comment on our characterization of the *dSERT* mutant. When characterizing a new mutation in a *Drosophila* protein, some manipulations are common, including experiments that show a decrease in the gene/protein expression (as we did here) and/or the phenotypic rescue of the mutation by re-expression of the wildtype protein. For instance, these were the approaches carried out to characterize the mutant for the *Drosophila* dopamine transporter (dDAT), known as *fumin* or *fmn*.[35] However, as important as this, is to actually show that the activity of the protein of interest is affected in the putative mutant. This was not carried out for the *fmn* mutant until several years later, by the group of Venton.[36] This is partly explained by the fact that only a limited number of research groups have developed neurochemical tools to actually study the efflux of neuroactive substances in *Drosophila* brain. In the case of our work, it is already mapped the site of the insertion in the dSERT gene, and therefore, our experiments serve to show that this is actually a mutant. For doing this, we use an electrochemical system we recently developed and described,[16,17] that allow us to truly assess the release of neuroactive substances in a fly brain preparation. Thus, our data demonstrate that this is a hypomorph *dSERT* mutant.

Molecular Modeling of dSERT. In order to modify the extracellular levels of serotonin, 4-MTA must interact with dSERT. We decided to obtain a structural characterization of the dSERT protein that could give us some insights on the ability of this protein to interact with ligands (in particular 4-MTA) and also to evaluate the stability of the interaction between the transporter and the amphetamine derivative.

For doing this, we first generated a 3D model of the dSERT protein structure, as explained in Materials and Methods. We used as template the 3D structure of the *Drosophila* Dopamine transporter (dDAT, PDB ID: 4XP9, 2.95 Å resolution[37]) because it shares a sequence identity bigger than 50% with the target sequence (sequence alignment is shown in Figure S1). Afterward, the model for dSERT was used to define the main interactions between dSERT and 4-MTA. Figure 4A shows a general view of the binding site of 4-MTA when docked at dSERT. As expected, this site (as well as the interactions drug-residues detected) coincides with the binding pocket occupied by amphetamine in the crystal structure of dDAT.[37] As shown in the close up in Figure 4A, 4-MTA docked at a cavity formed by F90, A91, D93, N96, M167, Y171, S328, L329, G330, F333, S429, T430, and G433 in the dSERT model, which is consistent with the residues described as important for ligand binding in the model for human SERT (e.g., D93 and Y171 in the dSERT correspond to D98 and Y176 in the human protein, respectively[38−40]), which have been recently corroborated in the crystal structure of human SERT.[41] Thus, an ionic interaction between the dSERT D93 residue and the ammonium group of the ligand and also a $\pi-\pi$ interaction between the Y171 residue in dSERT and the aromatic moiety of the ligand appeared as the major contributors for the stabilization of the protein−ligand complex.

In order to obtain more details about the specific interactions in the 4-MTA/dSERT complex we used molecular dynamics (MD) simulation. The plots of RMSD indicate that the drug−protein complex was well equilibrated and remained stable throughout the 20 ns simulation (Figure S2). As mentioned above, docking experiments revealed that several interactions between the protein and the ligand are formed, although the main ones are established by D93, F90, Y171 and S328. The temporal evolution of these interactions, as measured by the distance between the drug and each interacting residue is displayed in Figure 4B. Thus, a cation$-\pi$ interaction is observed between the ammonium group of 4-MTA and the dSERT F90 residue. The MD simulation also supports the interaction between S328 and 4-MTA, mediated by a hydrogen bond. In addition, a strong interaction is observed between the residue D93 with the ammonium group of 4-MTA, given that the distance between these groups decreases over time up to 1.6 Å (Figure 5, top left inset). Interestingly, at 19.5 ns the distance between D93 and 4-MTA increases over 3 Å, by the introduction of a water molecule between these groups (Figure 5, top right inset). The contribution of a water molecule to the stability of the interaction between the transporter and the ligand is a new finding that deserves further study. Thus, our modeling studies suggest a strong, specific interaction between 4-MTA and dSERT,

Behavioral Characterization of the *dSERT* Mutant. Overall, our data support the idea that the tools used in our study are directed to the same molecular target, the dSERT protein. With this validation, we decided to assess the contribution of the serotonin system, and particularly the dSERT protein, to complex behaviors in flies. We focused in three major aspects: olfactory processing, motor control, and an anxiety-related behavior, centrophobism.

It has been previously shown that serotonin modulates the activity of *Drosophila* AL neurons, and it has been proposed that this amine could be involved in the processing of olfactory information in this animal.[19] However, this is an idea that has not been actually tested. We postulated that if serotonin is involved in processing olfactory information in the AL, then the behavioral response of flies to odorants should be altered in *dSERT* mutants. In order to assess this, we used a behavioral assay[42] that allows us to evaluate different motor parameters and also the response to odorants. We studied the behavioral response of flies toward benzaldehyde (Bz), which has been described as one of the strongest aversive odorants in *Drosophila*.[43,44]

Control and *dSERT* mutant flies were recorded before any stimulus and then in the presence of Bz. In absence of any olfactory stimulus, flies do not show a naïve preference for any specific part of the arena (Figure S3). On the other hand Bz presentation induces a negative chemotaxis, which was evidenced as a movement toward the opposite side of the arena. A representative experiment is shown in Figure 5A. Data from different experiments is quantified as performance index (PI), and shows that, as hypothesized, fly exposure to Bz induces a negative chemotaxis (aversion), expressed as PI greater than zero (first bar, Figure 5B).

We then tested whether an acute pretreatment with 4-MTA (5 min before the assay) modifies the aversion to Bz in control flies. Our results show that 4-MTA (1 μM) generated a significant increase in the aversive response to Bz, an effect not observed at the other drug concentrations evaluated (Figure 5B). Similar results were observed when we treated control flies with other drugs known to increase serotonin extracellular levels, and whose actions depend on the SERT protein (Figure S4A).

Interestingly, mutant dSERT flies showed an aversive response to Bz of similar magnitude to that observed in control animals. However, the increased aversive response to Bz induced by 4-MTA was not observed in these flies (Figure 5C). Altogether, these data suggest that the initial aversive response

DOI: 10.1021/acschemneuro.7b00089
ACS Chem. Neurosci. 2017, 8, 2168−2179

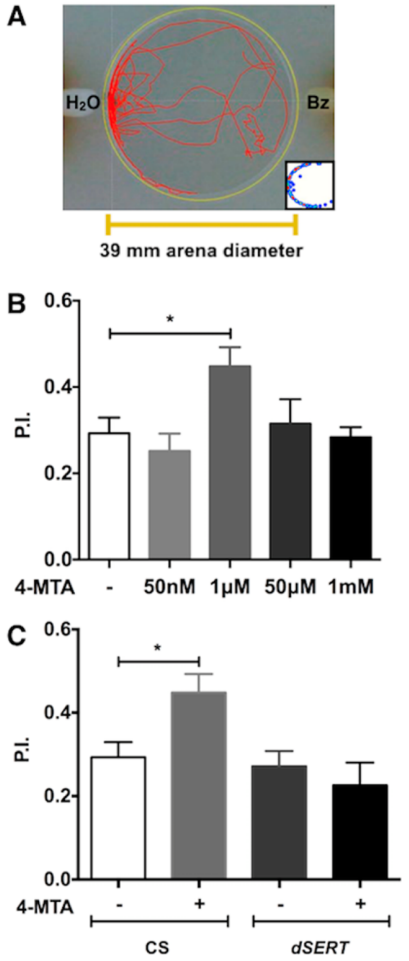

Figure 5. 4-MTA induces an increased aversive response to Bz that depends on dSERT. (A) Setup for behavioral assay. It is possible to track the movement of fly in a circular arena (red traces). In the representative experiment shown, it is observed the aversive effect of benzaldehyde (Bz) placed in the right side of the arena, as evidenced in the red trace and also in inset in lower right corner, as a heat map of the position of the fly during the experiment. (B) Exposure to 4-MTA (1 μM) induces an increased aversion to Bz in flies. Aversive olfactory response toward Bz, measured as positive performance index (PI) in control situation (absence of odorant, white bar, n = 25) and at different 4-MTA concentrations: 50 nM (n = 15 flies); 1 μM (n = 19 animals); 50 μM (n = 18 flies) and 1 mM (n = 17 flies). *p < 0.05, one-way ANOVA followed by Tukey post test when comparing groups. (C) Increase in aversion to Bz is not observed in *dSERT* mutants exposed to 4-MTA. Mean aversive responses (expressed as positive PI) in CS and *dSERT* mutant flies treated (indicated as "+") or not (labeled as "−") with 4-MTA (1 μM). Data shown corresponds to mean + SEM of n = 31, 18, 21, and 15 flies, in each experimental group, respectively. *p < 0.05, two-way ANOVA followed by Tukey post test.

toward Bz does not depend on the dSERT protein and/or serotonin, but that the increase in the olfactory response induced by 4-MTA depends on serotonergic neurotransmission and the operation of the transporter. This is consistent with previous reports that demonstrate that the serotonergic system innervates and modulate the activity of AL neurons in *Drosophila*.[19,20] Serotonergic systems innervating and modulating the activity of the neurons constituting the first relay olfactory center is not a particularity of invertebrates: it has been previously shown that serotonergic fibers innervate and modulate the activity of neurons forming the vertebrate olfactory bulb glomeruli.[45−47] Thus, the modulatory actions of serotonin on neurons of the first brain olfactory center would be a common theme in vertebrates and invertebrates. The mechanisms and consequences of this modulation are only partially understood and in this sense the mutant system described here is particularly well suited to further advance on this issue.

We and others have previously shown that serotonin contributes to motor control in *Drosophila* both at the larval[6,48,49] and adult stage.[50,51] Thus, it is possible that the acute treatment with 4-MTA and/or the genetic alteration of dSERT could affect the execution of motor programs in *Drosophila*, and idea we decided to assess. We studied several motor parameters but here show only three that are representative of locomotor behavior in adult flies: distance traveled, speed and activity time (Figure 6). Our results show no effect of 4-MTA (1 μM) in the three motor parameters studied (Figure 6). Interestingly, *dSERT* mutant flies show a significant increase in the three motor parameters studied as compared to control flies (Figure 6). Moreover we observed that 4-MTA treatment did not affect motor output in mutant animals.

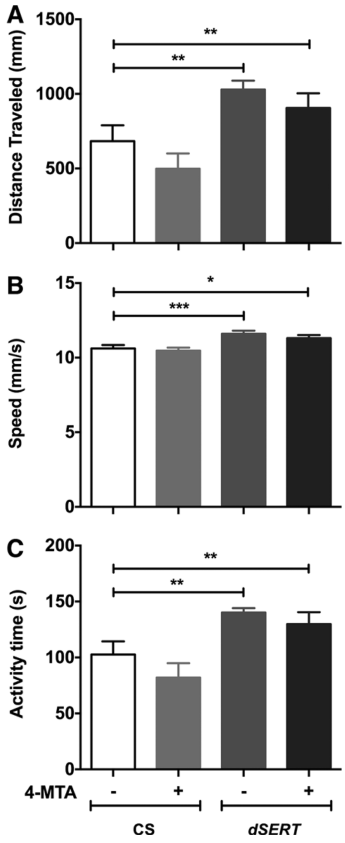

Figure 6. 4-MTA treatment does not affect locomotion in flies while *dSERT* mutant flies show increased basal locomotor behavior. Bars represent mean + SEM of distance traveled (A), activity time (B), or speed (C), in control (CS) or *dSERT* mutant flies, exposed (indicated "+") or not (labeled "−") to 4-MTA 1 μM. *p < 0.05, **P < 0.01, and ***p < 0.001 between identified experimental groups (n = 20, 14, 20, and 15 flies, respectively), two-way ANOVA followed by Tukey post test.

DOI: 10.1021/acschemneuro.7b00089
ACS Chem. Neurosci. 2017, 8, 2168−2179

Even though both the mutant and 4-MTA treatment are directed toward the same molecular target, dSERT, the difference between these two manipulations is its temporal dynamics: while the 4-MTA treatment is acute, only lasting 5 min and having no effect on animal development, the effect of the mutation is present over the entire lifespan of the animal. Therefore, our data would argue that although an acute increase in serotonin extracellular levels induced by 4-MTA has little or no effect on locomotion (Figure 6), it affects olfactory responses (Figure 5). It is possible to suggest that this is due to the differential action of this chemical on distinct serotonergic neural circuits and/or the differential contributions to these behaviors of different serotonergic pathways, as has been previously shown for two different behavioral outputs that depend on serotonin, mating and arousal.[52] On the other hand, the data obtained with *dSERT* mutant animals suggests that a modification of the serotonergic system affects normal development of circuits responsible for locomotion in adult flies. This is consistent with a previous study showing that tampering with the serotonergic system over fly development, by feeding *Drosophila* larvae blockers of dSERT, not only affects larval locomotion[53] but results also in altered adult fly motor behavior.[49]

It is well-known that the serotonergic system contributes in vertebrates to several complex behaviors, including anxiety.[1,54] As previously reported in mammals, *Drosophila* also shows a preference for the periphery in an arena, a behavior that has linked to anxiety.[55] With this in mind, we finally decided to evaluate centrophobism in flies, which can be quantified by comparing the preference of flies to be in the periphery as opposed to the center in the arena. Our results show a significant decrease in centrophobism in *dSERT* mutant flies as compared to control flies (Figure 7). Moreover, pharmacological increase of serotonin extracellular levels by fly exposure to 4-MTA results in reduced centrophobism. No further effect on centrophobism is observed in *dSERT* mutant flies fed with the amphetamine derivative, consistent with the idea that the molecular target of 4-MTA is dSERT (Figure 7). Similar results were observed when feeding flies with other drugs that increase serotonin extracellular levels in vertebrate systems, and whose molecular target is SERT (Figure S4B). Our data complements a recent report by Mohammad et al.,[14] where it was shown that that the expression of an RNAi for dSERT affects a different anxiety-like behavior in flies. Thus, altogether these data show that (1) the serotonergic system modulates centrophobism in adult flies; (2) 4-MTA induces a change in behavior in flies, which could be related to an anxious behavior; and (3) the effect of 4-MTA in *Drosophila* is mediated by dSERT. These data support the idea that the serotonergic system modulates anxiety-linked behaviors in flies, as it does in mammalian systems.[14] These results are in agreement with a model where increased serotonin levels promote exploratory behavior and suggest a decreased anxiety state in these flies.

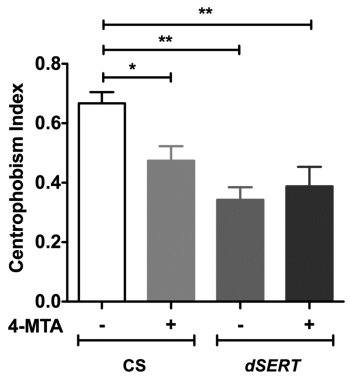

Figure 7. Centrophobism, an anxiety-associated behavior, depends on serotonergic neurotransmission in flies. The preference of flies for periphery, measured as centrophobism index, during control assays (no odorant present) in control strain (CS) and in dSERT mutant flies, fed (indicated as "+") or not (indicated as "−") with 4-MTA (1 μM). Data represents mean + SEM of n = 23, 18, 22, and 15 flies, respectively. *p < 0.05 and **p < 0.001, two-way ANOVA with Tukey post test, when comparing indicated experimental groups.

In sum, we have shown here that pharmacological and genetic manipulations that affect central serotonin levels modify responses to an aversive odorant, locomotor behavior and centrophobism, suggesting that this BA plays a key role in modulating a vast variety of functions and processes in the *Drosophila* brain as it does in mammals. In addition, the pharmacological responses observed both in control and dSERT mutant flies confirm the potential of this organism as model for low- to high-throughput screening of novel useful drugs.[5] Moreover, our work further supports the idea that given the evolutionary conservation of the serotonergic neurotransmission in vertebrate and invertebrate systems, it is possible to advance our comprehension of the molecular mechanisms underlying the contribution of this BA to behaviors, making use of the advantages offered by invertebrate animal models including *Drosophila*.

METHODS

Bioethical and Biosafety issues. All experimental procedures were approved by the Bioethical and Biosafety Committee of the Facultad de Ciencias Biológicas, Pontificia Universidad Católica de Chile and were conducted in accordance to the guidelines of the National Committee for Scientific and Technological Research, CONICYT and the Servicio Agrícola y Ganadero de Chile, SAG.

Flies. All experiments were carried out with male flies (3−7 days old). Flies were raised at 19 °C on a 12/12 h light/dark cycle and maintained on a standard yeast meal diet.

The *dSERT* mutant was obtained from the Bloomington *Drosophila* Stock Center (BDSC, line # 36004). This is a mutant generated in background y^1w, which was cantonized for at least 5 generations. Thus, as genetic controls we used Canton-S (CS). The *dSERT* mutant was originally generated by the group of Hugo Bellen, in the Gene Disruption Project.[11] It was generated by insertion of the Mi{MIC} transposable element in the 2R:24407821[-] position, in the intron that separates the exons 3 and 4 of the SERT *Drosophila* gene. The information on the site of the insertion can be found at http://www.ncbi.nlm.nih.gov/gss/JM029640. This transposable element contains in its sequence a splice acceptor followed by three stop codons.

Additional flies used in this work include dSERT-Gal4 and UAS-RNAi^{SERT} (lines #207777 and 11346, respectively, obtained from Vienna *Drosophila* Resource Center, Vienna, Austria); w1118; PBac{GH146-QF.P}53 P{QUAS-mtdTomato-3xHA}24A (from BDSC, line # 30037) and UAS-eGFP (which was already available at the Campusano lab).

Quantitative RT-PCR. We carried out a quantitative real time PCR to assess the change in expression of dSERT in control and mutant animals.[6,56] Briefly, RNA obtained from about 100 adult heads (50 mg of tissue) was treated with RQ1 RNase-free DNase (Promega). Reverse transcription was carried out with 600 ng of RNA (First Strand cDNA Synthesis kit, Thermo Scientific) according to manufacturer's instructions. Afterward, cDNA was amplified with 5× HOT FIREPol EvaGreen qPCR Mix Plus (Solis BioDyne), in the presence of specific primers. Reactions were carried out in Light

DOI: 10.1021/acschemneuro.7b00089
ACS Chem. Neurosci. 2017, 8, 2168−2179

Cycler 480 system (Roche). A first cycle of 15 min at 95 °C was followed by 15 s at 95 °C, 20 s at 59 °C and 30 s at 72 °C for 40 cycles. The final step was at 72 °C, 30 s. Quantification of PCR products for each genotype and each gene was carried out using the $2^{(-\Delta\Delta CP)}$ method. PCR reactions for each genotype and gene were carried out in duplicate, in each of three different biological replicas. Data for dSERT expression was normalized to expression of housekeeping gene GAPDH2. The primers used to amplify a sequence corresponding to exons 7 and 8 of the mRNA for dSERT (downstream the insertion site) were as follows: SERTF 5′-TGCTGGTCAACTTCCTGAAT-3′ and SERTR 5′-ATGAATAT-GGTCAGCAGGAACA-3′. PCR product was 200 bp, and efficiency of primers was 2.1932. Conditions for PCR reaction GAPDH2 gene were as indicated above, except that it was carried out with 150 ng of RNA. Primers for GAPDH2 were as follows: GAPDH2F, 5′-CGTTCATGCCACCACCGCTA-3′ and GAPDH2R, 5′-CCAC-GTCCATCACGCCACAA-3′. PCR product was 72 bp, and efficiency was 2.2422.

Reagents. (±) 4-MTA hydrochloride was synthesized as previously reported.[29] Serotonin, fluoxetine and nicotine were purchased from Sigma-Aldrich (St. Louis, MO, USA). All other reagents and salts used were of analytical grade.

Desiccation Assay. Three days old adult male flies were isolated and placed individually in 0.5 cm diameter glass tubes in absence of food and water. Flies were visually inspected every 3 h and surviving flies were counted. The assay was finished when the last fly of each experimental group/strain was dead. Data is shown as percentage of live flies overtime.

Fly Brain Dissection and Preparation for Neurochemical Analysis. In each experiment, an adult fly male was anesthetized under CO_2 and its brain removed. The tissue was pinned down to the bottom of a recording chamber (total volume 500 μL) so that the AL region was exposed. This preparation was superfused (3 mL/min) with a standard HEPES-buffered Tyrode solution (concentrations in mM: NaCl 140, KCl 4.5, HEPES 10, $MgCl_2$ 1.0, $CaCl_2$ 2.5, glucose 11; pH 7.2 continuously bubbled with air), at room temperature.

dSERT Expression in AL. Photomicrographs of brains of flies expressing tomato red protein in the AL region and GFP under the control of a dSERT-gal4 line were obtained at 40× magnification in an inverted LSM Fluoview 1000 (Olympus) confocal microscope and processed in ImageJ to generate the final images, as previously reported.[57]

High-Speed Chronoamperometric Recordings. Ex vivo brain recordings were performed as in refs 16 and 17 except that the carbon electrode was placed on top of the AL region, to better assess changes in the neuroactive molecules released after manipulations in this brain region. All drugs were freshly prepared in the Hepes-Tyrode solution described above and diluted to the desired working concentration. 4-MTA and nicotine were applied by a fast bolus injection (150 μL) into the recording chamber from a pipet located at about 1 mm from the brain surface. When indicated, brains were incubated with fluoxetine (100 μM) for 5 min before exposure to the serotonin (100 μM) challenge. Control experiments (in absence of brain tissue) were performed to discard that drugs generated a nonspecific signal in the system. Several manipulations were carried out in a single fly brain; each brain was used up to 2 h.

dSERT Modeling. A three-dimensional model of dSERT was generated using homology modeling. The crystal structure of dDAT available at the Protein Data Bank (PDBid 4XP1; resolution of 2.89 Å) was used as a template.[37] Models were prepared with MODELLER9v12[58] using standard parameters. The outcomes were ranked on the basis of the internal scoring function of the program. One hundred dSERT models were prepared and after stereochemical and energetic evaluations, the best structure was submitted to H++ server[59] to compute p*K* values of ionizable groups and to add missing hydrogen atoms according to the specified pH of the environment. Ions Na^+ and Cl^- were located inside of dSERT based on previous models[60,61] and were considered in all simulations. Then, the macromolecule was inserted into a 1-palmitoyl-2-oleoyl-*sn*-glycero-3-phosphocholine (POPC) membrane, solvated with water model TIP3, and ions were added creating an overall neutral system in 0.15 M NaCl. The final system was submitted to MD simulation (2 ns) using NAMD 2.10[62] and the NPT ensemble was used to perform the calculations. All other modeling conditions were as previously described.[28,63]

Molecular Docking and Dynamics. Ligands were constructed using Gaussian03,[64] and the partial charges of different compounds were corrected using ESP methodology. Based on crystallographic data,[37] the molecular docking of 4-MTA in dSERT was performed with the AutoDock 4.0 suite.[65] The grid maps were calculated using the autogrid4 option and centered on the dDAT-binding site. All other docking conditions were as previously described,[28] but a maximum number of 2.5×10^6 energy evaluations was used. The docked compound forming the receptor-drug complex was built using the lowest docked-energy binding position. The protein−ligand complex with the highest affinity (inferred from docking energy) was submitted to MD simulations (20 ns) to evaluate the stability of the complex and the characteristics of the main interactions. To this end, the same conditions described above were used.

Video Recording and Chemotaxis Assay. For behavioral assays, we used a setup previously described by the group of Brembs,[42] which we modified with his help. In brief, single flies were placed in a circular white arena (39 mm diameter, 2 mm high), with two pieces of cotton placed in opposite sides (see Figure 5A). The behavior of flies was recorded in this arrangement for 3 min at room temperature (23−25 °C). Afterward, one of the cottons was soaked with 100 μL of Bz (1% v/v in water), while the other was soaked with 100 μL of distilled water. Fly behavior was recorded for another 3 min. All video recordings were analyzed offline, using the tracking analysis software Buridan tracker.[42]

Data for centrophobism and different motor parameters were obtained as in.[42] In this work we show three motor parameters, distance traveled, activity time and speed, which better represent locomotor behavior in adult flies. In addition, heat maps that reflect the position of flies during control and Bz conditions, were generated. These maps were processed with ImageJ to calculate performance index (PI), a value that reflects the innate aversion of flies to Bz. To do that, the heat map was divided in two halves and PI was calculated according to the following formula:

$$PI = (AUC_{H_2O} - AUC_{Bz})/(AUC_{H_2O} + AUC_{Bz})$$

where AUC_{H_2O} = time spent in the water half and AUC_{Bz} = time spent in the Bz half.

Drug Exposure for Behavioral Assays. Male flies were food deprived for 15 h before beginning an experiment. Afterward, flies were fed different 4-MTA solutions (range 50 nM to 1 mM) or vehicle (5% sucrose and 0.6% propionic acid) in filter paper circles, for 5 min.

Statistical Analysis. Data presented corresponds to mean + SEM of indicated number of experiments (n). All statistical evaluations were carried out in GraphPad Prism software, using t test, one-way ANOVA, or two-way ANOVA followed by Tukey post test. Significance was defined with $p < 0.05$.

■ ASSOCIATED CONTENT

Supporting Information

The Supporting Information is available free of charge on the ACS Publications website at DOI: 10.1021/acschemneuro.7b00089.

Sequence alignment of dSERTand dDAT; RMSD of backbone atoms relative to the starting complex dSERT/4-MTA; fly movement tracking; effect of escitalopram or fluoxetine on olfactory response and centrophobism (PDF)

■ AUTHOR INFORMATION

Corresponding Authors

*E-mail: nlfuenzalida.u@gmail.com. Telephone: 562-2354-2133.

DOI: 10.1021/acschemneuro.7b00089
ACS Chem. Neurosci. 2017, 8, 2168−2179

*E-mail: jcampusano@bio.puc.cl.

ORCID

Jorge M. Campusano: 0000-0001-5254-8340

Author Contributions

S.H. and D.M.-M. contributed equally to this work. S.H., D.M.-M., A.F., E.G.P., P.I.-V., M.R.-P., R.V., N.F.-U., and J.M.C. designed experiments; S.H., D.M.-M., P.E., R.V.Z., E.F., A.F., and N.F.-U. conducted research; S.H., D.M.-M., P.E., A.F., R.V., N.F.-U., and J.M.C. analyzed data; S.H., D.M.-M., A.F., E.G.P., P.I.-V., M.R.-P., R.V., N.F.-U., and J.M.C. wrote the manuscript.

Funding

This work was supported by FONDECYT Grants No. 1141233 (J.M.C.), 1161375 (A.F.), 1130079 and 1171391 (E.G.P.), 1150615 (P.I.-V.) and 1170662 (M.R.-P.). S.H., N.F.-U., R.V.Z., and E.F. are supported by CONICYT PhD fellowships.

Notes

The authors declare no competing financial interest.

■ ACKNOWLEDGMENTS

We would like to thank Dr. Hugo Bellen and his group for some basic information on the generation of the *dSERT* mutant. We would also like to thank Dr. Bjoern Brembs on comments and ideas to setup the behavioral assay.

■ ABBREVIATIONS

4-MTA, 4-methylthioamphetamine; AL, Antennal Lobe; BA, biogenic amine; Bz, Benzaldehyde; CS, Canton S wildtype strain; DAT, dopamine plasma membrane transporter; dDAT, *Drosophila* dopamine plasma membrane transporter; dSERT, *Drosophila* serotonin plasma membrane transporter; MAO, monoamine oxidase; nAChR, nicotinic acetylcholine receptor; P.I, Performance Index; POPC, 1-palmitoyl-2-oleoyl-*sn*-glycero-3-phosphocholine; SERT, serotonin plasma membrane transporter

■ REFERENCES

(1) Olivier, B. (2015) Serotonin: a never-ending story. *Eur. J. Pharmacol. 753*, 2−18.

(2) Murphy, D. L., Lerner, A., Rudnick, G., and Lesch, K. P. (2004) Serotonin transporter: gene, genetic disorders, and pharmacogenetics. *Mol. Interventions 4* (2), 109−23.

(3) Kristensen, A. S., Andersen, J., Jorgensen, T. N., Sorensen, L., Eriksen, J., Loland, C. J., Stromgaard, K., and Gether, U. (2011) SLC6 neurotransmitter transporters: structure, function, and regulation. *Pharmacol Rev. 63* (3), 585−640.

(4) Martin, C. A., and Krantz, D. E. (2014) Drosophila melanogaster as a genetic model system to study neurotransmitter transporters. *Neurochem. Int. 73*, 71−88.

(5) Pandey, U. B., and Nichols, C. D. (2011) Human disease models in Drosophila melanogaster and the role of the fly in therapeutic drug discovery. *Pharmacol Rev. 63* (2), 411−36.

(6) Silva, B., Goles, N. I., Varas, R., and Campusano, J. M. (2014) Serotonin receptors expressed in Drosophila mushroom bodies differentially modulate larval locomotion. *PLoS One 9* (2), e89641.

(7) Liu, Y., Luo, J., Carlsson, M. A., and Nassel, D. R. (2015) Serotonin and insulin-like peptides modulate leucokinin-producing neurons that affect feeding and water homeostasis in Drosophila. *J. Comp. Neurol. 523* (12), 1840−63.

(8) Nall, A., and Sehgal, A. (2014) Monoamines and sleep in Drosophila. *Behav. Neurosci. 128* (3), 264−72.

(9) Sitaraman, D., LaFerriere, H., Birman, S., and Zars, T. (2012) Serotonin is critical for rewarded olfactory short-term memory in Drosophila. *J. Neurogenet. 26* (2), 238−44.

(10) Huang, X., Marona-Lewicka, D., and Nichols, D. E. (1992) p-methylthioamphetamine is a potent new non-neurotoxic serotonin-releasing agent. *Eur. J. Pharmacol. 229* (1), 31−8.

(11) Bellen, H. J., Levis, R. W., Liao, G., He, Y., Carlson, J. W., Tsang, G., Evans-Holm, M., Hiesinger, P. R., Schulze, K. L., Rubin, G. M., Hoskins, R. A., and Spradling, A. C. (2004) The BDGP gene disruption project: single transposon insertions associated with 40% of Drosophila genes. *Genetics 167* (2), 761−81.

(12) Kalueff, A. V., Ren-Patterson, R. F., and Murphy, D. L. (2007) The developing use of heterozygous mutant mouse models in brain monoamine transporter research. *Trends Pharmacol. Sci. 28* (3), 122−7.

(13) Murphy, D. L., Fox, M. A., Timpano, K. R., Moya, P. R., Ren-Patterson, R., Andrews, A. M., Holmes, A., Lesch, K. P., and Wendland, J. R. (2008) How the serotonin story is being rewritten by new gene-based discoveries principally related to SLC6A4, the serotonin transporter gene, which functions to influence all cellular serotonin systems. *Neuropharmacology 55* (6), 932−60.

(14) Mohammad, F., Aryal, S., Ho, J., Stewart, J. C., Norman, N. A., Tan, T. L., Eisaka, A., and Claridge-Chang, A. (2016) Ancient Anxiety Pathways Influence Drosophila Defense Behaviors. *Curr. Biol. 26* (7), 981−6.

(15) Luo, J., Becnel, J., Nichols, C. D., and Nassel, D. R. (2012) Insulin-producing cells in the brain of adult Drosophila are regulated by the serotonin 5-HT1A receptor. *Cell. Mol. Life Sci. 69* (3), 471−84.

(16) Fuenzalida-Uribe, N., Meza, R. C., Hoffmann, H. A., Varas, R., and Campusano, J. M. (2013) nAChR-induced octopamine release mediates the effect of nicotine on a startle response in Drosophila melanogaster. *J. Neurochem. 125* (2), 281−90.

(17) Fuenzalida-Uribe, N., Hidalgo, S., Varas, R., and Campusano, J. M. (2016) Study of the Contribution of Nicotinic Receptors to the Release of Endogenous Biogenic Amines in Drosophila Brain. In *Nicotinic Acetylcholine Receptor Technologies* (Li, M. D., Ed.), Springer Science+Business Media, New York.

(18) Gundelfinger, E. D., and Hess, N. (1992) Nicotinic acetylcholine receptors of the central nervous system of Drosophila. *Biochim. Biophys. Acta, Mol. Cell Res. 1137* (3), 299−308.

(19) Dacks, A. M., Green, D. S., Root, C. M., Nighorn, A. J., and Wang, J. W. (2009) Serotonin modulates olfactory processing in the antennal lobe of Drosophila. *J. Neurogenet. 23* (4), 366−77.

(20) Sizemore, T. R., and Dacks, A. M. (2016) Serotonergic Modulation Differentially Targets Distinct Network Elements within the Antennal Lobe of Drosophila melanogaster. *Sci. Rep. 6*, 37119.

(21) Giang, T., Rauchfuss, S., Ogueta, M., and Scholz, H. (2011) The serotonin transporter expression in Drosophila melanogaster. *J. Neurogenet. 25* (1−2), 17−26.

(22) Makos, M. A., Kim, Y. C., Han, K. A., Heien, M. L., and Ewing, A. G. (2009) In vivo electrochemical measurements of exogenously applied dopamine in Drosophila melanogaster. *Anal. Chem. 81* (5), 1848−54.

(23) Pyakurel, P., Privman Champaloux, E., and Venton, B. J. (2016) Fast-Scan Cyclic Voltammetry (FSCV) Detection of Endogenous Octopamine in Drosophila melanogaster Ventral Nerve Cord. *ACS Chem. Neurosci. 7* (8), 1112−9.

(24) Mathews, T. A., Fedele, D. E., Coppelli, F. M., Avila, A. M., Murphy, D. L., and Andrews, A. M. (2004) Gene dose-dependent alterations in extraneuronal serotonin but not dopamine in mice with reduced serotonin transporter expression. *J. Neurosci. Methods 140* (1−2), 169−81.

(25) Montanez, S., Owens, W. A., Gould, G. G., Murphy, D. L., and Daws, L. C. (2003) Exaggerated effect of fluvoxamine in heterozygote serotonin transporter knockout mice. *J. Neurochem. 86* (1), 210−9.

(26) Gobbi, M., Moia, M., Pirona, L., Ceglia, I., Reyes-Parada, M., Scorza, C., and Mennini, T. (2002) p-Methylthioamphetamine and 1-(m-chlorophenyl)piperazine, two non-neurotoxic 5-HT releasers in vivo, differ from neurotoxic amphetamine derivatives in their mode of action at 5-HT nerve endings in vitro. *J. Neurochem. 82* (6), 1435−43.

(27) Roman, D. L., Saldana, S. N., Nichols, D. E., Carroll, F. I., and Barker, E. L. (2004) Distinct molecular recognition of psychostimu-

DOI: 10.1021/acschemneuro.7b00089
ACS Chem. Neurosci. 2017, 8, 2168−2179

lants by human and Drosophila serotonin transporters. *J. Pharmacol. Exp. Ther. 308* (2), 679−87.
(28) Sotomayor-Zarate, R., Quiroz, G., Araya, K. A., Abarca, J., Ibanez, M. R., Montecinos, A., Guajardo, C., Nunez, G., Fierro, A., Moya, P. R., Iturriaga-Vasquez, P., Gomez-Molina, C., Gysling, K., and Reyes-Parada, M. (2012) 4-Methylthioamphetamine increases dopamine in the rat striatum and has rewarding effects in vivo. *Basic Clin. Pharmacol. Toxicol. 111* (6), 371−9.
(29) Hurtado-Guzman, C., Fierro, A., Iturriaga-Vasquez, P., Sepulveda-Boza, S., Cassels, B. K., and Reyes-Parada, M. (2003) Monoamine oxidase inhibitory properties of optical isomers and N-substituted derivatives of 4-methylthioamphetamine. *J. Enzyme Inhib. Med. Chem. 18* (4), 339−47.
(30) Scorza, M. C., Carrau, C., Silveira, R., Zapata-Torres, G., Cassels, B. K., and Reyes-Parada, M. (1997) Monoamine oxidase inhibitory properties of some methoxylated and alkylthio amphetamine derivatives: structure-activity relationships. *Biochem. Pharmacol. 54* (12), 1361−9.
(31) Roelofs, J., and Van Haastert, P. J. (2001) Genes lost during evolution. *Nature 411* (6841), 1013−4.
(32) Monastirioti, M. (1999) Biogenic amine systems in the fruit fly Drosophila melanogaster. *Microsc. Res. Tech. 45* (2), 106−21.
(33) Nassel, D. R., and Elekes, K. (1992) Aminergic neurons in the brain of blowflies and Drosophila: dopamine- and tyrosine hydroxylase-immunoreactive neurons and their relationship with putative histaminergic neurons. *Cell Tissue Res. 267* (1), 147−67.
(34) Python, F., and Stocker, R. F. (2002) Immunoreactivity against choline acetyltransferase, gamma-aminobutyric acid, histamine, octopamine, and serotonin in the larval chemosensory system of Dosophila melanogaster. *J. Comp. Neurol. 453* (2), 157−67.
(35) Kume, K., Kume, S., Park, S. K., Hirsh, J., and Jackson, F. R. (2005) Dopamine is a regulator of arousal in the fruit fly. *J. Neurosci. 25* (32), 7377−84.
(36) Vickrey, T. L., Xiao, N., and Venton, B. J. (2013) Kinetics of the dopamine transporter in Drosophila larva. *ACS Chem. Neurosci. 4* (5), 832−7.
(37) Wang, K. H., Penmatsa, A., and Gouaux, E. (2015) Neurotransmitter and psychostimulant recognition by the dopamine transporter. *Nature 521* (7552), 322−7.
(38) Celik, L., Sinning, S., Severinsen, K., Hansen, C. G., Moller, M. S., Bols, M., Wiborg, O., and Schiott, B. (2008) Binding of serotonin to the human serotonin transporter. Molecular modeling and experimental validation. *J. Am. Chem. Soc. 130* (12), 3853−65.
(39) Grouleff, J., Ladefoged, L. K., Koldso, H., and Schiott, B. (2015) Monoamine transporters: insights from molecular dynamics simulations. *Front. Pharmacol. 6*, 235.
(40) Jorgensen, A. M., Tagmose, L., Jorgensen, A. M., Topiol, S., Sabio, M., Gundertofte, K., Bogeso, K. P., and Peters, G. H. (2007) Homology modeling of the serotonin transporter: insights into the primary escitalopram-binding site. *ChemMedChem 2* (6), 815−26.
(41) Coleman, J. A., Green, E. M., and Gouaux, E. (2016) X-ray structures and mechanism of the human serotonin transporter. *Nature 532* (7599), 334−9.
(42) Colomb, J., Reiter, L., Blaszkiewicz, J., Wessnitzer, J., and Brembs, B. (2012) Open source tracking and analysis of adult Drosophila locomotion in Buridan's paradigm with and without visual targets. *PLoS One 7* (8), e42247.
(43) Knaden, M., Strutz, A., Ahsan, J., Sachse, S., and Hansson, B. S. (2012) Spatial representation of odorant valence in an insect brain. *Cell Rep. 1* (4), 392−9.
(44) Stensmyr, M. C., Dweck, H. K., Farhan, A., Ibba, I., Strutz, A., Mukunda, L., Linz, J., Grabe, V., Steck, K., Lavista-Llanos, S., Wicher, D., Sachse, S., Knaden, M., Becher, P. G., Seki, Y., and Hansson, B. S. (2012) A conserved dedicated olfactory circuit for detecting harmful microbes in Drosophila. *Cell 151* (6), 1345−57.
(45) Brill, J., Shao, Z., Puche, A. C., Wachowiak, M., and Shipley, M. T. (2016) Serotonin increases synaptic activity in olfactory bulb glomeruli. *J. Neurophysiol. 115* (3), 1208−19.
(46) Hardy, A., Palouzier-Paulignan, B., Duchamp, A., Royet, J. P., and Duchamp-Viret, P. (2005) 5-Hydroxytryptamine action in the rat olfactory bulb: in vitro electrophysiological patch-clamp recordings of juxtaglomerular and mitral cells. *Neuroscience 131* (3), 717−31.
(47) Liu, S., Aungst, J. L., Puche, A. C., and Shipley, M. T. (2012) Serotonin modulates the population activity profile of olfactory bulb external tufted cells. *J. Neurophysiol. 107* (1), 473−83.
(48) Rodriguez Moncalvo, V. G., and Campos, A. R. (2009) Role of serotonergic neurons in the Drosophila larval response to light. *BMC Neurosci. 10*, 66.
(49) Majeed, Z. R., Abdeljaber, E., Soveland, R., Cornwell, K., Bankemper, A., Koch, F., and Cooper, R. L. (2016) Modulatory Action by the Serotonergic System: Behavior and Neurophysiology in Drosophila melanogaster. *Neural Plast. 2016*, 7291438.
(50) Kamyshev, N. G., Smirnova, G. P., Savvateeva, E. V., Medvedeva, A. V., and Ponomarenko, V. V. (1983) The influence of serotonin and p-chlorophenylalanine on locomotor activity of Drosophila melanogaster. *Pharmacol., Biochem. Behav. 18* (5), 677−81.
(51) Nichols, C. D. (2007) 5-HT2 receptors in Drosophila are expressed in the brain and modulate aspects of circadian behaviors. *Dev. Neurobiol. 67* (6), 752−63.
(52) Pooryasin, A., and Fiala, A. (2015) Identified Serotonin-Releasing Neurons Induce Behavioral Quiescence and Suppress Mating in Drosophila. *J. Neurosci. 35* (37), 12792−812.
(53) Dasari, S., Viele, K., Turner, A. C., and Cooper, R. L. (2007) Influence of PCPA and MDMA (ecstasy) on physiology, development and behavior in Drosophila melanogaster. *Eur. J. Neurosci 26* (2), 424−38.
(54) Haller, J., Aliczki, M., and Gyimesine Pelczer, K. (2013) Classical and novel approaches to the preclinical testing of anxiolytics: A critical evaluation. *Neurosci. Biobehav. Rev. 37*, 2318−30.
(55) Chen, A. Y., Wilburn, P., Hao, X., and Tully, T. (2014) Walking deficits and centrophobism in an alpha-synuclein fly model of Parkinson's disease. *Genes Brain Behav 13* (8), 812−20.
(56) Campusano, J. M., Andres, M. E., Magendzo, K., Abarca, J., Tapia-Arancibia, L., and Bustos, G. (2005) Novel alternative splicing predicts a truncated isoform of the NMDA receptor subunit 1 (NR1) in embryonic rat brain. *Neurochem. Res. 30* (4), 567−76.
(57) Silva, B., Molina-Fernandez, C., Ugalde, M. B., Tognarelli, E. I., Angel, C., and Campusano, J. M. (2015) Muscarinic ACh Receptors Contribute to Aversive Olfactory Learning in Drosophila. *Neural Plast. 2015*, 658918.
(58) Sali, A., and Blundell, T. L. (1993) Comparative protein modelling by satisfaction of spatial restraints. *J. Mol. Biol. 234* (3), 779−815.
(59) Gordon, J. C., Myers, J. B., Folta, T., Shoja, V., Heath, L. S., and Onufriev, A. (2005) H++: a server for estimating pKas and adding missing hydrogens to macromolecules. *Nucleic Acids Res. 33*, W368−71.
(60) Forrest, L. R., Zhang, Y. W., Jacobs, M. T., Gesmonde, J., Xie, L., Honig, B. H., and Rudnick, G. (2008) Mechanism for alternating access in neurotransmitter transporters. *Proc. Natl. Acad. Sci. U. S. A. 105* (30), 10338−43.
(61) Penmatsa, A., Wang, K. H., and Gouaux, E. (2013) X-ray structure of dopamine transporter elucidates antidepressant mechanism. *Nature 503* (7474), 85−90.
(62) Phillips, J. C., Braun, R., Wang, W., Gumbart, J., Tajkhorshid, E., Villa, E., Chipot, C., Skeel, R. D., Kale, L., and Schulten, K. (2005) Scalable molecular dynamics with NAMD. *J. Comput. Chem. 26* (16), 1781−802.
(63) Pessoa-Mahana, H., Recabarren-Gajardo, G., Temer, J. F., Zapata-Torres, G., Pessoa-Mahana, C. D., Barria, C. S., and Araya-Maturana, R. (2012) Synthesis, docking studies and biological evaluation of benzo[b]thiophen-2-yl-3-(4-arylpiperazin-1-yl)-propan-1-one derivatives on 5-HT1A serotonin receptors. *Molecules 17* (2), 1388−407.
(64) Frisch, M. J., Trucks, G.W., Schlegel, H. B., Scuseria, G. E., Robb, M. A., Cheesman, J. R., Zakrzewski, V. G., Montgomery, J. A., Jr., Straatman, S., Dapprich, J. M. M., Daniels, A. D., Kudin, K. N.,

DOI: 10.1021/acschemneuro.7b00089
ACS Chem. Neurosci. 2017, 8, 2168−2179

Strain, M. C., Farkas, J. O., Tomasi, V. B., Cossi, M., Cammi, R., Mennucci, B., Pomelli, C., Adamo, S. C., Clifford, J. O., Petersson, G. A., Ayala, P. Y., Cui, Q., Morokuma, D. K., Malick, A. D. R., Raghavachari, K., Foresman, J. B., Cioslowski, J., Ortiz, J. V., Baboul, B. B. S. A. G., Liu, G., Liashenko, A., Piskorz, P., Komaromi, R. I., Gomperts, R. L. M., Fox, D. J., Keith, T., Al-Laham, M. A., Peng, C. Y., Nanayakkara, A., Challacombe, P. M. W. G. M., Johnson, B., Chen, W., Wong, J. L., Andres, C. G., Head-Gordon, M., Replogle, E. S., and Pople, J. A. (1998) *Gaussian 98*, Revision A.9, Gaussian Inc, Pittsburgh, PA.

(65) Morris, G. M., Goodsell, D. S., Halliday, R. S., Huey, R., Hart, W. E., Belew, R. K., and Olson, A. J. (1998) Automated Docking Using a LamarckianGenetic Algorithm and an EmpiricalBinding Free Energy Function. *J. Comput. Chem. 19* (14), 1639−1662.

DOI: 10.1021/acschemneuro.7b00089
ACS Chem. Neurosci. 2017, 8, 2168−2179

Appendix B: A published journal club article discussing the differential roles of RIM on synaptic plasticity in mammals' synapses

This is a published manuscript in The Journal of Neuroscience, discussing the findings reported by Kupferschmidt et al., (2019). As this manuscript was written by myself, I am the only contributor to this work.

Journal Club

Editor's Note: These short reviews of recent *JNeurosci* articles, written exclusively by students or postdoctoral fellows, summarize the important findings of the paper and provide additional insight and commentary. If the authors of the highlighted article have written a response to the Journal Club, the response can be found by viewing the Journal Club at www.jneurosci.org. For more information on the format, review process, and purpose of Journal Club articles, please see https://www.jneurosci.org/content/jneurosci-journal-club.

RIM1$\alpha\beta$ Are Required at the Corticostriatal Synapses for Habit Formation

Sergio Hidalgo[1,2]

[1]Departamento de Biología Celular y Molecular, Facultad de Ciencias Biológicas, Pontificia Universidad Católica de Chile, Santiago 8330025 Chile, and [2]School of Physiology, Pharmacology and Neuroscience, Faculty of Life Science, University of Bristol, Bristol BS8 1TD, United Kingdom

Review of Kupferschmidt et al.

Control of instrumental actions relies on a dual system of goal-directed and habit strategies (Liljeholm and O'Doherty, 2012). Goal-directed actions involve anticipation of rewards and are therefore sensitive to changes in the value of the outcome. Habits, in contrast, are well learned actions driven by a stimulus without regard to the outcome (Yin, 2008). Through repetition and learning, goal-directed strategies gradually evolve into less flexible habits (Yin, 2008; Gremel and Costa, 2013). This happens when the sensorimotor association becomes strong enough to overcome the expectancy of the outcome, allowing the brain to complete everyday actions with minimal effort.

The balance between goal-directed and habitual action is regulated by an intricate neuronal network in which the dorsal striatum plays a pivotal role (Liljeholm and O'Doherty, 2012; Corbit et al., 2013). Specifically, the dorsomedial striatum (DMS) regulates goal-directed strategies, while the dorsolateral striatum (DLS) is involved in action learning and habitual strategies (Yin, 2008; Liljeholm and O'Doherty, 2012; Nazzaro et al., 2012; Gremel and Costa, 2013). Thus, changes in DMS and DLS activity underlie switches from goal-directed to habitual action strategies (Yin et al., 2009; Santos et al., 2015). These changes in activity have been proposed to be regulated by glutamatergic projections from the cerebral cortex, which are the main source of excitatory signals to the striatum (Huerta-Ocampo et al., 2014).

In addition to postsynaptic changes in AMPA and NMDA receptors, which occur in the DLS in the late phases of skill learning and habit formation (Yin et al., 2009), recent findings suggest that presynaptic release dynamics in the dorsal striatum are important predictors for action learning (Kupferschmidt et al., 2017). For example, expression of CB1 cannabinoid receptors (CB1Rs) in cortical neurons projecting to the dorsal striatum are indispensable for habit formation (Gremel et al., 2016), and endocannabinoid-dependent long-term depression (eCB-LTD) of neurotransmitter release might be involved in this dependence (Wu et al., 2015).

Presynaptic release of neurotransmitters relies on a complex machinery that couples local calcium influx to synaptic vesicle fusion. Several proteins coordinate this process, including Rab3 interacting molecules (RIMs), one of the main components of the presynaptic active zone (Schoch et al., 2002). RIM proteins are encoded by four genes that give rise to seven isoforms; of these, the α and β isoforms encoded by the *Rims1* gene are the most studied (Kaeser and Südhof, 2005). RIM proteins are expressed ubiquitously in the CNS (Schoch et al., 2006), and they have been proposed to be coordinators of the components involved in short- and long-term synaptic plasticity at the active zone (Schoch et al., 2006). Interestingly, RIM1 deletion has different effects on plasticity at different synapse types (Kaeser and Südhof, 2005). For instance, RIM1α knock-out enhances short-term plasticity in hippocampal CA3–CA1 synapses (Schoch et al., 2002), whereas it disrupts long-term plasticity while sparing short-term plasticity in dentate gyrus mossy fibers (Castillo et al., 2002). Moreover, it has been shown in *ex vivo* (Chevaleyre et al., 2007; Grueter et al., 2010) and *in vitro* (Alonso et al., 2017) experiments that endocannabinoid-induced long- and short-term depression depends in part on RIM1α expression.

To determine whether RIM1 influences plasticity at corticostriatal synapses, Kupferschmidt et al. (2019) used Emx1::Cre;RIM1$^{-/-}$ mice, in which the RIM1 isoforms α and β were deleted selectively in excitatory neurons in the neocortex (RIM1$\alpha\beta$ cKO). As expected, this reduced the frequency of spontaneous

Received April 19, 2019; revised Aug. 3, 2019; accepted Aug. 7, 2019.

This work was supported by CONICYT Doctoral fellowship PFCHA-Doctorado Nacional-2116161. I thank Dr. Edgar Buhl for comments on the paper.

The author declares no competing financial interests.

Correspondence should be addressed to Sergio Hidalgo at s.hidalgosotelo@bristol.ac.uk.

https://doi.org/10.1523/JNEUROSCI.0896-19.2019

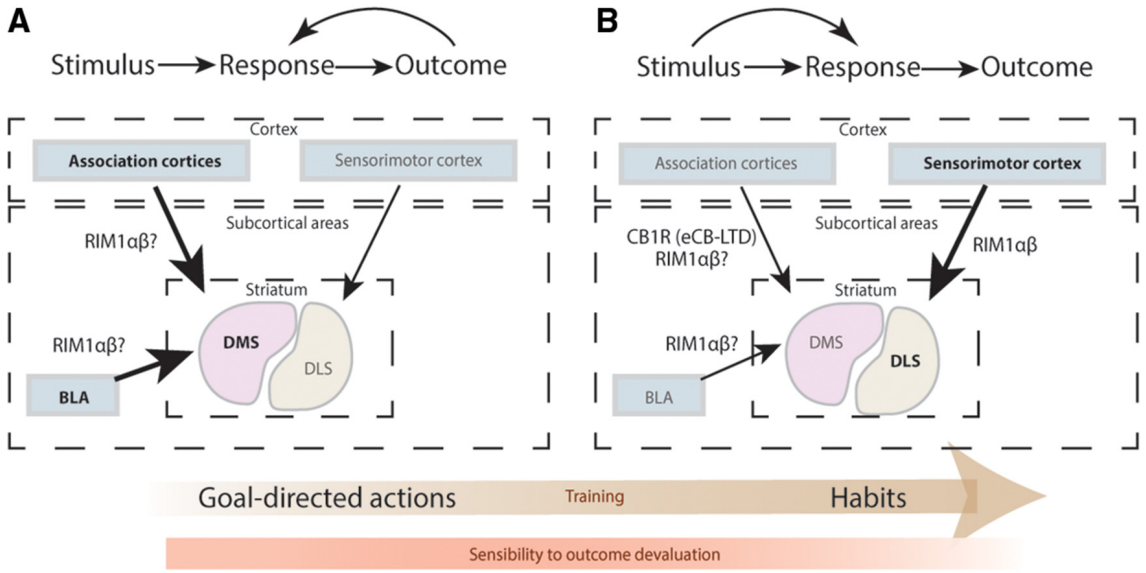

Figure 1. Simplified proposed mechanism for the shift from goal-directed to habitual strategies and the RIM1$\alpha\beta$ contribution to the corticostriatal network established by Kupferschmidt et al. (2019). ***A***, In the presence of a novel stimulus, actions are highly dependent on outcomes, indicative of goal-directed strategies. These are modulated mainly by the neural inputs from associative and limbic areas (like the BLA) to the DMS, while the DLS is disengaged. ***B***, After training or action learning, the stimulus becomes the driver of the action, indicative of habits. In this situation, projections from the sensorimotor cortex are strengthened, possibly through the contribution of RIM1$\alpha\beta$ in the presynaptic modulation of glutamate release. In addition, inputs from the associative cortices to the dorsal striatum (likewise the OFC terminals) are inhibited by eCB-LTD, a process dependent on CB1R. Whether RIM1$\alpha\beta$ is important in the inputs from cortical structures to the DMS is still unknown.

EPSCs in medium-sized spiny neurons (MSNs), the most abundant neurons in the DLS, without changing the amplitude of spontaneous events, indicating a defect in presynaptic vesicle release (Castillo et al., 2002; Schoch et al., 2006). In addition, responses evoked in MSNs by stimulation of corticostriatal fibers were significantly reduced in mutant mice, suggesting evoked release was also impaired.

To evaluate whether CB1R-dependent synaptic plasticity was also affected in RIM1$\alpha\beta$ cKO mice, the authors used different strategies to induce short- or long-term depression. First, depolarization-induced suppression of excitation (DSE) was used to induce short-term depression in corticostriatal synapses. Depolarizing neurons to 30 mV for 10 s induced similar amounts of depression in RIM1$\alpha\beta$ cKO and wild-type mice. Second, DHPG was used to induce long-term depression. Again, the extent of depression was similar in RIM1$\alpha\beta$ cKO and wild-type mice. Moreover, this effect was effectively blocked by a CB1R antagonist in both mutant and control animals. Therefore, both short- and long-term depression of neurotransmitter release were spared in the RIM1 cKO mice.

Next, Kupferschmidt et al. (2019) investigated how the reduction in basal neurotransmission between the cortex and the DLS in RIM1$\alpha\beta$ cKO mice affected goal-directed and habit-driven action. To do this, they used a self-paced instrumental task followed by a valuation test. Food-restricted mice were trained to press a lever to receive a food-pellet reward, using a random-interval reward schedule for several days; this protocol was previously shown to promote habit formation (Gremel et al., 2016). Bias to use a goal-directed or habitual action strategy was assessed after training by giving mice access to either a sucrose solution or food pellets before testing them on the lever-pressing task in the absence of the reward. Importantly, access to the food pellets before testing is expected to devalue the reward, whereas access to sucrose solution is not. If mice are using goal-directed strategies, they should press the lever fewer times in the devalued condition; but if they are using habitual strategies, the number of lever pressings should be indistinguishable in the two conditions. As expected, reward devaluation did not affect lever pressing in control animals, indicating habitual control of actions. In contrast, RIM1$\alpha\beta$ cKO mice were sensitive to the devaluation, as indicated by fewer lever presses compared with the wild-type and to the sucrose condition. This suggests that habit formation was impaired in these mice.

These findings are exciting for two main reasons. First, according to the "dual-system theory" of instrumental learning, goal-directed strategies, which depend on cortico-DMS synapses, have initial dominance over habits that rely on cortico–DLS synapses. Therefore, weakening the cortical transmission to DLS might be expected to bias the animals toward the use of goal-directed actions even when interval-schedule reward training is used to promote habits (Nazzaro et al., 2012). Indeed, the findings presented by Kupferschmidt et al. (2019) support this notion, where goal-directed strategies would be set by default when habits cannot be formed. Second, they suggest a RIM1-independent synaptic plasticity at corticostriatal synapses, different to what is observed in other synapses in the CNS. For example, in cultured cerebellar granule cells, using protocols of endocannabinoid-induced depression similar to the one used by Kupferschmidt et al. (2019), CB1R activation induced greater depression of neurotransmitter release in RIM1α-deficient cells than in wild-type, and this effect was rescued by re-expressing RIM1α (Alonso et al., 2017). Opposite results were found in hippocampal neurons and a subset of neurons in the core region of the nucleus accumbens (NAc): RIM1α depletion in these structures caused a reduction in the DHPG-induced eCB-LTD (Grueter et al., 2010). Given that eCB-LTD occurs in corticostriatal synapses and its relevance has been shown in several studies (Nazzaro et al., 2012; Wu et al., 2015), the lack of effect in the RIM1$\alpha\beta$ cKO mice shown by Kupferschmidt et al. (2019) suggests that, as in short- and long-term potentiation, short- and long-term

depression can be RIM1-dependent or independent, depending on the synapse type. Because RIMs proteins are ubiquitously expressed in the CNS, this also suggests a differential specialization of the neurotransmitter release machinery in different synapse types.

Excitatory synapses in other regions where RIM1$\alpha\beta$ have a predominant function might contribute to the phenotypes observed here. As stressed above, whereas DLS [which Kupferschmidt et al. (2019) examined] is engaged in later stages of action learning and habit formation, DMS is involved in goal-directed strategies (Liljeholm and O'Doherty, 2012; Gremel and Costa, 2013), and in early phases of training. Both the orbitofrontal cortex (OFC) and the basolateral amygdala (BLA) project to the DMS (Kelley et al., 1982; Gremel and Costa, 2013; Gremel et al., 2016). It has been shown that inhibition of OFC inputs to the dorsal striatum is necessary for habit formation, and this process depends on CB1Rs (Gremel and Costa, 2013; Gremel et al., 2016). The BLA was also shown to be involved in the process of goal-directed action learning; specifically, BLA lesions increase outcome devaluation (Corbit et al., 2013). Therefore, it is possible that the inability to set habitual strategies in the RIM1$\alpha\beta$ cKO mice arises from defective activation/inactivation balance of DMS by OFC and/or BLA, in addition to the reduction in basal neurotransmission at cortex-DLS synapses reported by Kupferschmidt et al. (2019) (Fig. 1).

By addressing the role of RIM1$\alpha\beta$ in the corticostriatal synapses, Kupferschmidt et al. (2019) have provided new evidence on the importance of basal corticostriatal neurotransmission in the balance between goal-directed and habitual strategies. Untangling these mechanisms will lead us to a better understanding of complex diseases, such as obsessive-compulsive disorder or drug-related seeking behavior, where this balance is biased toward habits. Moreover, the authors have presented exciting new data showing that RIM1 can differentially modulate neuronal plasticity, raising new questions about the molecular arrangement of presynaptic components at corticostriatal synapses.

References

Alonso B, Bartolomé-Martín D, Ferrero JJ, Ramírez-Franco J, Torres M, Sánchez-Prieto J (2017) CB1 receptors down-regulate a cAMP/Epac2/PLC pathway to silence the nerve terminals of cerebellar granule cells. J Neurochem 142:350–364.

Castillo PE, Schoch S, Schmitz F, Südhof TC, Malenka RC (2002) RIM1alpha is required for presynaptic long-term potentiation. Nature 415:327–330.

Chevaleyre V, Heifets BD, Kaeser PS, Südhof TC, Purpura DP, Castillo PE (2007) Endocannabinoid-mediated long-term plasticity requires cAMP/PKA signaling and RIM1α. Neuron 54:801–812.

Corbit LH, Leung BK, Balleine BW (2013) The role of the amygdala-striatal pathway in the acquisition and performance of goal-directed instrumental actions. J Neurosci 33:17682-17690.

Gremel CM, Chancey JH, Atwood BK, Luo G, Neve R, Ramakrishnan C, Deisseroth K, Lovinger DM, Costa RM (2016) Endocannabinoid modulation of orbitostriatal circuits gates habit formation. Neuron 90:1312–1324.

Gremel CM, Costa RM (2013) Orbitofrontal and striatal circuits dynamically encode the shift between goal-directed and habitual actions. Nat Commun 4:2264.

Grueter BA, Brasnjo G, Malenka RC (2010) Postsynaptic TRPV1 triggers cell type-specific long-term depression in the nucleus accumbens. Nat Neurosci 13:1519–1525.

Huerta-Ocampo I, Mena-Segovia J, Bolam JP (2014) Convergence of cortical and thalamic input to direct and indirect pathway medium spiny neurons in the striatum. Brain Struct Funct 219:1787–1800.

Kaeser PS, Südhof TC (2005) RIM function in short-and long-term synaptic plasticity. Biochem Soc Trans 33:1345–1349.

Kelley AE, Domesick VB, Nauta WJ (1982) The amygdalostriatal projection in the rat-an anatomical study by anterograde and retrograde tracing methods. Neuroscience 7:615–630.

Kupferschmidt DA, Juczewski K, Cui G, Johnson KA, Lovinger DM (2017) Parallel, but dissociable, processing in discrete corticostriatal inputs encodes skill learning. Neuron 96:476-489.e5.

Kupferschmidt DA, Augustin SM, Johnson KA, Lovinger DM (2019) Active zone proteins RIM1$\alpha\beta$ are required for normal corticostriatal transmission and action control. J Neurosci 39:1457–1470.

Liljeholm M, O'Doherty JP (2012) Contributions of the striatum to learning, motivation, and performance: an associative account. Trends Cogn Sci 16:467–475.

Nazzaro C, Greco B, Cerovic M, Baxter P, Rubino T, Trusel M, Parolaro D, Tkatch T, Benfenati F, Pedarzani P, Tonini R (2012) SK channel modulation rescues striatal plasticity and control over habit in cannabinoid tolerance. Nat Neurosci 15:284–293.

Santos FJ, Oliveira RF, Jin X, Costa RM (2015) Corticostriatal dynamics encode the refinement of specific behavioral variability during skill learning. eLife 4:e09423.

Schoch S, Castillo PE, Jo T, Mukherjee K, Geppert M, Wang Y, Schmitz F, Malenka RC, Südhof TC (2002) RIM1α forms a protein scaffold for regulating neurotransmitter release at the active zone. Nature 415:321–326.

Schoch S, Mittelstaedt T, Kaeser PS, Padgett D, Feldmann N, Chevaleyre V, Castillo PE, Hammer RE, Han W, Schmitz F, Lin W, Südhof TC (2006) Redundant functions of RIM1α and RIM2α in Ca^{2+}-triggered neurotransmitter release. EMBO J 25:5852–5863.

Wu YW, Kim JI, Tawfik VL, Lalchandani RR, Scherrer G, Ding JB (2015) Input- and cell-type-specific endocannabinoid-dependent LTD in the striatum. Cell Rep 10:75–87.

Yin HH (2008) From actions to habits: neuroadaptations leading to dependence. Alcohol Res Health 31:340–344.

Yin HH, Mulcare SP, Hilário MR, Clouse E, Holloway T, Davis MI, Hansson AC, Lovinger DM, Costa RM (2009) Dynamic reorganization of striatal circuits during the acquisition and consolidation of a skill. Nat Neurosci 12: 333–341.

Appendix C: A published article describing the role of L-Type Ca^{2+} Channels in tau-mediated memory impairments

This is a published manuscript in Frontier in Cellular Neuroscience, describing the effects of tau and the L-Type Ca^{2+} Channel, Ca-α1D, on memory and calcium handling in *Drosophila*. Here we showed that *tau* overexpression, as a model of Alzheimer's Disease, caused impaired memory. Moreover, knocking-down *Ca-α1D* in the MBs and MBs output neurons also impaired memory. Nonetheless, the knock-down of *Ca-α1D* improved memory performance in the *tau*-expressing flies to a level indistinguishable to the controls. We also showed that this was due to an increased expression of *Ca-α1D.* My contribution to this work, as co-first author, was to perform the experiments to assess the contribution of *Ca-α1D* in memory and the restore of phenotypes in the MBs output neurons. I also conducted the molecular assays to show the overexpression of *Ca-α1D* in tau flies.
As *CACNA1C*, the fly homologue of the *Ca-α1D* gene, is highly associated with schizophrenia, it was interesting to measure its role in learning and memory as a proxy to understand the cognitive impairments observed in patients with this disorder.

frontiers in Cellular Neuroscience

ORIGINAL RESEARCH
published: 10 September 2019
doi: 10.3389/fncel.2019.00409

Restoration of Olfactory Memory in *Drosophila* Overexpressing Human Alzheimer's Disease Associated Tau by Manipulation of L-Type Ca^{2+} Channels

*James P. Higham†, Sergio Hidalgo†, Edgar Buhl and James J. L. Hodge**

School of Physiology, Pharmacology and Neuroscience, University of Bristol, Bristol, United Kingdom

OPEN ACCESS

Edited by:
Miguel Medina, Biomedical Research Networking Center on Neurodegenerative Diseases (CIBERNED), Spain

Reviewed by:
Alfonso Martin-Pena, University of Florida, United States
Se-Young Choi, Seoul National University, South Korea
Amrit Mudher, University of Southampton, United Kingdom

***Correspondence:**
James J. L. Hodge
james.hodge@bristol.ac.uk

†These authors have contributed equally to this work

Specialty section:
This article was submitted to Cellular Neurophysiology, a section of the journal Frontiers in Cellular Neuroscience

Received: *29 March 2019*
Accepted: *26 August 2019*
Published: *10 September 2019*

Citation:
Higham JP, Hidalgo S, Buhl E and Hodge JJL (2019) Restoration of Olfactory Memory in Drosophila Overexpressing Human Alzheimer's Disease Associated Tau by Manipulation of L-Type Ca^{2+} Channels. Front. Cell. Neurosci. 13:409. doi: 10.3389/fncel.2019.00409

The cellular underpinnings of memory deficits in Alzheimer's disease (AD) are poorly understood. We utilized the tractable neural circuits sub-serving memory in *Drosophila* to investigate the role of impaired Ca^{2+} handling in memory deficits caused by expression of human 0N4R isoform of tau which is associated with AD. Expression of tau in mushroom body neuropils, or a subset of mushroom body output neurons, led to impaired memory. By using the Ca^{2+} reporter GCaMP6f, we observed changes in Ca^{2+} signaling when tau was expressed in these neurons, an effect that could be blocked by the L-type Ca^{2+} channel antagonist nimodipine or reversed by *RNAi* knock-down of the L-type channel gene. The L-type Ca^{2+} channel itself is required for memory formation, however, *RNAi* knock-down of the L-type Ca^{2+} channel in neurons overexpressing human tau resulted in flies whose memory is restored to levels equivalent to wild-type. Expression data suggest that *Drosophila* L-type Ca^{2+} channel mRNA levels are increased upon tau expression in neurons, thus contributing to the effects observed on memory and intracellular Ca^{2+} homeostasis. Together, our Ca^{2+} imaging and memory experiments suggest that expression of the 0N4R isoform of human tau increases the number of L-type Ca^{2+} channels in the membrane resulting in changes in neuronal excitability that can be ameliorated by *RNAi* knockdown or pharmacological blockade of L-type Ca^{2+} channels. This highlights a role for L-type Ca^{2+} channels in tauopathy and their potential as a therapeutic target for AD.

Keywords: tau, tauopathy, Alzheimer's disease, memory, L-type Ca2+ channels, *Drosophila*, GCaMP Ca2+ imaging

INTRODUCTION

The accumulation of the microtubule-associated protein tau (MAPT) within central neurons is a key histopathological feature of Alzheimer's disease (AD) (Kaufman et al., 2018; Nisbet and Gotz, 2018). Post-mortem AD brain samples contain the hallmark accumulation of extracellular amyloid beta (Aβ) plaques and intracellular neurofibrillary tangles (NFTs) of hyperphosphorylated tau, resulting in neurodegeneration and brain atrophy. The accumulation of tau is more correlated with the progression of AD pathology and symptoms than the magnitude of Aβ plaques

(Arendt et al., 2016). However, the mechanisms by which tau disrupts neuronal function, and consequently behavior, are not clear. Tau exists in six major isoforms formed by alternative splicing of exons 2 and/or 3 (0N, 1N or 2N) and 10 (3R or 4R) of the MAPT-17 gene (Buee et al., 2000). There is some evidence that 4R isoforms are upregulated in post-mortem brains, particularly within the hippocampus of AD patients (Boutajangout et al., 2004; Espinoza et al., 2008; Hasegawa et al., 2014), and show stronger affinity binding to tubulin and aggregation than 3R forms (Arendt et al., 2016). However, both 3R and 4R isoforms are present in NFTs, suggesting both play a role in pathology. The expression of 0N4R tau in model organisms can yield neuronal and behavioral dysfunction prior to the onset of neurodegeneration (Wittmann et al., 2001; Mershin et al., 2004). This suggests that tau's detrimental effect on neurons is sufficient to drive behavioral changes before neuronal death.

Patients with AD display memory impairment, and once the onset of neurodegeneration has occurred, treating the symptoms of AD becomes exceedingly difficult, so targeting the earlier signs of neuronal dysfunction is likely to be more efficacious. To this end, an understanding of how tau influences neuronal function is required. Disrupted calcium (Ca^{2+}) homeostasis including increased Ca^{2+} levels causing excitotoxicity has been posited as a key pathophysiology in AD, which may underpin the early stages of disease and precipitate neurodegeneration (Mattson and Chan, 2001; Brzyska and Elbaum, 2003; Canzoniero and Snider, 2005). Recent work suggests that these changes in neuronal excitability and Ca^{2+} signaling provide an important link between Aβ and tau pathology and disease progression (Spires-Jones and Hyman, 2014; Wu et al., 2016), but exactly how remains unknown. Different rodent models of tauopathy recapitulate some features of AD pathology including changes in excitability (Booth et al., 2016a,b), increased Ca^{2+} signaling (Wang and Mattson, 2014), neurodegeneration (Spillantini and Goedert, 2013), and impaired synaptic plasticity and memory (Arendt et al., 2016; Biundo et al., 2018). It is not clear what the source of increased Ca^{2+} is, however, increased levels of Ca^{2+} channels, such as the L-type voltage-gated Ca^{2+} channel (Ca_V1), have been shown to be upregulated in rodent models of AD, with blockers, such as nifedipine, being effective in trails to prevent the cognitive decline that occurs in AD (Coon et al., 1999; Anekonda et al., 2011; Goodison et al., 2012; Nimmrich and Eckert, 2013; Daschil et al., 2015). The role of voltage-gated Ca^{2+} channels in memory or AD has not been studied in *Drosophila*. *Drosophila* contains three different voltage-gated Ca^{2+} channel genes including the *DmCa1D* or *Ca-α1D* gene that encodes a high voltage-activated current and is equivalent to the vertebrate $Ca_V1.1$-1.4 genes that encode L-type Ca^{2+} channels (Worrell and Levine, 2008).

Alzheimer's disease and tauopathies have been modeled in *Drosophila* (Iijima-Ando and Iijima, 2010; Wentzell and Kretzschmar, 2010; Papanikolopoulou and Skoulakis, 2011), with targeted neuronal expression of human 0N4R tau causing neurodegeneration, shortened lifespan, circadian, sleep and motor deficits (Wittmann et al., 2001; Kerr et al., 2011; Sealey et al., 2017; Buhl et al., 2019; Higham et al., 2019). Furthermore, during development at the larval neuromuscular junction, motor neurons overexpressing human 0N3R or 0N4R caused a reduction in size and irregular and abnormally shaped synaptic terminals, a reduction in endocytosis and exocytosis and a reduction in high frequency synaptic transmission (Chee et al., 2005; Zhou et al., 2017). Also, while expression of tau 0N3R in the adult giant fiber system caused increased failure rate at high frequency stimulation, expression of 0N4R caused defects in stimulus conduction, response speed and conduction velocity (Kadas et al., 2019).

Learning and memory deficits can also be assessed in *Drosophila* using aversive olfactory classical conditioning (Malik et al., 2013; Malik and Hodge, 2014). Different mushroom body (MB) neuropils underpin specific phases of memory and are redundant during others (Pascual and Preat, 2001; Krashes et al., 2007; Davis, 2011). MB neurons send axons that terminate in lobed structures, with memory acquisition being mediated by the α′β′ lobe neurons and memory-storage by the αβγ neurons. In addition, a number of additional pairs of neurons innervate or are innervated by the MB and mediate different aspects of memory. For instance, the amnesiac expressing dorsal paired medial (DPM) and anterior paired lateral (APL) neurons are thought to consolidate and stabilize labile memory (Pitman et al., 2011). Finally, the MB innervate a pair of M4/6 MB output neurons via a cholinergic synapse, with optogenetic manipulation of the M4/6 neurons switching between appetitive and aversive memory (Barnstedt et al., 2016). Previous work has demonstrated that expression of tau in γ neurons caused a reduction in learning and 1.5 h memory in 3–5 days old young flies which were shown to still have their γ neurons intact, prior to their degeneration around day 45 (Mershin et al., 2004). Moreover, pan-neuronal 0N4R expression caused learning and long-term memory loss while 0N3R tau expression failed to do so (Sealey et al., 2017).

Therefore, *Drosophila* expressing human tau can be used to study AD relevant behaviors and their underlying neuronal mechanism, with loss of memory being possible prior to neurodegeneration. Although tau-mediated changes in neuronal properties are likely underpinning the memory impairment observed in *Drosophila* AD models, these changes have not been extensively studied in *Drosophila* MB neurons.

In this study, we determined the effect of human 0N4R tau expression in different neuropils of the *Drosophila* memory circuit on one-hour memory. We measured the effect of 0N4R tau on MB output neuron mediated memory and Ca^{2+} signaling and described a potential interaction between 0N4R tau with L-type voltage-gated Ca^{2+} channels which may underpin memory impairment.

RESULTS

To determine the effect of human tau 0N4R on memory, we targeted expression of the transgene to different neuronal populations of the *Drosophila* memory circuit and performed one-hour olfactory aversive conditioning. Driving expression of a human tau 0N4R transgene (Wittmann et al., 2001; Kerr et al., 2011; Higham et al., 2019) in the entire MB (*OK107-Gal4*

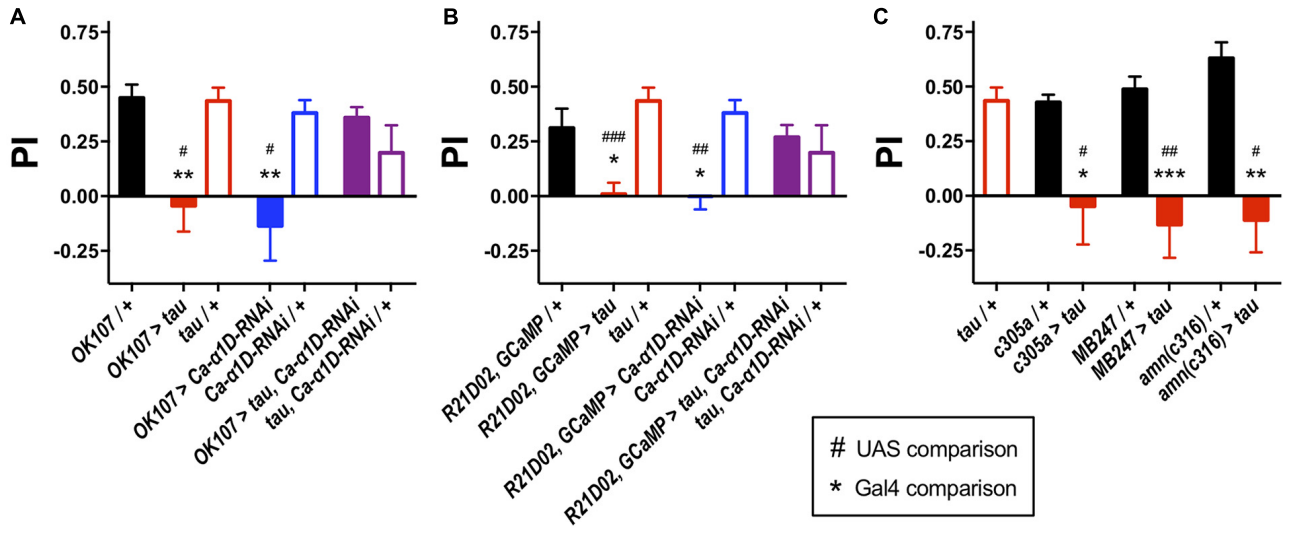

FIGURE 1 | Knock-down of L-type Ca^{2+} channels rescued tau-induced memory defects. **(A)** Tau expression in the MB (*OK107-Gal4*) ablated one-hour memory (n = 7 experiments with 50–100 flies each, red bar), as did the expression of an *RNAi* to the gene encoding the L-type Ca^{2+} channel alpha subunit (*Ca-α1D-RNAi*, n = 8, blue bar) compared to both Gal4 (n = 12, black bar) and UAS controls (tau, n = 11, open red bars; *Ca-α1D-RNAi*, n = 9, open blue bars). Co-expression of both transgenes (n = 12, purple bar) resulted in flies with a memory performance equivalent to that of control animals, as did the UAS controls (n = 4, open purple bar). **(B)** Likewise, expression of tau (n = 9) or *Ca-α1D-RNAi* (n = 6) in the MB efferent M4/6 neurons (*R21D02-Gal4*, n = 10) abolished memory. Memory was restored to wild-type levels by co-expression of both transgenes (n = 15). **(C)** Expression of tau in neuronal subpopulations of the MB impaired memory. Expression was driven in the α′β′ neurons (*c305a-Gal4*, n = 6 control, n = 4 tau), αβγ neurons (*MB247-Gal4*, n = 10 control, n = 7 tau) and dorsal paired medial neurons (*amn(c316)-Gal4*, n = 5 control, n = 4 tau). Data analyzed with Kruskal–Wallis test with Dunn's *post hoc* tests **(A,C)** or with one-way ANOVA with Dunnett's *post hoc* tests **(B)**. $^{*/\#}p < 0.05$, $^{**/\#\#}p < 0.01$, and $^{***/\#\#\#}p < 0.001$. Note that *UAS / +* controls are the same for each panel.

(Malik et al., 2013), p_{Gal4} = 0.004, p_{UAS} = 0.01, **Figure 1A**) yielded memory deficient flies. Similarly, when expressed in the memory-relevant M4/6 MB output neurons (Barnstedt et al., 2016), *R21D02-Gal4, GCaMP6f > tau* flies displayed greatly reduced memory performance compared to control counterparts (p_{Gal4} = 0.02, p_{UAS} < 0.001, **Figure 1B**). We also found that tau caused a significant reduction in one-hour memory when expressed in the α′β′ MB neurons (*c305a-Gal4* (Krashes et al., 2007), p_{Gal4} = 0.02, p_{UAS} = 0.01, **Figure 1C**), which mediate memory acquisition and in the memory-storing αβγ neurons (*MB247-Gal4* (Krashes et al., 2007), p_{Gal4} < 0.001, p_{UAS} = 0.003) and dorsal paired medial (DPM) neurons (*amn(c316)-Gal4*, p_{Gal4} = 0.002, p_{UAS} = 0.03), which consolidate and stabilize labile memory (Pitman et al., 2011). All animals used for aversive conditioning were aged 2–5 days and displayed naïve avoidance of shock (**Supplementary Table S1**). Likewise, all genotypes showed similar naïve avoidance of the odors used for olfactory conditioning (**Supplementary Table S1**). Thus, all genotypes were able to detect both odors and shock, verifying that memory defects were *bone fide* and not attributable to a sensorimotor defect.

To assess changes in Ca^{2+} handling which may underpin behavioral dysfunction, we imaged the M4/6 neurons in whole *ex vivo* brains using GCaMP6f as these neurons are pertinent to memory and single neurons can be visualized (Barnstedt et al., 2016). There did not appear to be a difference in baseline fluorescence of these neurons between control and tau-expressing animals (p = 0.5, **Figure 2A**), suggesting no effect on basal Ca^{2+} handling, assuming comparable GCaMP6f expression between genotypes. Bath application of high potassium chloride (KCl) concentration resulted in a robust and transient elevation in fluorescence which could be ameliorated by removing Ca^{2+} from the external solution (12.8 ± 1.0% of control, p = 0.003) or by adding cadmium (200 μM, 11.75 ± 11.75% of control, p = 0.009), a general blocker of *Drosophila* voltage-gated Ca^{2+} channels (Ryglewski et al., 2012), to the external solution (**Supplementary Figure S2A**). This indicated that the transient relies upon Ca^{2+} influx through voltage-gated Ca^{2+} channels, or that cadmium blocked presynaptic Ca^{2+} channels and, consequently, neurotransmitter release and activation of M4/6 neurons.

KCl-evoked Ca^{2+} transients in tau-expressing M4/6 neurons were almost three-fold greater than in control neurons (268.9 ± 45.2% of control, p = 0.005, **Figure 2B**). Since previous reports have documented the potential involvement of L-type Ca^{2+} channels in AD (Wang and Mattson, 2014; Coon et al., 1999), we tested whether the change in magnitude of Ca^{2+} transients in M4/6 neurons was dependent on these channels by applying the clinically-used L-type channel-selective blocker nimodipine (Nimmrich and Eckert, 2013; Terada et al., 2016). The addition of 5 μM nimodipine to the external solution had no effect on the magnitude of Ca^{2+} transients in control brains (p > 0.9, **Figure 2C**). However, the peak of the transient in tau-expressing neurons was sensitive to nimodipine and was reduced to a magnitude indistinguishable from control (98.9 ± 21.1% of control, p > 0.9). The elevated Ca^{2+} influx seen in these neurons may, therefore, be due to augmented L-type Ca^{2+} channels. To further investigate which type of voltage-gated Ca^{2+} channel

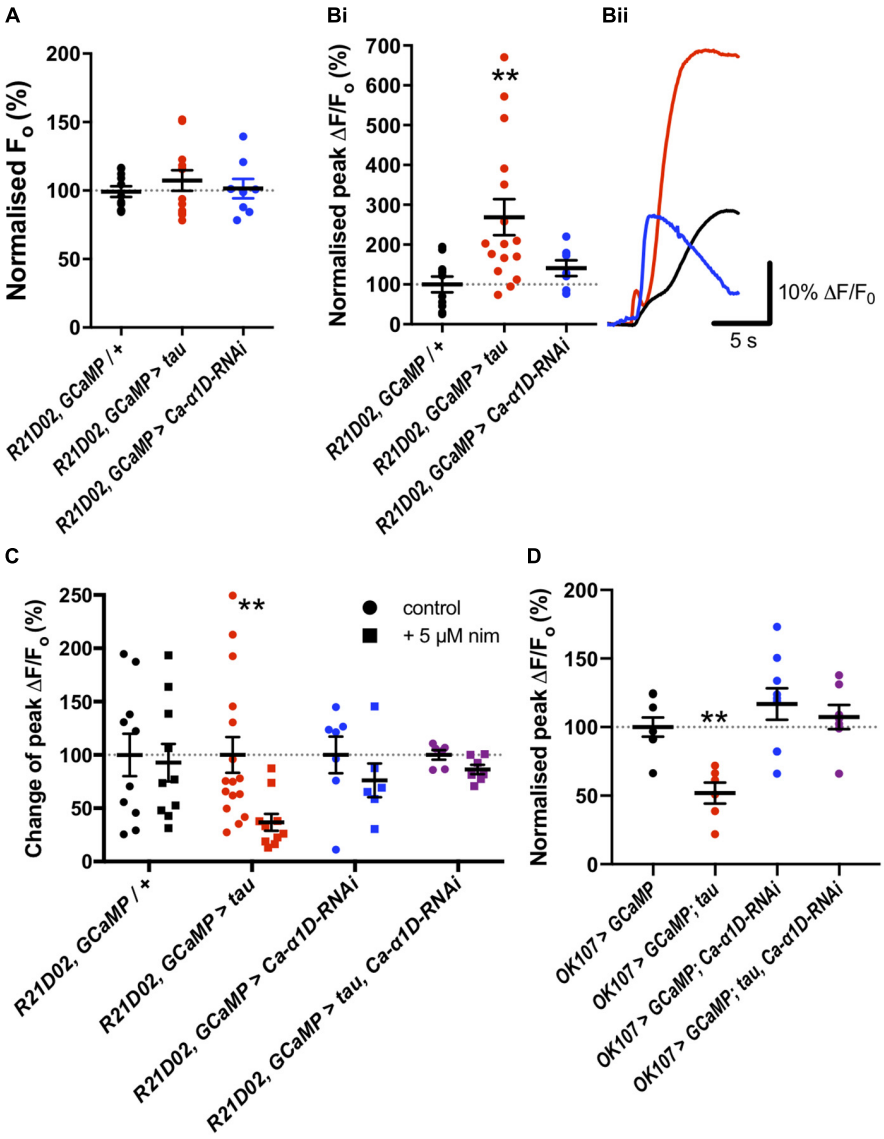

FIGURE 2 | Tau expression elevated nimodipine-sensitive Ca^{2+} channels in mushroom body (MB) and M4/6 neurons. **(A)** Basal Ca^{2+} levels were no different between control neurons and those expressing tau or *Ca-α1D-RNAi*. **(Bi)** However, the peak magnitude of Ca^{2+} transients were greater in the tau-expressing neurons than in control or *Ca-α1D-RNAi*-expressing neurons. **(Bii)** GCaMP6f relative fluorescence changes over time traces of M4/6 neurons in response to 100 mM KCl for control (black trace), tau (red trace) and *Ca-α1D-RNAi* (blue trace). **(C)** Ca^{2+} transients in control and *Ca-α1D-RNAi*-expressing neurons were not sensitive to the L-type Ca^{2+} channel blocker nimodipine (black and blue symbols, respectively). Driving tau expression in M4/6 neurons conferred sensitivity of Ca^{2+} transients to nimodipine (red symbols). The effect of tau on Ca^{2+} transient nimodipine sensitivity was ablated by co-expression of tau and *Ca-α1D-RNAi* in these neurons (purple symbols). Control for each genotype normalized to 100%. **(D)** Tau expression in the MB reduced peak fluorescence following a high KCl challenge; an effect reversed by co-expression of *Ca-α1D-RNAi*. Data analyzed with one-way ANOVA with Dunnett's *post hoc* tests panels **(A,D)**, with Kruskal–Wallis test with Dunn's *post hoc* tests panel **(B)** or with two-way ANOVA with Sidak's *post hoc* tests panel **(C)**. $^{*/\#}p < 0.05$, $^{**/\#\#}p < 0.01$, and $^{***/\#\#\#}p < 0.001$. Note that data for *OK107 > GCaMP* and *OK107 > GCaMP, tau* are reproduced from Higham et al. (2019).

mediated the Ca^{2+} influx, we also tested the effect of addition of the L-type and T-type Ca^{2+} channel blocker, amiloride (1 mM), to nimodipine on the KCl-induced Ca^{2+} transient, as this compound greatly reduced Ca^{2+} currents in cultured embryonic *Drosophila* giant neurons (Peng and Wu, 2007). Amiloride did not significantly reduce the peak of the Ca^{2+} transient in M4/6 neurons ($p = 0.2$, **Supplementary Figure S2B**). The lack of effect of amiloride likely indicates developmental or cell-specific differences in Ca^{2+} channel expression or that the voltage-gated Ca^{2+} channels blocked by amiloride largely overlap with nimodipine which do not contribute significantly to the Ca^{2+} transient in wild-type M4/6 neurons.

To corroborate our pharmacological data, we tested the nimodipine sensitivity of Ca^{2+} transients in M4/6 neurons co-expressing tau and an *RNAi* to the L-type Ca^{2+} channel gene (*UAS-Ca-α1D-RNAi*), that has been shown to reduce

L-type Ca^{2+} channel currents and protein levels by over 75% in *Drosophila* neurons (Kadas et al., 2017). Ca^{2+} transients in these neurons displayed a much reduced, and statistically insignificant ($p > 0.05$, **Figure 2C**), block by nimodipine compared to transients in neurons expressing tau alone (13.2% vs. 62.3% reduction in peak). This data shows that the elevated Ca^{2+} transients in tau-expressing M4/6 neurons rely on L-type Ca^{2+} channels. As L-type channels negatively regulate neuronal excitability (Worrell and Levine, 2008), *RNAi* mediated reduction of L-type Ca^{2+} channels increases neuronal activity (Kadas et al., 2017).

We went on to test the involvement of the L-type Ca^{2+} channel itself in memory by knocking down its expression with *RNAi*. Knock-down of *Ca-α1D* in the M4/6 neurons abolished one-hour memory ($p_{Gal4} = 0.03$, $p_{UAS} = 0.007$, **Figure 1B**). These animals exhibited no sensorimotor defects (**Supplementary Table S1**), verifying the observed phenotype as a genuine memory defect. In alignment with the lack of effect of nimodipine on the Ca^{2+} transient in control neurons, knock-down of the L-type channel had no effect on KCl-evoked Ca^{2+} influx in M4/6 cells ($p = 0.6$, **Figure 2B**).

We sought to resolve whether there was a behavioral interaction between 0N4R tau and the L-type Ca^{2+} channel by testing whether knocking down *Ca-α1D* could ameliorate the effect of tau on memory as it did on Ca^{2+} signaling. Strikingly, even though expression of human tau or *Ca-α1D-RNAi* removed memory alone, co-expression in M4/6 neurons yielded flies with memory performance indistinguishable from wild-type animals ($p_{Gal4} > 0.9$, $p_{UAS} > 0.9$, **Figure 1B**). We tested whether this restoration of memory could have been a consequence of *Gal4* dilution due to the presence of multiple transgenes. Expression of an innocuous gene, *UAS-GFP*, with either *UAS-tau* or *UAS-Ca-α1D-RNAi* yielded animals with impaired memory ($p = 0.02$ and 0.005, respectively, **Supplementary Figure S1**). This demonstrates that dilution of transgene expression is not responsible for the observed change in memory performance. Lastly, the expression of transgenes in the M4/6 output neurons had no effect on the animals' naïve sensorimotor behavior indicating that the effects seen in memory are not due to defective sensory responses (**Supplementary Table S1**).

To test if the apparent interaction between tau and L-type Ca^{2+} channels occurred in other neurons, we performed Ca^{2+} imaging of the entire MB (*OK107-Gal4*). The KCl-evoked Ca^{2+} response in this large population of neurons was reduced by the expression of tau (48.1% reduction, $p = 0.006$, **Figure 2D**; Higham et al., 2019), likely reflecting a reduction in excitability. MB neuronal architecture appeared grossly intact in tau-expressing animals (data not shown), and neurodegeneration has been shown not to play a significant role in memory defects at this age (Higham et al., 2019). In alignment with observations in M4/6 neurons, the expression of *Ca-α1D-RNAi* in the MB abolished one-hour memory ($p_{Gal4} = 0.001$, $p_{UAS} = 0.04$, **Figure 1A**) but did not affect the magnitude of the Ca^{2+} transient in these neurons ($p = 0.4$, **Figure 2D**). The co-expression of these two transgenes in the MB resulted in a Ca^{2+} transient which was no different in magnitude compared to control animals ($p > 0.9$, **Figure 2D**). The ablation of one-hour memory caused by tau or *Ca-α1D-RNAi* expression in MB neurons was also reversed by co-expression of both transgenes as these animals exhibited a memory performance equivalent to control animals ($p_{Gal4} > 0.9$, $p_{UAS} > 0.9$, **Figure 1A**).

The mechanism underlying tau-mediated augmentation of Ca^{2+} influx through L-type channels is not clear. It could be due to elevated expression of the *Ca-α1D* gene, increased trafficking to, or reduced recycling from, the plasma membrane or changes in single channel properties such as conductance or open probability. To investigate this further, we measured *Ca-α1D* expression in whole brain extracts by RT-qPCR. All transgenes were expressed in all neurons (*elav-Gal4*) to ensure changes in gene expression were detectable (**Figure 3**). *Ca-α1D-RNAi* knock-down reduced expression of the channel by 58% ($p < 0.05$), while expression of tau lead to a 68% ($p = 0.04$) increase in *Ca-α1D*. Interestingly, co-expression of tau and *Ca-α1D-RNAi* restored *Ca-α1D* to 72% ($p = 0.3$) of control fly levels. This strongly suggests that the effects observed in behavior and Ca^{2+} imaging are due to a change in *Ca-α1D* expression in the brain.

DISCUSSION

Selectively expressing tau in MB neuronal subsets revealed a non-specific adverse effect on memory processing (**Figure 1**). MB neurons sub-serving specific memory phases rely on different signaling molecules. For example, CaMKII is required in α′β′ neurons, but not αβγ, and vice versa for KCNQ channels (Cavaliere et al., 2013; Malik et al., 2013). This suggests that

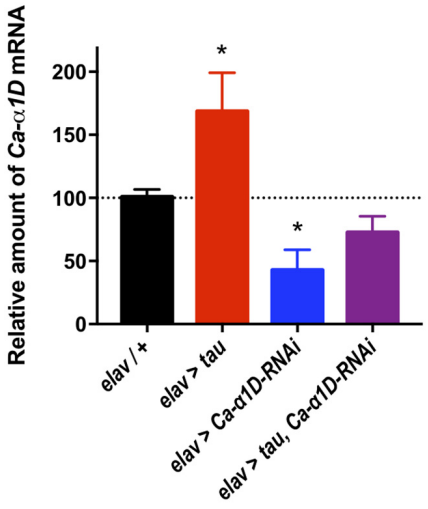

FIGURE 3 | Tau expression increased Ca^{2+} *channelα1D mRNA* levels. Pan-neuronal Tau expression led to a 68% increase in *Ca-α1D mRNA* levels compared to controls, while expressing a *RNAi* against *Ca-α1D* reduced its expression by 58%. Co-expression of the *RNAi* in tau expressing flies partially restored levels of *Ca-α1D* compared to controls. $n = 6$ biological replicates of 23 or more heads each for all groups. Data analyzed with one-way ANOVA with Holm-Sidak's *post hoc* tests. *$p < 0.05$.

tau either promiscuously interacts with and disrupts numerous intracellular components or disrupts a pathway common to all MB neurons. *In vivo* Ca^{2+} imaging of different MB neuronal subsets has revealed the importance of Ca^{2+} transient plasticity in olfactory associative memory (Yu et al., 2006; Sejourne et al., 2011). Following conditioning, MB neurons exhibit differential Ca^{2+} responses to the CS+ and CS- odors (Yu et al., 2006; Sejourne et al., 2011). In the β′ lobe dendrites of M4/6 neurons, exposure to an aversively conditioned CS+ odour results in a greater Ca^{2+} influx compared with CS-, with the reverse being true for appetitively conditioned odors (Owald et al., 2015). Other MB neurons display a similar distinction between CS+ and CS-, with these differences believed to coordinate avoidance or approach behavior. Given that tau expression aberrantly elevated stimulus-evoked Ca^{2+} influx, it is plausible that this interferes with conditioning-induced Ca^{2+} transient plasticity. Augmented Ca^{2+} entry via L-type channels in tau-expressing neurons may ablate the difference in Ca^{2+} influx between CS+ and CS-, rendering them indistinguishable at the cellular level.

The knock-down of the *Drosophila* L-type Ca^{2+} channel demonstrated its importance in both the MB and the M4/6 neurons for memory. This aligns with data from $Ca_v1.2$ knock-out mice, which are deficient in spatial memory tasks (Moosmang et al., 2005; White et al., 2008). Despite *R21D02, GCaMP6f > Ca-α1D-RNAi* and *OK107 > Ca-α1D-RNAi* flies being memory deficient, the M4/6 and MB neurons of these animals displayed no reduction in evoked Ca^{2+} entry, nor did nimodipine have any effect on the Ca^{2+} transient in control M4/6 neurons (**Figure 2**). This suggests that perhaps only a small population of L-type channels is present in these neurons. A previous electrophysiological study of Ca^{2+} currents in cultured *Drosophila* giant embryonic neurons revealed only a very small block by nifedipine, likely reflecting a low number of L-type channels (Peng and Wu, 2007). Likewise an electrophysiological and pharmacological study of the adult *OK107-Gal4* MB neurons again showed only a small contribution of L-type channels to their Ca^{2+} transients (Jiang et al., 2005). Fluorescence imaging using GCaMP may not be sufficiently sensitive to resolve such a small contribution to global Ca^{2+} influx – a contribution that is nonetheless important for cellular function and, hence, memory.

It is not known whether the L-type channel plays any role in the plasticity of Ca^{2+} transients in *Drosophila per se*. However, these channels are vital for the function of memory-associated neurons. The generation of medium and slow afterhyperpolarizations (AHPs), which are a period of prolonged hyperpolarized membrane potential following action potential firing, in hippocampal neurons is dependent on Ca^{2+} entry through L-type channels (Lancaster and Adams, 1986; Marrion and Tavalin, 1998; Bowden et al., 2001). Elevated Ca^{2+} entry would augment AHPs and suppress neuronal firing, thereby disrupting neural circuit function and the behavior subserved by that circuit. This is apparent in mice and rabbits, which exhibit an age-related memory decline with concomitant elevation of L-type Ca^{2+} channel expression and AHP magnitude in the hippocampus (Moyer et al., 1992; Nunez-Santana et al., 2014). This impairs stimulus-evoked changes in neuronal activity which underpin learning (Moyer et al., 2000). Blocking augmented AHPs in aged rabbits with nimodipine facilitated enhanced performance in associative learning tasks (Straube et al., 1990). L-type Ca^{2+} channels also negatively regulate neuronal excitability in *Drosophila* neurons (Worrell and Levine, 2008), and so their augmentation by tau may exert a similar effect on *Drosophila* neurons to that observed in aging mammals, with their knock-down resulting in increased firing of neurons (Kadas et al., 2017).

In M4/6 neurons, we observed raised evoked Ca^{2+} influx due to tau expression, while Ca^{2+} influx was suppressed in MB neurons (**Figures 2B,D**). Augmentation of the Ca^{2+} transient in single tau-expressing M4/6 neurons reflects the elevated Ca^{2+} influx through L-type channels, as the transients were reduced by nimodipine and L-type channel knock-down. However, in a large population of MB neurons (∼2500 neurons) the elevated Ca^{2+} influx through L-type channels is likely small relative to the reduced Ca^{2+} levels due to suppressed neuronal activity, therefore a reduction in the Ca^{2+} transient was observed. The reduced excitability of MB neurons was rescued by co-expression of *Ca-α1D-RNAi* as this manipulation opposes the suppression of excitability caused by tau (Kadas et al., 2017). Not only were the tau-induced Ca^{2+} signaling defects rescued by manipulation of L-type Ca^{2+} channels, but so was olfactory memory (**Figures 1A,B**). This lends further credence to the suggestion that tau interacts with the L-type Ca^{2+} channel and also shows that this interaction solely mediates memory dysfunction, at least in young animals.

Raised L-type Ca^{2+} channel expression has also been documented in other AD models, as well as in aging. In agreement with our data, L-type Ca^{2+} current density was elevated in CA1 neurons of 3 × Tg mice (Wang and Mattson, 2014), as were AHPs in the dorsomedial entorhinal cortex of rTg4510 mice (Booth et al., 2016a). Our data shows that wild-type 0N4R tau, as well as the frontotemporal dementia-associated P301L mutant expressed in 3 × Tg and rTg4510 mice, is capable of augmenting Ca^{2+} influx in neurons. What is more, elevated expression of a mammalian L-type Ca^{2+} channel ($Ca_V1.2$) was observed in a neuroblastoma cell line following transgenic $A\beta_{42}$ expression; this resulted in reduced cell viability and six-fold increase in Ca^{2+} influx, that could be ameliorated by the L-type Ca^{2+} channel dihydropyridine blockers, nimodipine and isradipine (Copenhaver et al., 2011). This study went on to show that the L-type channel blocker, isradipine could increase survival of *Drosophila* overexpressing human amyloid precursor protein (APP_{695}), as well as decreasing the accumulation of Aβ and phosphorylated tau in the triple transgenic AD mice (3 × TgAD) which express human Presenilin 1_{M146V}, $APP_{Swedish}$ and tau_{P30L}. This indicates that correcting defective Ca^{2+} handling in AD may be of therapeutic benefit, particularly as L-type Ca^{2+} channels appear to be relevant in the human AD brain, too.

Raised L-type Ca^{2+} channel expression has been documented in the brains of AD patients (Coon et al., 1999), with increased L-type channels thought to underlie the memory loss and neurodegeneration that occurs in dementia (Missiaen et al., 2000; Mattson and Chan, 2001; Canzoniero and Snider, 2005; Thibault et al., 2007). Our data shows that there is increased

expression of the *Drosophila* L-type Ca^{2+} channel, *Ca-α1D,* in tau expressing neurons, therefore suggesting conserved mechanisms of Aβ and tau-related calcium deficits across species (**Figure 3**). Importantly, clinical trials of L-type blockers show a slowing of cognitive decline in AD patients (Anekonda et al., 2011; Goodison et al., 2012; Nimmrich and Eckert, 2013).

In summary, using behavioral, physiological, pharmacological and molecular methods, we show that knock-down of the *Drosophila* L-type Ca^{2+} channel *Ca-α1D* can rescue tau mediated olfactory learning deficits by restoring Ca^{2+} handling in MB neurons.

MATERIALS AND METHODS

Drosophila Genetics

Flies were raised at a standard density with a 12 h:12 h light dark (LD) cycle on standard *Drosophila* medium (0.7% agar, 1.0% soya flour, 8.0% polenta/maize, 1.8% yeast, 8.0% malt extract, 4.0% molasses, 0.8% propionic acid, and 2.3% nipagen) at 25°C. Wild-type control was *Canton S w-* (*CSw-*) and *R21D02-GAL4, UAS-GCaMP6f* were kind gifts from Prof. Scott Waddell (University of Oxford). *UAS-human MAPT (TAU 0N4R) wild-type* (Wittmann et al., 2001; Kerr et al., 2011) was a kind gift from Prof. Linda Partridge (University College London), *UAS-GFP* was a gift from Prof. Mark Wu (John Hopkins University). The following flies were obtained from the Bloomington and Vienna fly stock centers: *OK107-Gal4* (Bloomington *Drosophila* stock center number BDSC:854), *c305a-Gal4* (BDSC:30829), *amn(c316)-Gal4* (BDSC:30830), *MB247-Gal4* (BDSC:50742), *elav-Gal4* (BDSC:8760), *UAS-GCaMP6f* (BDSC:42747) and *UAS-Ca-α1D-RNAi* flies [Vienna *Drosophila* resource center GD51491 (Kadas et al., 2017)].

Aversive Olfactory Conditioning

All memory experiments were carried out at 25°C and 70% relative humidity under dim red light. Flies were used for experiments after 2–5 days of aging at 25°C and 70% relative humidity in a 12-hour light: 12-hour dark environment. Using a previously published protocol (Mershin et al., 2004; Krashes et al., 2007; Kosmidis et al., 2010; Malik et al., 2013; Malik and Hodge, 2014; Barnstedt et al., 2016), groups of 25–50 flies were first transferred from food tubes into the training tube lined with an electrifiable grid. After acclimatization to the electrified tube for 90 s, flies were exposed to either 3-octanol (OCT, Sigma) or 4-methylcyclohexanol (MCH, Sigma) (conditioned stimulus, CS+) paired with twelve 70 V DC electric shocks (unconditioned stimulus, United States) over 60 s (shocks of duration 1.25 s with inter-shock latency of 3.75 s). This was followed by a 30 s rest period with no stimulus. Flies were then exposed to the reciprocal odour (CS−) for 60 s with no electric shock. Memory retention was tested one-hour post-conditioning (intermediate-term memory). To account for any innate bias the flies may have towards an odour, the CS + odour was reversed in alternate groups of flies and the performances from these two groups averaged to give $n = 1$. Moreover, the order of delivery of CS+ and CS− was alternately reversed.

To test memory, flies were placed at the choice point of a T-maze with one pathway exposed to CS+ and the other to CS−. After 120 s, the number of flies choosing each pathway was counted. Memory was quantified using the performance index (PI):

$$PI = \frac{N_{CS-} - N_{CS+}}{N_{CS-} + N_{CS+}}$$

where N_{CS-} and N_{CS+} is the number of flies choosing CS− and CS+, respectively. A $PI = 1$ indicates perfect learning where all flies chose CS−, and $PI = 0$ indicates a 50:50 split between CS− and CS+ and, therefore, no learning.

Calcium Imaging

GCaMP imaging was performed using previously published protocols (Cavaliere et al., 2012; Gillespie and Hodge, 2013; Malik et al., 2013; Schlichting et al., 2016; Shaw et al., 2018) with flies being anaesthetized on CO_2, decapitated and their brains dissected out of the head in extracellular saline containing (in mM): 101 NaCl, 1 $CaCl_2$, 4 $MgCl_2$, 3 KCl, 5 D-glucose, 1.25 NaH_2PO_4, and 20.7 $NaHCO_3$ adjusted to a final pH of pH 7.2 with an osmolality of 247–253 mmol/kg. Brains were held ventral side up in a recording chamber using a custom-made anchor and visualized with a 40× water-immersion lens on an upright microscope (Zeiss Examiner Z1).

Brains were superfused with extracellular saline (5 mL/min) as above and cells were depolarized by bath application of 100 mM KCl in extracellular solution (362 mmol/kg) for 15 s at 5 mL/min. Drug-containing or Ca^{2+}-lacking solutions were superfused over the brain for 60 s prior to imaging. The Ca^{2+}-lacking external solution contained 8 mM $MgCl_2$.

Images were acquired at 8 Hz with 50 ms exposure using a CCD camera (ZEISS Axiocam) and a 470 nm LED light source (Colibri, ZEISS) and recorded with ZEN (Zeiss, 4 frames/sec). Baseline fluorescence (F_0) was taken as the mean fluorescence during the 10 s (80 images) prior to the start of KCl perfusion. The change in fluorescence relative to baseline [$(F\text{-}F_0)/F_0$, where F is fluorescence at a given time] following KCl addition was recorded, and the peak change [$(F_{max}\text{-}F_0)/F_0$] was used as a metric of transient [Ca^{2+}] increase. Example traces were plotted using Origin 9 (Origin Lab).

All chemicals were purchased from Sigma-Aldrich (Gillingham, United Kingdom), except for nimodipine which was purchased from Tocris (Bristol, United Kingdom) and amiloride which was donated by Prof. David Sheppard (University of Bristol).

RT-qPCR

Relative measure of Ca-α1D expression levels was assessed by two-step qPCR. 2–5 days old male flies were anesthetized with CO_2 and decapitated, obtaining six biological replicates with 23 heads each. Total *RNA* was extracted from head lysates by organic phenol/chloroform method using TRIzol reagent (Invitrogen). *RNA* quantification was carried out in Nanodrop spectrophotometer (Thermo Scientific) and *RNA* integrity was checked by electrophoresis in 1% agarose gel. Samples were

treated with TURBO DNA-free kit (Invitrogen) in order to remove genomic DNA contamination. Reverse transcription was carried out using RevertAid First Strand cDNA Synthesis Kit (Thermo Scientific) following manufacturer's instructions, with 500 ng of *RNA* as template and Oligo (dT) as primer to amplify total *mRNA*. cDNA samples were stored at −20°C or used immediately for qPCR reactions.

Quantitative PCR reactions were carried out in QuantStudio 3 Real-Time PCR system (Applied Biosystems) using HOT FIREPol EvaGreen qPCR Mix Plus (Solis BioDyne). The primers used to amplify Ca-α1D *mRNA* were as follows: Ca1DF 5′-CCTTGAGGGCTGGACTGATG-3′ and Ca1DR 5′-ATCACGAAGAAGGCACCCAG-3′ with a PCR product expected size of 108 bp and 104% primer efficiency (**Supplementary Figure S3**). As a housekeeping gene, the following primers for GAPDH2 *mRNA* were used: GAPDH2F 5′-CGTTCATGCCACCACCGCTA-3′ and GAPDH2R 5′-CCACGTCCATCACGCCACAA-3′. The expected PCR product size was 72 bp and the primer efficiency was 100%. To activate DNA polymerase, a first step of 15 min at 95°C was used, followed by 50 cycles of 30 s at 95°C, 30 s at 60°C, followed by a 1 min 72°C elongation step. At the end of the experiment, a temperature ramp from 60°C to 95°C was used for melting curve analysis and the product fit to the predicted melting curve obtained by uMelt software (Dwight et al., 2011). Quantification for each genotype and each gene was carried out using the $2^{(-\Delta\ \Delta\ Ct)}$ method and data was expressed as a percentage of change.

Analysis

All data were analyzed using Prism 7 (GraphPad Inc.). Data were scrutinized to check they met the assumptions of parametric statistical tests, and non-parametric, rank-based alternatives were used where appropriate. Details of statistical tests used are in figure legends. Data are presented as mean ± standard error of mean.

DATA AVAILABILITY

The raw data supporting the conclusion of this manuscript will be made available by the authors, without undue reservation, to any qualified researcher.

AUTHOR CONTRIBUTIONS

All authors devised and performed the experiments, and wrote and edited the manuscript. JH secured the funding.

FUNDING

This work was supported by a CONICYT-PCHA/Doctorado Nacional/2016-21161611 studentship to SH. GW4 accelerator (GW4-AF2-002), Alzheimer's Research United Kingdom network grant, Alzheimer's Society undergraduate grants and Leverhulme Trust grant (RPG-2016-318) to JH. The funders had no other part in research.

ACKNOWLEDGMENTS

The authors are grateful to Drs. Linda Partridge, Scott Waddell, and Mark Wu for providing the fly stocks, and Drs. Kofan Chen, Bilal Malik, and Neil Marrion for helpful advice and comments on the manuscript.

SUPPLEMENTARY MATERIAL

The Supplementary Material for this article can be found online at: https://www.frontiersin.org/articles/10.3389/fncel.2019.00409/full#supplementary-material

REFERENCES

Anekonda, T. S., Quinn, J. F., Harris, C., Frahler, K., Wadsworth, T. L., and Woltjer, R. L. (2011). L-type voltage-gated calcium channel blockade with isradipine as a therapeutic strategy for Alzheimer's disease. *Neurobiol. Dis.* 41, 62–70. doi: 10.1016/j.nbd.2010.08.020

Arendt, T., Stieler, J. T., and Holzer, M. (2016). Tau and tauopathies. *Brain Res. Bull.* 126, 238–292. doi: 10.1016/j.brainresbull.2016.08.018

Barnstedt, O., Owald, D., Felsenberg, J., Brain, R., Moszynski, J. P., Talbot, C. B., et al. (2016). Memory-Relevant mushroom body output synapses are cholinergic. *Neuron* 89, 1237–1247. doi: 10.1016/j.neuron.2016.02.015

Biundo, F., Del Prete, D., Zhang, H., Arancio, O., and D'Adamio, L. (2018). A role for tau in learning, memory and synaptic plasticity. *Sci. Rep.* 8:3184. doi: 10.1038/s41598-018-21596-3

Booth, C. A., Ridler, T., Murray, T. K., Ward, M. A., de Groot, E., Goodfellow, M., et al. (2016a). Electrical and network neuronal properties are preferentially disrupted in dorsal, but not ventral, medial entorhinal cortex in a mouse model of tauopathy. *J. Neurosci.* 36, 312–324. doi: 10.1523/JNEUROSCI.2845-14.2016

Booth, C. A., Witton, J., Nowacki, J., Tsaneva-Atanasova, K., Jones, M. W., Randall, A. D., et al. (2016b). Altered intrinsic pyramidal neuron properties and pathway-specific synaptic dysfunction underlie aberrant hippocampal network function in a mouse model of tauopathy. *J. Neurosci.* 36, 350–363. doi: 10.1523/JNEUROSCI.2151-15.2016

Boutajangout, A., Boom, A., Leroy, K., and Brion, J. P. (2004). Expression of tau mRNA and soluble tau isoforms in affected and non-affected brain areas in Alzheimer's disease. *FEBS Lett.* 576, 183–189. doi: 10.1016/j.febslet.2004.09.011

Bowden, S. E., Fletcher, S., Loane, D. J., and Marrion, N. V. (2001). Somatic colocalization of rat SK1 and D class ($Ca_V1.2$) L-type calcium channels in rat CA1 hippocampal pyramidal neurons. 21:RC175. doi: 10.1523/JNEUROSCI.21-20-j0006.2001

Brzyska, M., and Elbaum, D. (2003). Dysregulation of calcium in Alzheimer's disease. *Acta Neurobiol. Exp.* 63, 171–183.

Buee, L., Bussiere, T., Buee-Scherrer, V., Delacourte, A., and Hof, P. R. (2000). Tau protein isoforms, phosphorylation and role in neurodegenerative disorders. *Brain Res. Brain Res. Rev.* 33, 95–130. doi: 10.1016/s0165-0173(00)00019-9

Buhl, E., Higham, J. P., and Hodge, J. J. L. (2019). Alzheimer's disease-associated tau alters *Drosophila* circadian activity, sleep and clock neuron electrophysiology. *Neurobiol. Dis.* 130:104507. doi: 10.1016/j.nbd.2019.104507

Canzoniero, L. M., and Snider, B. J. (2005). Calcium in Alzheimer's disease pathogenesis: too much, too little or in the wrong place? *J. Alzheimers Dis.* 8, 147–154; discussion 209–115.

Cavaliere, S., Gillespie, J. M., and Hodge, J. J. (2012). KCNQ channels show conserved ethanol block and function in ethanol behaviour. *PLoS One* 7:e50279. doi: 10.1371/journal.pone.0050279

Cavaliere, S., Malik, B. R., and Hodge, J. J. (2013). KCNQ channels regulate age-related memory impairment. *PLoS One* 8:e62445. doi: 10.1371/journal.pone.0062445

Chee, F. C., Mudher, A., Cuttle, M. F., Newman, T. A., MacKay, D., Lovestone, S., et al. (2005). Over-expression of tau results in defective synaptic transmission in *Drosophila* neuromuscular junctions. *Neurobiol. Dis.* 20, 918–928. doi: 10.1016/j.nbd.2005.05.029

Coon, A. L., Wallace, D. R., Mactutus, C. F., and Booze, R. M. (1999). L-type calcium channels in the hippocampus and cerebellum of Alzheimer's disease brain tissue. *Neurobiol. Aging* 20, 597–603. doi: 10.1016/s0197-4580(99)00068-8

Copenhaver, P. F., Anekonda, T. S., Musashe, D., Robinson, K. M., Ramaker, J. M., Swanson, T. L., et al. (2011). A translational continuum of model systems for evaluating treatment strategies in Alzheimer's disease: isradipine as a candidate drug. *Dis. Models Mech.* 4, 634–648. doi: 10.1242/dmm.006841

Daschil, N., Kniewallner, K. M., Obermair, G. J., Hutter-Paier, B., Windisch, M., Marksteiner, J., et al. (2015). L-type calcium channel blockers and substance P induce angiogenesis of cortical vessels associated with beta-amyloid plaques in an Alzheimer mouse model. *Neurobiol. Aging* 36, 1333–1341. doi: 10.1016/j.neurobiolaging.2014.12.027

Davis, R. L. (2011). Traces of *Drosophila* memory. *Neuron* 70, 8–19. doi: 10.1016/j.neuron.2011.03.012

Dwight, Z., Palais, R., and Wittwer, C. T. (2011). uMELT: prediction of high-resolution melting curves and dynamic melting profiles of PCR products in a rich web application. *Bioinformatics* 27, 1019–1020. doi: 10.1093/bioinformatics/btr065

Espinoza, M., de Silva, R., Dickson, D. W., and Davies, P. (2008). Differential incorporation of tau isoforms in Alzheimer's disease. *J. Alzheimers Dis.* 14, 1–16. doi: 10.3233/jad-2008-14101

Gillespie, J. M., and Hodge, J. J. (2013). CASK regulates CaMKII autophosphorylation in neuronal growth, calcium signaling, and learning. *Front. Mol. Neurosci.* 6:27. doi: 10.3389/fnmol.2013.00027

Goodison, W. V., Frisardi, V., and Kehoe, P. G. (2012). Calcium channel blockers and Alzheimer's disease: potential relevance in treatment strategies of metabolic syndrome. *J. Alzheimes Dis.* 30(Suppl. 2), S269–S282. doi: 10.3233/JAD-2012-111664

Hasegawa, M., Watanabe, S., Kondo, H., Akiyama, H., Mann, D. M., Saito, Y., et al. (2014). 3R and 4R tau isoforms in paired helical filaments in Alzheimer's disease. *Acta Neuropathol.* 127, 303–305. doi: 10.1007/s00401-013-1191-9

Higham, J. P., Malik, B. R., Buhl, E., Dawson, J. M., Ogier, A. S., Lunnon, K., et al. (2019). Alzheimer's disease associated genes ankyrin and tau cause shortened lifespan and memory loss in *Drosophila*. *Front. Cell. Neurosci.* 13:260. doi: 10.3389/fncel.2019.00260

Iijima-Ando, K., and Iijima, K. (2010). Transgenic *Drosophila* models of Alzheimer's disease and tauopathies. *Brain Struct. Funct.* 214, 245–262. doi: 10.1007/s00429-009-0234-4

Jiang, S. A., Campusano, J. M., Su, H., and O'Dowd, D. K. (2005). *Drosophila* mushroom body Kenyon cells generate spontaneous calcium transients mediated by PLTX-sensitive calcium channels. *J. Neurophysiol.* 94, 491–500. doi: 10.1152/jn.00096.2005

Kadas, D., Klein, A., Krick, N., Worrell, J. W., Ryglewski, S., and Duch, C. (2017). Dendritic and Axonal L-Type calcium channels cooperate to enhance motoneuron firing output during *Drosophila* larval locomotion. *J. Neurosci.* 37, 10971–10982. doi: 10.1523/JNEUROSCI.1064-17.2017

Kadas, D., Papanikolopoulou, K., Xirou, S., Consoulas, C., and Skoulakis, E. M. C. (2019). Human Tau isoform-specific presynaptic deficits in a *Drosophila* central nervous system circuit. *Neurobiol. Dis.* 124, 311–321. doi: 10.1016/j.nbd.2018.12.004

Kaufman, S. K., Del Tredici, K., Thomas, T. L., Braak, H., and Diamond, M. I. (2018). Tau seeding activity begins in the transentorhinal/entorhinal regions and anticipates phospho-tau pathology in Alzheimer's disease and PART. *Acta Neuropathol.* 136, 57–67. doi: 10.1007/s00401-018-1855-6

Kerr, F., Augustin, H., Piper, M. D., Gandy, C., Allen, M. J., Lovestone, S., et al. (2011). Dietary restriction delays aging, but not neuronal dysfunction, in *Drosophila* models of Alzheimer's disease. *Neurobiol. Aging* 32, 1977–1989. doi: 10.1016/j.neurobiolaging.2009.10.015

Kosmidis, S., Grammenoudi, S., Papanikolopoulou, K., and Skoulakis, E. M. (2010). Differential effects of Tau on the integrity and function of neurons essential for learning in *Drosophila*. *J. Neurosci.* 30, 464–477. doi: 10.1523/JNEUROSCI.1490-09.2010

Krashes, M. J., Keene, A. C., Leung, B., Armstrong, J. D., and Waddell, S. (2007). Sequential use of mushroom body neuron subsets during *Drosophila* odor memory processing. *Neuron* 53, 103–115. doi: 10.1016/j.neuron.2006.11.021

Lancaster, B., and Adams, P. R. (1986). Calcium-dependent current generating the afterhyperpolarization of hippocampal neurons. *J. Neurophysiol.* 55, 1268–1282. doi: 10.1152/jn.1986.55.6.1268

Malik, B. R., Gillespie, J. M., and Hodge, J. J. (2013). CASK and CaMKII function in the mushroom body alpha'/beta' neurons during *Drosophila* memory formation. *Front. Neural Circ.* 7:52. doi: 10.3389/fncir.2013.00052

Malik, B. R., and Hodge, J. J. (2014). *Drosophila* adult olfactory shock learning. *J. Vis. Exp.* 90:e50107.

Marrion, N. V., and Tavalin, S. J. (1998). Selective activation of Ca^{2+}-activated K^+ channels by co-localized Ca^{2+} channels in hippocampal neurons. *Nature* 395, 900–905. doi: 10.1038/27674

Mattson, M. P., and Chan, S. L. (2001). Dysregulation of cellular calcium homeostasis in Alzheimer's disease: bad genes and bad habits. *J. Mol. Neurosci.* 17, 205–224. doi: 10.1385/jmn:17:2:205

Mershin, A., Pavlopoulos, E., Fitch, O., Braden, B. C., Nanopoulos, D. V., and Skoulakis, E. M. (2004). Learning and memory deficits upon TAU accumulation in *Drosophila* mushroom body neurons. *Learn Mem.* 11, 277–287. doi: 10.1101/lm.70804

Missiaen, L., Robberecht, W., van den Bosch, L., Callewaert, G., Parys, J. B., Wuytack, F., et al. (2000). Abnormal intracellular Ca^{2+}homeostasis and disease. *Cell Calcium* 28, 1–21. doi: 10.1054/ceca.2000.0131

Moosmang, S., Haider, N., Klugbauer, N., Adelsberger, H., Langwieser, N., Muller, J., et al. (2005). Role of hippocampal $Ca_v1.2$ Ca^{2+} channels in NMDA receptor-independent synaptic plasticity and spatial memory. *J. Neurosci.* 25, 9883–9892. doi: 10.1523/jneurosci.1531-05.2005

Moyer, J. R. Jr., Power, J. M., Thompson, L. T., and Disterhoft, J. F. (2000). Increased excitability of aged rabbit CA1 neurons after trace eyeblink conditioning. *J. Neurosci.* 20, 5476–5482. doi: 10.1523/jneurosci.20-14-05476.2000

Moyer, J. R. Jr., Thompson, L. T., Black, J. P., and Disterhoft, J. F. (1992). Nimodipine increases excitability of rabbit CA1 pyramidal neurons in an age- and concentration-dependent manner. *J. Neurophysiol.* 68, 2100–2109. doi: 10.1152/jn.1992.68.6.2100

Nimmrich, V., and Eckert, A. (2013). Calcium channel blockers and dementia. *Br. J. Pharmacol.* 169, 1203–1210.

Nisbet, R. M., and Gotz, J. (2018). Amyloid-beta and Tau in Alzheimer's Disease: novel pathomechanisms and non-pharmacological treatment strategies. *J. Alzheimers Dis.* 64, S517–S527. doi: 10.3233/JAD-179907

Nunez-Santana, F. L., Oh, M. M., Antion, M. D., Lee, A., Hell, J. W., and Disterhoft, J. F. (2014). Surface L-type Ca^{2+} channel expression levels are increased in aged hippocampus. *Aging Cell* 13, 111–120. doi: 10.1111/acel.12157

Owald, D., Felsenberg, J., Talbot, C. B., Das, G., Perisse, E., Huetteroth, W., et al. (2015). Activity of defined mushroom body output neurons underlies learned olfactory behavior in *Drosophila*. *Neuron* 86, 417–427. doi: 10.1016/j.neuron.2015.03.025

Papanikolopoulou, K., and Skoulakis, E. M. (2011). The power and richness of modelling tauopathies in *Drosophila*. *Mol. Neurobiol.* 44, 122–133. doi: 10.1007/s12035-011-8193-1

Pascual, A., and Preat, T. (2001). Localization of long-term memory within the *Drosophila* mushroom body. *Science* 294, 1115–1117. doi: 10.1126/science.1064200

Peng, I. F., and Wu, C. F. (2007). *Drosophila cacophony* channels: a major mediator of neuronal Ca^{2+} currents and a trigger for K^+ channel homeostatic regulation. *J. Neurosci.* 27, 1072–1081. doi: 10.1523/jneurosci.4746-06.2007

Pitman, J. L., Huetteroth, W., Burke, C. J., Krashes, M. J., Lai, S. L., Lee, T., et al. (2011). A pair of inhibitory neurons are required to sustain labile memory in the *Drosophila* mushroom body. *Curr. Biol.* 21, 855–861. doi: 10.1016/j.cub.2011.03.069

Ryglewski, S., Lance, K., Levine, R. B., and Duch, C. (2012). Ca_v2 channels mediate low and high voltage-activated calcium currents in *Drosophila*

motoneurons. *J. Physiol.* 590, 809–825. doi: 10.1113/jphysiol.2011.222836

Schlichting, M., Menegazzi, P., Lelito, K. R., Yao, Z., Buhl, E., Dalla Benetta, E., et al. (2016). A neural network underlying circadian entrainment and photoperiodic adjustment of sleep and activity in *Drosophila*. *J. Neurosci.* 36, 9084–9096. doi: 10.1523/JNEUROSCI.0992-16.2016

Sealey, M. A., Vourkou, E., Cowan, C. M., Bossing, T., Quraishe, S., Grammenoudi, S., et al. (2017). Distinct phenotypes of three-repeat and four-repeat human tau in a transgenic model of tauopathy. *Neurobiol. Dis.* 105, 74–83. doi: 10.1016/j.nbd.2017.05.003

Sejourne, J., Placais, P. Y., Aso, Y., Siwanowicz, I., Trannoy, S., Thoma, V., et al. (2011). Mushroom body efferent neurons responsible for aversive olfactory memory retrieval in *Drosophila*. *Nat. Neurosci.* 14, 903–910. doi: 10.1038/nn.2846

Shaw, R. E., Kottler, B., Ludlow, Z. N., Buhl, E., Kim, D., Morais da Silva, S., et al. (2018). In vivo expansion of functionally integrated GABAergic interneurons by targeted increase in neural progenitors. *EMBO J.* 37:e98163. doi: 10.15252/embj.201798163

Spillantini, M. G., and Goedert, M. (2013). Tau pathology and neurodegeneration. *Lancet Neurol.* 12, 609–622. doi: 10.1016/s1474-4422(13)70090-5

Spires-Jones, T. L., and Hyman, B. T. (2014). The intersection of amyloid beta and tau at synapses in Alzheimer's disease. *Neuron* 82, 756–771. doi: 10.1016/j.neuron.2014.05.004

Straube, K. T., Deyo, R. A., Moyer, J. R. Jr., and Disterhoft, J. F. (1990). Dietary nimodipine improves associative learning in aging rabbits. *Neurobiol. Aging* 11, 659–661. doi: 10.1016/0197-4580(90)90033-v

Terada, S., Matsubara, D., Onodera, K., Matsuzaki, M., Uemura, T., and Usui, T. (2016). Neuronal processing of noxious thermal stimuli mediated by dendritic Ca^{2+} influx in *Drosophila* somatosensory neurons. *eLife* 5:e12959. doi: 10.7554/eLife.12959

Thibault, O., Gant, J. C., and Landfield, P. W. (2007). Expansion of the calcium hypothesis of brain aging and Alzheimer's disease: minding the store. *Aging Cell* 6, 307–317. doi: 10.1111/j.1474-9726.2007.00295.x

Wang, Y., and Mattson, M. P. (2014). L-type Ca^{2+} currents at CA1 synapses, but not CA3 or dentate granule neuron synapses, are increased in 3xTgAD mice in an age-dependent manner. *Neurobiol. Aging* 35, 88–95. doi: 10.1016/j.neurobiolaging.2013.07.007

Wentzell, J., and Kretzschmar, D. (2010). Alzheimer's disease and tauopathy studies in flies and worms. *Neurobiol. Dis.* 40, 21–28. doi: 10.1016/j.nbd.2010.03.007

White, J. A., McKinney, B. C., John, M. C., Powers, P. A., Kamp, T. J., and Murphy, G. G. (2008). Conditional forebrain deletion of the L-type calcium channel $Ca_V1.2$ disrupts remote spatial memories in mice. *Learn. Mem.* 15, 1–5. doi: 10.1101/lm.773208

Wittmann, C. W., Wszolek, M. F., Shulman, J. M., Salvaterra, P. M., Lewis, J., Hutton, M., et al. (2001). Tauopathy in *Drosophila*: neurodegeneration without neurofibrillary tangles. *Science* 293, 711–714. doi: 10.1126/science.1062382

Worrell, J. W., and Levine, R. B. (2008). Characterization of voltage-dependent Ca2+ currents in identified *Drosophila* motoneurons in situ. *J. Neurophysiol.* 100, 868–878. doi: 10.1152/jn.90464.2008

Wu, J. W., Hussaini, S. A., Bastille, I. M., Rodriguez, G. A., Mrejeru, A., Rilett, K., et al. (2016). Neuronal activity enhances tau propagation and tau pathology in vivo. *Nat. Neurosci.* 19, 1085–1092. doi: 10.1038/nn.4328

Yu, D., Akalal, D. B., and Davis, R. L. (2006). *Drosophila* alpha/beta mushroom body neurons form a branch-specific, long-term cellular memory trace after spaced olfactory conditioning. *Neuron* 52, 845–855. doi: 10.1016/j.neuron.2006.10.030

Zhou, L., McInnes, J., Wierda, K., Holt, M., Herrmann, A. G., Jackson, R. J., et al. (2017). Tau association with synaptic vesicles causes presynaptic dysfunction. *Nat. Commun.* 8:15295. doi: 10.1038/ncomms15295

Conflict of Interest Statement: The authors declare that the research was conducted in the absence of any commercial or financial relationships that could be construed as a potential conflict of interest.